SESS REPORT 2019

The State of Environmental Science in Svalbard – an annual report

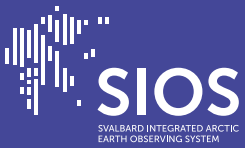

SESS REPORT 2019

The State of Environmental Science in Svalbard – an annual report

Floor van den Heuvel, Christiane Hübner,
Malgorzata Błaszczyk, Martin Heimann,
Heikki Lihavainen (Editors)

SESS report 2019
The State of Environmental Science in Svalbard
– an annual report

ISSN 2535-809X (printed)
ISSN 2535-6321 (pdf)
ISBN 978-82-691528-7-6 (printed, stapled)
ISBN 978-82-691528-6-9 (pdf)

Publisher: Svalbard Integrated Arctic Earth Observing System (SIOS)
Editors: Floor van den Heuvel, Christiane Hübner,
Malgorzata Błaszczyk, Martin Heimann, Heikki Lihavainen
Editor popular science summaries: Janet Holmén
Layout: Melkeveien designkontor, Oslo

CITATION:
Entire report: Van den Heuvel F, Hübner C, Błaszczyk M, Heimann M, Lihavainen H (eds) 2020: SESS report 2019, Svalbard Integrated Arctic Earth Observing System, Longyearbyen
Chapters in report: All authors (2020) Title of chapter. In: Van den Heuvel et al. (eds): SESS report 2019, Svalbard Integrated Arctic Earth Observing System, Longyearbyen, pp. xx - xx

The report is published as electronic document, available from the SIOS web site www.sios-svalbard.org/SESSreport

Contents

Foreword

The Svalbard Integrated Arctic Earth Observing System (SIOS) is an international multi-disciplinary research infrastructure for observing the Arctic Earth. SIOS concentrates on long-term observations important for global environmental and climate change, to observe, attribute and describe the effects of the change. The central instrument for developing SIOS, guiding the next years' work within SIOS and reporting the achievements during the last year is this annual SESS report.

The integrating theme of SIOS is to understand the processes in the interfaces between different earth system science disciplines and their dependencies on each other in the changing environment. As a holistic multidisciplinary research infrastructure, SIOS has huge potential to improve our understanding of the sweeping changes in our Arctic environment. Huge potential often also entails huge challenges. We as SIOS together are challenged but strive incessantly towards attaining the SIOS goals. International and multidisciplinary also means multilingual in a scientific environment. Finding a common language is a challenge indeed, but facilitated by strong common interests towards Arctic research. The science and research in different spheres have matured in different manners and directions, and to align them to the shared SIOS goals we need this common language. The SESS report is one integrative tool to improve the communication between spheres.

To be able to attain the potential described above, SIOS has defined the first set of core data, which in a broad sense are state variables important for global environmental diagnostics, describing energy and mass exchange and the combined effect of human perturbations and environmental change on organism, populations and ecosystems. Core data will be produced over time such that scientists can plan experiments leaning on a trustworthy source of the core data streams. This backdrop of data produced by SIOS is a vital enhancement in making Svalbard an even better research platform for the international research community. The SESS report is instrumental to exploring, developing and defining the next generation of core data and thus the proliferation of Svalbard research.

The SESS report is a way to develop the observing system; the recommendations in the SESS reports are used as prioritising instruments in developing and optimising the research infrastructure. This year's report includes reviews of existing data and activities, data summaries and updates from last year's chapters. It is a unique description of current activities and collaboration, as well as recommendations for the future in Svalbard research.

Without the voluntary work of the editorial board (Floor van den Heuvel, Martin Heimann, and Malgorzata Błaszczyk) this report would have never seen the light of day. We deeply appreciate their invaluable devotion towards this report. The help of Janet Holmén in turning the scientific language into understandable popular science form is appreciated. The anonymous reviewers made an important contribution to the chapters with their constructive suggestions: the scientific world relies on scientists' willingness to act as reviewers. Finally, thanks to the authors of the SESS report 2019; your contribution to science in Svalbard is indispensable. Now the task lies with us, SIOS and the SIOS Knowledge Centre, to take your recommendations to the SIOS consortium to discuss feasibility, set priorities, and strive for timely implementation.

Longyearbyen, December 2019

Prof. Heikki Lihavainen
Director, SIOS

Kim Holmén
Chair of Board of Directors, SIOS

Christiane Hübner
Information Officer, SIOS

Authors from following institutions contributed to this report:

AARI	Arctic and Antarctic Research Institute, Russia
AMU	Adam Mickiewicz University, Poland
ASC	Andøya Space Center, Norway
AU	Aarhus University, Denmark
AWI	Alfred Wegener Institute, Helmholtz Centre for Polar and Marine Research, Germany
Bates College	Bates College, USA
CIRA	Cooperative Institute for Research in the Atmosphere, Colorado State University, USA
CPR-Survey	Continuous Plankton Recorder Survey, Marine Biological Association, U.K.
CPS	Centre for Polar Studies, University of Silesia, Poland
CU	Clemson University, USA
DC	Dartmouth College, USA
GFZ	German Research Centre for Geosciences, Germany
Hampshire College	Hampshire College, USA
IGF PAS	Institute of Geophysics, Polish Academy of Sciences, Poland
IGRAS	Institute of Geography, Russian Academy of Sciences, Russia
IIM	Italian Navy Hydrographic Institute, Italy
IMR	Institute of Marine Research, Norway
INAR	Institute for Atmospheric and Earth System Research, University of Helsinki, Finland
Insubria Univ	Insubria University, Italy
IOPAN	Institute of Oceanology Polish Academy of Sciences, Poland

ISP-CNR.....Institute of Polar Sciences, National Research Council of Italy, Italy
JAXA.....JAXA Institute of Space and Aeronautical Science, Japan
JB Hyp Devices .....JB Hyperspectral Devices, Germany
JHI .....The James Hutton Institute, UK
Lund Univ.....Lund University, Sweden
MET Norway .....Norwegian Meteorological Institute, Norway
NASA.....NASA Goddard Space Flight Center, USA
NCSR.....National Center for Scientific Research, Greece
NGI .....Norwegian Geotechnical Institute, Norway
NINA .....Norwegian Institute for Nature Research, Norway
NIPR .....National Institute of Polar Research, Japan
NORCE .....Norwegian Research Centre AS, Norway
NORSAR.....NORSAR, Norway
NPI.....Norwegian Polar Institute, Norway
OGS.....National Institute of Oceanography and Applied Geophysics, Italy
SLU .....Swedish University of Agricultural Sciences, Sweden
SU .....Stockholm University, Sweden
U IOWA.....University of Iowa, USA
UAF .....University of Alaska, USA
UiO .....University of Oslo, Norway
UiT .....UiT, The Arctic University of Norway, Norway
UNIMiB.....University of Milano-Bicocca, Italy
UNIS.....University Centre in Svalbard, Norway
Univ Bolzano .....Free University of Bozen-Bolzano, Italy
UP.....University of Perugia, Italy
UU .....Uppsala University, Sweden

Executive Summary

Floor van den Heuvel[1], Christiane Hübner[2], Malgorzata Błaszczyk[3], Martin Heimann[4], Heikki Lihavainen[2]

1 Ecole Polytechnique Fédérale de Lausanne, Environmental Remote Sensing Laboratory, Lausanne, Switzerland; 2 SIOS Knowledge Centre, Longyearbyen, Norway; 3 University of Silesia, Faculty of Natural Sciences, Sosnowiec, Poland; 4 Max-Planck-Institute for Biogeochemistry, Jena, Germany

The Arctic constitutes a key "hotspot" in the global Earth System. It is currently warming faster than the rest of the Earth due to several critical feedback processes of global importance, e.g. the land and sea ice albedo effect. This warming promotes a host of changes in interconnected environmental parameters, from the oceans, ice and ecosystems at the surface, past the clouds to the stratosphere. Understanding, quantifying and ultimately predicting changes in these interactions using complex Earth system models constitutes a critical challenge in Earth system science. Meeting this challenge requires comprehensive observations in the Arctic domain.

Due to its location at the crossroads of major atmospheric and oceanic currents, as well as its accessibility and the presence of important international research infrastructures, Svalbard constitutes a perfect location for observing and studying Arctic climate change and its impacts on high latitude terrestrial and oceanic ecosystems. The chapters in this report document the current status of the Arctic environment as observed in Svalbard in 2019, and highlight research conducted within SIOS.

In Svalbard, conditions during the 2017/18 hydrological year were markedly warmer than the previous year. Despite a longer freezing season, mean air temperatures were higher at all measurement locations in Svalbard.

This continued warming has had repercussions on the terrestrial system through a decrease in the depth and duration of snow cover, as well as an increased frequency of rain-on-snow events. These changes have led to increases in plant productivity, permafrost active layer thickness and ground temperatures.

While enhanced vegetation growth has positive effects on the population sizes of grazers in Svalbard, such as reindeer and geese, rain-on-snow events and the resulting thick layer

of ice raises herbivore mortality rates by blocking their access to food. Enhanced grubbing by grazers in search of food extends the exposure of permafrost to warming, while changes in the snow- and vegetation cover affects the amount of solar radiation reflected back into the atmosphere. Thus, changes within the terrestrial system can both affect other parts of this system and feed back into the atmosphere.

Increased monitoring of permafrost at different locations and greater depths, as well as enhanced use of remote sensing techniques to monitor both ground instability and vegetation growth are necessary for better quantification of the observed changes. The complex interactions between climatic variables and the Arctic tundra ecosystem and species, require long-term, adaptive food-web based monitoring.

Glaciers and ice caps are among the most eye-catching indicators documenting changes in the global climate. Svalbard holds only a tiny fraction of the glacier area in the Arctic, but represents a wide range of glacier types. All reported pan-Svalbard estimates show a decrease in glacier mass balance, likely as a result of atmospheric and oceanic warming. Fast glacial retreat in Svalbard causes expansion of fjords and proglacial areas, and increases freshwater input into marine environments, influencing regional albedo and energy balance.

Collaborative research programmes across (and outside) the glaciological community are required to better assess the future evolution of glacier cover. Long-term *in situ* measurements and models focus on surface ablation. Frontal ablation, however, is understudied. Estimates of ablation processes at the glacier front – calving and submarine melting – have hitherto been forced to rely on outdated information and low-resolution methods. Long-term trends and changes in seasonal calving patterns can be now observed in near real-time with cryoseismological monitoring. Expansion of the seismological network and integration of seismic observations with other monitoring methods are expected to provide a more accurate and more complete quantification of the global warming footprint on Svalbard's cryosphere.

Currents from both the Atlantic and the Arctic Oceans strongly influence the climate in Svalbard through input of warm or cold water. More frequent warm water inputs from

the Atlantic in combination with higher ocean and air temperatures impact sea ice extent, thickness and duration, as well as the snow cover on the sea ice. Reduced ice cover diminishes the amount of solar radiation reflected back into space, as the darker water absorbs solar radiation and warms up, further accelerating sea ice melting. Loss of sea ice, oceanic warming and freshwater inputs from glacier melt also affect marine ecosystems, for example by changing species' ranges and increasing phytoplankton productivity.

Extending the established *in situ* sea ice monitoring at Svalbard with autonomous technology and remote sensing tools would provide a robust suite of complementary monitoring methods. An integrated observation system and enhancement of monitoring activities with additional biogeochemical and molecular sensors is recommended. This would give us a more comprehensive overview of the biological and chemical changes in oceans and fjords.

The characteristics of natural and anthropogenic aerosols are fundamental for our understanding of changes in the Arctic system as the impact of aerosols and their various feedback mechanisms are still very uncertain. Aerosols are solid or liquid particles suspended in the air. Oceans and sea ice are sources of natural cloud condensation nuclei; aerosols that can act as a seed for cloud droplets. Among these are aerosols released from sea spray, secondary aerosols originating from phytoplankton-emitted dimethyl sulphide and iodine emissions from sea ice. More open water and increased phytoplankton activity may impact the chemical composition of the aerosols and thus cloud formation. In addition, natural cloud condensation nuclei may originate from emissions of biogenic vapours from plants and animals as a result of increased terrestrial primary production on land.

Black carbon aerosols, mostly of anthropogenic origin, warm the atmosphere through their capacity to absorb solar radiation while suspended in the atmosphere or in clouds. Black carbon may also affect the physical and radiative properties of clouds or, when deposited on the ground, impact the regional radiation balance by reducing snow and ice surface albedo.

Extension of the current instrumentation for aerosol detection in the atmosphere to other locations in Svalbard, and improved comparability among different measurement techniques, would improve our understanding of how aerosols of both natural and anthropogenic origin end up in the Arctic atmosphere. Supplementing the infrastructure for the vertical probing of atmospheric variables with drones, unmanned aerial vehicles, and balloons will not only enhance our understanding of the Arctic atmosphere, but also facilitate the use and interpretation of remote sensing observations.

The upper polar atmosphere is strongly influenced by solar winds, which heat and structure the thermosphere. During 2018/19, five Grand Challenge Initiative – Cusp rockets were successfully launched through daytime auroras over Svalbard. Unique data sets were collected to explore solar wind forcing of particle acceleration, turbulence, atmospheric heating and outgassing that may influence the upper boundaries of the polar atmosphere.

The editors thank the many researchers who have contributed articles for the SESS Report 2019. Reading about how the SIOS projects have advanced has been a rewarding experience.

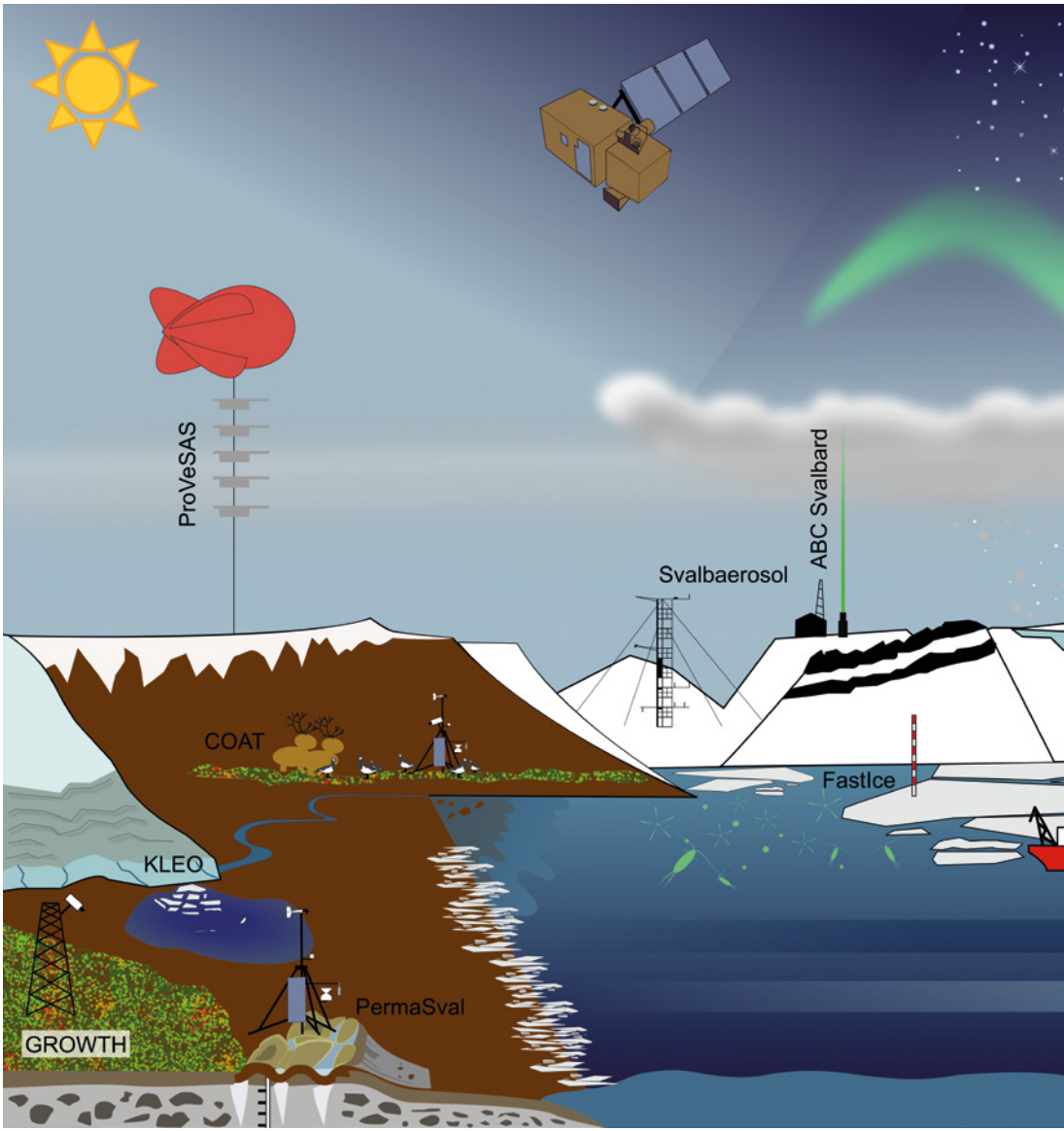
ProVeSAS
ABC Svalbard
Svalbaerosol
COAT
FastIce
KLEO
PermaSval
GROWTH

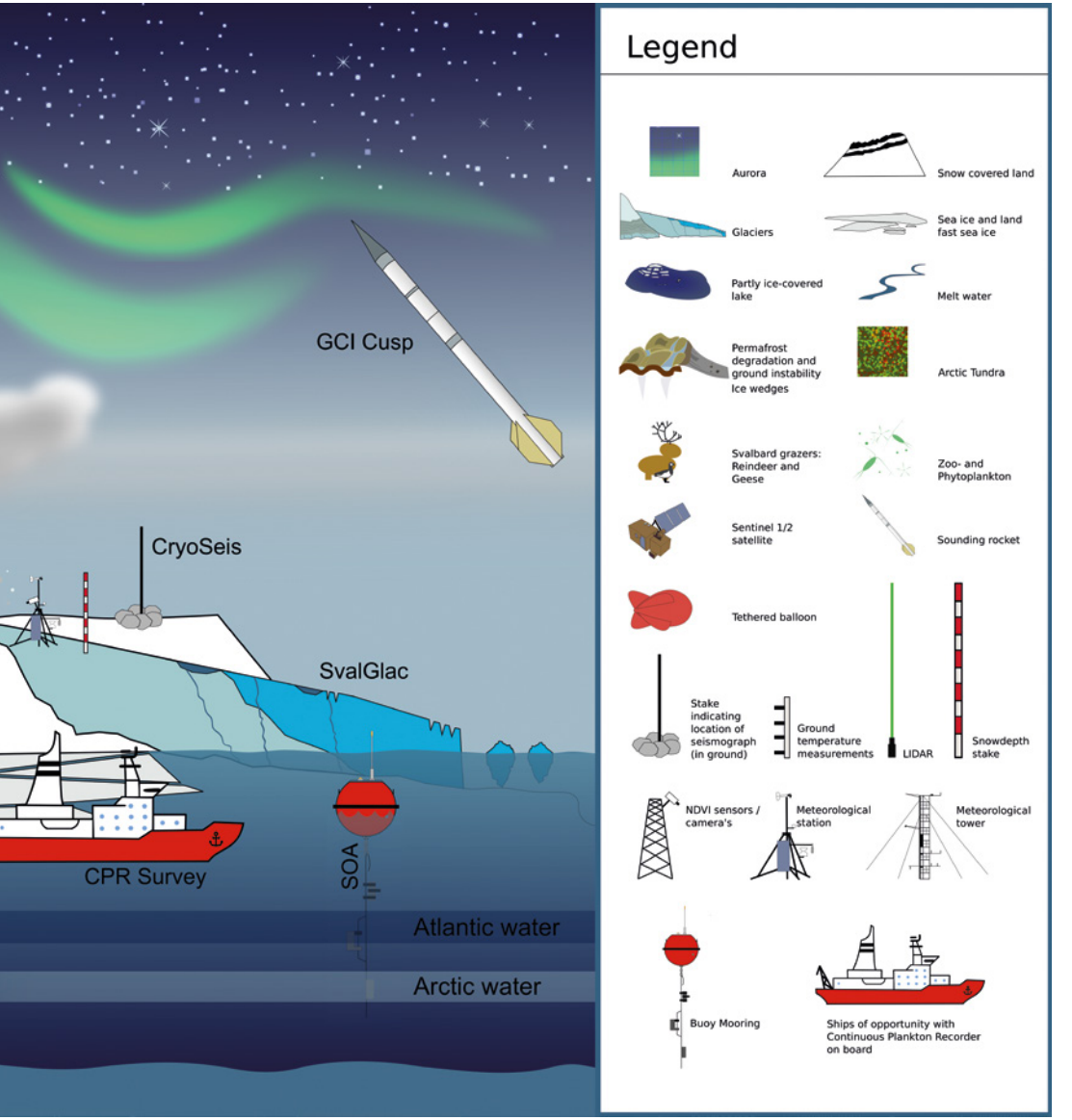
GCI Cusp
CryoSeis
SvalGlac
CPR Survey
SOA
Atlantic water
Arctic water
Legend
Aurora
Snow covered land
Glaciers
Sea ice and land fast sea ice
Partly ice-covered lake
Melt water
Permafrost degradation and ground instability Ice wedges
Arctic Tundra
Svalbard grazers: Reindeer and Geese
Zoo- and Phytoplankton
Sentinel 1/2 satellite
Sounding rocket
Tethered balloon
Stake indicating location of seismograph (in ground)
Ground temperature measurements
LIDAR
Snowdepth stake
NDVI sensors / camera's
Meteorological station
Meteorological tower
Buoy Mooring
Ships of opportunity with Continuous Plankton Recorder on board

CHAPTER 1

Automatic phenology cameras (phenocams) capture the timing of plant green-up, growth and senescence in Adventdalen. (Photo: Stein Rune Karlsen)

Sentinel satellite-based mapping of plant productivity in relation to snow duration and time of green-up (GROWTH)

Click here for full chapter

HIGHLIGHTS

Annual plant production provides food for wildlife and plays a key role in the global carbon budget. With new SIOS data and existing data from Adventdalen, close to Longyearbyen, we have a unique possibility to measure plant production at different scales.

AUTHORS

SR Karlsen (NORCE)
L Stendardi (Univ Bolzano)
L Nilsen (UiT)
E Malnes (NORCE)
L Eklundh (Lund Univ)
T Julitta (JB Hyp Devices)
A Burkart (JB Hyp Devices)
H Tømmervik (NINA)

Svalbard's climate is undergoing dramatic changes, but how this will influence plant productivity is largely unknown. Understanding these changes at the ecosystem level requires that we use data from different sources – including satellites – to assess climate-induced effects on plant vitality and productivity. However, measuring plant productivity is a challenging task. For the Adventdalen area we use radar satellite data to map snow and ice in the melting season and optical satellite data to map the start and peak of the growing season. The satellite data can be related to plant productivity, but must be interpreted based on measurements done in the field.

An observation system for continuous field monitoring of vegetation was established

in Adventdalen in Svalbard in 2015. This system consists of field-based racks with various sensors and cameras, which are placed in different vegetation types. The system has successfully recorded the timings of green-up, plant growth and senescence since its establishment.

To further increase the usefulness of the observation system, we need to develop methods to validate the satellite data with data from the sensors and cameras on the racks in Adventdalen. This would allow more accurate estimates of plant productivity over broader regions and scaling up to all of Svalbard. The most advanced instrument in this observation system is a state-of-the-art spectrometer that measures radiances and sun-induced fluorescence; it was deployed in Adventdalen in the summer of 2019. This expensive instrument can give even better estimates of plant productivity and can also be used to calibrate the other measurements and the satellite data. However, the observation system as currently configured in Adventdalen does not provide sufficient data on bryophytes (mosses).

RECOMMENDATIONS

There is a need to develop methodologies that combine field-based measurements and near-ground sensors of plant productivity with data from Sentinel satellites in order to validate satellite data and provide more accurate estimates of plant productivity at large spatial scales. The plant observation system in Adventdalen should be expanded to include more measurements on mosses.

Longyearbyen – Adventdalen. Onset of growing season 2018. (NORCE – Norwegian Research Centre)

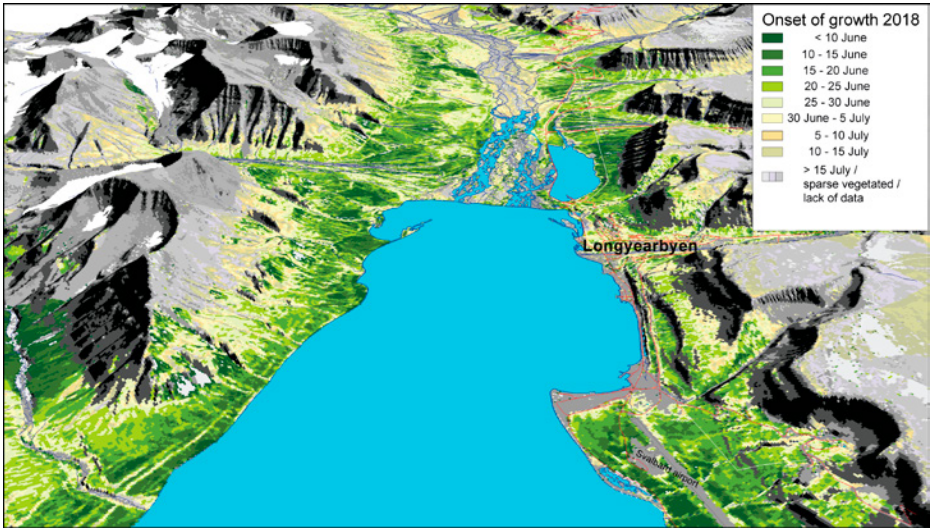

CHAPTER 2

COAT has five food web monitoring modules. The Svalbard reindeer is the focus of one of them. (Photo: Tore Nordstad/NPI)

Climate-Ecological Observatory for Arctic Tundra (COAT)

Click here for full chapter

HIGHLIGHTS

COAT is a scientifically robust observation system that enables long-term, real-time detection, documentation, understanding and predictions of climate impacts on Arctic tundra ecosystems. COAT aims to be an ecosystem-based, long-term, adaptive monitoring programme, based on a food-web approach.

AUTHORS

ÅØ Pedersen (NPI)
J Stien (NINA)
S Albon (JHI)
E Fuglei (NPI)
K Isaksen (Met Norway)
G Liston (CIRA)
JU Jepsen (NINA)
J Madsen (AU)
VT Ravolainen (NPI)
AK Reinking (CIRA)
EM Soininen (UiT)
A Stien (NINA)
R van der Wal (SLU)
NG Yoccoz (UiT)
RA Ims (UiT)

COAT is a response to the urgent international calls for establishment of observation systems that make it possible to gain insight into how climate impacts Arctic tundra. COAT Svalbard is an essential component of SIOS and serves to optimise and integrate the ecosystem-based terrestrial monitoring.

Variations from year to year and differences from place to place make long-term monitoring essential to support the complex decisions involved in conservation, management and policymaking. The COAT approach is holistic, covering entire ecosystems by integrating information about living and non-living factors over time

and space, with clearly defined monitoring goals.

Monitoring modules within COAT Svalbard track five key climate-sensitive food web pathways as well as climate parameters that determine how those pathways function (www.coat.no). Each module is described in terms of expected direct and indirect relationships between organisms in the food web pathways, and how climate and management interventions might influence these interactions. The programme is implemented according to a peer-reviewed Science Plan with a solid foundation in the scientific literature. COAT Svalbard focuses on two contrasting Arctic regions: Nordenskiöld Land and Brøggerhalvøya and surrounding areas. The vertebrate populations being monitored in these areas currently appear to be stable or growing. However, the lack of long-term monitoring of the vegetation communities on which these animals rely hinders understanding of bottom-up processes within the food web. COAT aims to fill these gaps and provide new insight into how climate change impacts High Arctic tundra ecosystems.

RECOMMENDATIONS

We recommend coordinating research infrastructure and observational measurements at similar spatial and temporal scales to predict and understand climate impacts on Svalbard tundra. Specifically, we recommend increasing the number of full-scale automatic weather stations, developing high-resolution physically based snow models from joint data sources, and developing more relevant variables to describe ecosystem functioning and processes.

Integrated data from SIOS and COAT will demonstrate in practice how coordinated monitoring can help answer crucial research questions about the ecosystem.

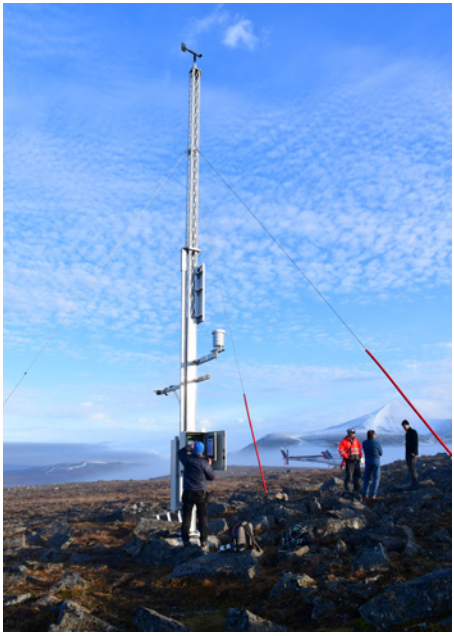

Researchers check an automatic weather station, newly established at Janssonhaugen, Nordenskiöld Land, Svalbard. (Photo: Ketil Isaksen/MET)

A researcher carrying out the annual Svalbard reindeer population abundance census in Adventdalen to provide information on total number of animals, mortality and reproduction. (Photo: Elin Vinje Jenssen/NPI)

CHAPTER 3

Water column monitoring on Linnévatnet. (Photo: Michael Retelle)

Environmental Monitoring in the Kapp Linné-Grønfjorden Region (KLEO)

Click here for full chapter

HIGHLIGHTS

1. Regional temperatures in Kapp Linné–Grønfjorden have risen
2. Lake ice formation in the fall has recently been delayed to as late as December
3. Peak river flow in six of the last eight years is due to late-season rain
4. AARI has done intensive hydrologic and precipitation studies

AUTHORS

M Retelle (UNIS, Bates College)
H Christiansen (UNIS)
A Hodson (UNIS)
A Nikulina (AARI)
M Osuch (IGF PAS)
K Poleshuk (AARI)
K Romashova (AARI)
S Roof (Hampshire College)
L Rouyet (NORCE, UiT, UNIS)
S Strand (UNIS, UiO)
I Vasilevich (AARI)
T Wawrzyniak (IGF PAS)

The Kapp Linné–Grønfjorden region is an ideal and strategic location for an interdisciplinary long-term environmental observatory in the coastal region of western Spitsbergen at the mouth of Isfjorden. The regional climate is greatly influenced by its maritime setting with higher mean annual air temperature and greater precipitation than the more continental interior regime in central Spitsbergen. With the recent intensified Atlantification of the northern Barents Sea, environmental monitoring studies along the west Spitsbergen coast may serve as an early warning system in a changing climate.

The Kapp Linné Environmental Observatory (KLEO) was formulated as an international collaborative site within the Svalbard Integrated Arctic Earth Observing System (SIOS) as a regional centre with a research focus on hydroclimate, snow and ice cover, permafrost, ecology and paleoclimate. KLEO research sites extend from the west coast of Spitsbergen at the mouth of Isfjorden, to the eastern shore of Grønfjord.

The Kapp Linné Environmental Observatory provides an ideal training ground for the next generation of arctic scientists who will take on the challenges of the 21st century. The proximity to the University Centre in Svalbard (UNIS) and the AARI Barentsburg Research Station provides a highly motivated and well-trained workforce for addressing critically important environmental research issues.

RECOMMENDATIONS

The network of environmental monitoring installations and environmental sampling in the Kapp Linné–Grønfjorden region should be maintained and improved in this period of changing climate. In addition, we encourage an increase in interdisciplinary research, including long-term studies of both terrestrial and aquatic ecology.

Understanding regional variability in hydroclimate will be an increasingly important issue in Svalbard in the 21st century. Regional precipitation gradients, water storage in glacier ice and groundwater, and the role of groundwater as a water source and a factor in shaping the bio-geosphere are significant but poorly understood issues that must be addressed.

Linnédalen (Linnéelva, Linnévatnet and Linnébreen) looking south across the outlet of Linnévatnet. (Photo: Michael Retelle)

Physical limnological monitoring on Linnévatnet. (Photo: Margaret Holzer)

CHAPTER 4

The calving front of Paierlbreen terminating in the Hornsund Fjord (Photo: Dominik Cyran)

New data, new techniques and new challenges for updating the state of Svalbard glaciers (SvalGlac)

Click here for full chapter

HIGHLIGHTS

- We assess the mass balance of all Svalbard glaciers since year 2000
- Glaciers over all of Svalbard are losing mass, at rates depending on location
- Updated quantification of calving and better understanding of surges are urgently needed

AUTHORS

TV Schuler (UIO, UNIS)
A Glazovsky (IGRAS)
JO Hagen (UIO)
A Hodson (UNIS)
J Jania (CPS)
A Kääb (UIO)
J Kohler (NPI)
B Luks (IGF PAS)
J Malecki (AMU)
G Moholdt (NPI)
V Pohjola (UU)
W van Pelt (UU)

Glacier mass balance is the budget between snow accumulation and melting of snow and ice. Where glaciers terminate in the ocean, calving of icebergs constitutes an additional mechanism of mass loss, though it is more difficult to assess than snow accumulation and surface melting. The SvalGlac report reviews new technologies and new data that have become available in the past 20 years to update previous assessments. We find that glaciers all over Svalbard are losing mass, with rates depending on geographical location and glacier size. Smaller glaciers in southern Spitsbergen experience highest rates of mass loss while large ice caps in Northeast Svalbard are closer to a balance situation. However, variations from year to year are large and long-term observations are needed to recognise trends. These

Close-up of Basin-3, a surging outlet glacier from Austfonna, Nordaustlandet. (Photo: T.V. Schuler)

RECOMMENDATIONS

- To close the knowledge gaps, we recommend further development of Svalbard as a glacier laboratory by
- investing in instrumentation and data sharing to overcome lack of crucial data
- supporting pilot projects that can provide missing information where appropriate methodology already exists, and
- strengthening the glaciological community to collaboratively develop research programmes to improve process understanding.

spatial patterns and temporal evolution are also supported by modelling studies that calculate surface mass balance based on meteorological data, and by studies applying satellite remote sensing.

The only available estimate of calving needs updating, especially with regard to year-to-year and seasonal variations. Several large surges have occurred in the past few years, strongly influencing the amount of ice discharged into the ocean. A glacier surge is a switch from a slow to fast flowing mode, sometimes happening periodically. The mechanisms responsible for surges are not well understood but several Svalbard-based studies shed new light on these processes.

The most important gaps are:

- our incomplete understanding of surging, both the process itself and its implications for Svalbard glacier mass balance
- incomplete basic data coverage for quantification of calving and
- imited information about glacier mass balance and meltwater runoff in a future climate.

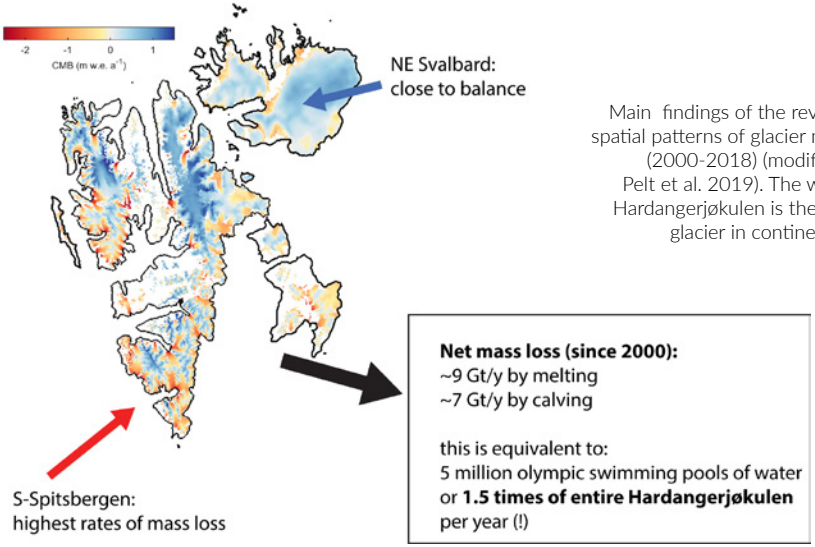

Main findings of the review showing spatial patterns of glacier mass balance (2000-2018) (modified after Van Pelt et al. 2019). The widely known Hardangerjøkulen is the sixth largest glacier in continental Norway.

CHAPTER 5

Fieldwork on Holtedalfonna where a temporary seismic station was deployed in April 2016. (Photo: A Köhler)

Seismological monitoring of Svalbard's cryosphere: current status and knowledge gaps (CRYOSEIS)

Click here for full chapter

HIGHLIGHTS

Cryoseismology can track changes in seasonal patterns of glacial seismicity and sub-surface properties over decades, allowing us to assess the effects of climate change in the cryosphere. Better seismic station coverage in Svalbard would enhance use of cryoseismology in environmental research.

AUTHORS

A Köhler (NORSAR)
W Gajek (IGF PAS)
M Malinowski (IGF PAS)
J Schweitzer (NORSAR)
M Majdanski (IGF PAS)
W Geissler (AWI)
M Chamarczuk (IGF PAS)
A Wuestefeld (NORSAR)

The new research field of cryoseismology studies ground shaking (seismic waves) generated in the frozen part of our planet. The shaking is caused by processes such as icequakes related to the movement of glaciers, glacier calvings, and flowing meltwater. Climate change affects processes at glaciers such as calving and causes changes in the permanently frozen ground (permafrost) in polar regions. Cryoseismology can measure these changes using seismic waves.

Accessibility and well-developed logistics mean that Svalbard is much easier to work in than other regions in the Arctic or the Antarctic, and make Svalbard a natural laboratory to study changes in the cryosphere induced by climate change.

Continuous seismic data collection in Svalbard (going back as long as decades) allows us to observe long-term trends and changes in seasonal patterns of glacial seismicity or sub-surface structures (permafrost). High temporal resolution of seismic data provides much more detail, e.g. about the calving process, than satellite images and helps us estimate the mass of ice that glaciers lose due to calving. Strong calving in Svalbard can be registered at great distances (up to 100 km) and measurements are fully independent of visibility, which allows for observation of calving regardless of polar night or bad weather conditions. This report briefly presents cryoseismology, its capabilities and methods within a global context, highlights recent research activity in Svalbard and suggests directions for future research and development of seismological infrastructure.

RECOMMENDATIONS

- The permanent seismic station network in Svalbard should be extended to improve detectability and location of glacier seismicity.
- A continuous automatic near-real-time detection system for seismic events (calvings, surges, etc.) should be implemented.
- Using resources of a common instrument pool for cryosphere research in Svalbard, multi-disciplinary, integrated field experiments with direct observations of cryosphere processes should be carried out.
- New technologies and methods (such as fibre-optic cables, noise interferometry, machine learning) that have just started being employed in seismology should be adopted in Svalbard to foster the cryoseismological research.

Extracting data from a temporary seismic station close to Ny-Ålesund in April 2016. (Photo: A Köhler)

Hansbreen terminus. (Photo: W Gajek)

CHAPTER 6

View from the observatory on Zeppelinfjellet near Ny-Ålesund over the northern part of inner Kongsfjorden, in April 2018. From here, regular sea ice observations are performed. In the picture, sea ice is recognisable in the distance to the right. (Photo: M Semmling)

Long-term monitoring of landfast sea ice extent and thickness in Kongsfjorden, and related applications (FastIce)

Click here for full chapter

HIGHLIGHTS

Systematic monitoring of landfast sea ice in Kongsfjorden, Svalbard, since 2003 improved understanding of its variability and long-term changes. After 2006, the ice cover was less extensive in space and time, and thinner than earlier. Results have also contributed to process and validation studies.

AUTHORS

S Gerland (NPI)
O Pavlova (NPI)
D Divine (NPI)
J Negrel (NPI)
S Dahlke (AWI)
AM Johansson (UiT)
M Maturilli (AWI)
M Semmling (GFZ)

Landfast sea ice (ice anchored to the shore) covers the inner parts of Kongsfjorden, Svalbard, in winter and spring, and is an important feature for the physical and biological fjord systems. Systematic fast-ice monitoring for Kongsfjorden, as a part of a long-term project at the Norwegian Polar Institute (NPI), started in 2003. It includes ice extent mapping and in situ measurements of ice and snow thickness. The permanent presence of NPI staff at Ny-Ålesund Research Station enables regular in situ fast-ice thickness measurements as long as the fast ice is accessible. In addition, daily visits to the observatory on the mountain Zeppelinfjellet close to Ny-Ålesund allow regular ice observations (weather, visibility, and daylight permitting). Monitoring of the sea ice conditions in Kongsfjorden can be used to demonstrate and investigate phenomena

related to climate change in the Arctic.

Fjord ice begins to form in the inner part of Kongsfjorden between December and March. After that the ice grows in thickness and extent, and then decreases until it melts or breaks off and drifts out of the fjord between April and June. Before 2006, ice often stretched from the interior to the central fjord parts, but in later years the ice has mainly been restricted to the inner fjord. Moreover, the ice was usually at least 0.6 m thick, in contrast to recent years with thickness often only about 0.2 m. The snow cover thickness on the ice in spring has also decreased, which can be partly explained by shorter fast ice seasons. The reason for less ice in Kongsfjorden after 2006 is considered to be a combination of the influence of warmer water and higher air temperatures in winter.

RECOMMENDATIONS

- Continue the monitoring as a robust and affordable initiative. While keeping consistency in the methods, consider introducing modern and autonomous technology
- Continue developing tools based on satellite remote sensing to support the monitoring
- Continue refining sea ice model components to improve the understanding of changes and variability observed

This monitoring has contributed to a number of process and validation studies, for example to improve satellite remote sensing techniques and the understanding of atmosphere–ice–ocean interaction.

Monitoring of sea ice thickness and freeboard (the vertical distance between ice and water surfaces) in Kongsfjorden is done from drill holes, usually drilled with an auger 5 cm in diameter, here from spring 2015. In addition, snow thickness is measured. (Photo: S Gerland)

CHAPTER 7

Sea ice loss leads to increased emission of compounds from phytoplankton and other living organisms, including dimethylsulphide and iodine, which can then form cloud condensation nuclei. (Photo: Mikko Sipilä)

Multidisciplinary research on biogenically driven new particle formation in Svalbard (SVALBAEROSOL)

Click here for full chapter

HIGHLIGHTS

Sea ice loss accelerates formation of cloud condensation nuclei (CCN) in the Arctic, leading to feedbacks to Arctic climate. We propose upgrades to aid resolution of mechanisms of CCN long-term monitoring of how relevant quantities change with warming Arctic environment.

AUTHORS

M Sipilä (INAR)
CJM Hoppe (AWI)
A Viola (ISP-CNR)
M Mazzola (ISP-CNR)
R Krejci (SU)
P Zieger (SU)
L Beck (INAR)
T Petäjä (INAR)

Climate change in the Arctic is reflected in decreased snow cover, thawing permafrost, increased productivity on land, and especially loss of sea ice. The latter accelerates climate warming and further sea ice decline. However, it may also increase phytoplankton productivity, thus increasing concentrations of cloud "seeds", cloud condensation nuclei (CCN), which in turn largely determine how clouds interact with light and affect Earth's energy balance. Therefore, change in CCN concentration may speed up or slow down climate warming in the Arctic. However, the mechanisms leading to CCN production over ice-covered and open Arctic waters are not known in detail. In addition, increasing emissions of vapours from plants and animals as a result of increased primary production on land may affect natural CCN production.

RECOMMENDATIONS

To resolve the details of CCN production and to monitor changes in the process chain from emissions to CCN formation we recommend upgrading the SIOS observation system. The following upgrades in Ny-Ålesund (Gruvebadet laboratory and Zeppelin observatory) are proposed:

- Mass spectrometer systems capable of measuring aerosol precursor vapours and naturally charged ion clusters
- Instrumentation for recording size distribution of naturally charged ion clusters and aerosol particles
- Instrumentation for recording neutral 1-3 nm clusters

Since phytoplankton is likely a key driver of secondary CCN formation we also propose:

- Systematic long-term monitoring of phytoplankton populations and their production of sulphur-containing compounds in Kongsfjorden

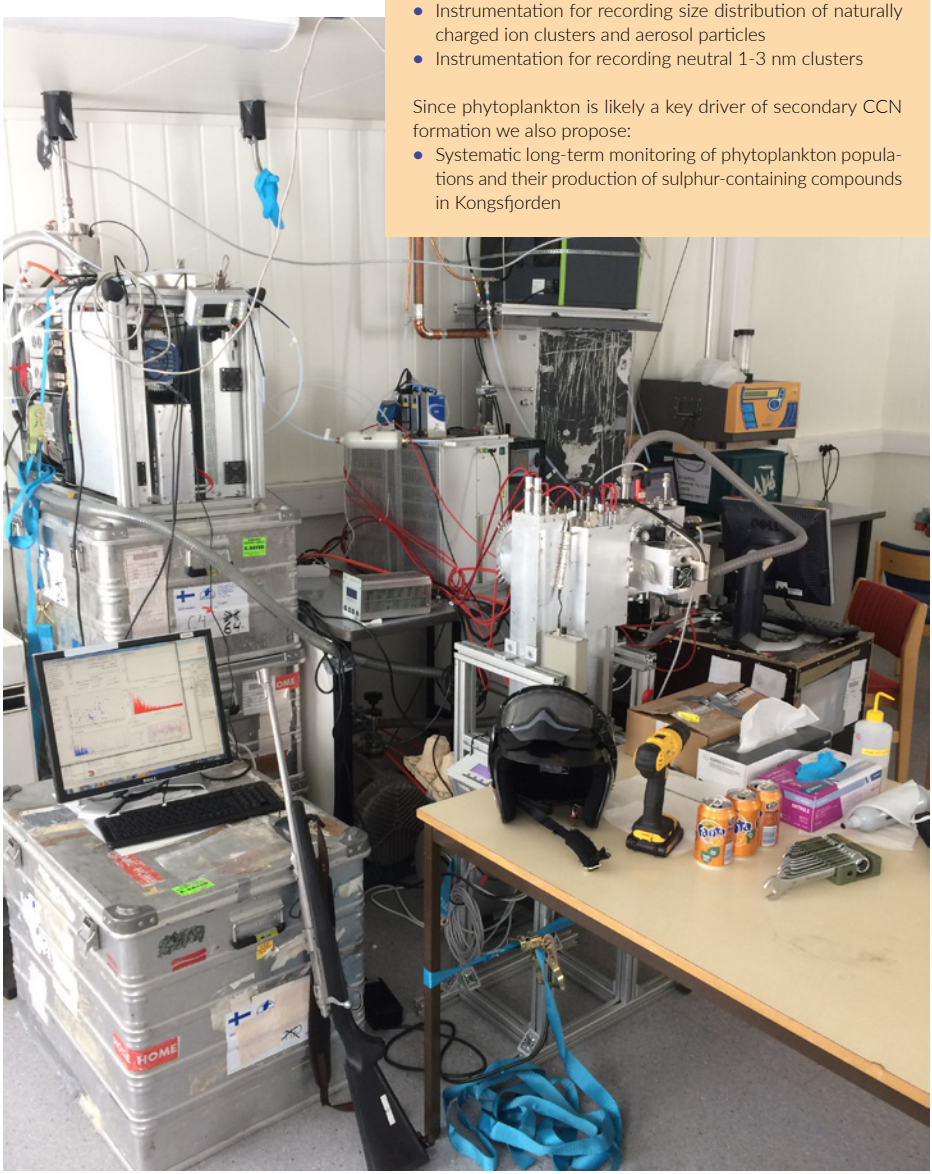

Gruvebadet laboratory in Ny-Ålesund filled with mass spectrometers and other instrumentation relevant for resolving and monitoring the formation of aerosols and cloud condensation nuclei. (Photo: Mikko Sipilä)

CHAPTER 8

Zeppelin observatory (near mountain top) from Gruvebadet (foreground). (Photo: Mauro Mazzola)

Atmospheric black carbon in Svalbard (ABC Svalbard)

Click here for full chapter

HIGHLIGHTS

Black carbon in Svalbard has been monitored continuously for more than 10 years at two adjacent sites at different altitudes, and during short research campaigns in various parts of the archipelago. The complexity of atmospheric dynamics promotes variable vertical profiles of black carbon.

AUTHORS

S Gilardoni (ISP-CNR)
A Lupi (ISP-CNR)
M Mazzola (ISP-CNR)
DM Cappelletti (UP)
B Moroni (UP)
L Ferrero (UNIMiB)
P Markuszewski (IOPAN)
A Rozwadowska (IOPAN)
R Krejci (SU)
P Zieger (SU)
P Tunved (SU)
L Karlsson (SU)
S Vratolis (NCSR)
K Eleftheriadis (NCSR)
AP Viola (ISP-CNR)

Black carbon particles are emitted into the atmosphere during combustion and reside in the air for days. Once emitted, they can be transported across thousands of kilometres and reach remote locations, like the Arctic. In the polar regions, black carbon has extremely important impacts on climate and environment. Because of its dark colour, it absorbs incoming solar radiation and can warm the atmosphere. Furthermore, black carbon that settles on the white surface of snow and ice favours their melting.

Black carbon has been measured for decades in Svalbard, continuously at the high-altitude Zeppelin observatory, and during the warm seasons at the low-altitude Gruvebadet observatory, both near Ny-Ålesund village. Although the data show matching seasonal oscillations, the concentrations are generally higher at Gruvebadet, suggesting an impact of local emissions and demonstrating the complexity of vertical dynamics in the atmosphere. In 2018, unlike previous years, the two sites registered very similar concentrations. In Svalbard, the long-term records of black carbon measurements are complemented by short-term observations, performed during intensive experiments, cruises along the coasts, and vertical profile measurements. Such measurements reveal a large spatial variability of local black carbon sources and the impact of ship emissions. Vertical profiles clearly show the presence of black carbon layers at high altitude (above 1 km) during spring, likely due to long-range transport of pollution from lower latitudes during conditions of Arctic haze.

RECOMMENDATIONS

- Improve comparability among different techniques currently used to measure black carbon.
- Develop a correction algorithm for optical measurements specifically designed for the Arctic environment.
- Increase spatial and temporal coverage of black carbon vertical profile measurements.
- Promote measurement of carbon flux in dry and wet deposition (dry=as particles; wet=with precipitation).
- Favour integration of atmospheric and cryospheric measurements by establishing joint discussion platforms and integrated databases.
- Improve understanding of black carbon's properties as cloud condensation nuclei (cloud seeds).

Hornsund 2006 cruise.
(Photo: Anna Rozwadowska)

Measuring black carbon vertical profiles.
(Photo: David Cappelletti)

CHAPTER 9

Aerial view of Ny-Ålesund, as seen from a drone. (Photo: Rune Storvold)

Probing the vertical structure of the lower atmosphere over Svalbard (ProVeSAS)

Click here for full chapter

HIGHLIGHTS

- Interest in using tethered balloons and drones to study the vertical structure of the lower atmosphere over Svalbard is growing.
- Most studies of Svalbard's lower atmosphere are done in Ny-Ålesund or during cruises.
- Most measurements are done in spring/summer.
- About 60 papers on this topic have been published.

AUTHORS

M Mazzola (ISP-CNR)
AP Viola (ISP-CNR)
DM Cappelletti (UP)
C Ritter (AWI)
R Storvold (NORCE)

Understanding the causes and mechanisms of climate change requires an enormous number of continuous and accurate measurements. To measure atmospheric parameters along the vertical profile, one must either fly the instrumentation or infer such information at a distance from the emissions or reflections of components in the atmosphere (remote sensing). Techniques that use one of these approaches have been developed since the 1940s. However, both approaches suffer from limitations on the accuracy of the measurements and the amount of information that can be obtained. Recent technological development has enabled production of small, low-cost sensors with capabilities similar to those used in the laboratory. These sensors can be installed on balloons or small unmanned aerial

vehicles, allowing direct measurements in the lower atmosphere. With more accurate information on the status of the atmosphere, researchers can refine their mathematical data interpretation techniques.

The research station in Ny-Ålesund is already well equipped for a number of standard vertical profile measurements. Fewer activities are performed at other stations in Svalbard. This is clear from the studies we cited in our contribution: about 60 papers. Half were based on remote sensing, 22 on balloons (tethered or free), 5 on dropsondes and 5 on drones. Although we do not claim that this list is exhaustive, it may represent the status of activities in Svalbard. The limited air traffic in the Arctic means that carrying out measurements with balloons and small radio-controlled airplanes is easier than elsewhere.

RECOMMENDATIONS

- Studies of the lower atmosphere should be encouraged by simplifying the process of obtaining flight permits, and by creating specific infrastructure, such as hangars for the recovery of vehicles, runways dedicated to take-off/landing of drones, sites dedicated to the launch and recovery of balloons, and compressors for helium recovery.
- Activities during the dark season should be increased, despite the logistical challenges, as most campaigns are currently performed during spring and summer.
- We recommend improved coordination between the different groups involved in this type of research. Data visibility and availability should also be increased.

Tethered balloon and LIDAR beam during the January 2019 campaign in Ny-Ålesund. (Photo: Gregory Tran)

CHAPTER 10

Permafrost drill site on pingo in Adventdalen.
(Photo: Ulrich Neumann, Kolibri Geo Services)

Permafrost temperatures and active layer thickness in Svalbard during 2017/2018 (PermaSval)

Click here for full chapter

HIGHLIGHTS

During the 2017-2018 hydrological year mean annual ground temperatures observed in Svalbard ranged from -1.2°C to -5.1°C. The duration of active layer freeze-back varied from 2 to 151 days. Active layer thickness at the observation sites varied in summer 2018 between 64 cm and 463 cm.

AUTHORS

HH Christiansen (UNIS)
GL Gilbert (UNIS, NGI)
N Demidov (AARI)
M Guglielmin (Insubria Univ)
K Isaksen (MET Norway)
M Osuch (IGF PAS)
J Boike (AWI)

Permafrost temperature presented in this report, including the first full year of ground temperature data from the Hornsund area, indicate that the north-south gradient present in air temperatures is also present in ground temperatures in Svalbard. Permafrost temperatures are warmest in Hornsund in the south, intermediate in Barentsburg and Kapp Linne in the central part, and lowest around Ny-Ålesund in the northern part and in the centrally located Adventdalen area. The ground is warmest near the coasts (e.g. Kapp Linne and Hornsund) and in areas with thicker snow cover during winter (e.g. Endalen and Bayelva). Mean annual ground temperatures measured at the depth of zero annual amplitude or lowermost sensor

varied from -1.2°C (Hornsund, 12 m depth) to -5.1°C (Breinosa and Old Auroral Station, 10 m depth). During the 2017-2018 hydrological year, the duration of active layer freeze-back in Svalbard varied from 2 days at Breinosa to 151 days at Endalen. Active layer thickness ranged in summer 2018 between 64 cm (Breinosa) and 463 cm (Hornsund).

RECOMMENDATIONS

- Maintain existing permafrost and active layer monitoring networks and instrumentation.
- Expand the permafrost monitoring network and make the data on this essential climate variable available online.
- Assess the response of permafrost landscapes to changes in climate by obtaining more knowledge about the ground ice content.
- Investigate avenues to increase the time-scale of permafrost observations.
- Continue to develop remote sensing tools for monitoring permafrost conditions and landscape response.
- Improve interdisciplinary networking on permafrost-related issues.

Ground thermal snapshot (minimum, mean, and maximum temperatures) measured in the upper 10–30 m of the permafrost observation boreholes in Svalbard during the 2017-2018 hydrological year.

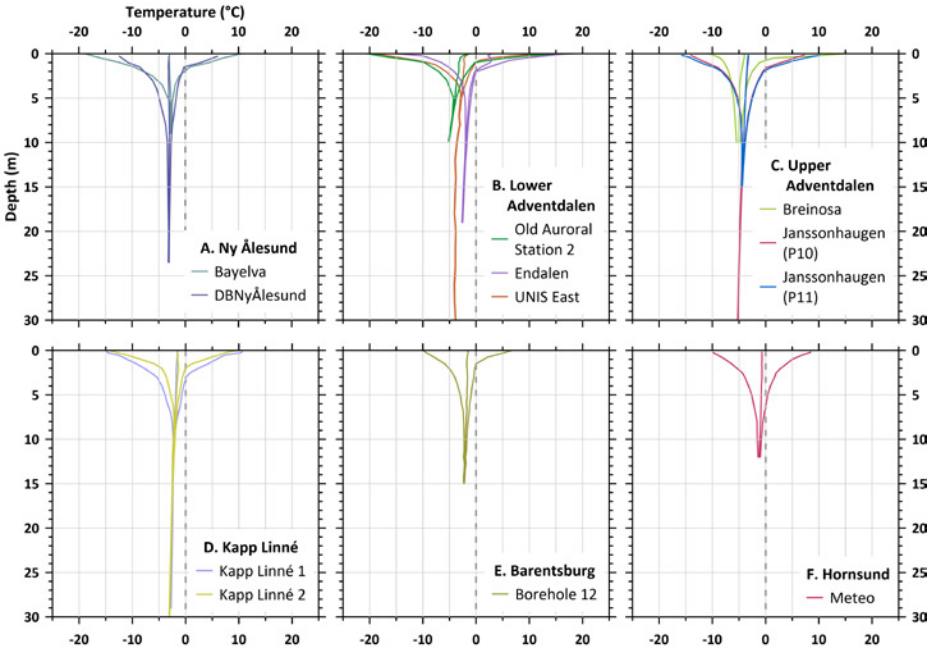

CHAPTER 11

Operations at the stern of RV *Alliance* during mooring deployment west of Svalbard. (Photo: Fixed GoPro camera)

Spitsbergen Oceanic and Atmospheric interactions (SOA)

Click here for full chapter

HIGHLIGHTS

Observations gathered in the deep sea west of Svalbard reveal oscillations in temperature and salinity during winter months. Longer time-series collected in the Arctic Ocean are essential to identify and analyse anomalies and events that can affect global circulation and climate.

AUTHORS

M Bensi (OGS)
V Kovačević (OGS)
L Langone (ISP-CNR)
S Miserocchi (ISP-CNR)
M Demarte (IIM)
R Ivaldi (IIM)

Off the Svalbard archipelago, in the eastern Fram Strait, at 1000 m depth along the continental slope, we observed temperature and salinity fluctuations that were more prominent between October and April. Data were acquired employing an oceanographic mooring deployed at 76°N 013°E from June 2014. Since then, the most noteworthy episode lasted more than 15 days in December 2016/January 2017 when the temperature rose from the typical value of -0.9°C to over 2°C. At the same time, bottom currents increased significantly, to 85 cm/s. Normally, these bottom currents flow around 10-15 cm/s. This region is characterized by the passage of Atlantic Water flowing northward in the upper layer, bringing relatively warm water to the Arctic Ocean. Below 800 m depth, the Norwegian Deep Sea Water, colder and less salty, also flows northward.

Thanks to the scientific community that carries out measurements both in the ocean and in the atmosphere, we know that the Arctic is progressively warming up; we see this in the gradual melting of sea ice and ice on land. However, it is not clear how much of this warming is caused by human activities and what consequence it will have. In order to record and to study environmental changes and anomalies, we need time series. To provide robust climate data, such series must span decades. Achieving this goal requires great effort in terms of international collaborations, both economic and scientific.

RECOMMENDATIONS

Many processes must be taken into consideration when studying oceanographic time series from the area west of Svalbard. These include atmospheric phenomena such as wind, evaporation and air pressure oscillations at the sea surface, but also the ocean's internal oscillations induced by tides and formation of dense water plumes. Possible implications for biogeochemical aspects, e.g., the carbon cycle and the marine food web, also need further attention. Lastly, it will be important to probe how global ocean circulation might be affected by changes in oceanic heat content associated with the variability in the properties and volume of inflowing Atlantic water and/or with vertical mixing processes that extend into the deep ocean. How much these processes will affect global circulation is still an open question.

Buoys of the oceanographic mooring before deployment. The researchers will not see them again for an entire year. (Photo: Manuel Bensi)

Drone flying over sea ice during the High North 2018 cruise. (Photo: Manuel Bensi)

CHAPTER 12

Planktonic crab larvae.
(Photo: Martin Edwards)

The Continuous Plankton Recorder Survey – Monitoring plankton in the Nordic Sea (CPR Survey)

Click here for full chapter

HIGHLIGHTS

The Pacific diatom *Neodenticula seminae* (an indicator of trans-Arctic migration) was recorded off Svalbard in 2016, the easternmost observation of this diatom in the Nordic Seas.

AUTHORS

M Edwards (CPR-Survey)
P Helaouet (CPR-Survey)
C Ostle (CPR-Survey)
D Johns (CPR-Survey)
M Wootton (CPR-Survey)
E Strand (IMR)
E Bagoien (IMR)

The Continuous Plankton Recorder (CPR) survey monitors plankton in the waters around Svalbard and south to northern Norway. Within this region of the Nordic Seas, the CPR survey adds to and complements other monitoring methods by providing a broader spatial and temporal perspective. Most other surveys are coastal or are sporadically sampled through time. The CPR survey also adds value by providing data covering several decades at the Atlantic basin scale that can help disentangle and interpret changes observed in the Nordic Seas and help predict changes over coming decades. For example, regions that currently support Arctic ecosystems will instead support sub-Arctic systems within the next 10 to 20 years (if not sooner). The biological signals of change we see further south in Atlantic sub-polar systems now can be used to detect the early warning signs of change in the Arctic.

To develop the observation system further, the CPR survey currently works closely with Norwegian scientists to coordinate its sampling on board "ships of opportunity". These are often cargo vessels that regularly ply the same route. They are outfitted with instruments that automatically and routinely collect a range of data on oceanographic parameters. The Norwegian FerryBox system is one such ship of opportunity.

RECOMMENDATIONS

The CPR survey, by coordinating its sampling programme with the FerryBox system, can obtain valuable complementary information such as pCO_2 in the waters where the sampling was done.

It is envisioned that in the near future the CPR survey will form part of a more integrated observation system within this region and enhance its monitoring with an additional suite of biogeochemical and molecular sensors. It will also endeavour to explore possible synergies between other oceanographic monitoring and the biological monitoring conducted by the CPR survey. Although commercial shipping in the Arctic is sparse, CPR monitoring could be expanded by using other ships of opportunity that operate in this region, such as tourist vessels.

The distribution of the Pacific diatom species *N. seminae* in the Northern Hemisphere from CPR records in the North Pacific and records from the North Atlantic from 1998. The species was recorded off Svalbard in 2016, its most easterly observation in the North Atlantic.

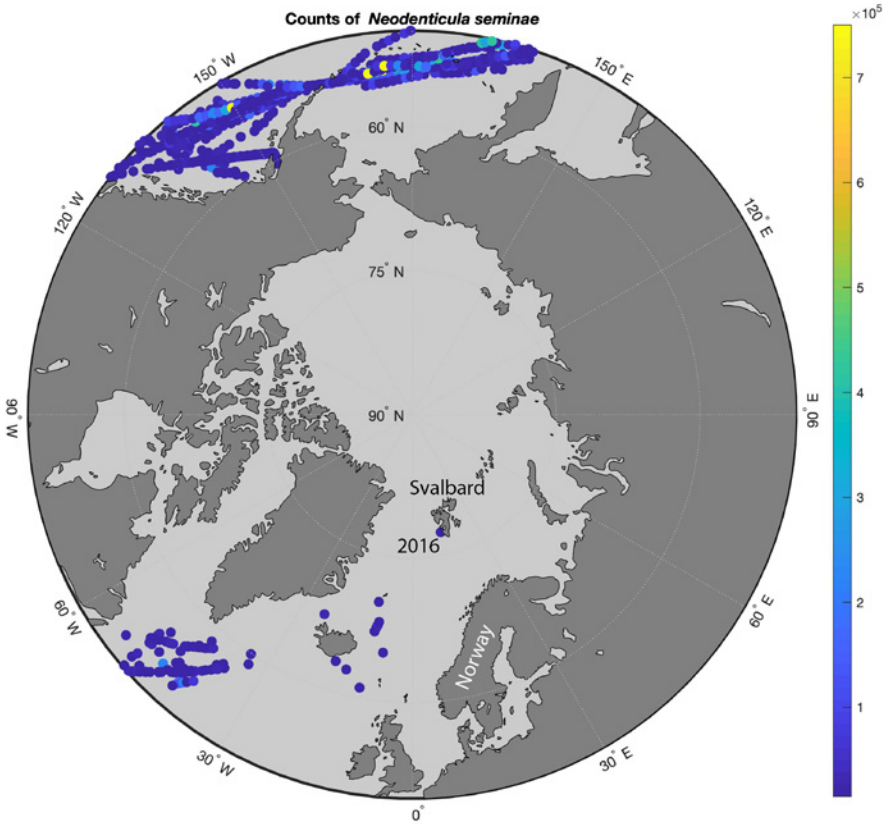

CHAPTER 13

Svalbard is the only place in the world where we can explore the daytime Northern lights (cusp aurora) with sounding rockets. ICI-5, equipped with two 4DSpace modules, each carrying six daughter payloads as big as ice hockey pucks, is a first attempt at 3D measurement of ionospheric turbulence. (Illustration: Trond Abrahamsen, Andøya Space Center)

Grand Challenge Initiative – Cusp: observational network for solar wind-driven dynamics of the top atmosphere (GCI-Cusp)

Click here for full chapter

HIGHLIGHTS

In winter 2018/19, five Grand Challenge Initiative – Cusp rockets were successfully launched through energetic daytime auroras over Svalbard. Unique data sets to explore solar wind forcing of particle acceleration, turbulence, atmosphere heating and outgassing were collected.

AUTHORS

J Moen (UiO, UNIS)
A Spicher (UiO)
T Takahashi (UiO, NIPR)
DE Rowland (NASA)
C Kletzing (U IOWA)
J LaBelle (DC)
M Larsen (CU)
M Conde (UAF)
Y Saito (JAXA)
K Blix (ASC)

The Grand Challenge Initiative – Cusp (GCI-Cusp) is a strategic research coordination between Norway, Japan, and the US. Eight sounding rockets were successfully launched during winter 2018/19, and three more are scheduled in December 2019. Polar cusps are two funnel-shaped regions in the Earth's magnetic field, where solar wind particles can directly enter the polar atmosphere. Collisions between these particles and the atmosphere produce the Northern lights. Cusp aurora is the scientific term for the Northern lights in daytime. Svalbard is a world-class laboratory for studying the cusp.

The polar atmosphere is strongly influenced by the solar wind. The GCI-Cusp questions are related to the physics of how the solar

wind couples the top of the atmosphere at the poles and the effects it has: how auroral particles are accelerated by waves along magnetic field lines in the cusp, and how these energy inputs lead to heating, upwelling and outgassing of Earth's atmospheric gasses into space. The Norwegian rocket, ICI-5, launched 26 November 2019, equipped with 12 daughter payloads for 3D imaging of turbulent vortices within the Northern lights. This turbulence sometimes causes severe disturbances/black-out of radio signals. Unfortunately, due to roll rate anomaly the daughters did not spin out. Efforts will be made to redo this novel experiment.

The initial processing of the GCI-Cusp data is ongoing and looks very promising. Some data suggest a new method of remotely detecting the cusp using VLF waves. As a world first for sounding rocket experiments, data collected within the GCI-Cusp programme will be made openly and easily available to all users through the SIOS data management system.

RECOMMENDATIONS

For the future, the SIOS partners should invest in a high-resolution 4D (time and space) all-sky imaging system to enhance the cusp-observational network. Key parameters derived from routine ground optical and radar instruments should be given status as SIOS core data.

Strategic efforts should be made to become a central partner in the GCI-Mesosphere Lower Thermosphere rocket initiative. Together, GCI-Cusp and GCI-M/LT will contribute to optimizing an ESS programme that monitors the vertical coupling of atmospheric layers from sea surface to space and provides knowledge crucial to weather and climate prediction models.

ICI-5 rocket lift-off from SVALRAK Ny-Ålesund 07:43 UT on 26 November 2019. The near-vertical green trace is the LIDAR beam. (Photo: Helge Markussen)

Sentinel satellite-based mapping of plant productivity in relation to snow duration and time of green-up (GROWTH)

Stein Rune Karlsen[1], Laura Stendardi,[2], Lennart Nilsen[3], Eirik Malnes[1], Lars Eklundh[4], Tommaso Julitta[5], Andreas Burkart[5], Hans Tømmervik[6]

1 NORCE Norwegian Research Centre AS, P.O.Box 6434 Tromsø, Norway
2 Faculty of Science and Technology, Free University of Bozen-Bolzano, 39100 Bolzano, Italy
3 The Arctic University of Norway, NO-9037 Tromsø, Norway
4 Department of Physical Geography and Ecosystem Science, Lund University, Sölvegatan 12, SE-223 62 Lund, Sweden
5 JB Hyperspectral Devices, Am Botanischen Garten 33, 40225 Düsseldorf, Germany.
6 Norwegian Institute for Nature Research (NINA), FRAM – High North Research Centre for Climate and the Environment, PO Box 6606, Langnes, NO-9296 Tromsø, Norway

Corresponding author: Stein Rune Karlsen,

Keywords: Sentinel-1, Sentinel-2, FLOX, snow, phenology, plant productivity

1. Introduction

Plant productivity (g biomass / m^{2}*y) is fundamental to Arctic tundra ecosystem's functions and services. Annual plant production is vital for wildlife, it plays a key role in the global carbon budget, nutrient cycling, surface energy budget and large-scale climate. However, measuring plant productivity is a challenging task. Carrying out long-term field-based studies of plant productivity is labour intensive, and only few time-series exist for the Arctic. On Svalbard, the only long time-series of field-based measurements is from Semmeldalen on Nordenskiöld Land peninsula (van der Wal and Stien 2014). Satellite image-aided analysis of plant productivity provides a method for determining spatially complete coverage that can be used to interpolate traditional ground-based estimations of biomass and production. Several remotely sensed Normalised Difference Vegetation Index (NDVI) based studies covering large areas of northern high latitudes indicate increased vegetation greenness during the last few decades (Myneni et al. 1997; Epstein et al. 2013; Xu et al. 2013; Park et al. 2016; Vickers et al. 2016), but with mostly less increase or even regionally a decreasing trend since approximate the millennium shift (Bhatt et al. 2013). However, only a few of these large-scale studies (Epstein et al. 2012, Raynolds et al. 2012) have used extensive plant biomass data for validation, and then only data from one season, not catching the annual variation. Additionally, Guay et al. (2014), who used mean NDVI for June-August to investigate trends from different satellite datasets (e.g. MODIS, Spot Vegetation, and different versions of the GIMMS dataset), showed that temporal trends were highly dependent on the dataset used. Each year the NOAA Arctic Report Card is presented, showing the research on Arctic tundra vegetation dynamics from the previous year (Epstein et al. 2018). But most of the observations therein are linked to satellites with coarse spatial resolution. However, in Svalbard, the field data from Semmeldalen (van der Wal and Stien 2014) were linked to a time-series of clear-sky MODIS satellite data for the 2000-2014 period (Karlsen et al. 2018) and referred to in the Arctic Report Card (Epstein et al. 2018). This regional study (covering Nordenskiöld land) also utilizes phenological maps showing onset of growth (Karlsen et al. 2014), and showed that the best fit between field data and MODIS data was with time-integrated NDVI from onset to peak of the growing season. This study revealed large differences between years in plant production, a strong link to summer temperatures, and a possible link to sea-ice distribution (Macias-Fauria et al. 2017). However, only relative differences in the spatiotemporal pattern of plant production were found, partly due to the coarse resolution of MODIS data (250x250m^{2}). Hence, there is a need to develop methodologies to map actual plant productivity in terms of grams of biomass per square meter per year (g / m^{2}*y). With the new generation of satellite data, in particular Sentinel-1 and Sentinel-2 data, we have frequent coverage combined with high spatial and spectral resolution, allowing us to work at the plant community level. In addition, automatic field and near-field sensors and cameras for ecological monitoring have become cheaper and with higher capacity and more capabilities in recent years.

In this State of Environmental Science in Svalbard (SESS) report, we show different datasets, Svalbard Integrated Arctic Earth Observing System (SIOS) based and others, in the Adventdalen valley area, close to Longyearbyen, which can be linked and utilized in plant productivity measurements. Further, Svalbard is undergoing dramatic climatic changes, with periods of heavy rain instead of steady snow cover in autumn, and mild periods in mid-winter creating ice or even snow free spots have occurred several times in the last years (Bjerke et al. 2017). How these extreme climatic events and changes in snow duration, snow properties, and time-of-green-up affect the plant growth is largely unknown at the plant community and ecosystems level, and there is a need to provide more accurate proxies of plant productivity at large spatial scales. Clearly, there is a valuable opportunity for developing methodologies that combine field-based measurements and near ground sensors of plant productivity with Sentinel data in order to validate satellite data and provide more accurate estimates of plant productivity at different spatial scales.

2. Overview of existing data

Several SIOS-based and other datasets located in Adventdalen, close to Longyearbyen, can be combined in measuring plant productivity and to detect climatic drivers. The datasets are both satellite data (Sentinel) and from field-based measurements/near ground sensors.

2.1 Satellite data

2.1.1 Time-series of Sentinel-1 data

The instrument #42 (Snow parameter retrieval using remote sensing satellites) belongs to the cryosphere module of the project SIOS-InfraNor[1]. We have pre-processed Sentinel-1 Ground Range Detected (GRD) data from the interferometric wide swath mode (10 m pixel spacing) HH and HV polarization over Nordenskjold land. The time series started in 2015 with a few scenes, and gradually increased to regular 2 scenes per 6 day repeat cycles in 2018. Figure 1 shows a composition of three backscatter Sentinel-1 images in the HV channel, corresponding to different periods of the year 2018 (March, May and July). Sentinel-1 also provides Extended Wide Swath data (40 m pixel spacing) but this product will be considered later. C-band SAR (5.6 GHz) is only sensitive to wet snow. Wet snow maps can thus be provided on a regular basis (2.3 scenes per week) independent of cloud conditions. This is a big advantage in contrast to optical data like Sentinel-2 which require cloud-free conditions. In addition to wet snow, C-band SAR data can also provide indications of thawing/freezing conditions in the active permafrost layer and on the soil

1 https://sios-svalbard.org/InfraNor

moisture.

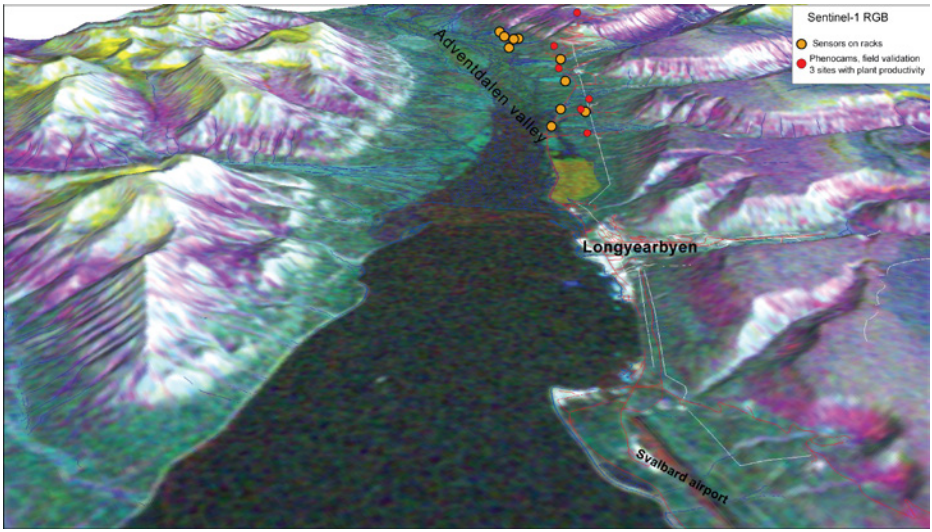

Figure 1: RGB composition of three Sentinel-1 HV images from Adventdalen: 1 March 2018 (red), 29 July 2018 (green), 30 May 2018 (blue). The colours identify patterns in the surfaces, deriving from the different backscattering mechanisms. The dark blues and blues across the figure represent low-changing features such as the sea or the airport, the green colours the vegetated areas, the purple represents bare soil or rocks, while yellow features surfaces, which are affected by major variations, i.e. wet snow in July.

2.1.2 Time-series of clear-sky Sentinel-2 data

Within the SIOS-InfraNor instruments # 52 (Time-series of medium resolution satellite data) time-series of clear-sky Sentinel-2 (S2) are processed. Due to the northern location S2 data are obtained almost daily, and with Sentinel-2B data in addition from July 2017, often twice a day. The data covering Adventdalen are obtained between approximate 11:30 and 13:30 UTC. Frequent fog and clouds, snow and ice, a short growing season, and often weak response from the vegetation characterize Svalbard, and make cloud masking on the archipelago a challenging task. The cloud detection provided with the bottom-of-atmosphere Sentinel-2 product (L2A) often fails and is of limited value. In particular, detection of shadows from cloud, clouds over sparsely vegetated areas, thin clouds, and shadows from cirrus often fails. In processing clear-sky time-series we combined several methods, included visual quality control. For most of the images used, we manually masked out the cloudy parts by drawing polygons around them, using several different cloud-detection algorithms to aid this work, depending of the cloud type and time of season. This is time-consuming work, but it is only done once and ensures that most of the noise in the datasets is removed and that most (>80%) of the noise-free data are retained. All Nordenskiöld Land will be

processed for the years 2016-2018 for the period late April to late September. For this late April to late September period for the Adventdalen valley floor, the results show 12-15 cloud-free days in 2016, 16-22 days in 2017, and 15-21 days in 2018. However, the days were not evenly disturbed throughout the season, and fewer cloud-free days were obtained in the surrounding mountains. Next the cloud-free pixels were interpolated to daily data. For the indices NDVI and Normalised Difference Snow Index (NDSI) a Kernel Ridge Regression machine learning method was used for interpolation, combined with Savitzky-Golay filtering. In most cases the processing of S2 data to bottom-of-atmosphere (L2A) worked, however, in some images errors were found in terrain correction or in atmospheric correction. The reason for this needs further investigations. Due to the limited cloud-free days available, we have so far only used top-of-atmospheric data (L1C), since removing the L2A products with errors will further decrease the number of days with cloud-free data. From this clear-sky time-series of daily NDVI/NDSI data we extracted the last day of snow cover, onset of growth (Figure 2) and time-integrated NDVI from onset to peak of the season (OP NDVI) (Figure 3). The OP NDVI data indicate annual plant production but needs further validation with the field data and near-ground sensors/camera data to obtain gram living green biomass per square meter per year.

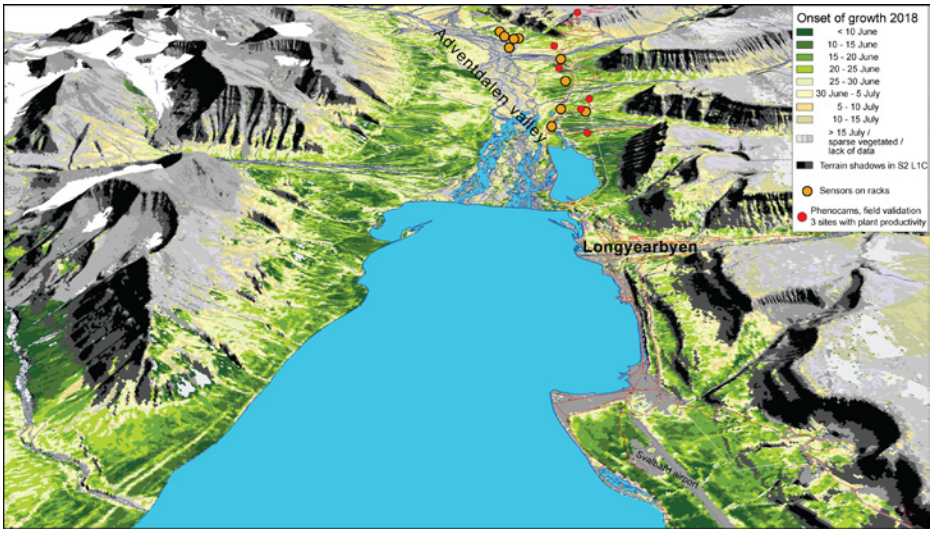

Figure 2: Onset of the growing season for the year 2018. Extracted from time-series of clear-sky Sentinel-2 NDVI data.

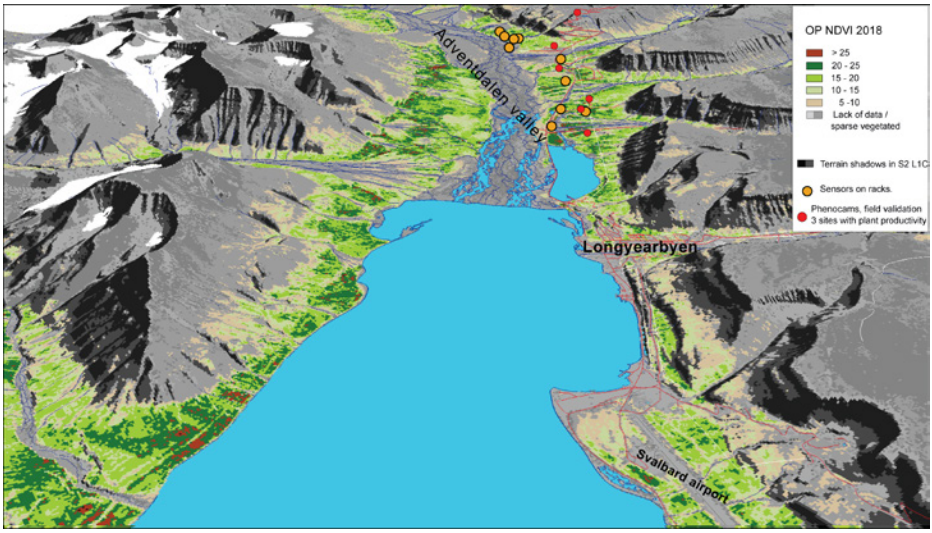

Figure 3: Time-integrated NDVI from onset of growth to peak of growth (OP NDVI) for the year 2018. Extracted from time-series of clear-sky Sentinel-2 NDVI data. The values indicate the annual plant productivity, but need to be validated from in-situ data.

2.2 Field data and near-ground remote sensing data

2.2.1 Imaging and non-imaging sensors on racks

SIOS-InfraNor Instrument #44 is an automatic system for monitoring vegetation and environmental seasonal changes (phenology) on Svalbard (AsMovEn). Ten racks and three landscape cameras are distributed within the lower part of Adventdalen. The racks have basic equipment comprising one Red-Green-Blue (RGB) camera, non-imaging NDVI and photochemical reflectance index (PRI)-sensors and a sensor measuring both soil moisture and temperature. In addition, some have additional equipment like a thermal infrared sensor measuring surface temperature and a sensor recording the PRI. For calibration purposes, hemispheric NDVI and PRI sensors were mounted on some racks measuring incoming radiation. Retrieval of greenness indices like GRVI (Green-Red Vegetation Index) and NDVI showed that these indices successfully recorded timing of the green-up and plant growth periods and senescence in all six plant species/groups in the period 2015-2018, and the first year is reported (Anderson et al. 2016). Figure 4 shows NDVI versus surface temperature from the end of April to the beginning of October 2017 from one of the racks. Data were recorded in the Arctic bell-heather (*Cassiope tetragona*) heath on the lower part of an alluvial fan.

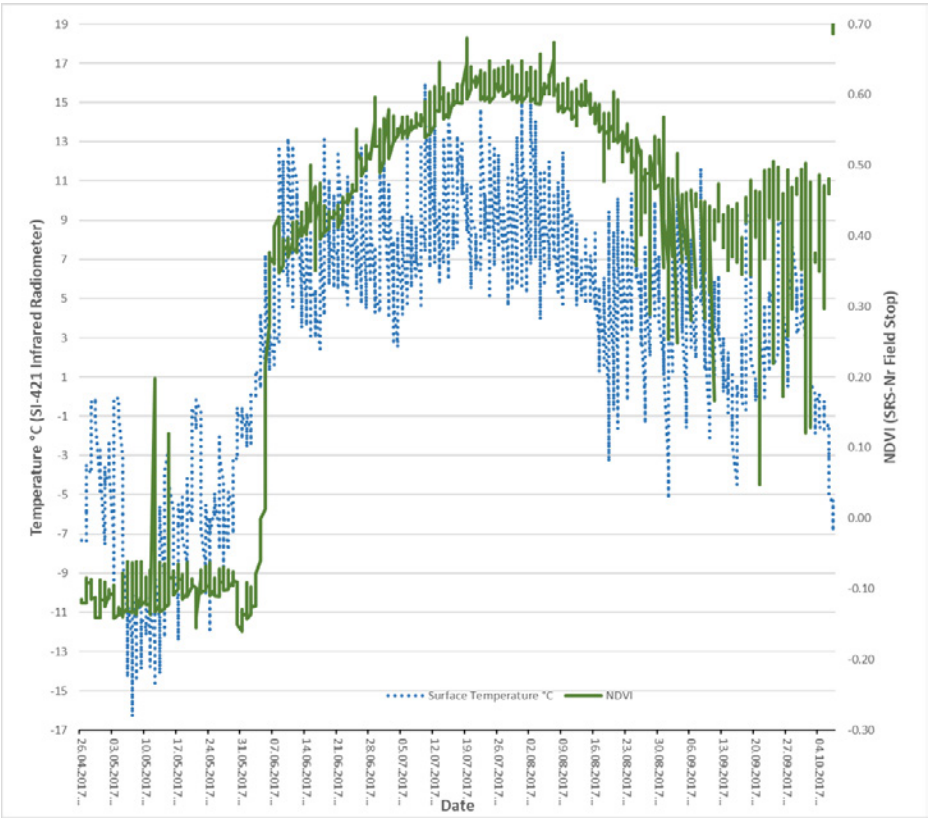

Figure 4: Example of selected data from one of the ten racks in Adventdalen. Plot showing NDVI versus surface temperature as measured by the infrared radiometer in heath vegetation (*Cassiope tetragona- Dryas octopetala* type) for the 2017 season.

2.2.2 Sun-Induced measurements by the spectroscopy system FLoX

SIOS-InfraNor instrument #49 (FLoX), is a state-of-the-art spectrometer that measure Sun-Induced Fluorescence (SIF), which is a new global proxy for GPP (Gross Primary Production). The instrument was established in Adventdalen in beginning of June 2019. Passive Sun-induced chlorophyll fluorescence (SIF) is a radiation flux emitted by chlorophyll molecules in the red (RSIF) and far red region (FRSIF) and provides a better direct proxy for photosynthesis independent of ancillary information or modelling steps which is needed by other methods (Yang et al. 2015). SIF occurs as a direct result of light absorption by the chlorophyll complex during photosynthesis (Porcar-Castell et al. 2014). SIF can be acquired from ground- and satellite-based observations (Yang et al. 2015, Frankenberg et al. 2014) like the FLoX-instrument established close to and within the foot print of the Eddy-Covariance tower (Pirk

et al. 2017) in Adventdalen (Figure 5). The eddy covariance technique (EC) is a widely used atmospheric measurement technique to measure and calculate vertical turbulent fluxes within atmospheric boundary layers and determine exchange rates of trace gases (like CO_2 and methane) and hence the net ecosystem exchange of CO_2 (NEE) over agricultural lands and natural ecosystems (Pirk et al. 2017). The SIF-measurements acquired by the FLoX-system on the ground and similar systems are good proxies for EC-measurements and will become important ground calibration sites for satellite-based systems.

Figure 5: Sun-Induced measurements by the spectroscopy system FLoX. The FLoX-system (foreground) is established near and within the footprint of the Eddy-Covariance station (in background) in Adventdalen (Photo: Lennart Nilsen).

The FLOX (JB Hyperspectral Devices, Düsseldorf, Germany) is a field spectrometer designed for continuous and long-lasting high-resolution spectral measurements of radiances and for SIF retrieval at the top-of-canopy. The spectrometer technical specifications in terms of spectral coverage, resolution and signal-to-noise (SNR) were designed based on the FLEX mission instrument specifications (Drusch et al. 2017, Coppo et al. 2017). The FLOX is equipped with two grating spectrometers: (i) QEPro (Ocean Optics, Largo FL, USA) with high spectral resolution (FWHM~0.3 nm; SSI~0.15 nm) in the fluorescence emission range

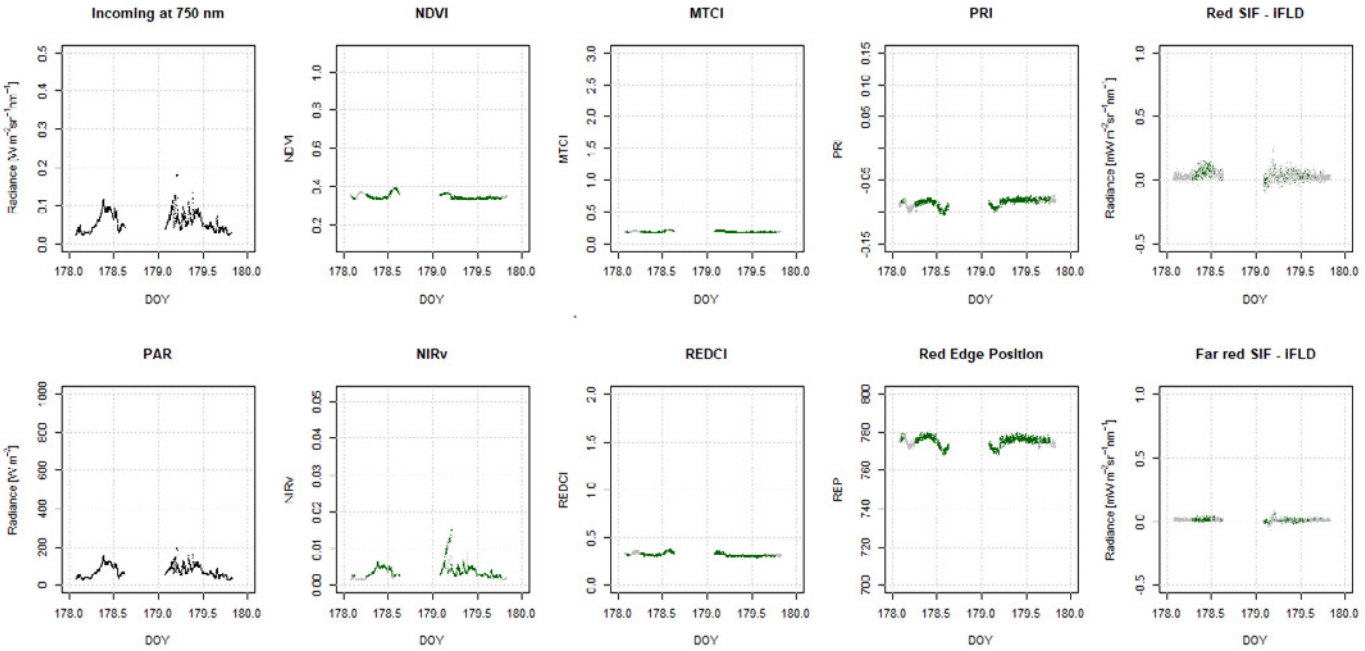

Figure 6: Measurements by the spectroscopy system FLoX during Day no: 178 and 179 in June 2019. NDVI: Normalized Difference Vegetation Index; MTCI = MERIS terrestrial chlorophyll index; PRI= Photochemical Reflectance Index; PAR: Photosynthetic Active Radiation, NIR_V: Near Infrared Reflectance of terrestrial vegetation (the product of total scene NIR reflectance NIR_T) and NDVI; REDCI: between 52S and 52N; Red Edge position: Results are reported as the wavelength of the maximum derivative of reflectance in the vegetation red edge region of the spectrum in microns from 690 nm to 740 nm; and the Sun-Induced fluorescence measurements at Red: and Far red: used the FLD-method.

650 nm–800 nm; (ii) FLAME S (Ocean Optics, Largo FL, USA) covering the full range of VIS-NIR (FWHM~1.7 nm; SSI~0.6 nm). The spectrometer's entrance is split towards two optical fibres that lead to a cosine receptor measuring the downwelling radiance and a bare fibre measuring the canopy upwelling radiance.

Preliminary results on only few data from the growing season 2019, indicate that the calibration of the data remained good during the cold Svalbard weather conditions. Since 2019 is considered to be a test season, this is encouraging. Figure 6 shows various parameters and indices that can be extracted from the FLoX-measurements like that the chlorophyll content (MTCI) was rather low but changing during the growing season. SIF was very low and could be explained by low incoming radiance and low chlorophyll content of the vegetation (Figure 6). In the limited processed data, Vegetation Indices (Vis) are not showing strong daily dynamics, since the VIs like the NDVI are not directly related to physiological changes. Usually these VIs are affected by directional effects (Bidirectional Reflectance Distribution Functions (BRDFs) and change during the day according to the sun position and sun angle. In the data processed, most of the time it was cloudy, so light was mainly diffuse light, in this case the directional effect would have less important effect on the results. The FLoX-measurements of SIF may provide better estimates of start and end of the growing season across the Arctic regions than the satellite-derived vegetation indices like Enhanced vegetation Index (EVI) and NDVI (Luus et al. 2017). They found that the EVI-based seasonality measure indicates that spring "green-up" occurred 9 days prior to SIF-based estimates, and that the SIF-based estimates agreed with aircraft and carbon-flux tower measurements of CO_2. Further analysis will be run when the dataset from the whole growing season 2019 (June-September) is retrieved.

2.2.3 Phenocams

In order to monitor plant phenophases in field, eight to nine phenocams (trail cameras, mainly type LTL Acorn) were used in the Adventdalen for the 2014-2019 period (Figure 7). The placement of the cameras was designed to be up-scaled to the resolution of Sentinel-2 data.

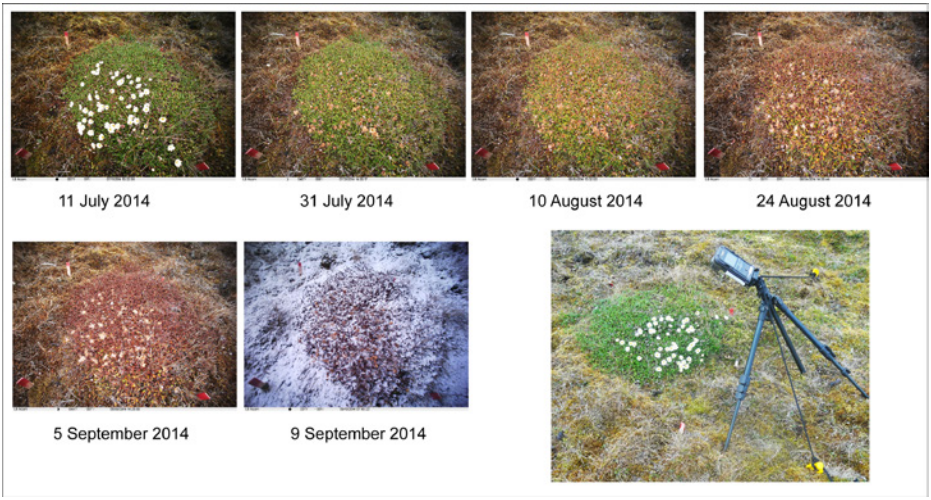

Figure 7: Eight or nine cameras in Adventdalen have been used since 2014 to document plant phenology. The example shows selected images of mountain avens (*Dryas octopetala*) for the July to September 2014 period.

2.2.4 Field measurements of plant productivity

Annual field measurements of plant productivity were collected from tundra-grass (*Dupontia fisheri*) and woodrush (*Luzula confusa*) in the Adventdalen valley area (Stendardi and Karlsen 2016). About 1600 measurements of the length of leaves were done annually for the 2015 to 2019 period. The measurements are from five sites, two on tundra-grass and three on woodrush. The sites were selected where the species was dominant and covered large enough area for up-scaling to Sentinel data. The results show annual biomass (g / $m^{2*}y$) measured on 18 x 18 cm^2 plots with 100% plant cover, up-scaled to 1 x 1 m^2 (Figure 8). The sites have some co-location with phenocams and the sensors on racks. The measurements were done by The Free University of Bolzano, Italy, in cooperation with NORCE.

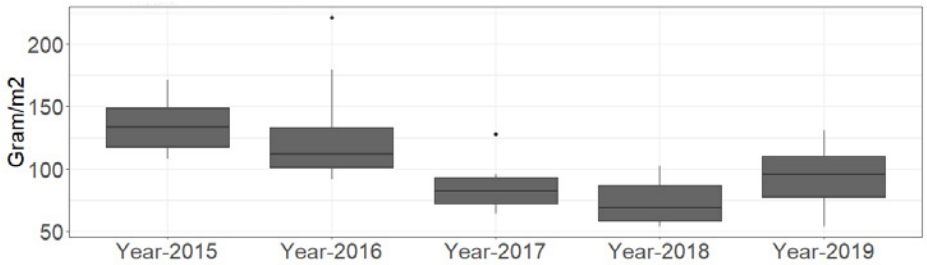

Figure 8: Example of annual plant production measured on the ground on woodrush (*Luzula confusa*) in the Adventdalen valley. Squares of 18 x 18 cm^2 with 100% plant cover is measured and up-scaled to 1 x 1 m^2.

2.2.5 Other data

A carbon flux tower with adjacent automatic flux chambers is installed in Adventdalen, belonging to Lund University (P.I. Torben Christensen, currently with Aarhus University). The measurements have been discontinued the last few years but there is potential for collecting valuable data on carbon fluxes and gas emissions from the tundra vegetation. Multispectral sensors (Skye non-imaging radiometers) exist but are not yet installed.

2.2.6 Connection to other SIOS work

The satellite data and field measurements in Adventdalen presented here have connections and synergies with other work presented in this issue. The chapter 'The Environmental Monitoring in the Kapp Linné-Grønfjorden Region' (Retelle et al. 2020) includes some related ecological work. The Adventdalen observation work has an obvious synergy to the chapter 'Climate-Ecological Observatory for Arctic Tundra' (Pedersen et al. 2020), and their study of the food web. The active-layer thickness impacts the vegetation and the Adventdalen observations presented here, have a connection to the chapter 'Permafrost thermal snapshot and active-layer thickness in Svalbard 2016-2017' (Christiansen 2020).

3. Unanswered questions

- For which species and plant communities and with what accuracy can plant productivity be measured with the available data in Adventdalen?
- What is the best ground-image resolution and which spectral features provide the best time-serial data for recording plant species phenology and productivity?
- How can we combine and analyse data through different spatial scales from field data, and near ground sensor data to Sentinel data? Can information on plant productivity from one scale explain pattern observed at larger scales?
- How do we measure bryophyte annual productivity, on the ground, with near ground sensors, and with Sentinel data?
- How do we identify and measure climatic drivers for plant productivity on the scale of plant communities?
- What is the diurnal (day and night) pattern of photosynthesis as measured by SIF?
- What is the growing season variation in measured environmental parameters, SIF and vegetation indices (VIs)? And how does the low sun elevation on Svalbard influence these parameters?

4. Recommendations for the future

- There is a need for developing methodologies that combine field-based measurements and near ground sensors on plant productivity with Sentinel data in order to validate satellite data and provide more accurate estimates of plant productivity at large spatial scales.
- There is a need to determine how the NDVI-sensor data relate to plant productivity data in order to quantify productivity as gram per square meter per year (g / m^2*y).
- There is a need for a detailed Sentinel-based vegetation map covering larger part of Svalbard in order to up-scale from the Adventdalen area.
- There is a need for a more detailed study of the effects of bryophytes upon remote sensed vegetation indices in order to analyse their contribution to both the spatial and temporal patterns of vegetation development. This should include plant productivity measurements on moss-tundra (preferably *Tomentypnum nitens - Aulacomnium turgidum* type), on sites which can be up-scaled with Sentinel data.
- There is a need to develop methods to use the FLoX-measurements, and especially SIF measurements, as calibration for different ongoing and coming satellite sensor systems. This includes studies on how FLoX-measurements can act as valuable proxies for photosynthesis and carbon fluxes at present time and in the future, and to study how the SIF measurements both from surface (FLoX) and space can be used for better detection of the start, peak and end of the growth season.

5. Data availability

Table 1: Different datasets, SIOS based and others, in the Adventdalen valley area, close to Longyearbyen, which can be linked and utilized in plant productivity measurements.

Data	Description	Provider, data access
Time-series of Sentinel-1 data	SIOS-InfraNor instrument #42 (Snow parameter retrieval using remote sensing satellites),	NORCE Technology. Will be on server by early 2020. Contact: Eirik Malnes.
Time-series of Sentinel-2 data	Time-series of cloud-free Sentinel-2 data (SIOS-InfraNor instruments # 52) covering Nordenskiöld Land for the period 2016-2018	NORCE Climate. Will be on server by early 2020. Contact: Stein Rune Karlsen.
FLoX	SIOS-InfraNor instrument #49 (FLoX). The FLoX is a spectroscopy system for the unsupervised retrieval of Sun-Induced-Fluorescence (SIF) and spectrally resolved reflectance.	Norwegian Institute for Nature Research (NINA). Contacts: Hans Tømmervik (NINA) and Lennart Nilsen (UiT)
Imaging and non-imaging sensors on rack	SIOS-InfraNor instrument #44. Establishment of an automatic system for monitoring vegetation and environmental seasonal changes on Svalbard. Ten racks and three landscape cameras are distributed within the lower part of Adventdalen.	The Arctic University of Norway. Contact: Lennart Nilsen.
Plant production measurements	Plant productivity measurements on two graminoides at 6 sites in Adventdalen. Annual measurements from 2015 to 2019.	Faculty of Science and Technology, Free University of Bozen-Bolzano, Italy. Contact: Laura Stendardi.
Phenocams	Eight to nine phenocams cameras in Adventdalen observing phenology. One photo each hour from 10am to 3pm, from early June to early September for the 2014-2019 period.	NORCE Climate. Contact: Stein Rune Karlsen.

Acknowledgements

This work was supported by the Research Council of Norway, project number 251658, Svalbard Integrated Arctic Earth Observing System - Knowledge Centre (SIOS-KC).

References

Anderson HB, Nilsen L, Tømmervik H, Karlsen SR, Nagai S, Cooper EJ (2016) Using ordinary digital cameras in place of near-Infrared sensors to derive vegetation indices for phenology studies of high Arctic vegetation. Remote Sens 8:847. https://doi.org/10.3390/rs8100847

Bhatt US, Walker DA, Raynolds MK, Bieniek PA, Epstein HE, Comisio JC, Pinzon JE, Tucker CJ, Polyakovl V (2013) Recent declines in warming and vegetation greening trends over Pan-Arctic tundra. Remote Sens 5:4229-4254. https://doi.org/10.3390/rs5094229

Bjerke JW, Treharne R, Vikhamar-Schuler D, Karlsen SR, Ravolainen V, Bokhorst S, Phoenix G., Bochenek Z, Tømmervik H (2017) Understanding the drivers of extensive plant damage in boreal and Arctic ecosystems: Insights from field surveys in the aftermath of damage. Sci Total Environ 599-600:1965–1976, https://doi.org/10.1016/j.scitotenv.2017.05.050

Christiansen HH, Gilbert GL, Demidov N, Guglielmin M, Isaksen K, Osuch M, Boike J (2020) Permafrost temperatures and active-layer thickness in Svalbard during 2017/2018. In: Van den Heuvel et al. (eds): SESS report 2019, Svalbard Integrated Arctic Earth Observing System, Longyearbyen, 236 - 249 . https://sios-svalbard.org/SESS_Issue2

Coppo P, Taiti A, Pettinato L, Francois M, Taccola M, Drusch M (2017) Fluorescence imaging spectrometer (FLORIS) for ESA FLEX mission. Remote Sens 9:649. https://doi.org/10.3390/rs9070649

Drusch M, Moreno J et al. (2017) The FLuorescence EXplorer Mission Concept-ESA's Earth Explorer 8. IEEE Trans Geosci Remote Sens 55:1273–1284. https://doi.org/10.1109/TGRS.2016.2621820

Epstein HE, Raynolds MK, Walker DA, Bhatt US, Tucker CJ and Pinzon JE (2012) Dynamics of aboveground phytomass of the circumpolar Arctic tundra during the past three decades. Environ Res Lett 7:015506. https://doi.org/10.1088/1748-9326/7/1/015506

Epstein HE, Myers-Smith I, Walker DA (2013) Recent dynamics of arctic and sub-arctic vegetation Environ Res Lett 8:8015040. https://doi.org/10.1088/1748-9326/8/1/015040

Epstein H, Bhatt U, Raynolds M, Walker D, Forbes B, Phoenix G, Bjerke J, Tømmervik H, Karlsen SR, Myneni R, Park T, Goetz S and Jia G (2018) Tundra Greenness. https://arctic.noaa.gov/Report-Card/Report-Card-2018/ArtMID/7878/ArticleID/777/

Frankenberg C, O'Dell C, Berry J, Guanter L, Joiner J, Köhler P, Pollock R, Taylor TE (2014), Prospects for chlorophyll fluorescence remote sensing from the Orbiting Carbon Observatory-2. Remote Sens Environ 147:1–12. https://doi.org/10.1016/j.rse.2014.02.007

Guay KC, Beck PSA, Berner LT, Goetz SJ (2014) Vegetation productivity patterns at high northern latitudes: a multi-sensor satellite data assessment. Global Change Biol 20:3147–3158. https://doi.org/10.1111/gcb.12647

Karlsen SR, Elvebakk A, Høgda KA, Grydeland T (2014) Spatial and temporal variability in the onset of the growing season on Svalbard, Arctic Norway—measured by MODIS-NDVI satellite data. Remote Sens 6:8088-8106. https://doi.org/10.3390/rs6098088

Karlsen SR, Anderson H, van der Wal R, Hansen B (2018) A new NDVI measure that overcomes data sparsity in cloud-covered regions predicts annual variation in ground-based estimates of high arctic plant productivity. Environ Res Lett 13:025011. https://doi.org/10.1088/1748-9326/aa9f75

Luus KA, Commane R et al. (2017) Tundra photosynthesis captured by satellite-observed solar-induced chlorophyll fluorescence, Geophys Res Lett 44:1564–1573. https://doi.org/10.1002/2016GL070842

Macias-Fauria M, Karlsen SR, Forbes BC (2017) Disentangling the coupling between sea ice and tundra productivity. Sci Rep. 7:8586. https://doi.org/10.1038/s41598-017-06218-8

Myneni RB, Keeling CD, Tucker CJ, Asrar G, Nemani RR (1997) Increased plant growth in the northern high latitudes from 1981 to 1991. Nature 386:698–702. https://doi.org/10.1038/386698a0

Park T, Ganguly S, Tømmervik H, Euskirchen ES, Høgda KA, Karlsen SR, Brovkin V, Nemani RR, Myneni RB (2016) Changes in growing season duration and productivity of northern vegetation inferred from long-term remote sensing data. Environ Res Lett.11:084001. https://doi.org/10.1088/1748-9326/11/8/084001

Pedersen ÅØ, Stien J, Albon S, Fuglei E, Isaksen K, Liston G, Jepsen JU, Madsen J, Ravolainen VT, Reinking AK, Soininen EM, Stien A, van der Wal R, Yoccoz NG, Ims RA (2020) Climate-Ecological Observatory for Arctic Tundra. In: Van den Heuvel et al. (eds): SESS report 2019, Svalbard Integrated Arctic Earth Observing System, Longyearbyen, 58 - 83 . https://sios-svalbard.org/SESS_Issue2

Pirk N, Sievers J, Mertes J, Parmentier FJW, Mastepanov M, Christensen, TR (2017) Spatial variability of CO2 uptake in polygonal tundra: assessing low-frequency disturbances in eddy covariance flux estimates. Biogeosciences 14:3157–3169. https://doi.org/10.5194/bg-14-3157-2017

Porcar-Castell A, Tyystjärvi E, Atherton J, van der Tol C, Flexas J, Pfündel EE, Moreno J, Frankenberg C, Berry JA (2014) Linking chlorophyll a fluorescence to photosynthesis for remote sensing applications: Mechanisms and challenges. J Exp Bot 65:4065–4095. https://doi.org/10.1093/jxb/eru191

Raynolds MK, Walker DA, Epstein HE, Pinzon JE, Tucker CJ (2012) A new estimate of tundra-biome phytomass from trans-Arctic field data and AVHRR NDVI. Rem Sens Letters. 3:403–411. https://doi.org/10.1080/01431161.2011.609188

Retelle M, Christiansen H, Hodson A, Nikulina A, Osuch M, Poleshuk K, Romashova K, Roof S, Rouyet L, Strand SM, Vasilevich I, Wawrzyniak T (2020) Environmental Monitoring in the Kapp Linné-Grønfjorden Region. In: Van den Heuvel et al. (eds): SESS report 2019, Svalbard Integrated Arctic Earth Observing System, Longyearbyen, 84 - 107 . https://sios-svalbard.org/SESS_Issue2

Stendardi L, Karlsen SR (2016) Monitoring of plant productivity in relation to climate on Svalbard. Norut Report 07/2016. 14 pp.

Van der Wal R, Stien A (2014) High-arctic plants like it hot: a long-term investigation of between-year variability in plant biomass. Ecology 95:3414–27. https://doi.org/10.1890/14-0533.1

Vickers H, Høgda KA, Solbø S, Karlsen SR, Tømmervik H, Aanes R, Hansen BB (2016) Changes in greening in the high Arctic: insights from a 30 year AVHRR max NDVI dataset for Svalbard. Environ Res Lett.11:105004. https://doi.org/10.1088/1748-9326/11/10/105004

Xu L, Myneni RB et al. (2013) Temperature and vegetation seasonality diminishment over northern lands. Nat Clim Chang 3:581–586. https://doi.org/10.1038/NCLIMATE1836

Yang X, Tang J, Mustard J, Lee JE, Rossini M, Joiner J, Munger, JW, Kornfeld A, Richardson AD (2015) Solar-induced chlorophyll fluorescence that correlates with canopy photosynthesis on diurnal and seasonal scales in a temperate deciduous forest, Geophys Res Lett 42:2977–2987, https://doi.org/10.1002/2015GL063201

Climate-Ecological Observatory for Arctic Tundra (COAT)

Åshild Ønvik Pedersen[1], Jennifer Stien[2], Steve Albon[3], Eva Fuglei[1], Ketil Isaksen[4], Glen Liston[5], Jane U. Jepsen[2], Jesper Madsen[6], Virve T. Ravolainen[1], Adele K. Reinking[5], Eeva M. Soininen[7], Audun Stien[2], René van der Wal[8], Nigel G. Yoccoz[7] and Rolf A. Ims[7]

1 Norwegian Polar Institute, Fram Centre, NO-9296 Tromsø, Norway
2 Norwegian Institute for Nature Research, Fram Centre, NO-9296 Tromsø, Norway
3 The James Hutton Institute, Craigiebuckler Aberdeen AB 15 8 QH, Scotland
4 Norwegian Meteorological Institute, 0313 Oslo, Norway
5 Cooperative Institute for Research in the Atmosphere, Colorado State University, 80523 Fort Collins, Colorado, USA
6 Aarhus University, Department of Bioscience, DK-8410 Rønde, Denmark
7 UiT – Arctic University of Norway, Department of Arctic and Marine Biology, NO-9037, Tromsø, Norway
8 Swedish University of Agricultural Sciences (SLU), Dept. of Ecology, Ulls väg 16, 75651 Uppsala, Sweden

Corresponding author: Åshild Ønvik Pedersen, aashild.pedersen@npolar.no

Keywords: Adaptive monitoring, climate change, ecological monitoring, ecosystem based monitoring, food-web, long-term, management, terrestrial

1. Introduction

1.1 Background

Arctic tundra is one of the Earth's largest terrestrial biomes comprising the terrestrial ecosystems north of the continuous boreal forest. A predicted average temperature increase, of up to 10 °C by the turn of the century (Hansen et al. 2014; Hanssen-Bauer et al. 2019) will result in large and unforeseeable impacts on these ecosystems that will have pervasive implications locally and globally (CAFF 2013; Ims and Ehrich 2013; Meltofte et al. 2013). The Climate Ecological Observatory for Arctic Tundra (COAT) is a response to the urgent international calls for establishment of scientifically robust observation systems that will enable long-term, real-time detection, documentation, understanding and predictions of climate impacts on Arctic tundra ecosystems. COAT aims to be a fully ecosystem-based, long-term, adaptive monitoring programme, based on a food-web approach (Ims et al. 2013; www.coat.no). It is implemented from a peer reviewed Science Plan (Ims et al. 2013) based on a comprehensive review of the scientific literature on the functioning, structure and known drivers of terrestrial Arctic ecosystems. COAT focuses on two Norwegian Arctic regions, the Low Arctic Varanger peninsula and high Arctic Svalbard (Figure 1) that provide pertinent contrasts in Arctic tundra system complexity and climate and management regimes. COAT Svalbard is an essential component of the Svalbard Integrated Arctic Earth Observing System (SIOS) and serves to optimize and integrate the ecosystem-based terrestrial monitoring. This chapter will summarize the COAT Svalbard programme, with the goal of opening an avenue to increased integration of data within the SIOS community.

1.2 Climate impact path models

Understanding the functioning and structure of food webs is a key for predicting the response of tundra ecosystems to drivers of change (Post et al. 2009). The Svalbard tundra food web is relatively simple (Box 1), although the interactions between trophic levels can result in complex dynamics (Ims et al. 2013). COAT Svalbard contains six monitoring modules (five food web modules and a crosscutting climate module) (Figure 2). Each of the five food web modules (Box 2) is based on a *conceptual model* that outlines a set of *monitoring targets* in terms of climate sensitive key species or functional species groups in the tundra food web and *a priori* hypotheses for their key process relations. Climate and environmental management interventions are included as the main drivers of these relations. The purpose of the conceptual food web is to form a basic framework for data-driven causal analyses and predictions of climatic effects on the monitoring targets, quantify relationships between the monitoring targets and infer how management could be effective in mitigating predicted unwanted effects. Indeed, as COAT aims to be management relevant,

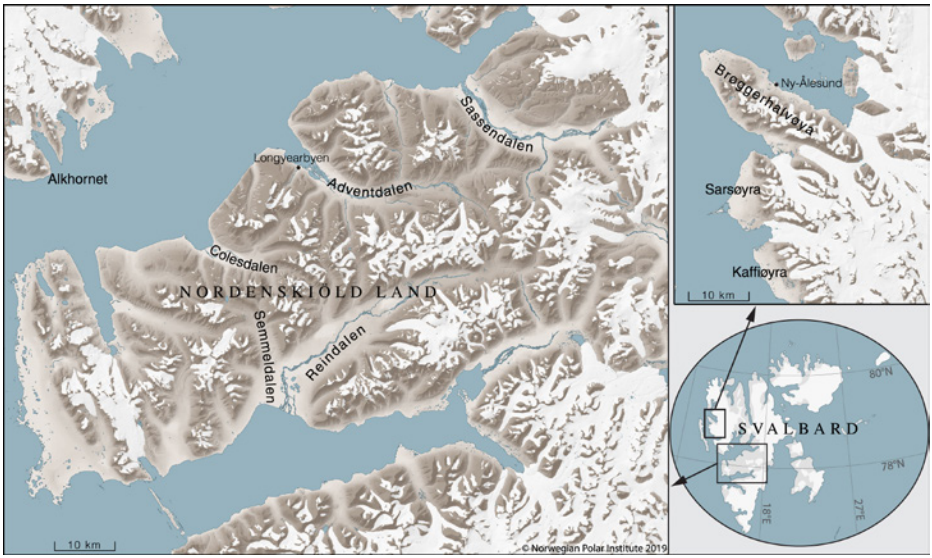

Figure 1: Map of the COAT Svalbard study regions (lower right) in Nordenskiöld Land (left) and Forlandssundet (Brøggerhalvøya, Sarsøyra and Kaffiøyra) (upper right). Figure: Bernt Bye/NPI.

the conceptual models particularly highlight monitoring targets and process relations that may be subjected to local management actions. The climate module covers the main climatic variables (Figure 2) that are expected to act as drivers on species or functional groups in the food web modules. An important output of the climate module is the generation of high-quality weather data from automatic weather stations that cover the most important ecological gradients (e.g. coast to inland sites). Weather data are used to calibrate spatial and temporal snow models (see Liston and Elder 2006 for an example), as the cryosphere has a key role in determining the dynamics of the Svalbard tundra ecosystem (e.g. Stien et al. 2012; Hansen et al. 2013).

1.3 Conceptual models, monitoring targets, state variables and analyses

Each conceptual model outlines (1) key ecological interactions (trophic or competitive) between monitoring targets, (2) the most likely pathways for impacts of climate change and (3) the options and pathways for management to alleviate or mitigate negative pressure impacts (see Lindenmayer and Likens 2009; 2010a,b; 2011 for description of the use of conceptual models in long-term monitoring). Although climate change is expected to be the main driver of ecological change, other drivers can be locally or regionally important. In the COAT models these local pressures are represented by the management-impact pathways, because local pressures such as harvesting, development of infrastructure and

Box 1. Svalbard terrestrial tundra ecosystem

Compared to many other tundra ecosystems, even in equivalent bioclimatic subzones, the Svalbard food web is relatively simple, and some typical Arctic key-stone species and food chains are missing. The isolated geographical positioning of the archipelago, possibly together with certain attributes of the climate, are main reasons for this. The key herbivore species present are one ungulate (the endemic Svalbard reindeer), one species of ptarmigan (the endemic Svalbard rock ptarmigan) and two species of migrating geese (the pink-footed and the barnacle goose). The predator/scavenger guild is also depauperate with the main species being the Arctic fox and the glaucous gull, the latter being a species that also make extensive use of marine food sources Indeed, marine subsidies (both in terms of nutrient and energy) to the terrestrial ecosystems are more profound in the coastal areas of Svalbard than in many other High Arctic regions (Ims and Ehrich 2013). Migrating passerines (e.g. snow bunting) and shore birds (e.g. purple sandpipers) add to the species diversity and abundance of prey in the summer season (Kovacs and Lydersen 2006). Contrary to what is found in most tundra food-webs (Ims and Fuglei 2005), small and medium-sized mammalian herbivores (rodents and hares) and specialist predators are functionally absent on Svalbard (Strøm and Bangjord 2004). Only a local introduced population of sibling vole is spatially restricted to the area around a sea bird colony in Grumant, Nordenskiöld Land peninsula (Henttonen et al. 2001). Figure from Ims et al (2013).

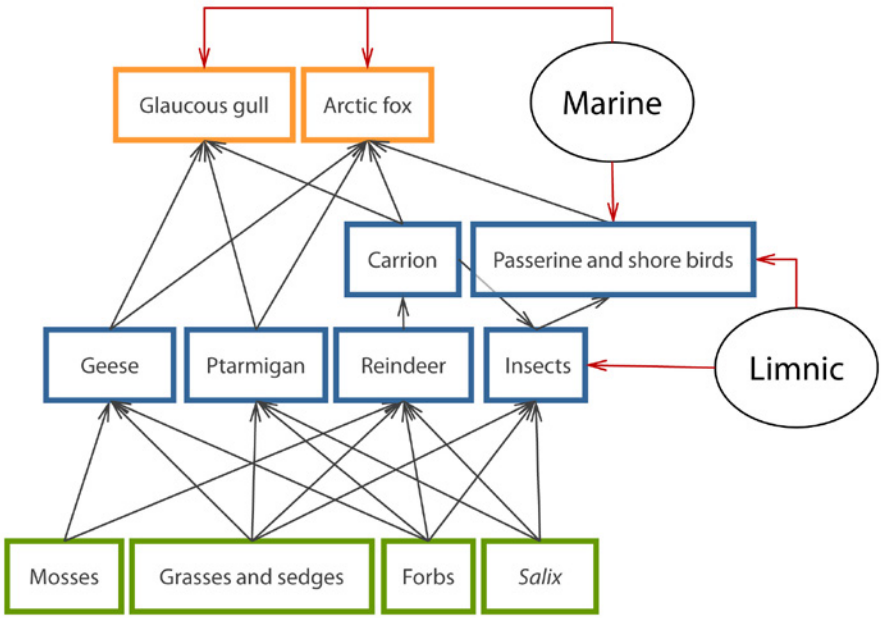

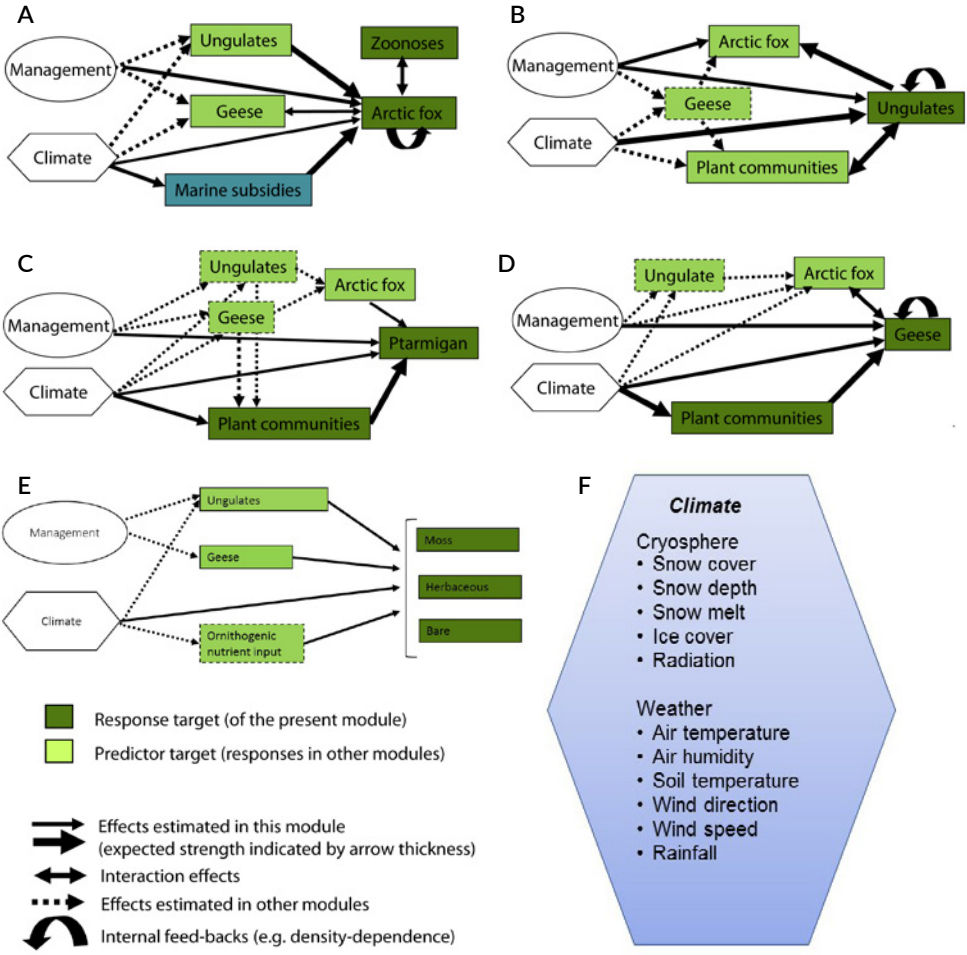

Figure 2: The conceptual models representing the five food web modules and the climate module of COAT Climate - ecological Observatory for Arctic Tundra (after Ims et al. 2013). Each model specifies climate and management impact pathways on prioritized monitoring targets. A. Arctic fox module, B. Reindeer module, C. Ptarmigan module and D. Goose module, E. Moss tundra module and F. Climate module, including the main climate state variables that are relevant to the monitoring components in the food web modules. See Box 2 for a summary of key attributes for each conceptual food web module.

increased traffic in principle can be dealt with by appropriate local management actions (Figure 2 and Box 2). Furthermore, monitoring targets that are subject to management actions are prioritized in COAT. Additional criteria for inclusion as a monitoring target were high climate sensitivity, high importance as conservation targets (e.g. endemic species) and high usefulness for comparative scientific analysis in a circumpolar context.

Box 2. Key attributes and motivations behind the five food-web modules

The Arctic fox model (Figure 2A) targets (1) the *Arctic fox* because it is functionally the most important predator within the terrestrial food-web and (2) *Arctic fox parasites* and *diseases* that represent dangerous zoonones (rabies, toxoplasmosis and parasites) for humans. Management options and local pressures are harvesting and regulating traffic. Potentially important climate impact paths are change of herbivore abundance and changing sea ice extent. Additionally, the Arctic fox is the terrestrial species most subjected to bioaccumulation of long-distance transported pollutants.

The reindeer model (Figure 2B) targets the *Svalbard reindeer* and (2) *plant communities* containing the main forage plants. The endemic Svalbard reindeer have increased in abundance and expanded their spatial range (Le Moullec 2019). Recent studies have revealed direct sensitivity of the reindeer to climate (Hansen et al. 2011; Hansen et al. 2013; Hansen et al. 2019a). The reindeer has a key role in *plant community* dynamics (see van der Wal et al. 2001; van der Wal et al. 2004) and a strong influence on the population dynamics of the Arctic fox (Eide et al. 2004). Management options and local pressures are recreational hunting.

The ptarmigan model (Figure 2C) targets (1) the *Svalbard rock ptarmigan* and (2) *plant communities* containing the main forage plants. The key climate-impact pathway affecting ptarmigan is predicted to be indirectly mediated by phenological changes in food plants and reproduction (Henden et al. 2017; Beard et al. 2019). Management options and local pressures are recreational hunting. In a conservation perspective, the Svalbard ptarmigan is an endemic sub-species that appears in low, but increasing densities, which contrast most other ptarmigan populations (Fuglei et al. 2019).

The goose model (Figure 2D) targets (1) the two goose species (*pink-footed* and *barnacle goose*) and (2) the *plant communities* they interact with. Geese have high impact on Arctic plant communities (e.g. Abraham et al. 2005; Speed et al. 2009; Madsen et al. 2011), their important interactions with the Arctic fox that determines their breeding success (Layton-Matthews et al. 2019b), as well as the many issues that relate to the management of long-distant migrants. Management options are hunting on flyways and wintering grounds (Madsen and Williams 2012).

The **moss tundra model** (Figure 2E) targets moist moss tundra that can occur in 3 alternative states; a *thick moss layer*, *herbaceous plant dominated* and *bare patches* and focuses on the transitions between these states (Ravolainen et al. 2019) . The key climate-pathway is predicted to be warm summer temperatures that can be indirectly mediated by increased abundance of herbivores leading to shifts in vegetation states via grazing, trampling and fertilization, and by nutrient input from seabirds and geese. The module also monitors *Dryas octopetala* vegetation, changes caused by winter damage and permafrost processes, and comprises a landscape scale remote sensing component.

Each of the conceptual models is further detailed by sets of *state variables*. While the *monitoring targets* are broad categories of interest (Figure 2 and Box 2), the state variables are the specific aspects of these monitoring targets that are sampled at relevant spatial and temporal scales, e.g. abundance, mortality, reproduction, body mass and demography (for a complete list see Ims et al. 2013). Many monitoring targets are involved in several conceptual models, often as a response target in one conceptual model while being a predictor target (driver) in other models (Figure 2). This affects the sampling designs for targets; each target has to be sampled at a temporal and spatial scale that is suitable for all the ecological processes it is involved in. Climate affects several processes in all the conceptual models. This implies that many state variables describing climate have to be sampled using an intensive study design, and at spatial scales appropriate for evaluating monitoring targets. For example, vegetation changes need to be monitored using a fine-scale spatial sampling design. To understand how climate affects vegetation, monitoring of climate state variables related to vegetation requires a study design that matches the vegetation sampling localities and spatial scale. Regarding temporal scaling, the timing of certain events requires simultaneous monitoring data with high temporal resolution across several trophic levels (cf. example of trophic mismatch below). To facilitate data-driven causal analyses and predictions the conceptual models of COAT need to be translated into statistical models. Indeed, a key purpose of the formulation of the conceptual models is to define the structure (the skeleton) of dynamical structural equation models (Grace et al. 2016). These statistical models will be analysed to both identify causal relations and provide short-term predictions (Ims et al. 2013).

1.4 Adaptive monitoring for understanding novel ecosystem processes

Ecological monitoring programmes need to be driven by questions and hypotheses of causality to be powerful tools for scientific inference and management decisions (Yoccoz et al. 2001; Legg and Nagy 2006; Nichols and Williams 2006; Lindenmayer and Likens 2009; Lindenmayer and Likens 2010b). In COAT, the conceptual models formulate these hypotheses. COAT further sets the conceptual models in an adaptive monitoring protocol framework (Lindenmayer and Likens 2009) (Box 3). This framework allows for a robust hypothetico-deductive approach that combines observational time-series of state variables (e.g. key climatic drivers such snow cover and temperature and food web response variables). The overall aim of the adaptive protocol is to attain increased knowledge of the effects of climate change on food web interactions and inference of optimal and adaptive management interventions in novel and unpredictable environments. An active interphase with management and stakeholders is implicit in the framework and is integral to understanding ecosystem functioning. Through the project SUSTAIN[1], COAT currently

1 www.sustain.uio.no/

Box 3. Design protocol for monitoring the COAT Svalbard tundra ecosystem.

Adaptive monitoring - a design for long-term, real-time monitoring in rapidly changing and novel environments.

Food-web dynamics are represented by conceptual models (Figure 2) describing the direct and indirect links between key drivers (climate and management), and key monitoring targets (species, communities, functional guilds) anticipated to reflect the functioning and structure of the tundra ecosystem. Predictions of relationships between monitoring targets and drivers are set by *a priori* hypotheses. Hypotheses are tested via experimental manipulations or by using observational study design. This results in understanding of the effectiveness of management actions and climate impacts on monitoring targets. Hierarchical multi-scale (both temporal and spatial) sampling design allows discrimination between changes of monitoring target caused by external drivers and internal processes. Sampling is undertaken, followed by analyses and interpretation of resulting data. We particularly focus on short-term predictions or forecasts that can be compared with observations. The resulting improved knowledge of food-web interactions are discussed with stakeholders (including management) and disseminated to the public. The protocol is adapted as necessary and the steps are reiterated to allow long-term adaptive management of the ecosystem component to mitigate adverse effects of climatic change on the Svalbard tundra ecosystem. COAT thus follows the adaptive monitoring protocols by (Lindenmayer and Likens (2009).

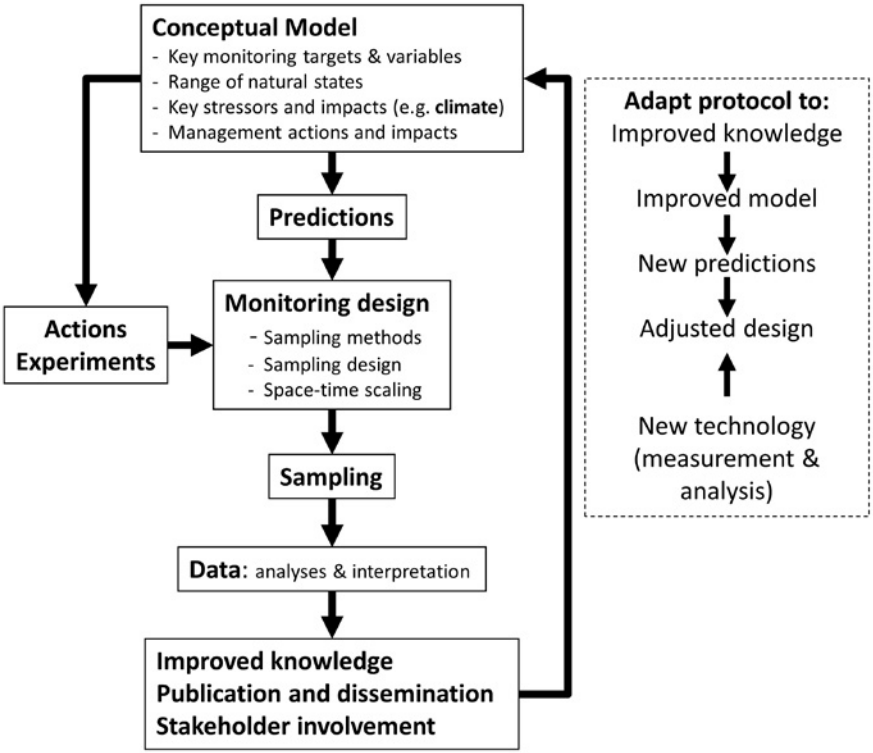

investigates the utility of a Strategic Foresight Protocol as a vehicle for providing such an active interphase between ecosystem science and end-users (Ims and Yoccoz 2017)

2. Current status and trends in the Svalbard terrestrial ecosystem

In this section, we give a brief summary of status and trends in monitoring targets and processes described in the conceptual climate impact path models. We mainly review the results from monitoring targets for which long time series are available and present hypotheses and predictions (i.e. expressed in the conceptual COAT models; Figure 2) that will be tested in future analyses when adequate data have become available.

2.1 Climate characteristics and ecological implications

There have been several recent reviews of Svalbard's current climate and trends therein (e.g. Gjelten et al. 2016; Isaksen et al. 2016; Vikhamar-Schuler et al. 2016; Renner et al. 2018; Hanssen-Bauer et al. 2019; IPCC 2019). Below we summarize the main conclusions and give a brief summary of expected ecological implications.

Temperature has increased (3 – 5 ˚ C between 1971 and 2017) in all seasons - with the largest increase in winter and the smallest in summer (Figure 3A) (Isaksen et al. 2016; Hanssen-Bauer et al. 2019). The winters are milder and characterized by fewer cold winter days (Gjelten et al. 2016) and more days with precipitation falling as rain (Figure 3B). Warmer July temperatures (Figure 3C) signal a change in characteristics of the plant growing season and July temperature is therefore a key indicator of a climatic region, and the basis for the climatic delineation of the Arctic bioclimatic subzones (CAVM Team 2003). Changes in mean July temperature on Svalbard indicate that climatically, the majority of the Svalbard tundra has shifted an entire bio-climatic sub-zone (Figure 3C) (Vikhamar-Schuler et al. 2016; Jepsen et al. 2019). Climatic change in these zones is expected to be accompanied by significant alteration of ecosystems and focal components with knock-on effects on function, structure and productivity (IPCC 2019).

Higher temperatures have led to winter rain becoming more frequent (Figure 4a), resulting in a regime shift in winter climate. Both the spatial occurrence and thickness of basal ice increased strongly with the annual amount of winter rain (Peeters et al. 2019). However, considerable spatial variation exists (Figure 4b), particularly along gradients from coast to inland (Peeters et al. 2019). Increased frequency of rain-on-snow, resulting in basal ground ice formation has negative impacts on population growth rates of the winter resident species of the vertebrate animal community (Stien et al. 2012; Hansen et al. 2013). Basal ground ice damages vegetation (Milner et al. 2016; Bjerke et al. 2017) and prevents

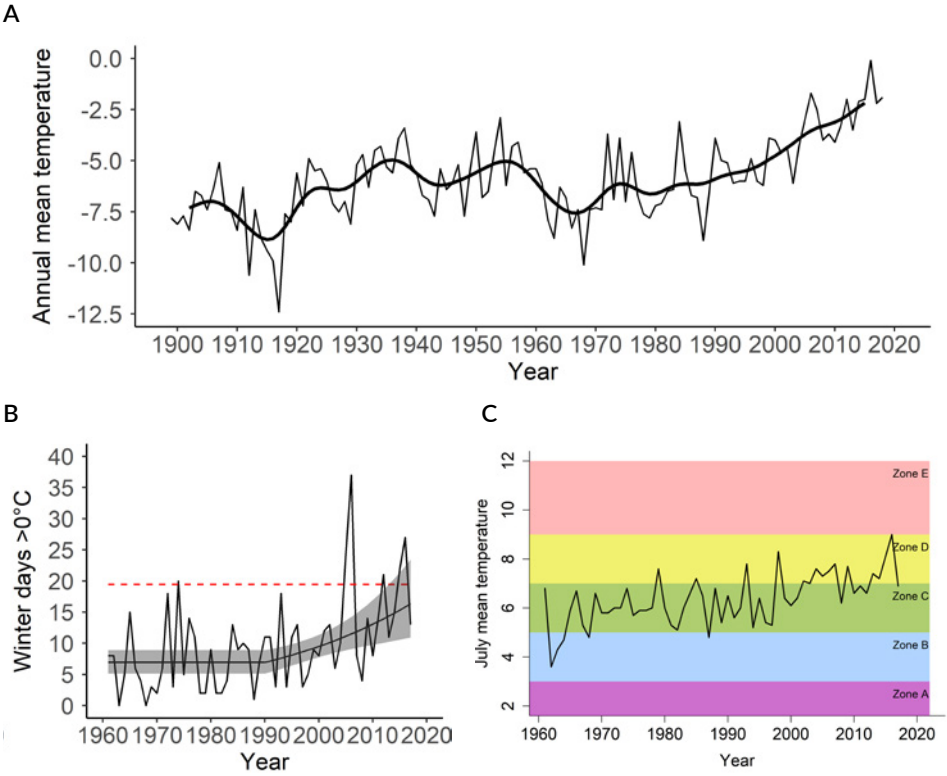

Figure 3: A: Observed trends in annual temperature in the Svalbard terrestrial tundra ecosystem. Mean annual temperature at Svalbard Airport meteorological station (1899-2018). The thick black line shows the long-term variability at the decadal scale (Nordli et al. 2014; Isaksen et al. 2016). B: The number of winter days (daily mean temperature > 0°C), for Svalbard Airport meteorological stations (1961-2017). The rate of change, relative to the 1961-1990 normal period, is shown with ±2SE and the dashed red line indicates 2SD of variation observed in the normal period 1961-1990 (modified from Jepsen et al. 2019). C: The mean July temperature of Svalbard Airport meteorological station (1961-2017) against the climatic boundaries of the Arctic bioclimatic subzones. After year 2000, this part of Svalbard has, climatically, shifted from subzone C (Middle Arctic tundra Zone) to subzone D (Southern Arctic Tundra Zone) (modified from Jepsen et al. 2019).

herbivores accessing food. Increased winter mortality of Svalbard reindeer in turn affects food availability for the Arctic fox (*Vulpes lagopus*) (Eide et al. 2012). It is still unclear whether the winters have become so mild that they make forage more accessible (due to snow melting) rather than locking away access to foraging grounds (due to ground ice formation).

Hydrological characteristics are changing due to increased precipitation and snowmelt patterns (see Gallet et al. 2019 for a review). The annual average surface run-off has increased by more than a third, mainly due to increased glacier melt and increased winter precipitation. This may increase glacial lake outburst floods as well as affecting erosion

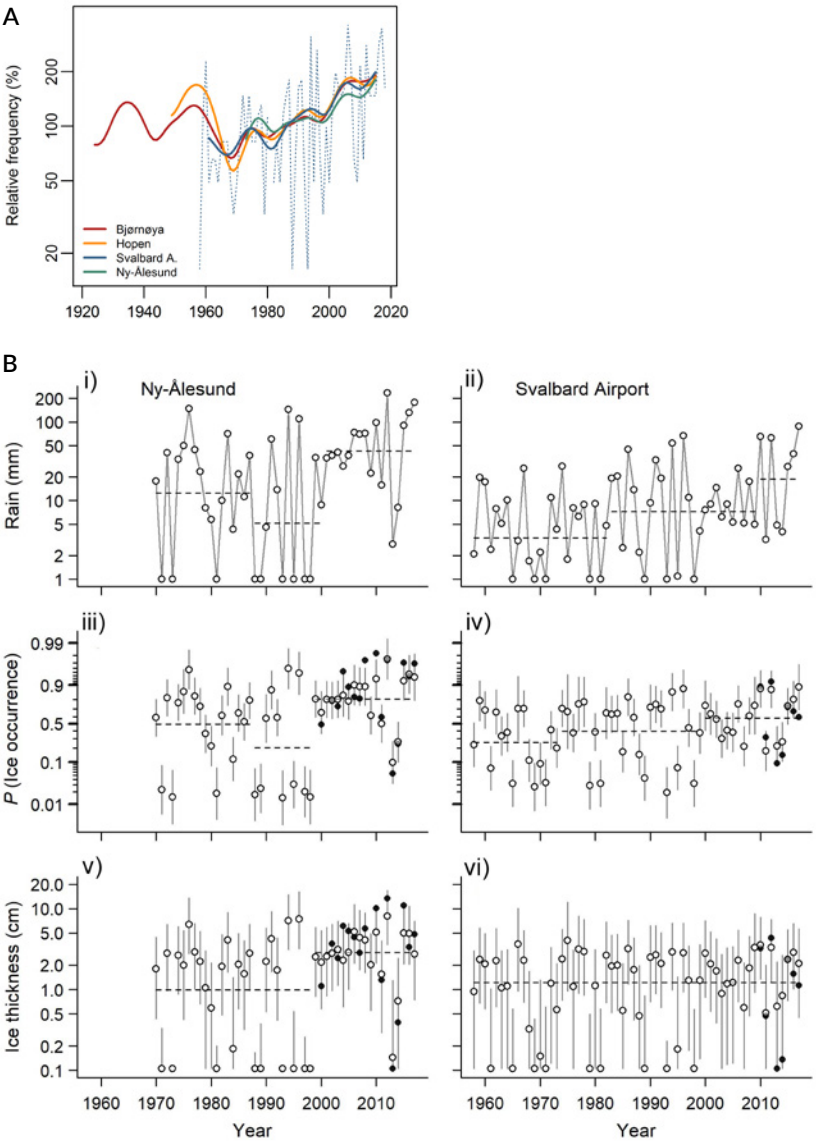

Figure 4: Observed trends in precipitation and ice characteristics of the terrestrial Svalbard. A) number of days per year relative to the 1971-2000 average of observed precipitation and a daily mean temperature over 0˚C (Hanssen-Bauer et al. 2019); B) Regime shifts in rain and basal ground ice: Historical amounts of winter rain (i - ii) and past modelled basal ground ice occurrence (iii – iv) and basal ground ice thickness (v - vi). Data from two meteorological stations: Ny-Ålesund, NW coast (i, iii, v) and Svalbard Airport, central Spitsbergen (ii, iv, vi). Average observed values up to 200 m elevation are included as black dots (or grey when overlapping with model estimates). Horizontal dashed lines indicate average values before and after observed regime shifts (i) 1987, 2000, (ii) 1982, 2009, (iii) 1987, 1998 (iv) 1973, 1999 (v) 1998 (vi) no change point observed (Peeters et al. 2019).

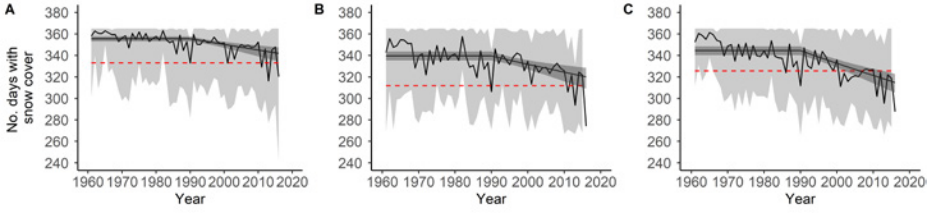

Figure 5: Number of days with snow cover for the three bioclimatic subzones Arctic Polar Desert Zone (A), Northern Arctic Tundra Zone (B) and Middle Arctic Tundra Zone (C) (extracted from Østby et al. 2017). The rate of change, relative to the 1961-1990 normal period, is shown with 2.5% - 97.5% confidence intervals. The dashed red line indicates 2SD of variation observed in the normal period (modified from Jepsen et al. 2019).

intensity and sediment supply to rivers (Hanssen-Bauer et al. 2019). The snow season has decreased by approximately 20 days since the middle of the last century and this trend is expected to continue decreasing, resulting in shifts in spring- and winter onset (Hanssen-Bauer et al. 2019). Snow cover duration is decreasing everywhere in the High Arctic, but most rapidly in the Middle-Arctic Tundra Zone (subzone A) (Jepsen et al. 2019) (Figure 5).

Changes in season length have a range of implications for food web interactions. Earlier springs may lead to phenological mismatch between egg laying and food resources for Svalbard rock ptarmigan (*Lagopus muta hyperborea*) (Ims et al. 2013; Wann et al. 2019), but data on this are still not available. Alternatively, an extended grazing season may have a positive effect on reproduction and habitat suitability for herbivores (Jensen et al. 2008; Albon et al.

2017; Layton-Matthews et al. 2019b; Rivrud et al. 2019). Furthermore, patterns of snow melt may determine the extent and intensity of disturbance of the tundra by geese grubbing

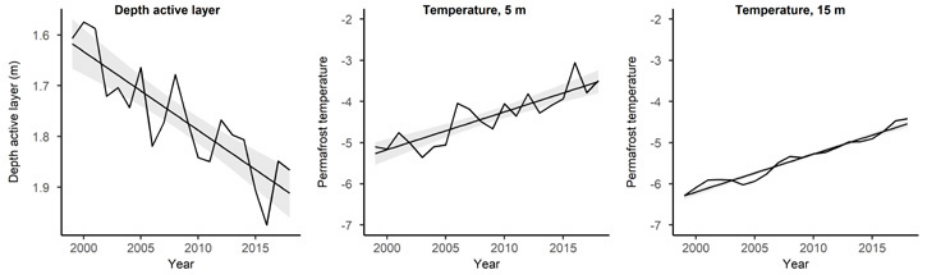

Figure 6: Trends in depth of the active layer (left) and permafrost temperatures (Sept. 1st) at 5 meters (middle) and 15 meters (right) depth in Adventdalen in central Spitsbergen (Isaksen pers. comm.: www.mosj.no). Trend lines indicate the estimated linear rate of change and shading indicates ±2SE (modified from Jepsen et al. 2019).

for belowground food items in early spring (Pedersen et al. 2013b; Pedersen et al. 2013c; Anderson et al. 2016) and breeding success (Madsen et al. 2007; Jensen et al. 2014).

Increased air temperature and precipitation are resulting in an annual reduction in permafrost depth in High Arctic Svalbard (Hanssen-Bauer et al. 2019). This leads to an associated increase in annual and seasonal temperature of permafrost layers and active soil layer (Isaksen et al. 2007; Etzelmüller et al. 2011) (Figure 6), which in turn can increase instability of slopes, hydrology and vegetation, especially where permafrost layers exist in sediments (Hanssen-Bauer et al. 2019).

Sea ice reductions are most pronounced in Svalbard and the Barents Sea area (Onarheim et al. 2018). The loss of sea ice and the earlier retreat in spring also have implications for the terrestrial ecosystem. The retreat in spring has on average been two weeks earlier per decade since 1979 (Laidre et al. 2015). Whereas the local/sub-regional component is attributed to sea breeze (cold air advection from ice-covered ocean onto adjacent land during the growing season), the large-scale component might reflect co-variability of sea ice and tundra productivity due to a common forcing (North Atlantic Oscillation) (Macias-Fauria et al. 2017). In addition, sea ice loss reduces the possibilities for Arctic fox hunting and scavenging on this substrate (Gaston et al. 2012; Fuglei and Tarroux 2019) and reindeer movement (Hansen et al. 2010).

These changing climatic conditions have a profound effect on the state of the cryosphere, which in turn determines the timing and extent of the growing season and the available resources for plants and animals. The snowscapes of Svalbard are highly heterogeneous, due to steep climatic gradients from coast to inland and a complex topography. Hence the monitoring design for measuring climate state variables needs to capture this variation. The COAT automated weather stations that will be in place within 2021, combined with field observations and experiments are essential to measure a suite of state variables necessary to predict and forecast effects from climate change on the Svalbard tundra food web. Such measures will be strengthened and complemented by additional remote sensing and ground based measurements of the cryosphere. The fine scale meteorological data will be used to calibrate landscape-scale snow models to improve our understanding of climate change on biotic processes in the tundra ecosystem.

2.2 Primary productivity

An increase in the temperature on Svalbard has led to increased primary production as measured by plant biomass (van der Wal and Stien 2014). Individual plants across habitats, plant functional types and species grow better in warm summers (van der Wal and Stien 2014; Milner et al. 2018; Le Moullec et al. 2019) given sufficient moisture (Elmendorf et al.

2012). However, satellite-based measures of plant biomass, which use the plant productivity index NDVI is more difficult to use in Svalbard than elsewhere due to frequent cloud cover. Different studies have adopted different approaches and this has led to conflicting conclusions regarding the validity of a link between NDVI and plant biomass (Johansen and Tommervik 2014; Vickers et al. 2016; Karlsen et al. 2018). However, the high-resolution spatial layers mapping plant productivity from Sentinel-2 data may be a key to disentangle some of the current issues observed (Karlsen et al. 2020).

Vegetation productivity is influenced by multiple abiotic and biotic factors. Experimental studies from Svalbard show plant growth responses to ice- and frost damage in the winter (Milner et al. 2016). Furthermore, herbivores may affect the vegetation negatively through grazing, trampling and grubbing (Van der Wal and Brooker 2004), but also have more indirect effects through increased fertilization and nutrient recycling (Ravolainen et al. 2019). The main grazers on Svalbard have both increased in population size in recent decades (Le Moullec et al. 2019; Figure 7). Finally, seabirds have a fertilising impact on vegetation, bringing nitrogen of marine origin into the terrestrial ecosystem (Zwolicki et al. 2013; Zwolicki et al. 2016).

The moss tundra vegetation presently functions as a hotspot of primary production and herbivore diversity. Direct climate effects as well as indirect effects from changes in abundance of herbivores and seabirds may cause a change from a moss dominated slow nutrient cycling system to herbaceous dominated faster nutrient cycling system. The moss tundra vegetation module will use a combination of field- and remote sensing monitoring techniques to provide data for estimating direct and indirect effects of climate on vegetation (Ravolainen et al. 2019).

2.3 Changes in higher trophic levels

2.3.1 Reindeer

Svalbard reindeer (*Rangifer tarandus platyrhynchus*) are key herbivores in the Svalbard tundra ecosystem, maintaining grass communities in an otherwise moss dominated ecosystem (Van der Wal and Brooker 2004). The reindeer population lacks influential predators and insect harassments, and harvest is strictly regulated to such low levels that it is not expected to affect population dynamics. Reindeer abundance on Svalbard has increased two-fold during the last decades (Le Moullec et al. 2019). However, monitored coastal and inland populations have contrasting trajectories (Hansen et al. 2019b; Le Moullec 2019). The population on the Nordskiöld Land peninsula has increased, while the population on the more northerly Brøggerhalvøya has remained stable at lower abundance levels (Hansen et al. 2019b). The Svalbard reindeer populations show large annual fluctuations in numbers but appear to be spatially synchronized by annual winter weather variability (Aanes et al. 2003;

Stien et al. 2012; Hansen et al. 2019b).

Long-term individual based studies of the population in Nordenskiöld Land peninsula have given insight into the mechanisms of the drivers of population dynamics - with contrasting effects of summer and winter climate determining the population trend. When summers and autumns are warm, reindeer body masses are higher in the autumn and even in the following spring, likely associated with higher plant productivity and extended grazing seasons (Albon et al. 2017). However, reindeer body mass is during the spring strongly influenced by rain-on-snow events, which also determine vital rates and ultimately variability in population growth rates (Albon et al. 2017). In winters with extensive basal ground ice, larger numbers of reindeer die, mainly through increased mortality of the youngest and oldest individuals, when the population is at high densities (Stien et al. 2012; Hansen et al. 2013). Recent analyses of long-term data sets of biological and weather state variables show that more frequent rain-on-snow events reduce extinction risk and stabilize population dynamics at lower levels due to interactions between age structure and density dependence (Hansen et al. 2019a).

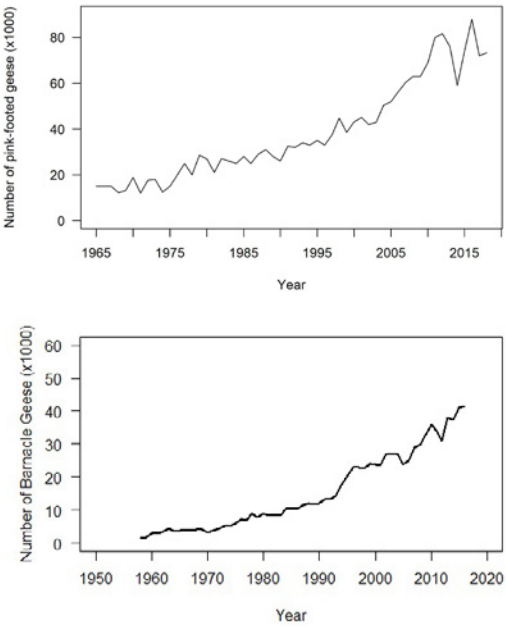

Figure 7: Left panel: Population size of pink-footed goose (upper) and barnacle goose (lower) in Svalbard. Goose counts are carried out on their wintering grounds in the UK (modified after Jensen et al. 2018; Johnson et al. 2018). Right panel: Impacts of intense pink-footed goose grubbing. Photo: Jesper Madsen.

Reindeer can have local effects on plant biomass. Further, they also modify the tundra vegetation communities (van der Wal et al. 2001; Van der Wal and Brooker 2004), and changes in reindeer abundance are expected to have knock on effects on composition, structure and productivity of the Svalbard tundra. Currently, there is lack of information on potential resource competition with geese, although the numbers of both species are increasing. Furthermore, the changing dynamics of rain-on-snow events are likely to play a large role in constraining the abundance and population growth rates of reindeer (Hansen et al. 2019a).

2.3.2 Svalbard rock ptarmigan

The Svalbard rock ptarmigan is an endemic sub-species restricted to Svalbard and Franz Josef Land. It is the only resident herbivore bird in the tundra ecosystem (Løvenskiold 1964), and the most important predator is the Arctic fox (Steen and Unander 1985). Currently, they are subject to local harvest (Soininen et al. 2016). Annual monitoring of spring densities of territorial males reveals low abundances (1-3 males per km^2) with moderate temporal fluctuations and no significant linear trends for the period 2000-2013 (Pedersen et al. 2012; Soininen et al. 2016). However, since 2014 the spring density has increased and reached a density level between 3-5 males per km^2 with a current positive trend (Fuglei et al. 2019). The temporal fluctuation in spring densities is partly driven by inter-annual variation in rain-on-snow events with population reductions in years with high occurrence of winter rain (Hansen et al. 2013). The monitoring data indicate an increasing trend in spring density, however, hunting statistics (i.e. bag size and the proportion of juveniles in the bag), show the opposite trend (Soininen et al. 2016). The discrepancies between these time-series are currently under interpretation. The Svalbard rock ptarmigan has limited amount of suitable breeding habitats available (< 4 %), which is also suggested to be one limiting factor for the breeding population (Pedersen et al. 2017).

Svalbard rock ptarmigan is predicted to be both directly and indirectly impacted by climate change (Ims et al. 2013; Henden et al. 2017). Rain-on-snow events, have already been shown to have direct negative effects on the population growth rate (Hansen et al. 2013). Moreover, increased weather variability in spring and summer is predicted to affect the onset of breeding and chick survival (Ims et al. 2013). Newborn ptarmigan chicks have a highly specialized diet of *Bistorta vivipara* bulbils (Unander et al. 1985). This is likely to make them vulnerable to phenological mismatch with their preferred food plants (Ims et al. 2013). A warmer summer climate may have a positive effect on the ptarmigan population through increased plant productivity, but warmer, icy winters that cause widespread damage to especially *Dryas* vegetation (Milner et al. 2016; Bjerke et al. 2017) that ptarmigan rely on in the spring, may have negative effects. The increasing populations of pink-footed geese may have a negative impact on ptarmigan forage resources through their intensive grazing and grubbing that remove important food plants (Ims et al. 2013).

2.3.3 Geese

Geese are key herbivorous species in the Svalbard tundra ecosystems, even though they are seasonal migrants spending just four months of the year in the archipelago (Madsen et al. 1999). All three species (pink-footed goose, barnacle goose and brent goose; *Branta bernicla*) have increased in recent years, but barnacle and pink-footed geese have seen the biggest increases (Clausen and Craggs 2018; Jensen et al. 2018; Madsen et al. 2018). The increases are due to a combination of increased overwintering survival due to increased protection from hunting and changed agricultural practices along their flyways (Johnson et al. 2018).

Svalbard geese are directly affected by changes in climate, as earlier snowmelt allows earlier nesting, and leads to increased nesting success (Madsen et al. 2007; Jensen et al. 2014; Layton-Matthews et al. 2019b). The climatically driven changes are likely to allow goose population densities to increase and distributions to expand (Jensen et al. 2008; Wisz et al. 2008).Particularly, the spring foraging by pink-footed geese (grubbing) has resulted in the changes of vegetation community composition, structure and function (Kuijper et al. 2006; van der Wal et al. 2007; Pedersen et al. 2013a). Grubbing leads to destruction of roots and rhizomes of food species and adjacent moss carpets concentrated in the fen regions (Fox et al. 2006). Multi-annual grubbing hampers regeneration and the removal of large amounts of plant material can have knock on effects for net ecosystem change (van der Wal et al. 2007). Removal of moss and trampling modifies the vegetation community, leading to increased soil temperature and enhanced graminoid growth (van der Wal et al. 2000; Gornall et al. 2009). However, vegetation degradation appears to be moderated by inter-annual variation in snowmelt patterns that structure grubbing activity (Anderson et al. 2016).

Arctic fox feed on geese, and can regulate goose population growth by predation of goslings (Eide et al. 2004; Madsen et al. 2007; Anderson et al. 2019; Layton-Matthews et al. 2019a). Barnacle geese are also vulnerable to egg predation by polar bears (*Ursus maritimus*) (Prop et al. 2015). The increasing populations impact negatively on the Svalbard rock ptarmigan population through the geese's removal of the tundra vegetation (Ims et al. 2013) or positively by a reduction in predation compatible with apparent mutualism and/or prey swamping mechanisms (Pedersen et al. 2018).

2.3.4 Arctic fox

Arctic fox is the only terrestrial mammalian apex predator and scavenger in the tundra ecosystem (Eide et al. 2004; Eide et al. 2005). It links the terrestrial food web to subsidies from the marine food web through prey, such as sea birds and seal carcasses (Prestrud 1992; Ims et al. 2013). Because Svalbard lacks cyclically fluctuating small rodents like lemmings, the Arctic fox population belongs to the coastal ecotype. Stable resources from the marine ecosystem subsidize this type, and population levels are generally more stable

compared to other types of Arctic fox populations in the Arctic. It is also an important carrier of zoonoses (animal born parasites/diseases that may spill over to humans) (Sørensen et al. 2005; Prestrud et al. 2007; Mørk et al. 2011).

The monitored Arctic fox populations show considerable annual variation in abundance, but the long-term population abundance trend is stable to slightly increasing, although they are locally trapped in parts of the monitoring areas (Eide et al. 2012; Layton-Matthews et al. 2019a). Their population dynamics are likely to be affected both directly and indirectly by climate. Arctic foxes may be indirectly negatively affected by the reduced availability of marine prey in the winter due to reduced sea ice cover that is habitat for important prey species, e.g. ringed seal (Tarroux et al. 2012), and in the summer due to the collapse of some seabird colonies (Descamps et al. 2013; Descamps et al. 2017). The Arctic fox abundance and reproduction is positively related to the amount of reindeer carcasses on the tundra (Eide et al. 2012; Hansen et al. 2013). However, this results in a one-year delayed negative impact on the population growth rate of foxes after severe winters (Hansen et al. 2013). Additionally, a warmer spring and summer has a positive influence on the amount and breeding success of geese (Madsen et al. 2007; Jensen et al. 2014), with likely subsequent positive effects on Arctic fox population dynamics (Ims et al. 2013). Winter sea ice allows dispersal, migration, and interchange of genes between the Svalbard population and other circumpolar ranges (Ehrich et al. 2012; Fuglei and Tarroux 2019). Thus, the reduction in sea ice extent (Gaston et al. 2012) may have consequences for population structure, robustness and long-term viability of the Arctic fox populations (Fuglei and Tarroux 2019).

2.4. Overall trends in monitoring targets

Currently abundance of monitored vertebrate populations appears to be stable or increasing for reindeer, ptarmigan, fox and geese (Jensen et al. 2018; Fuglei et al. 2019; Hansen et al. 2019b; www.mosj.no). There could be several reasons for this. The herbivores in the food webs that are monitored involve resident and migratory species that are at the northern edge of their range. They are adapted to harsh conditions, i.e. food limitation and extreme cold, but show considerable plasticity so that improved carrying capacity of the tundra during the summer season allows for better condition, and hence increased reproduction. Stochastic perturbations in the form of large-scale rain on snow, causing ground ice is still impacting annual variability in population growth rate, but the timing, scale and frequency of such impact may no longer be as severe as earlier described (Hansen at al. 2013), perhaps because improved conditions during the summer have increased the resilience of individuals to the severe weather events in winter. Recently, Hansen et al. (2019a) documented that such severe events have a temporary stabilizing effect on population size of reindeer rather than negative effects. Tundra plants respond immediately to increased summer temperature by increased growth (Van de Val and Stien 2014), but as of yet we are unable to quantify

the expected bottom-up effects of increased plant growth on higher trophic levels in the food web. While there has been a shift in bioclimatic sub-zone towards a Low Arctic climatic zone, therefore providing a growth season suitable for a higher diversity of plants and with a potential for establishment of other functional groups (e.g. shrubs), any change at plant community level is so far not apparent. This may be due to the fact that there may be long time-lags in such vegetation community level responses. However, there is presently a lack of long-term monitoring data to document community level transitions in vegetation types that may be particularly prone to such transitions and the eventual cascading impacts this may have on food web dynamics and ultimately overall ecosystem function. COAT aims to fill such gaps by establishing the required long-term monitoring and model-based analyses for disentangling changes in key food web processes and thereby provide a better understanding of how climate change impacts High Arctic tundra ecosystems.

3. Challenges and recommendations for the future

Long-term monitoring is instrumental for environmental conservation, management and policy making to (1) establish how various anthropogenic pressures affect the environment and to (2) assess the effectiveness of management actions. However, from originally being an activity initiated and governed by environmental management bodies and policy makers, environmental monitoring has now become a distinct scientific discipline (Lindenmayer and Likens 2009, 2010a, 2010b; Lindenmayer et al. 2011). The World Meteorological Organization (www.public.wmo.int/en) directs its attention to the aspects of climate variability and change that impact the environment. The observational data of weather and climate that are collected through the networks of observing, data-transmitting and forecasting systems, keep policy-makers informed about the state of the environment so that they are in a better position to prevent its further degradation.

In this context, research infrastructures are instrumental to the state variable monitoring of the multiple aspects of climate change and its impacts. Addressing complex issues requires a holistic ecosystem- based adaptive approach, achieved through integration of relevant biotic and abiotic measurements at appropriate spatial and temporal scales with clearly defined goals and targets for monitoring (Haase et al. 2018; Musche et al. 2019). Several key priorities for the development of research infrastructures have recently emerged. These relate to for instance interoperability among different research infrastructures by developing standard measurements of state variables, co-location of measurements at ecological relevant spatial and temporal scales, harmonizing methods, and establishing both methods and tools for data integration, including observation, experiments and modelling (Musche et al. 2019).

The COAT monitoring system, including the field infrastructure is currently under implementation at the core of the SIOS land module. This offers opportunities for

co-location of research infrastructure and state variable measurements at similar scales, as well as production of common data products and models.

For the infrastructure implementation phase, we have the following recommendations:

Co-location of research infrastructure: Full-scale automatic weather stations are core infrastructure of COAT's climate observation network. Currently, two stations are in place (Janssonhaugen and Reindalspasset) and in total eight stations are planned across the extent of COAT's monitoring areas. They measure a range of abiotic state variables across ecological gradients that are expected to change. Research infrastructure for measurements of other abiotic and biotic state variables ought to be co-located with the COAT weather stations and the corresponding climate-monitoring network. Such co-location is planned within COAT, but to date it mainly includes biotic state variables relevant for COAT food web models. Incorporation of a broader range of abiotic state variables related to snow cover properties, permafrost and energy balance would be beneficial as it will allows for development of joint products relevant to both monitoring of the biosphere and the cryosphere.

Focus on snow: The ecosystem impact of changing snow pack properties in a warming climate is a particularly central theme in COAT and a generally important arena for interdisciplinary research between ecology and geophysics. Besides the co-location of research infrastructure and measurements outlined above, there is a need to develop a data-model fusion system that merges available observational datasets on snow properties with state-of-the-science, high-resolution (1- to 500-meter scale), physically based snow models. The goal of this data-enhancement system is to create accurate, spatially distributed, time evolving, datasets that can be used to better understand relationships between ecosystem processes. Several climate impact pathways formulised by COAT conceptual models are driven by changes in snow cover properties. State-of-the art monitoring of such pathways is dependent on snow modelling products and joint efforts will contribute to this. Moreover, the development of new ecosystem-relevant synthesis variables from the snow modelling work is needed for COAT's statistical food web models to improve quantitative predictions about climate change impacts on species or functional species groups.

For the long-term running COAT's adaptive monitoring program (i.e. after the initial infrastructure implementation phase is completed in 2021) we have the following recommendations:

New methods and technologies: Ecosystem science has entered an era where new technologies allows for automatic measurements of biotic state variables that are more spatially extensive and temporally highly resolved data than the traditional manual measurements. An important component of adaptive monitoring is to include new methods and instruments that can significantly improve our ability to detect changes and attribute them to drivers. Such new methodological developments also include analytical tools

that aid the assimilation and processing of large amounts of raw sensor data to operative ecological state variables, as well as refined statistical models that can be used for more robust causal inferences and short-term predictions based on these state variables.

Interphase with end-users: It is COAT's ambition to be highly relevant to policy makers and managers. Given the prospects of extreme climate change, Arctic ecosystems are likely to become transformed beyond scientists' current powers to make predictions and managers' abilities to perform mitigations and adaptations. This grand challenge requires more sincere efforts to make the kind of structured interphases between monitoring-based ecosystem science and end-users that are presently tried within COAT (Ims and Yoccoz 2017).

4. Data availability

Integration of the variety of state variables is essential to COAT's ecosystem-based approach and geographically distributed observation network. To achieve this, COAT will use a custom-made data portal. The portal will be directly accessible through COAT's web site, and have both meta- and raw data available. The COAT data portal is currently tested by different types of datasets and will be operational in 2020. COAT data portal describes detailed metadata for each dataset, using formats in compliance with international standards. These metadata are reassessed on a yearly basis to make sure that they describe current practices and that no information is lost because of changes in methods and/or designs. The COAT data portal builds on international metadata standards (DCAT, schema.org-structured data and ISO 19115/CSW) and the digital SIOS infrastructure will be able to "harvest" metadata and state variables from this portal.

Acknowledgements

This work was supported by the Research Council of Norway, project number 251658, Svalbard Integrated Arctic Earth Observing System – Knowledge Centre (SIOS-KC) and Tromsø Science Foundation. We thank Matteo De Stefano for contributing text to the section on data availability, Ingrid M. G. Paulsen for helping with figures and photos, and Inger-Hansen Bauer and Bart Peeters for use of published figures.

References

Aanes R, Saether BE, Solberg EJ, et al. (2003) Synchrony in Svalbard reindeer population dynamics. Can J Zool Zoologie 81:103-110

Abraham KF, Jefferies RL, Alisauskas RT (2005) The dynamics of landscape change and snow geese in mid-continent North America. Glob Change Biol 11:841-855

Albon SD, Irvine J, Halvorsen O, et al. (2017) Contrasting effects of summer and winter warming on body mass explain population dynamics in a food-limited Arctic herbivore. Glob Change Biol 23:1374-1389

Anderson HB, Fuglei E, Madsen J, van der Wal R (2019) High-Arctic nesting geese occupying less favourable nest sites are more vulnerable to predation. Polar Res 38 https://doi.org/10.33265/polar.v38.3352

Anderson HB, Speed JDM, Madsen J, et al (2016) Late Snow Melt Moderates Herbivore Disturbance of the Arctic. Ecoscience 23:29-39

Beard KH, Kelsey KC, Leffler AJ, Welker JM (2019) The Missing Angle: Ecosystem Consequences of Phenological Mismatch. Trends Ecol Evol 34:885-888

Bjerke JW, Treharne R, Vikhamar-Schuler D, et al. (2017) Understanding the drivers of extensive plant damage in boreal and Arctic ecosystems: Insights from field surveys in the aftermath of damage. Sci Tot Environ 599:1965-1976

CAFF (2013) Arctic Biodiversity Assessment: Report for Policy Makers. Conservation of Arctic Flora and Fauna (CAFF), Akureyri, Iceland

CAVM Team (2003) Circumpolar Arctic Vegetation Map. (1:7,500,000). Conservation of Arctic Flora and Fauna (CAFF) Anchorage, Alaska, US Fish and Wildlife Service

Clausen P, Craggs A (2018) East Atlantic (Greenland/Svalbard) light-bellied brent *Branta bernicla hrota*. Conservation of Arctic Flora and Fauna, Akureyri, Iceland

Descamps S, Aars J, Fuglei E, et al. (2017) Climate change impacts on wildlife in a High Arctic archipelago - Svalbard, Norway. Glob Change Biol 23:490-502

Descamps S, Strom H, Steen H (2013) Decline of an Arctic top predator: synchrony in colony size fluctuations, risk of extinction and the subpolar gyre. Oecologia 173:1271-1282

Ehrich D, Carmichael L, Fuglei E (2012) Age-dependent genetic structure of Arctic foxes in Svalbard. Polar Biol 35:53-62

Eide NE, Eid PM, Prestrud P, Swenson JE (2005) Dietary responses of Arctic foxes *Alopex lagopus* to changing prey availability across an Arctic landscape. Wildlife Biol 11:109-121

Eide NE, Jepsen JU, Prestrud P (2004) Spatial organization of reproductive Arctic foxes *Alopex lagopus*: responses to changes in spatial and temporal availability of prey. J Anim Ecol 73:1056-1068

Eide NE, Stien A, Prestrud P, Yoccoz NG, Fuglei E (2012) Reproductive responses to spatial and temporal prey availability in a coastal Arctic fox population. J Anim Ecol 81:640-648

Elmendorf SC, Gregory HRH, Hollister RD, et al. (2012) Global assessment of experimental climate warming on tundra vegetation: heterogeneity over space and time Ecol Lett 15:164-175

Etzelmüller B, Schuler T, Isaksen K, et al. (2011) Modeling the temperature evolution of Svalbard permafrost during the 20th and 21st century. Cryosphere 5:67-79

Fox TA, Francis IS, Bergersen E (2006) Diet and habitat use of Svalbard Pink-footed Geese *Anser brachyrhynchus* during arrival and pre-breeding periods in Adventdalen. Ardea 94:691-699

Fuglei E, Henden JA, Callahan CT, et al. (2019) Circumpolar status of Arctic ptarmigan: Population dynamics and trends. Ambio. https://doi.org/10.1007/s13280-019-01191-0

Fuglei E, Tarroux A (2019) Arctic fox dispersal from Svalbard to Canada: one female's long run across sea ice. Polar Res 38. https://doi.org/10.33265/polar.v38.3512

Gallet JC, Björkman MP, Borstad CP, Hodson AJ, Jacobi HW, Larose C, Luks B, Schuler TV, Spolaor A, Urazgildeeva A, Zdanowicz C (2019) Snow research in Svalbard: current status and knowledge gaps. In: Orr et al. (eds): SESS report 2018, Svalbard Integrated Arctic Earth Observing System, Longyearbyen, pp. 82-107. https://sios-svalbard.org/SESS_Issue1

Gaston AJ, Gavrilo M, Ebert C (2012) Ice bridging as dispersal mechanism for Arctic terrestrial vertebrates and the possible consequences of reduced sea ice cover. Biodiversity 13:182–190

Gjelten H, Nordli Ø, Isaksen K, et al. (2016) Air temperature variations and gradients along the coast and fjords of western Spitsbergen. Polar Res 35:29878

Gornall JL, Woodin SJ, Jonsdóttir IS, van der Wal R (2009) Herbivore impacts to the moss layer determine tundra ecosystem response to grazing and warming. Oecologia 161:747-758

Grace JB, Anderson TM, Smith MD, et al. (2016) Integrative modelling reveals mechanisms linking productivity and plant species richness. Nature 529:390

Haase P, Tonkin J, Stoll S, et al. (2018) The next generation of site-based long-term ecological monitoring: Linking essential biodiversity variables and ecosystem integrity. Sci Tot Environ 613:1376-1384

Hansen B, Isaksen K, Benestad R, et al (2014) Warmer and wetter winters: characteristics and implications of an extreme weather event in the High Arctic. Env Res Lett 9 https://iopscience.iop.org/article/10.1088/1748-9326/9/11/114021

Hansen BB, Aanes R, Herfindal I, Kohler J, Sæther BE (2011) Climate, icing, and wild Arctic reindeer: past relationships and future prospects. Ecology 92:1917-1923

Hansen BB, Aanes R, Saether BE (2010) Partial seasonal migration in high-Arctic Svalbard reindeer (*Rangifer tarandus platyrhynchus*). Can J Zool 88:1202-1209

Hansen BB, Gameleon M, Albon SD, et al. (2019a) More frequent extreme climate events stabilize reindeer population dynamics. Nat Commun 10:1616

Hansen BB, Grøtan V, Aanes R, et al. (2013) Climate events synchronize the dynamics of a resident vertebrate community in the High ArcticArctic. Science 339:313-315

Hansen BB, Pedersen ÅØ, Peeters B, et al. (2019b) Spatial heterogeneity in climate change decouples the long-term dynamics of wild reindeer populations in the high Arctic. Glob Change Biol 00:1-13

Hanssen-Bauer I, Førland EJ, Hisdal H, et al. (2019) Climate in Svalbard 2100 – a knowledge base for climate adaptation. Norwegian Environment Agency (Miljødirektoratet), Oslo, Norway

Henden JA, Ims RA, Fuglei E, Pedersen ÅØ (2017) Changed Arctic-alpine food web interactions under rapid climate warming: implication for ptarmigan research. Wildlife Biol https://doi.org/10.2981/wlb.00240

Henttonen H, Fuglei E, Gower CN, et al (2001) *Echinococcus multilocularis* on Svalbard: introduction of an intermediate host has enabled the local life-cycle Parasitology 123:547-552

Ims RA, Ehrich D (2013) Arctic terrestrial Ecosystem. Chapter 13. In: Arctic Biodiversity Assessments. Meltofte, H. (ed.) Conservation of Arctic Flora and Fauna (CAFF), Akureyri, Iceland

Ims RA, Fuglei E (2005) Trophic interaction cycles in tundra ecosystems and the impact of climate change. Bioscience 55:311-322

Ims RA, Jepsen JU, Stien A, Yoccoz NG (2013) Science Plan for COAT: Climate-ecological Observatory for Arctic Tundra. Fram Centre, Tromsø

Ims RA, Yoccoz NG (2017) Ecosystem-based monitoring in the age of rapid climate change and new technologies Curr Opin Env Sust 29:170-176

IPCC (2019) Summary for Policymakers. In: IPCC Special Report on the Ocean and Cryosphere in a Changing Climate [H.-O. Pörtner, D.C. Roberts, V. Masson-Delmotte, P. Zhai, M. Tignor, E. Poloczanska, K. Mintenbeck, M. Nicolai, A. Okem, J. Petzold, B. Rama, N. Weyer (eds.)]. In press

Isaksen K, Nordli Ø, Førland EJ, et al (2016) Recent warming on Spitsbergen—Influence of atmospheric circulation and sea ice cover.J Geophys Res: Atmospheres 121: 11,913-11,931

Isaksen K, Sollid JL, Holmlund P, Harris C (2007) Recent warming of mountain permafrost in Svalbard and Scandinavia. J Geophys Res-Earth Surf 112 https://doi.org/10.1029/2006jf000522

IUCN (2009) Species and climate: More than just the polar bear. Species Survival Commission (SSC). doi:www.iucnredlist.org

Jensen GH, Madsen J, Johnson FA, Tamstorf MP (2014) Snow conditions as an estimator of the breeding output in High-Arctic pink-footed geese *Anser brachyrhynchus*. Polar Biol 37:1-14

Jensen GH, Madsen J, Nagy S, Lewis M (2018) AEWA international single species management plan for the barnacle goose (Branta leucopsis): Russia/Germany & Netherlands population, East Greenland/Scotland & Ireland population, Svalbard/South-west Scotland population. AEWA Technical Series, Bonn, Germany

Jensen RA, Madsen J, O'Connell M, et al (2008) Prediction of the distribution of Arctic-nesting pink-footed geese under a warmer climate scenario. Glob Change Biol 14:1-10

Jepsen JU, Arneberg P, Ims RA, Siwertsson A, Yoccoz NG (2019) Test av fagsystemet for økologisk tilstand. Erfaringer fra pilotprosjekter for arktisk tundra og arktisk del av Barentshavet NINA Rapport 1674 Norsk institutt for naturforskning

Johansen B, Tommervik H (2014) The relationship between phytomass, NDVI and vegetation communities Svalbard. Int J Appl Earth Obs Geoinf 27:20-30

Johnson FA, Høj Jensen G, Clausen KK, Madsen JC (2018) Adaptive Harvest Management for the Svalbard Population of Pink-Footed Geese 2018 Progress Summary (*Anser brachyrhynchus*). AEWA EGMP Technical, Report No 9 Bonn, Germany

Karlsen SR, Anderson HB, van der Wal R, Hansen BB (2018) A new NDVI measure that overcomes data sparsity in cloud-covered regions predicts annual variation in ground-based estimates of high Arctic plant productivity Env Res Lett 13. https://doi.org/10.1088/1748-9326/aa9f75

Karlsen SR, Stendari L, Nilsen L, Malnes E, Eklundh L, Julitta T, Burkhart A, Tømmervik H (2020) Sentinel based mapping of plant productivity in relation to snow duration and time of green-up. In: Van den Heuvel et al. (eds): SESS report 2019, Svalbard Integrated Arctic Earth Observing System, Longyearbyen, 42 - 57 . https://sios-svalbard.org/SESS_Issue2

Kovacs KM, Lydersen Ce (2006) Birds and mammals of Svalbard Norwegian Polar Institute, Tromsø:203

Kuijper DPJ, Bakker JP, Cooper EJ, et al (2006) Intensive grazing by Barnacle geese depletes High Arctic seed bank. Can J Bot-Rev Can Bot 84:995-1004

Laidre KL, Stern H, Kovacs, KM, et al. (2015) Arctic marine mammal population status, sea ice habitat loss, and conservation recommendations for the 21st century. Cons Biol 29:724-737

Layton-Matthews K, Hansen BB, Grotan V, et al (2019a) Contrasting consequences of climate change for migratory geese: Predation, density dependence and carryover effects offset benefits of High-Arctic warming. Glob Change Biol https://doi.org/10.1111/gcb.14773

Layton-Matthews K, Loonen M, Hansen B, et al (2019b) Density-dependent population dynamics of a high Arctic capital breeder, the barnacle goose. J Anim Ecol 88 https://doi.org/10.1111/1365-2656.13001

Le Moullec M (2019) A century of recovery from overharvest in a warming High-Arctic: the successful conservation story of endemic Svalbard reindeer J Wildlife Manage 83:1676-1686

Le Moullec M, Buchwal A, van der Wal R, et al (2019) Annual ring growth of a widespread high Arctic shrub reflects past fluctuations in community-level plant biomass. J Ecol 107:436-451

Legg CJ, Nagy L (2006) Why most conservation monitoring is, but need not be, a waste of time. J Environ Manage 78:194-199

Lindenmayer DB, Likens GE (2009) Adaptive monitoring: a new paradigm for long-term research and monitoring. Trends Ecol Evol 24:482-486

Lindenmayer DB, Likens GE (2010a) Effective ecological monitoring. CSIRO Publishing, Collingwood, Vic., Australia

Lindenmayer DB, Likens GE (2010b) The science and application of ecological monitoring. Biol Cons 143:1317-1328

Lindenmayer DB, Likens GE, Haywood A, Miezis L (2011) Adaptive monitoring in the real world: proof of concept. Trends Ecol Evol 26:641-646

Liston GE, Elder K (2006) A distributed snow-evolution modeling system (SnowModel). J Hydrometeorol 7:1259-1276

Løvenskiold HL (1964) Avifauna Svalbardensis Norsk Polarinstitutt Skrifter 129

Macias-Fauria M, Karlsen SR, Forbes BC (2017) Disentangling the coupling between sea ice and tundra productivity in Svalbard. Sci Rep-UK 7 https://doi.org/10.1038/s41598-017-06218-8

Madsen J, Cracknell G, Fox AD (eds) (1999) Goose Populations of the Western PaleArctic. A review of status and distribution. vol 48. Wetlands International Publication. Wetlands International, Wageningen, The Netherlands. National Environmental Research Institute, Rønde, Denmark,

Madsen J, Jaspers C, Tamstorf MP, et al (2011) Long-term effects of grazing and global warming on the composition and carrying capacity of graminoid marshes for moulting geese in East Greenland. Ambio 40:638-649

Madsen J, Jensen GJ, Cottaar F, et al. (2018) Svalbard pink-footed goose: Population status report 2017-2018. AEWA European goose management platform, Leeuwarden, the Netherlands

Madsen J, Tamstorf M, Klaassen M, et al. (2007) Effects of snow cover on the timing and success of reproduction in High-Arctic pink-footed geese *Anser brachyrhynchus* Polar Biol 30:1363-1372

Madsen J, Williams JH (2012) International species management plan for the svalbard population of the pink-footed goose *Anser brachyrhynchus* AEWA Technical report no 48

Meltofte H, Barry T, Berteaux D, et al. (2013) Arctic Biodiversity Assesment. Synthesis. Conservation of Arctic Flora and Fauna (CAFF),

Milner JM, Stien A, van der Wal R (2018) Retrospective growth analysis of the dwarf shrub *Cassiope tetragona* allows local estimation of vascular plant productivity in high Arctic Svalbard. J Veg Sci 29:943-951

Milner JM, Varpe O, van der Wal R, Hansen BB (2016) Experimental icing affects growth, mortality, and flowering in a high Arctic dwarf shrub. Ecol Evol 6:2139-2148

Musche M, Adamescu M, Angelstam P, et al. (2019) Research questions to facilitate the future development of European longterm ecosystem research infrastructures: A horizon scanning exercise. J Environ Manage 250: 109479

Mørk T, Bohlin J, Fuglei E, et al (2011) Rabies in the Arctic fox population, Svalbard,Norway. J Wildlife Dis 47:945-957

Nichols JD, Williams BK (2006) Monitoring for conservation. Trends Ecol Evol 21:668-673

Nordli O, Przybylak R, Ogilvie AEJ, Isaksen K (2014) Long-term temperature trends and variability on Spitsbergen: the extended Svalbard Airport temperature series, 1898-2012. Polar Res 33 https://doi.org/10.3402/polar.v33.21349

Onarheim IH, Eldevik T, Smedsrud LH, Stroeve JC (2018) Seasonal and regional manifestation of Arctic sea ice loss. J Clim 31:4917-4932

Pedersen ÅØ, Speed JDM, Tombre IM (2013a) Prevalence of pink-footed goose grubbing in the Arctic tundra increases with population expansion. Polar Biol 36:1569-1575

Pedersen ÅØ, Stien J, Eidesen PB, et al. (2018) High goose abundance reduces nest predation risk in a simple rodent-free High-Arctic ecosystem. Polar Biol 41:619-627

Pedersen ÅØ, Tombre I, Jepsen JU, et al (2013b) Spatial patterns of goose grubbing suggest elevated grubbing in dry habitats linked to early snowmelt. Polar Res 32 https://doi.org/10.3402/polar.v32i0.19719

Pedersen ÅØ, Tombre I, Jepsen JU, et al (2013c) Spatial patterns of goose grubbing suggest elevated grubbing in dry habitats linked to early snowmelt. Polar Res32:19719

Peeters B, Pedersen ÅØ, Loe LE, et al. (2019) Spatiotemporal patterns of rain-on-snow and basal ice in high Arctic Svalbard: detection of a climate-cryosphere regime shift. Environ Res Lett 14 https://doi.org/10.1088/1748-9326/aaefb3

Post E, Forchhammer MC, Bret-Harte MS, et al. (2009) Ecological dynamics across the Arctic associated with recent climate change. Science 325:1355-1358

Prestrud KW, Aasbakk KW, Fuglei E, et al. (2007) Serosurvey for Toxoplasma gondii in Arctic fox and its source species of infection in the high Arctic of Svalbard. Vet Parasitol 150:6-12

Prestrud P (1992) Food-habits and observations of the hunting behavior of Arctic foxes, *Alopex-lagopus*, in svalbard. Can Field Nat 106:225-236

Prop J, Aars J, Bårdsen BJ, et al. (2015) Climate change and the increasing impact of polar bears on bird populations. Front Ecol Evol 25 http://dx.doi.org/10.3389/fevo.2015.00033

Ravolainen VT, Soininen EM, Jónsdóttir IS, et al (2019). High Arctic ecosystem states: conceptualizing vegetation change for long-term monitoring and research. Sumbitted to AMBIO

Renner AHH, Sundfjord A, Janout MA, et al (2018) Variability and redistribution of heat in the atlantic water boundary current north of svalbard. J Geophys Res: Oceans 123:6373-6391

Rivrud IM, Meisingset EL, Loe LE, Mysterud A (2019) Future suitability of habitat in a migratory ungulate under climate change. Proc R Soc B: Biol Sci 286:20190442

Soininen E, Fuglei E, Pedersen ÅØ (2016) Complementary use of density estimates and hunting statistics: different sides of the same story? Eur J Wildl Res https://doi.org/10.1007/s10344-016-0987-z

Speed JDM, Woodin SJ, Tommervik H, et al (2009) Predicting habitat utilization and extent of ecosystem disturbance by an increasing herbivore population. Ecosystems 12:349-359

Steen JB, Unander S (1985) Breeding biology of the Svalbard rock ptarmigan *Lagopus mutus hyperboreus*. Ornis Scand 16:191-197

Stien A, Ims RA, Albon SD, et al. (2012) Congruent responses to weather variability in high Arctic herbivores. Biol Lett 8:1002-1005

Strøm H, Bangjord G (2004) The birds and mammal fauna of Svalbard. In: P Prestrud, H Strøm, and H Goldman, editors A catalogue of the terrestrial and marine animals of Svalbard Norwegian Polar Institute Skrifter 20:123–137

Sørensen KK, Mørk T, Sigurdardottir OG,et al (2005) Acute toxoplasmosis in three wild Arctic foxes (*Alopex lagopus*) from Svalbard; one with co-infections of Salmonella enteritidis PT1 and Yersinia pseudotuberculosis serotype 2b. Res Vet Sci 78:161-167

Tarroux A, Bety J, Gauthier G, Berteaux D (2012) The marine side of a terrestrial carnivore: intra-population variation in use of allochthonous resources by Arctic foxes. PLoS One 7 https://doi.org/10.1371/journal.pone.0042427

Unander S, Mortensen A, Elvebakk A (1985) Seasonal changes in crop content of the Svalbard Ptarmigan *Lagopus mutus hyperboreus*. Polar Res 3:239-245

van der Wal R, Bardgett RD, Harrison KA, Stien A (2004) Vertebrate herbivores and ecosystem control: cascading effects of faeces on tundra ecosystems. Ecography 27:242-252

van der Wal R, Brooker R, Cooper E, Langvatn R (2001) Differential effects of reindeer on high Arctic lichens. J Veg Sci 12:705-710 Van der Wal R, Brooker RW (2004) Mosses mediate grazer impacts on grass abundance in Arctic ecosystems. Funct Ecol 18:77-86

van der Wal R, Egas M, van der Veen A, Bakker J (2000) Effects of resource competition and herbivory on plant performance along a natural productivity gradient. J Ecol:317-330

van der Wal R, Sjögersten S, Woodin SJ, et al. (2007) Spring feeding by pink-footed geese reduces carbon stocks and sink strength in tundra ecosystems. Glob Change Biol13:539-545

van der Wal R, Stien A (2014) High Arctic plants like it hot: a long term investigation of between-year variability in plant biomass across habitats and species. Ecology 95:3414–3427

Vickers H, Hogda KA, Solbo S, et al (2016) Changes in greening in the high Arctic: insights from a 30 year AVHRR max NDVI dataset for Svalbard Environ Res Lett 11 https://doi.org/10.1088/1748-9326/11/10/105004

Vikhamar-Schuler D, Isaksen K, Haugen JE, et al (2016) Changes in winter warming events in the nordic Arctic region. J Clim 29:6223-6244

Wann GT, Aldridge CL, Seglund AE, et al (2019) Mismatches between breeding phenology and resource abundance of resident alpine ptarmigan negatively affect chick survival. Ecol Evol 9:7200-7212

Wisz M, Dendoncker N, Madsen J, et al. (2008) Modelling pink-footed goose (*Anser brachyrhynchus*) wintering distributions for the year 2050: potential effects of land-use change in Europe. Divers Distrib 14:721-731

Yoccoz NG, Nichols JD, Boulinier T (2001) Monitoring of biological diversity in space and time. Trends Ecol Evol 16:446-453

Zwolicki A, Zmudczynska-Skarbek K, Matula J, et al (2016) Differential responses of Arctic vegetation to nutrient enrichment by plankton- and fish-eating colonial seabirds in spitsbergen Front Plant Sci 7 https://doi.org/10.3389/fpls.2016.01959

Zwolicki A, Zmudczynska-Skarbek KM, Iliszko L, Stempniewicz L (2013) Guano deposition and nutrient enrichment in the vicinity of planktivorous and piscivorous seabird colonies in Spitsbergen. Polar Biol 36:363-372

Østby TI, Schuler TV, Hagen JO, et al (2017) Diagnosing the decline in climatic mass balance of glaciers in Svalbard over 1957-2014. Cryosphere 11:191-215

Environmental Monitoring in the Kapp Linné-Grønfjorden Region (KLEO)

Michael Retelle[1,2], Hanne Christiansen[1], Andy Hodson[1], Anna Nikulina[3], Marzena Osuch[4], Ksenia Poleshuk[3], Kseniia Romashova[3], Steve Roof[5], Line Rouyet[6,7,1], Sarah Marie Strand[1,8], Igor Vasilevich[3], Tomasz Wawrzyniak[4]

1 University Centre in Svalbard, Arctic Geology Department, Longyearbyen, Norway
2 Bates College, Lewiston, Maine, USA
3 Arctic and Antarctic Research Institute, St Petersburg, Russia
4 Institute of Geophysics Polish Academy of Sciences, Warsaw, Poland
5 Hampshire College, Amherst, USA
6 NORCE Norwegian Research Centre AS, Tromsø, Norway
7 UiT, The Arctic University of Norway, Department of Geosciences, Norway
8 University of Oslo, Department of Geosciences, Norway

Corresponding author: Michael Retelle, mretelle@bates.edu

Keywords: Hydroclimate, Arctic monitoring, periglacial geomorphology, permafrost

1. Introduction

The ability to understand and predict environmental changes in Svalbard is highly dependent on the availability of detailed and long-term records of baseline environmental data from a regional network across the archipelago. The Kapp Linné region provides a strategic location for a dedicated long-term environmental observatory in the western coastal region of the Nordenskiöldland Peninsula. This region is greatly influenced by the Atlantic High Arctic maritime climate regime (Eckerstorfer and Christiansen 2011) with higher mean annual air temperature and greater precipitation than the more continental interior regime in central Spitsbergen (Humlum 2002). With the recent intensified Atlantification of the northern Barents Sea (Nilsen et al. 2016; Barton et al. 2018), environmental monitoring studies along the Nordenskiöldland coast may help to serve as an early warning system for climate change and accompanying environmental responses across the Svalbard archipelago.

The Kapp Linné Environmental Observatory (KLEO) was formulated as an international collaborative site within the Svalbard Integrated Arctic Earth Observing System (SIOS) to contribute the results of long-term and interdisciplinary environmental monitoring in the Kapp Linné region to the State of Environmental Science in Svalbard (SESS) report 2019 and to enhance future collaboration among researchers. In this report we will provide: (1) an introduction to the study area with an inventory of ongoing research programs, instrumental installations and archived data within the SIOS network, (2) highlight recent, significant developments in hydroclimate research and (3) provide an outline for future developments in collaborative interdisciplinary environmental research.

The KLEO research sites span an area extending from the west coast of Spitsbergen at the mouth of Isfjorden, to the eastern shore of Grønfjord (Figure 1). The regional physiography is strongly controlled by both the bedrock type and the structural architecture of the northwest-striking West Spitsbergen Fold Belt (Dallman 2015). In the west, the Isfjordflya terrain along the coast is the northern extension of the 40 km long Nordenskiöldkysten strandflat complex, a low-lying Precambrian bedrock platform that is mantled by prominent set of gravel raised beach deposits (Landvik et al. 1987). Isfjord Radio, the long-standing weather station at Kapp Linné is situated at the northern tip of the strandflat. A prominent ridgeline of sharp peaks, comprised of pre-Cambrian phyllite (Ohta et al. 1992) reaches up to 780 meters in elevation and separates the coastal strandflat from Linnédalen and defines the western margin of Linnédalen watershed. The sharp ridge is incised with numerous well-defined cirques (some with small glaciers) and flanked by steep, coarse alluvial fans and several rock glaciers. The broad central valley of Linnédalen is oriented NNW along bedrock strike, is approximately 14 km long and up to 2 km wide, and is floored by light-coloured Carboniferous quartzite (Ohta et al. 1992).

Linnébreen, at the southern head of the valley, is a small polythermal valley glacier (currently

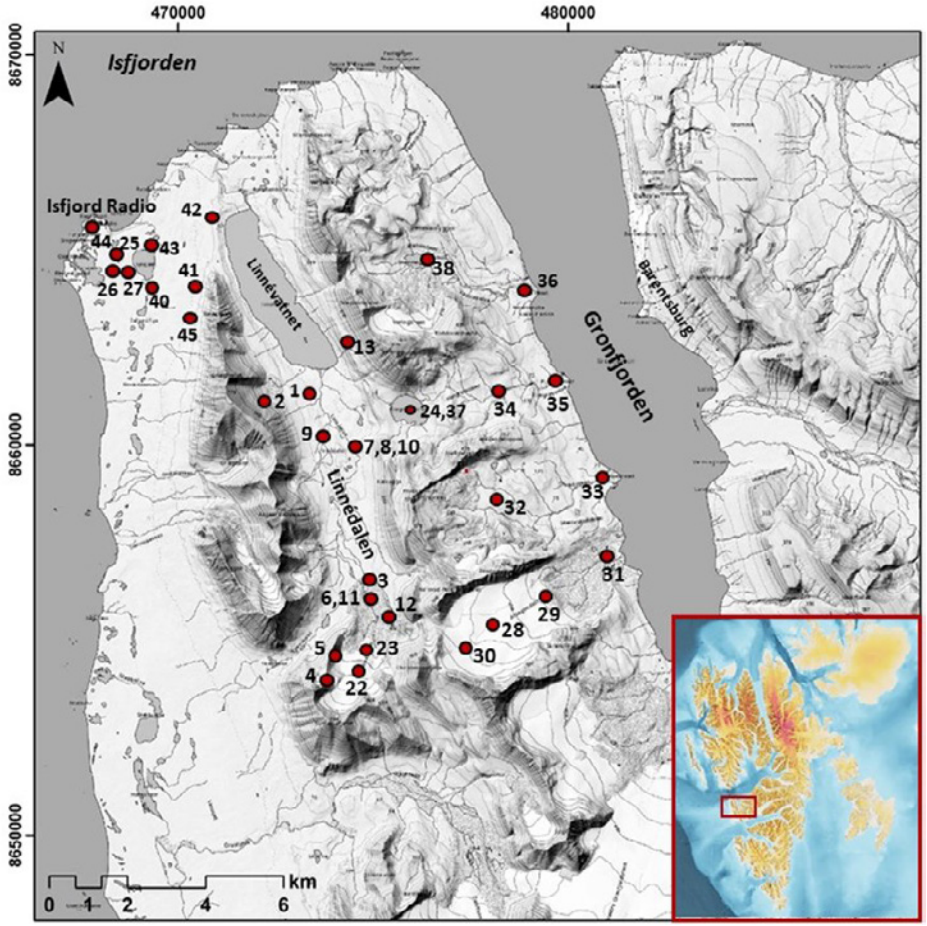

Figure 1: Location map of the Nordenskiöldkysten - Kapp Linné - Grønfjorden region. Inset map of Svalbard archipelago shows field area in red box. Numbers are monitoring instruments and installations. Refer to Appendix for descriptions.

approx. 2 km long) which resides in a steep bedrock amphitheatre and contributes meltwater to Linnéelva which flows almost 7 km to Linnévatnet (which will be described in more detail below). The eastern wall of Linnédalen is flanked by a ridge of Permian-age sedimentary rocks including dolomite, limestone, gypsum, and sandstone. This sedimentary sequence extends northeast of Linnévatnet to the Vardeborgsletta area where numerous karst features including dolines and sinkholes have been described by Salvigsen and Elgersma (1985). Kongressvatnet, a unique sulfate-rich 57-meter deep meromictic karst lake (Boyum and Kjensmo 1970; Guilizzoni et al. 2006; Holm et al. 2011), is situated in the saddle between Linnédalen and Grønfjorden in this same karst terrain. This unique lake yearly

exhibits significant changes in lake level as a result of karst drainage. The eastern flank of the ridge is comprised of younger east-dipping sedimentary strata of Mesozoic age which are well exposed in the classic Festningen section along the Isfjorden shore at the western mouth of Grønfjorden (Mørk and Worsley 2006). Several east-facing cirque glaciers, Aldegondebreen and Vøringbreen, and the more extensive Grønfjordbreen valley glacier complex are located along this ridge. Grønfjorden and the terrain to the east occupies an incised plateau topography due to the flat-lying Cenozoic-age sedimentary rocks of the Van Mijenfjorden Group, which contains the coal-bearing Firkanten Formation mined in Barentsburg and around Longyearbyen (Ohta et al. 1992).

2. Overview of existing knowledge

Relatively easy logistical access to Kapp Linné and Barentsburg, coupled with existing research infrastructure at sites across Kapp Linné, in Linnédalen and in the Grønfjorden region provides a solid foundation on which to continue monitoring and observations and to develop new environmental monitoring studies. Current long-term monitoring studies highlighted in this report include hydroclimate monitoring and paleoclimate studies in Linnédalen (initiated in 2003), UNIS faculty and student research focused in permafrost and periglacial geomorphology (initiated in 2004) and studies in cryo-hydrology and paleoecology in the adjacent Grønfjord region by the University Centre in Svalbard (UNIS) and Barentsburg Science Center researchers. Figure 1 illustrates a location map of instruments and installments in the region. An array of instrumentation in the 31 km^2 catchment of Linnédalen documents changes in the glacial-fluvial-lake system including an automated weather station, snow and water temperature sensors, time-lapse cameras, and moorings deployed in Linnévatnet. Development of the instrumental network in the watershed was initially supported by grants from the U.S. National Science Foundation Polar Programs and monitoring efforts have been sustained in recent years by faculty-student research at UNIS. A detailed list of the installations and instruments and their respective data series is shown in Appendix 1.

Regional Climatology: The Isfjord Radio meteorological station (78.0623°N 13.6157°E, 7 m a.s.l). is located on Kapp Linné at the southern edge of the mouth of Isfjorden. The first meteorological station was established on 1 September 1934 and was operating until 30 June 1941, then was destroyed by the actions of war. On 1 September 1946, the station was re-established at the same location. The measurements and observations have been conducted as one of the WMO indexed stations with the international numbering system 01013 until 30 June 1976. From this date onwards, the station was no longer used for climatological purposes; however an automatic weather station was re-established again for the periods 1 Jan 1997 – 5 Feb 2002, 20 Jun 2002 – 6 Dec 2004, and from 10 Sep 2014 to present. For the climatological description in this report, the data were homogenised

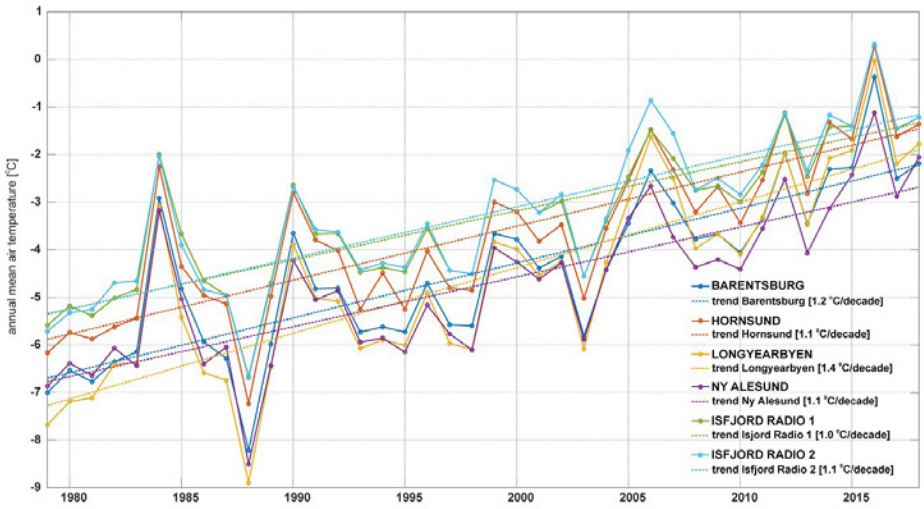

Figure 2: Variability of annual mean air temperatures in 1979-2018 at Barensburg, Hornsund, Longyearbyen, Ny-Ålesund, and two homogenised series for Isfjord Radio 1 and 2, where gaps were filled using data from Barentsburg and Longyearbyen respectively.

for the period 1979-2018 using the aforementioned original series together with the reconstructed daily series by linear regression from neighbouring stations in Barentsburg and Longyearbyen as predictors. Warm and humid air transported by extratropical cyclones from lower latitudes and warm West Spitsbergen current have a significant influence on the climate of Isfjord Radio, which is maritime and mild, concerning its high latitude. The long-term (1979-2018) mean annual air temperature (MAAT) is -3.4°C. The coldest month is March with the average temperature -10.0°C and the warmest July with 5.8°C.

A comparison of the mean annual air temperatures and their trends per decade at meteorological stations: Barentsburg (WMO Site 20107), Hornsund (WMO Site 01003), Svalbard Lufthavn (WMO Site 01008), Ny-Ålesund (01007) and Isfjord Radio is shown in Figure 2. In the case of Isfjord Radio, there are two homogenised series where gaps in the data series were filled using linear regression on data from Barentsburg (Isfjord Radio 1) and Longyearbyen (Isfjord Radio 2). The trends were estimated by the modified Mann-Kendall test (Mann 1945; Kendall 1975; Hamed and Rao 1998). The slope of the trend was estimated using the Sen's method (Sen 1968). A statistically significant increase in annual mean air temperatures at all stations shows that air temperature in the whole western and central part of Spitsbergen is shaped by the common sets of climatic processes that have broad impacts on the Atlantic Arctic (Osuch and Wawrzyniak 2017). The tendency is the same, and the range of these changes is from 1.0°C per decade at Isfjord Radio 1, to 1.4°C per decade in Longyearbyen.

Table 1: Comparison of mean monthly air temperature between Barentsburg, Hornsund, Longyearbyen, Ny-Ålesund and two reconstructed time series from Isfjord Radio. Measurements cover the period from 1979 to 2018.

Site	JAN	FEB	MAR	APR	MAY	JUN	JUL	AUG	SEP	OCT	NOV	DEC	Annual
Barenstburg	-11.3	-11.9	-12.0	-9.5	-3.1	2.4	6.1	5.2	1.4	-4.1	-7.3	-10.0	-4.5
Hornsund	-9.7	-9.7	-10.2	-8.1	-2.5	2.1	4.6	4.2	1.8	-2.7	-5.7	-8.6	-3.7
Longyearbyen	-12.1	-12.6	-12.6	-9.8	-2.7	3.1	6.6	5.6	1.5	-4.3	-7.7	-10.7	-4.6
Ny Ålesund	-11.4	-12.0	-12.0	-9.4	-2.8	2.4	5.5	4.4	0.7	-4.7	-7.7	-10.2	-4.8
Isfjord Radio 1	-9.4	-9.8	-10.0	-7.8	-2.2	2.7	5.8	5.1	1.9	-2.9	-5.8	-8.2	-3.4
Isfjord Radio 2	-9.3	-9.7	-9.7	-7.5	-1.9	2.8	5.7	5.0	1.8	-2.9	-5.8	-8.2	-3.3

A comparison of mean monthly conditions at the investigated stations during the period 1979-2018 is presented in Table 1. The span of observed mean monthly air temperatures during the year is varying between stations. The smaller difference is observed at Isfjord Radio and Hornsund while higher for Longyearbyen and Barentsburg due to the smaller influence of the ocean.

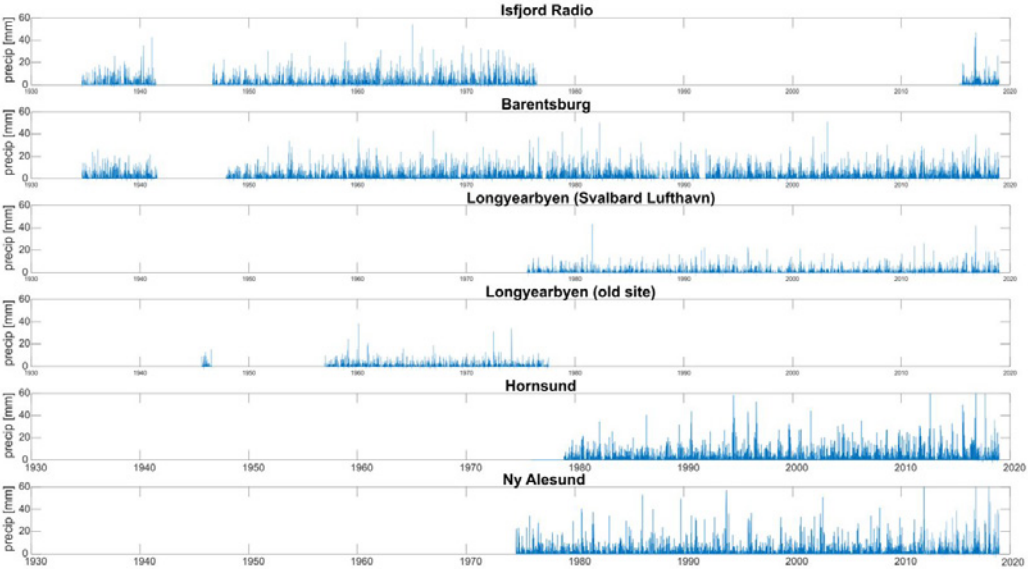

Figure 3: Diurnal sum of precipitation time series at meteorological sites in Spitsbergen in the period 1934-2018.

Measurements of daily sum precipitation at Isfjord Radio started on 1 September 1934 and were conducted in the same periods as air temperature described in the previous section. Precipitation time series at the six meteorological sites in Spitsbergen: Isfjord Radio, Barentsburg, Longyearbyen (old site), Longyearbyen (Svalbard Lufthavn), Hornsund, and

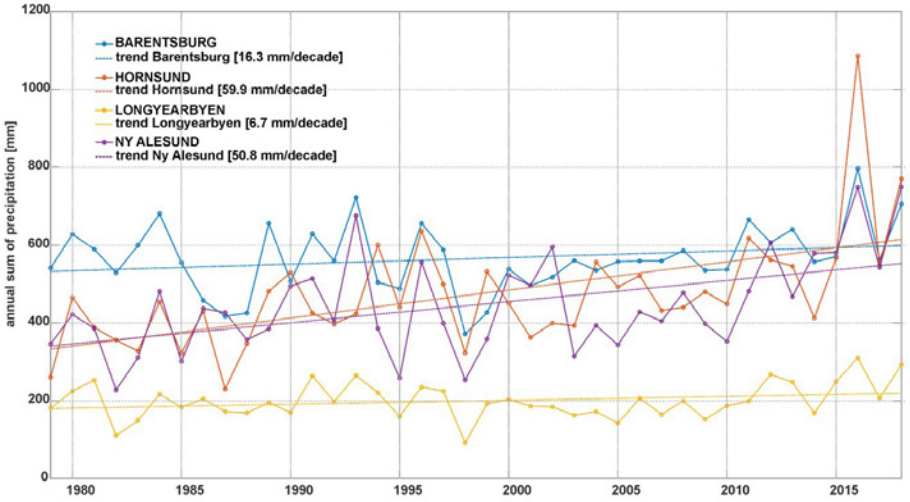

Figure 4: Variability of an annual sum of precipitation in 1979-2018 at Barentsburg, Hornsund, Longyearbyen, and Ny-Ålesund.

Ny-Ålesund are presented in Figure 3. Precipitation was not observed continuously at these sites before 1979. There are gaps and breaks in data that make current precipitation trend analyses difficult or impossible. As no data are available for Isfjord Radio for period 1 Jan 1979 - 2 May 2015 and in some shorter periods, the analyses were performed for other stations (Figure 4). The more detailed description is provided in this section for the Barentsburg data, located 14.5 km to the East from Isfjord Radio.

A comparison of the mean monthly sum of precipitation at the investigated stations during the period 1979-2018 is presented in Table 2. The highest annual precipitation is observed at Barentsburg (565 mm) and the lowest at Longyearbyen (200 mm). Hornsund and Ny-Ålesund have similar sums of precipitation. Although there are differences in the amount of precipitation between stations, their seasonal runs are generally similar. The driest months at all stations are May and June. The highest precipitation occurs in September at Hornsund and Ny-Ålesund, in November at Barentsburg, and in August at Longyearbyen. The span of the observed mean monthly sum of precipitation during the year

Table 2: Mean monthly sum of precipitation over period 1979-2018 at Barentsburg, Hornsund, Longyearbyen, and Ny-Ålesund.

Site	JAN	FEB	MAR	APR	MAY	JUN	JUL	AUG	SEP	OCT	NOV	DEC	Annual
Barentsburg	60	51	56	41	30	21	28	40	55	61	63	59	565
Hornsund	35	29	29	22	24	29	46	55	76	54	40	35	474
Longyearbyen	18	18	18	10	7	9	18	24	23	16	19	19	200
Ny Ålesund	51	41	45	26	18	16	29	39	57	41	44	39	446

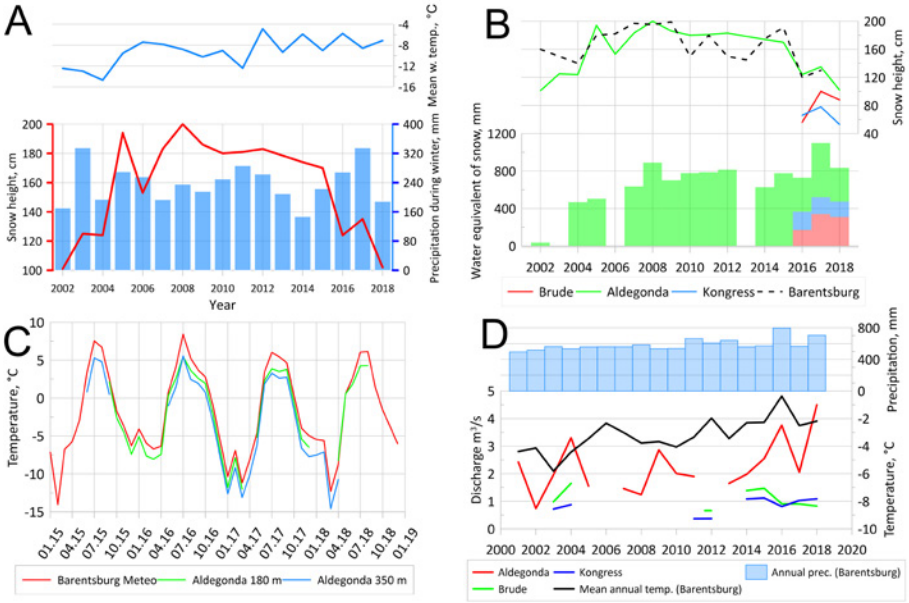

Figure 5: **A:** Variability of average snow cover height on Aldegonda glacier compared to average temperature and precipitation amount during the winter period (December-March); **B:** Variability of average snow cover height in Brude and Kongress river catchments, Aldegonda glacier and weather station in Barentsburg. **C:** Variability of average monthly temperature on weather stations in Barenstburg and Aldegonda glacier from 2015 to 2019; **D:** Variability of average water discharges of Aldegonda, Brude and Kongress rivers compared to annual precipitation and mean annual temperature in Barentsburg.

is varying between stations. The smallest difference is observed at Longyearbyen located in the inner part of the Spitsbergen island, with a more continental climate compared to the other stations.

Groundwater and Surface Water Hydrology in the Grønfjorden Region: Since 2001, the Arctic and Antarctic Research Institute (AARI) has been providing hydrological observations on the west shore of Grønfjorden in the Aldegonda, Bryde and Kongress watersheds. Snow cover observations (height, density, stratification) are carried out during the period of maximum snow accumulation (Figure 5A,B), and during the summer, continuous records of water and sediment discharge are collected. Complete observations on the rivers have been conducted since 2016. In addition to these observations on Aldegondabreen, two autonomous meteorological stations provide measurements at different altitudes (Figure 5C).The available data indicate a weak relationship between the average annual temperature, total annual precipitation and average river discharge (Figure 5D). The seasonal hydrographs of the rivers Aldegonda, Bryde, and Kongress correlate well with each other, despite the

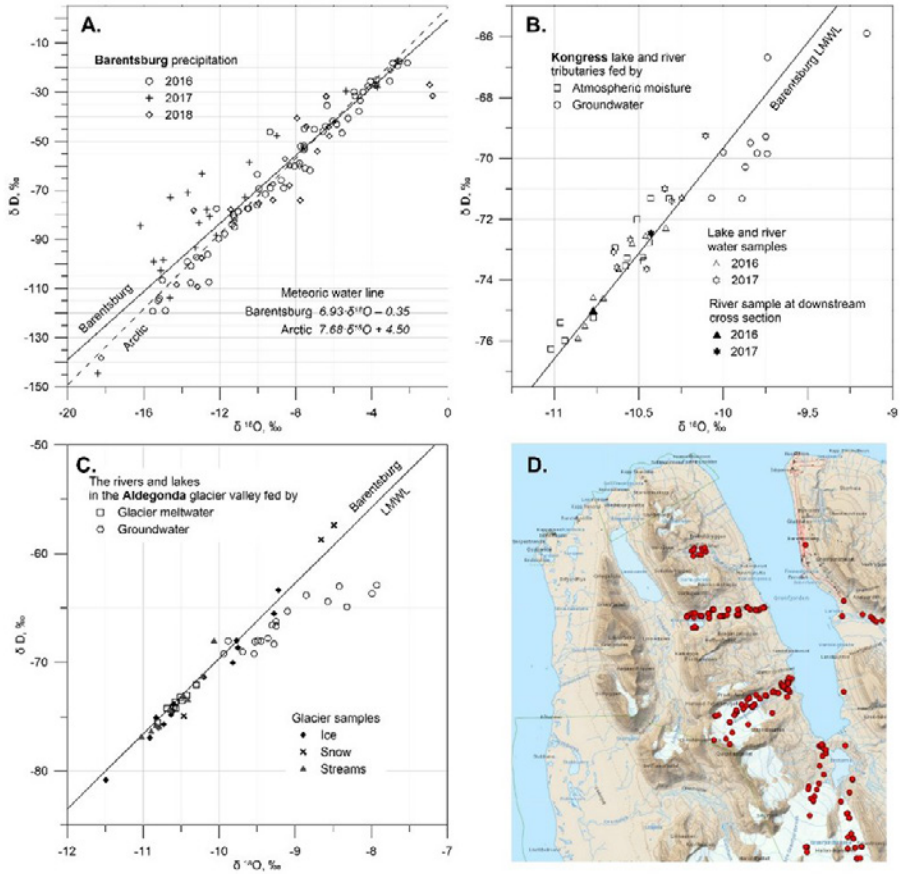

Figure 6: Isotopic composition of precipitation at Barentsburg meteorological station, surface and groundwater in Grønfjorden region. **A:** Meteoric water line (concentration of deuterium (δD) as a function of the concentration of oxygen-18 (δ18O): Barentsburg water line is calculated in 2016-2017, Arctic water line is drawn after Wetzel 1990; **B:** Isotopic signature of Kongressvatnet and adjacent rivers; **C:** Isotopic signature of Aldegondabreen snow, ice, meltwater and groundwater; **D:** Map of sampling sites for water isotopic composition, 2016-2018.

different types of river sources (Bryde and Aldegonda are glacier-fed rivers, Kongress lake- and snow-fed river). This is because the melting of the snow cover and liquid precipitation make a significant contribution to the annual river flow in all watersheds.

In 2016 at the Barentsburg research station AARI renewed the collecting of atmospheric precipitation samples for stable isotopic composition (δ18Oand δD) conducted in 1975-1981 by the Institute of Geography, Russian Academy of Sciences. Terrestrial waters, glacier snow, and ice have been sampled as well in the region of Grønfjorden in 2016-2018,

enabling the water isotopes to provide a record of water source changes for the future. The local meteoric water line (Figure 6A) has been drawn from the isotopic composition of samples taken in 2016-2017 and is defined as δD=6,93δ18O-0,35 (Skakun et al. 2019). The data of 2018 agree closely with the local Meteoric Water Line (LMWL), but show a slightly lower slope coefficient, indicating potential changes in moisture and water sources. Data from Barentsburg (1975-1981, 2016-2017) and Isfjord Radio 1960-1976 (Dansgaard 1964, IAE/WMO 2006) show that monthly mean isotopic composition of precipitation correlates well with monthly mean air temperature values, but the correlation varies between the winter and summer seasons. Isotopic composition in Ny-Ålesund and Hornsund poorly correlate with air temperature and depends on wind direction, ice formation in the fjords and other factors (Skakun et al. 2019).

The isotopic composition in Kongressvatnet showed that in spite of the dominance of meteoric water sources in the lake, there is strong inter-annual variability that indicates variations in groundwater recharge (Figure. 6B). The tributaries of Kongresselva also have different sources of water – thirteen of them have meteoric water (snowmelt and rain), and 8 have a groundwater source. At Aldegondabreen River, ice, snow and stream water (Figure 6C) collected on the glacier surface had isotopic composition close to LMWL, but the small lakes in the forefield are isotopically heavier due to evaporation and groundwater input. Lakes and streams further down the valley increasingly exhibit a deuterium excess (d-excess), demonstrating the sensitivity of stable isotopes to changing groundwater inputs, which are detectable in many of the watersheds on the west side of Grønfjorden.

Hydroclimate Research in the Glaciated Linnédalen Watershed: At the upper reaches of the watershed, the small valley glacier Linnébreen has been in steady retreat; earlier studies (2003-2013) detailed a sustained negative mass balance. Analysis of available imagery and annual mapping of the terminus since 2004 has shown that the glacier front has retreated approximately 1.8 km since 1936 and 1 km between 1995 and 2019 (Figure 7).

Downvalley from Linnébreen, a major research emphasis in Linnédalen since 2003 has been to monitor seasonal and interannual environmental processes in the glacier-river-lake system. Since lakes are situated in the lowest part of watersheds and they record inputs from physical, chemical and biological processes over short to long temporal scales, they can be acknowledged as sentinels of climate and environmental change (Williamson et al. 2009). In the Linnédalen watershed, integration of meteorological data, time-lapse photography, and temperature and sediment trap analysis provides a detailed archive of snow cover and melt, seasonal lake ice duration on Linnévatnet and timing and duration of fluvial activity including extreme events.

Linnévatnet (12 m a.s.l.) is a cold monomictic lake (Boyum and Kjensmo 1978) with the long axis oriented in an NNW-SSE direction along bedrock strike (Figure 1). The Linnévatnet

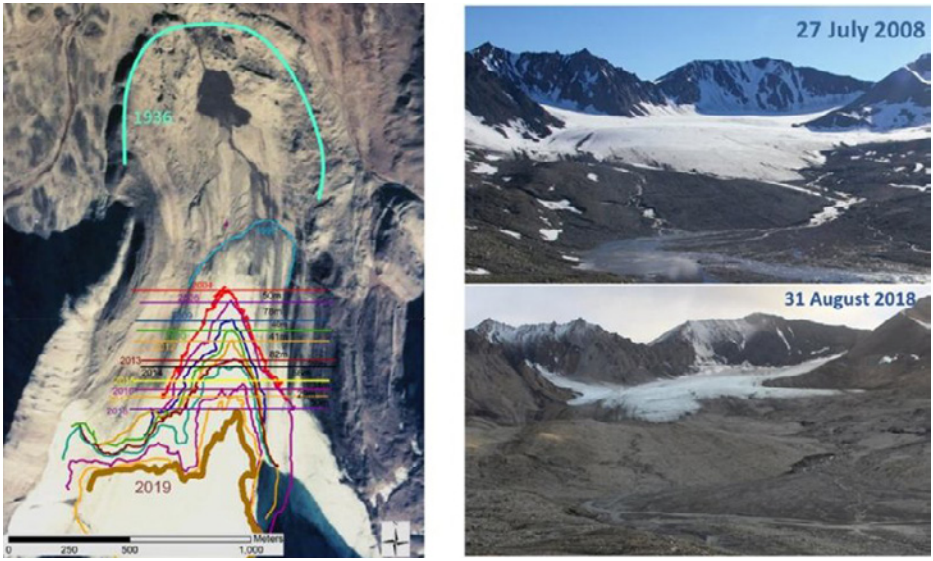

Figure 7: Left: A Map of Linnébreen showing ice margin positions from 1936 to present. The positions in 1936 and 1995 were obtained from air photographs and superimposed on georeferenced image from 1995. Positions from 2004 to 2019 are GPS tracks on georeferenced image. **Right:** Images of Linnébreen terminus from the time-lapse camera on Linnébreen Little Ice Age lateral moraine (view to the south).

watershed has an area of 27 km^2, of which 1.7 km^2 (6.3%) is glaciated (Snyder et al. 2000). There are three main basins: the SW and SE basins (11 and 16 meters depth, respectively) are located near the main inflow from Linnéelva in the south and separated by a bedrock ridge. The deeper main basin to the north has a maximum depth of 35 meters. The main inflow from Linnéelva enters the lake in the SE corner and a smaller braided stream in the SW corner originating in a cirque on Griegfjellet. Smaller inflows enter the lake from the numerous alluvial fans that drain snow and icy patches in gullies above the lake.

Temperature profiles in the lake, time-lapse imagery, and satellite remote sensing show that the ice-free season on Linnévatnet has been increasing over the last decade. Increases in ice-free duration have been documented throughout the Arctic (Lehnherr et al. 2018; Šmejkalová et al. 2016; Prowse et al. 2011; Magnuson et al. 2000). In-situ water temperature data collected at multiple depths at six locations since 2003 in Linnévatnet provide a unique opportunity to study the processes of lake ice formation and demise, and understand the climatic factors that are driving the decrease in ice cover duration. The work combines in-situ measurements with visible and near-infrared surface reflectance data from the Moderate Resolution Imaging Spectroradiometer (MODIS) to observe changes in reflectance of Lake Linné from 2000 – 2017 to determine the timing of summer ice-off (Cao et al. 2018). Sentinel-1 microwave backscatter data from Fall 2014 - Spring 2018 are

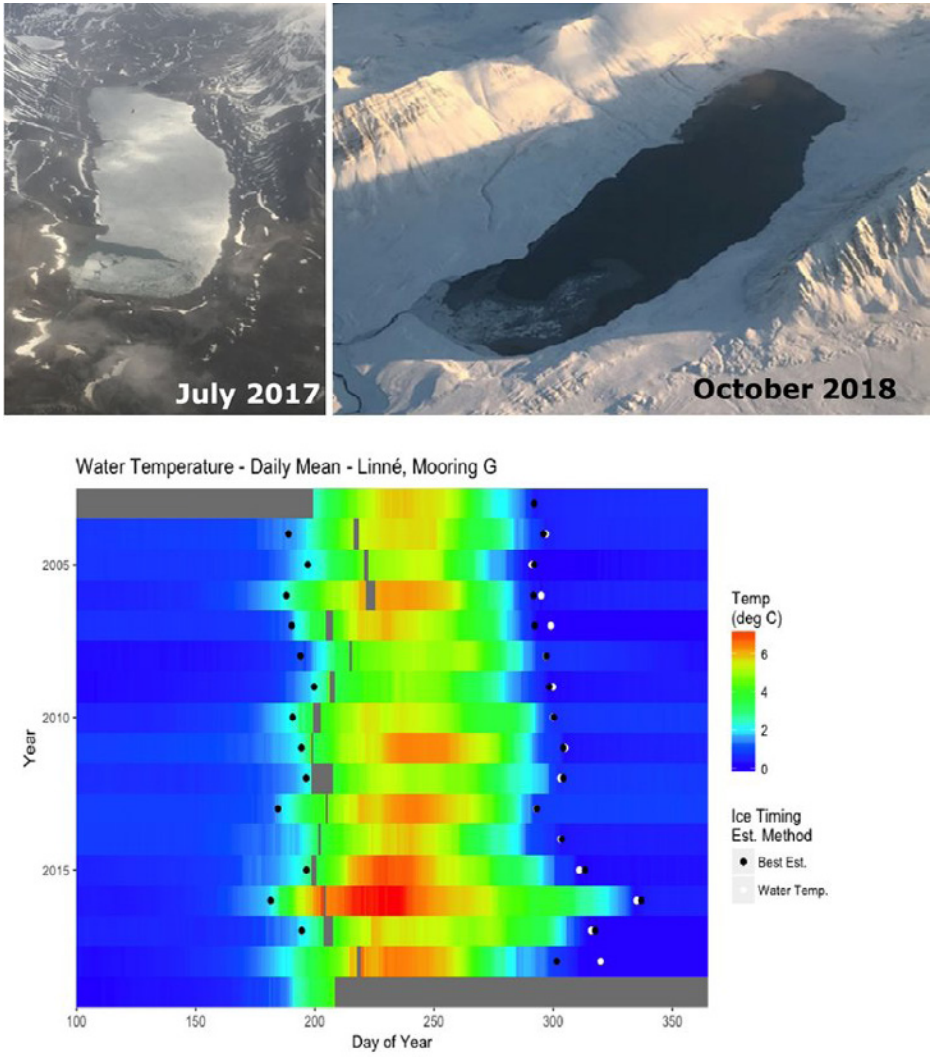

Figure 8: Upper: Photographs of Linnévatnet from commercial air flight 3 July 2017 and 9 October 2018 during breakup and freeze-up respectively. **Lower:** Plot of Linnévatnet. Daily mean water temperature 2003-2018 and best estimates of breakup and freezeup (dots). View to the south and southeast respectively.

also used to identify ice-on and ice-off dates, after correcting for satellite view angle effects. These results support an overall decrease in annual duration of lake ice cover in this part of Svalbard (Figure 8 lower panel). Contrary to patterns described for elsewhere in the Arctic (e.g. Šmejkalová et al. 2016; Magnuson et al. 2000), we do not see significant trends in the

timing of summer lake ice breakup (breakup has occurred between 3rd week of June and the middle of July). However, we see significant changes in the timing of lake ice formation in the autumn. Prior to 2013, lake ice cover always formed during the second half of October. Since 2013, we have observed several years in which lake ice cover did not form until late November or early December. Our ongoing work is exploring relationships between Kapp Linné area air temperature and Linnévatnet ice cover, and possible influences of the Arctic and North Atlantic Oscillations.

Analysis of meteorological data, time-lapse imagery and detailed grain size analysis of sediment traps has been used to characterise each year of sediment trap deployment (Figure

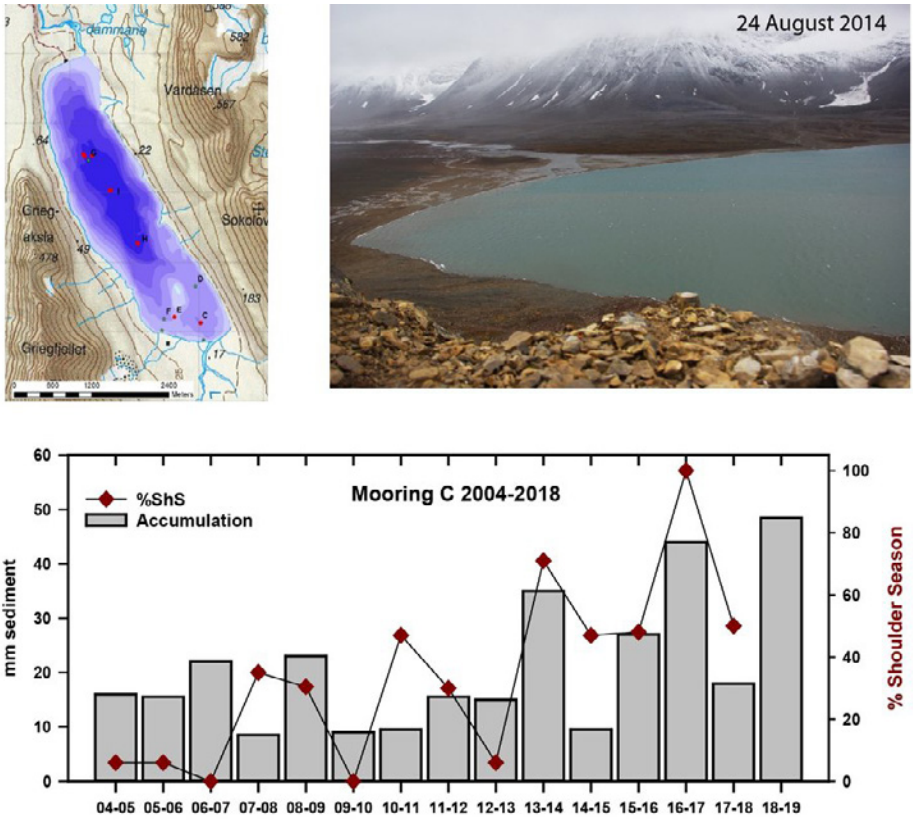

Figure 9: Upper left: Bathymetry of Linnévatnet and location of moorings (red dots). **Upper right:** Linnévatnet, view to the southwest from the "Plumecam" during river discharge event in late August 2014. **Lower:** Plot of accumulation from 2004 to 2018 in sediment trap from delta proximal mooring C. Red diamonds indicate percentage of accumulation in late summer-fall "shoulder season" (%ShS).

9 Top left), ca. 1 August to 31 July. Over the period 2013 to 2018 the general hydrological regime has shifted from one where peak discharge and lake sedimentation occurring during spring and early summer snowmelt (Schiefer et al. 2017) to one in which peak flow occurs during late summer and fall "shoulder season" as a result of intense late-season rainstorms (Nowak and Hodson 2013). In 2005, 2006, 2008, 2009, and 2012, the spring snowmelt processes were dominant; however the late-season mode has been the dominant mode in 6 of the past 8 years (Figure 9 bottom panel). In September 2015, approximately 70% of the annual sediment accumulation in sediment traps occurred over the course of 36 hours during a late summer rain event. Two storms in October and November 2016 produced floods and debris flows in the Linnédalen watershed with sediment yield exceeding all of the previous 13 years of observation. The late-season storms generally occur when the active layer is thickest at the end of the summer and sediments are easily mobilised along with residual sediment in stream channels.

Remote Sensing: Remote sensing techniques based on satellite Synthetic Aperture Radar (SAR) and optical images are powerful tools to upscale the investigation of large and hard-to-access Arctic environments. Past and on-going research projects in Svalbard have shown that remote sensing is valuable for A) the investigation of ground dynamics in periglacial areas using SAR Interferometry (InSAR) (Rouyet et al. 2019), B) the study of wet snow, ice cover on lakes and freeze/thaw cycles using SAR backscatter analysis (Eckerstorfer et al. 2017), and C) the mapping of vegetation (Johansen et al. 2012) and the onset of the growing season (Karlsen et al. 2014) using multi-spectral optical images.

In Kapp Linné, ground dynamics products document the distribution and timing of ground displacements along the line-of-sight of the SAR sensors during the snow-free season. Figure 10A shows the distribution of thaw subsidence in flat areas and creep on west-facing slopes between June and September 2018. Snow and ice cover products provide information about the distribution of wet snow and ice on water surfaces, useful to detect rain-on-snow events during the winter, the onset of the snow melting in spring and the timing of ice cover on lakes. Figure 10B is a snapshot for the 17th of July 2017 when snow is getting wet in the upper slopes and the ice covering Linnévatnet is melting. Vegetation products document the occurrence and distribution of the flora in the study area. Figure 10C shows the 18-units vegetation map in Kapp Linné based on Landsat TM/ETM+ imagery from 1987-2002.

Permafrost and Periglacial Geomorphology: Since 2004 observations of active layer temperatures in the most widespread periglacial landforms such as a beach ridge (43 in Figure 1), a snowpatch site (42 in Figure 1), a rock glacier (45 in Figure 1) and a solifluction sheet (41 in Figure 1) have been carried out primarily in the northern part of the strandflat in the study area. In 2008 as part of the IPY Thermal State of Permafrost (TSP Norway) project three boreholes were drilled into the permafrost for ground thermal monitoring

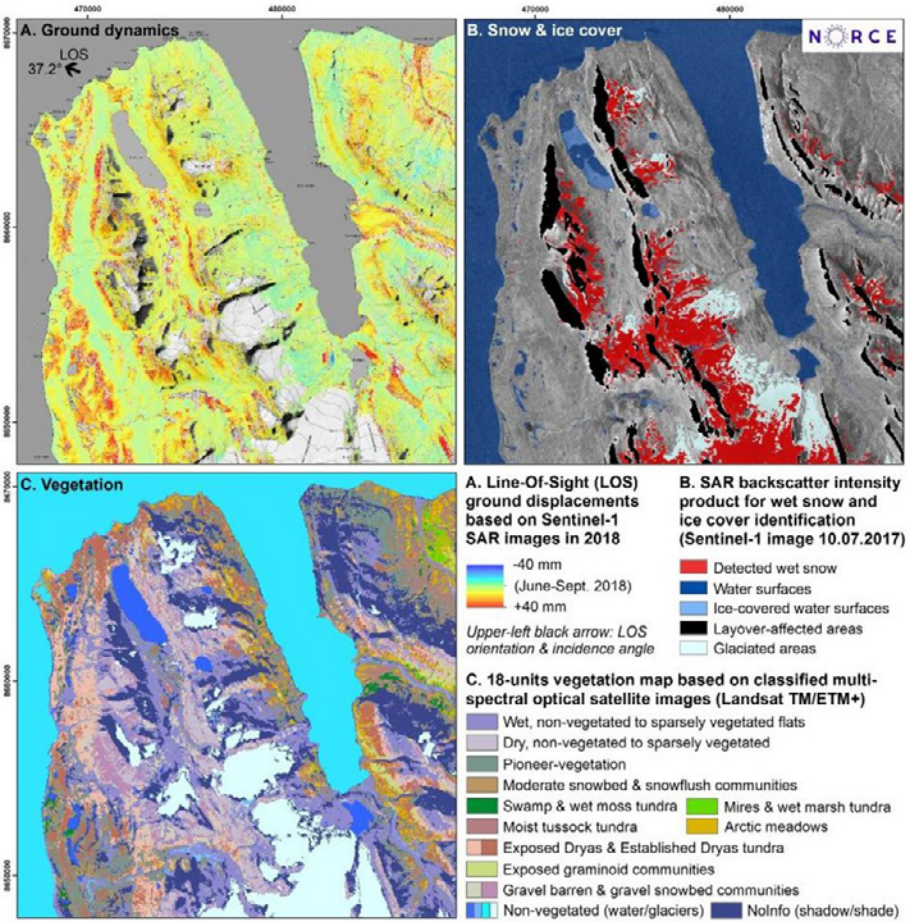

Figure 10: Examples of satellite remote sensing products in Kapp Linné.

(Christiansen et al. 2019). One borehole is 30 m deep and drilled into a bedrock outcrop (25 in Figure 1), another borehole is 39 m and drilled into beach ridge sediments laying over bedrock (26 in Figure 1). The third borehole was drilled 4 m through organic deposits and into beach ridge sediment (27 in Figure 1) but has been destroyed by a polar bear. These three boreholes are located approximately 1 km south of Isfjord Radio and are 200 m apart. Permafrost conditions in the two deep boreholes are compared to other permafrost observation sites in Svalbard in Christiansen et al. (2019) and in Christiansen et al. (2020). Generally the permafrost along the west coast in the study area is relatively warm as discussed for the last two hydrological years. This is reflecting the location close to the sea, with the top permafrost temperatures higher than -2°C and the deeper permafrost

temperatures (15-20 m) higher than -3°C recorded in both the strandflat at Kapp Linné and in the marine terrace in the Barentsburg area (Christiansen et al. 2019). The active layer varies from around 3 m thickness in the bedrock to approximately 1.5 m in sediments in the study area including data from both Kapp Linné and the Barentsburg area (Christiansen et al. 2020). Frost heave, thaw settlement, and downslope displacement of soil is measured at a solifluction station at the western flank of Griegfjellet (41 in Figure 1). A time-lapse camera takes daily photographs of the solifluction station, allowing for the assessment of snow conditions and ground heaving and settling. The ground temperature and solifluction station data have been used together with remote sensing backscatter data for improved process dynamics assessing ground deformation and subsidence in the landscape around Kapp Linné (Eckerstorfer et al. 2017).

3. Unanswered questions

Groundwater and Surface Water Hydrology: There are several urgent research needs that must be addressed if we are to properly understand the response of Svalbard's water budget to the marked climate changes described above. These are: i) the precipitation gradient across Nordenskiöldland is virtually unknown for rainfall, making data products from modern climate models or real data from our sparse network of rain gauges very difficult to distribute over the mountain environment; ii) we have traditionally neglected change in any water store other than glacier ice, providing no basis for accounting for how ground-thaw and the loss of ground ice will contribute to water supply and geomorphic processes; and iii) research in Svalbard has greatly neglected groundwater as a water source and bio-geomorphic agent. Due to the complexity of cold region hydrological systems, a catchment response can vary depending on permafrost thawing and lead to an increased storage capacity of affected soils and a higher contribution of groundwater to river discharge. Hydrological modelling of polar catchments with varying active layer thicknesses requires analysis of non-stationarity of environmental conditions and their influence on simulated runoff. It should be taken into account for simulation of recent, past and future conditions. Developing our work in the Kapp Linné region via multi-institutional collaboration will, therefore, provide a much-needed alternative site to the now-defunct glacier-groundwater system studied in the past at Vestre Broggerbreen in Ny-Ålesund and unglaciated catchment Fuglebekken in Hornsund (Wawrzyniak et al. 2017). This new collaboration, first initiated in 2007 between UK and AARI and recently with IGF PAS researchers, will involve the instrumentation of four adjacent watersheds lying on identical rock types, yet with different lake or glacier cover proportions. Comparative watershed approaches have yielded significant insights into the influence of changing glacier cover in the past and is well-placed to provide empirical data resources for the future.

Paleoclimate/Paleohydrology: The annually laminated sediment record in Linnévatnet provides a long-term and high-resolution record of hydro-climatic variability for this part of Svalbard. Annual layering varies in thickness and structure in response to the amount and timing of sediment delivered by runoff from snow and glacier melt, and precipitation events. The sediment record provides a context for understanding the recent shift in hydrology by addressing two significant questions: (1) are there periods in the past ca. 1,000 years where lake sedimentation is similar to the current warm, wet Arctic scenario or (2) are we looking at a "new normal"? To address this important question, a new study, funded by U.S. NSF Polar Programs (R.S. Bradley, UMass, USA and M. Retelle, UNIS/Bates College USA) will use long term records of annually laminated sediments to reconstruct rainfall-related events and determine if and when similar conditions occurred in the past.

Paleoecology: The paleoenvironmental history of western Nordenskiöld land or Grønfjorden area has been studied by the RussianScientific Center on Spitsbergen, at Barentsburg, since 2015. The paleogeographical study is focused on landscapes, geomorphological features, Quaternary sediments, lake bottom sediment outcrops, etc. All are the key to understanding the environmental dynamics and climatic changes of the Late Pleistocene and Holocene. Taxonomic description of diatom complexes that are forming today in ecologically different environments (karst lakes, small lagoons, big lakes, streams, marine littoral zone, shore zone) will provide an accurate analogue for paleoecological reconstructions in the future. As a well-studied area, Linnédalen is the perfect location for environmental and paleoenvironmental monitoring.

4. Recommendations for the future

1. It is vitally important to maintain and improve the network of environmental monitoring installations and environmental sampling in this critical region during this period of rapidly changing climate. In addition, we will strive to encourage an increase in interdisciplinary research. Some examples that are currently being pursued include long-term studies of both terrestrial and aquatic ecology and aquative microbiology and biogeochemistry.

2. Understanding regional variability in hydroclimate will be an increasingly important issue in Svalbard in the 21st Century. Poorly understood regional precipitation gradients, understanding the contributions of water storage in glacier ice and groundwater, and groundwater as a water source and a bio-geormorphic agent are significant issues that must be addressed.

3. The recent recognition of the Kapp Linné Environmental Observatory in the SIOS network provides the capability of linking with research in other High Arctic interdisciplinary observatories where similar hydroclimate, permafrost and limnological research is

undertaken including the Zackenberg station in Greenland (Mernild et al. 2007) and the Ward Hunt Island Observatory (Comte et al. 2018) and Cape Bounty Arctic Watershed Observatoriy (LaFrenière and Lamoureux 2019) in the Canadian High Arctic archipelago.

4. Continued support for the Kapp Linné Environmental Observatory provides an ideal training ground for the next generation of Arctic scientists who will take on the challenges of the 21st Century. The proximity to UNIS and the AARI Barentsburg Research Station provides a highly motivated and well-trained workforce for addressing critically important environmental research issues.

5. Synergy with other SIOS Programmes

The Kapp Linné Environmental Observatory is an interdisciplinary and international collaborative with a focus on hydroclimate, permafrost and periglacial research and education. Permafrost research at Kapp Linné is already a part of the Svalbard-wide network of permafrost boreholes and active layer monitoring stations however other natural connections can easily be forged with other SIOS research teams including hydrology (planned river discharge monitoring on Linnéelva), snow and glacier research, and terrestrial ecology.

6. Data availability

Data used in this report came from a wide variety of sources, including publicly accessible online databases. Table 3 lists datasets used in this report, data provider or owner, and notes on how to access data. A primary goal for KLEO project members is to make relevant data and metadata accessible through the SIOS data access point.

Table 3: Data used in this report and access information.

Data Category	Data descriptions	Temporal coverage	Location or spatial coverage	Data information, providers and access
Regional Climatology	Meteorological stations on Svalbard	Varies by station	Svalbard	The Norwegian Meteorological Institute: http://eklima.met.no https://aisori.meteo.ru/ClimateR/ Institute of Geophysics Polish Academy of Sciences: https://monitoring-hornsund.igf.edu.pl/index.php/login
Groundwater and Surface Water Hydrology	Snow cover observations Water and sediment discharge Precip and surface water isotopic composition	2002 to present 2006 to present	Aldegonda-breen, Kongress, Bryde, Aldegonda watersheds Barentsburg station	Available by request to Anna Nikulina, Arctic and Antarctic Research Institute Hydrogen and oxygen isotopes in precipitation: https://www.iaea.org/services/networks/gnip
Linnédalen Watershed Hydroclimate data	Weather station temperature time series Water temperature times series Time lapse camera images Glacier mass balance measurements (2005-2010) Annual sediment trap grain size and mass accumulations	2003 to present	Linnédalen watershed	Most data are available at https://arcticdata.io/catalog/view/doi:10.18739/A2VH5CH5P See Schiefer et al., 2017 Additional data available by request to Steve Roof, Hampshire College
KLEO region Remote sensing	Synthetic Aperture Radar (SAR)	1987 to present	Kapp Linné region	See Rouyet et al., 2019
Permafrost	Borehole temperature records	2004 to present	Kapp Linné region	Global Terrestrial Network for Permafrost (GTN-P): https://gtnp.arcticportal.org/

Acknowledgements

This work was supported by the Research Council of Norway, project number 251658, Svalbard Integrated Arctic Earth Observing System - Knowledge Centre (SIOS-KC). We are grateful to SIOS for encouraging the development of the Kapp Linné Environmental Observatory and this report through support for a workshop on August 2019. Research in Linnédalen was supported initially through several grants from the U.S. National Science Foundation Office of Polar Programs (Svalbard REU) and most recently facilitated through a summer course, *AG220 Environmental Change in the High Arctic Environment of Svalbard* at the University Centre in Svalbard. Since 2003 over 100 students have contributed to the environmental database though their research contributions in the Svalbard REU and UNIS AG220. We greatly appreciate the support of Spitsbergen Travel and most recently Basecamp Explorer for access to Isfjord Radio as a research station.

References

Barton BI, Lenn YD, Lique C (2018) Observed Atlantification of the Barents Sea causes the Polar Front to limit the expansion of winter sea ice. J Phys Oceanogr 48(8):1849-1866

Bøyum A, Kjensmo J (1970) Kongressvatn. A crenogenic meromictic lake at Western Spitsbergen. Arch Hydrobiol, 67:542–552

Bøyum A, Kjensmo J (1978) Physiography of Lake Linnévatn, Western Spitsbergen. In: Proceedings: 20th Congress, Internationale Vereinigung fur Theoretische und Angewandte Limnologie

Cao J, Roof S, Werner A, Gunn G, Bunting E, Tuttle S (2018) Comparison of Arctic Lake Ice Cover Timing on Svalbard Using Satellite and In-Situ Data. Am Geophys Ann Mtg, Washington DC, December 2018

Christiansen HH, Gilbert GL, Demidov N, Guglielmin M, Isaksen K, Osuch M, Boike J (2019) Permafrost thermal snapshot and active-layer thickness in Svalbard 2016-2017. In: Orr et al (eds): SESS report 2018, Svalbard Integrated Arctic Earth Observing System, Longyearbyen, pp. 26–47. https://sios-svalbard.org/SESS_Issue1

Christiansen HH, Gilbert GL, Demidov N, Guglielmin M, Isaksen K, Osuch M, Boike J (2020) Permafrost temperatures and active-layer thickness in Svalbard during 2017/2018. In: Van den Heuvel et al. (eds): SESS report 2019, Svalbard Integrated Arctic Earth Observing System, Longyearbyen, 236 - 249 . https://sios-svalbard.org/SESS_Issue2

Comte J, Culley AI, Lovejoy C, and Vincent WF 2018, Microbial connectivity and sorting in a High Arctic watershed, ISME J, 12 2988-3000.

Dallmann WK (Ed.) (2015) Geoscience Atlas of Svalbard. Norsk Polarinstitutt.Report Series No. 148.

Dansgaard W (1964) Stable isotopes in precipitation. Tellus 16:436-468. https://doi.org/10.3402/tellusa.v16i4.8993

Eckerstorfer M, Christiansen HH (2011) The "High Arctic maritime snow climate" in central Svalbard. A Antarct Alp Res 43(1):11-21

Eckerstorfer M, Malnes E, Christiansen HH (2017) Freeze/thaw conditions at periglacial landforms in Kapp Linné, Svalbard, investigated using field observations, in situ, and radar satellite monitoring. Geomorphology. 293:433-447

Guilizzoni P, Marchetto A, Lami A, Brauer A, Vigliotti L, Musazzi S, Langone L, Manca M, Lucchini F, Calanchi N, Dinelli E (2006) Records of environmental and climatic changes during the late Holocene from Svalbard: palaeolimnology of Kongressvatnet. J Paleolimnol 36(4):325-351

Hamed KH, Rao R (1998) A modified Mann-Kendall trend test for autocorrelated data. J Hydrol. 204: 182–196

Holm TM, Koinig KA, Andersen T, Donali E, Hormes A, Klaveness D, Psenner R (2011) Rapid physicochemical changes in the high Arctic Lake Kongressvatn caused by recent climate change. Aqua Sci 74(3):385-395

Humlum O (2002) Modelling late 20th century precipitation in Nordenskiold Land, Svalbard, by geographic means. -Norw J Geog 56: 96-103

IAEA/WMO (2006) International Atomic Energy Agency/ World Meteorological Organization. Global Network of Isotopes in Precipitation. The GNIP Database. Accessible at: https://www.iaea.org/services/networks/gnip

Johansen BE, Karlsen SR, Tømmervik H (2012) Vegetation mapping of Svalbard utilising Landsat TM/ ETM+ data. Polar Rec 48(1):47-63

Karlsen S, Elvebakk A, Høgda K, Grydeland T (2014) Spatial and temporal variability in the onset of the growing season on Svalbard, Arctic Norway—measured by MODIS-NDVI satellite data. Remote Sens 6(9):8088-8106

Kendall MG (1975) Rank Correlation Methods. Charles Griffin: London

Lafrenière MJ, Lamoureux SF (2019) Effects of changing permafrost conditions on hydrological processes and fluvial fluxes. Earth Sci Rev 191:212-223.

Landvik JY, Mangerud J, Salvigsen O (1987) The Late Weichselian and Holocene shoreline displacement on the west-central coast of Svalbard. Polar Res 5(1):29-44

Lehnherr I, St. Louis VL, Sharp M, Gardner AS, Smol JP, Schiff SL, Muir DCG, Mortimer CA, Michelutti N, Tarnocai C, St. Pierre KA, Emmerton, CA, Wiklund, JA, Köck, G, et al. (2018) The world's largest High Arctic lake responds rapidly to climate warming: Nat Commun 9 https://doi.org/10.1038/s41467-018-03685-z

Magnuson, JJ, Robertson, DM, Benson, BJ, Wynne, RH, Livingstone, DM, Arai, T et al. (2000). Historical trends in lake and river ice cover in the Northern Hemisphere. Science 289:1743-1746

Mann H (1945) Nonparametric tests against trend. Econometrica 13(3):245–259

Mernild SH, Sigsgaard C, Rasch M, Hasholt B, Hansen BU, Stjernholm M, Petersen D. Climate, river discharge and suspended sediment transport in the Zackenberg River drainage basin and Young Sound/Tyrolerfjord, Northeast Greenland, 1995–2003. Carbon cycling in Arctic marine ecosystems. Case study Young Sound, ed. S. Rysgaard, RN Glud, and TM Roberts. 2007:24-43.

Mørk A, Worsley D (2006) The Festningen section. Norsk Geologisk Forening (NGF) Abstracts and Proceedings, 3: 31-35

Nilsen F, Skogseth R, Vaardal-Lunde J, Inall, M (2016) A Simple Circulation Model: Intrusion of Atlantic Water on the West Spitsbergen Shelf. J Phys Oceanogr 46:1209-1230

Nowak A, Hodson, A (2013) Hydrological response of a High-Arctic catchment to changing climate over the past 35 years: a case study of Bayelva watershed Svalbard. Polar Res, 32:0

Ohta Y, Hjelle A, Andresen A, Dallmann WK, Salvigsen O (1992) Geological map of Svalbard 1:100,000, sheet B9G Isfjorden, Temakart 16, Norsk Polarinstitutt, Oslo

Osuch M, Wawrzyniak T (2017) Inter- and intra-annual changes of air temperature and precipitation in western Spitsbergen. Int J Climatol 37:3082– 3097, https://doi.org/10.1002/joc.4901

Prowse T, Alfredsen K, Beltaos S, Bonsal B, Duguay C, Korhola A., McNamara J, Pienitz R, Vincent WF, Vuglinsky V and Weyhenmeyer GA (2011) Past and Future Changes in Arctic Lake and River Ice. AMBIO, 40(S1): 53–62. https://doi.org/10.1007/s13280-011-0216-7

Rouyet L, Lauknes TR, Christiansen HH, Strand SM, Larsen Y (2019) Seasonal dynamics of a permafrost landscape, Adventdalen, Svalbard, investigated by InSAR. Rem Sens Env 231:111236

Salvigsen O, Elgersma A (1985) Large-scale karst features and open taliks at Vardeborgsletta, outer Isfjorden, Svalbard. Polar Res 3(2):145-153

Schiefer E, Kaufman D, McKay N, Retelle M, Werner A, Roof S (2017) Fluvial suspended sediment yields over hours to millennia in the High Arctic at proglacial Lake Linnévatnet, Svalbard. Earth Surf Proc Land 43(2): 482-498

Sen PK (1968) Estimates of the regression coefficient based on Kendall's tau. J Am Stati Assoc 63: 1379–1389. https://doi.org/10.2307/2285891

Skakun AA, Chikhachev KB, Ekaykin AA, Kozachek AV, Vladimirova DO, Veres AN, Verkulich SR, Sidorova OR, Demidov NE (2020) Stable isotopic content of atmopshericprecipitation and natural waters in the vicinity in the vicinity of Barentsburg (Svalbard). Ice and Snow (Led and Sneg) 60 (1): xx–xx. accepted [in Russian]

Šmejkalová T, Edwards ME, Dash J (2016) Arctic lakes show strong decadal trend in earlier spring ice-out: Sci Rep, 6: https://doi.org/10.1038/srep38449

Snyder JA, Werner A, Miller GH (2000) Holocene cirque glacier activity in western Spitsbergen, Svalbard: sediment records from proglacial Linnévatnet. The Holocene 10:(5)555-563

Wawrzyniak T, Osuch M, Nawrot A, Napiórkowski JJ (2017) Run-off modelling in an Arctic unglaciated catchment (Fuglebekken, Spitsbergen). Ann Glaciol 58 (75): 36–46. https://doi.org/10.1017/aog.2017.8

Wetzel K (1990) Isotopic Peculiarities of Meteoric Water in Polar Regions. Isotopenpraxis Isotopes in Environmental and Health Studies 26:11–13. https://doi.org/10.1080/10256019008624211

Williamson CE, Saros JE, Vincent WF, Smol JP (2009) Lakes and reservoirs as sentinels, integrators, and regulators of climate change. Limnol Oceanogr 54(6 part2): 2273-2282

Appendix

Metadata for Kapp Linné-Gronfjorden installations and instrumentation. Numbers refer to sites on Figure 1 in the text. Mooring sites are shown on map in Figure 9.

LOCATION	Map #	Installation	Latitude	Longitude	Record Length
Linnédalen	1	Remote weather station	78,027	13,85	2003-2019*
	2	Air temperature	78,02435	13,80961	2003-2019*
	3	Air temperature	77,981	13,911	2003-2019*
	4	Air temperature	77,95876	13,88705	2003-2019*
	5	Air temperature	77,96721	13,904	2003-2019*
	6	Snow tree (snow depth)	77,98	13,911	2003-2019*
	7	Snow tree (snow depth)	78,016	13,881	2003-2019*
	8	Snow tree (snow depth)	78,02366	13,877	2003-2019*
	9	Stream temperature.	78,024	13,863	2004-2019
	10	Stream temperature	78,016	13,881	2004-2019
	11	Stream temp.	77,981	13,91	2004=2019
	12	Time lapse camera	78,02537	13,81784	2007-2019
	13	Time lapse camera	78,031	13,902	2007-2019
Linnévatnet Moorings	14	Mooring C	78,03217	13,86084	2003-2019
	15	Intervalometer	78,03206	13,86062	2003-2019
	16	Mooring C Spring deployment	78,03217	13,86084	2003-2019
	17	Mooring D	78,0373	13,85713	2003-2019
	18	Mooring E	78,03278	13,84386	2003-2019
	19	Mooring F	78,03257	13,83683	2003-2019
	20	Mooring G	78,05276	13,78557	2003-2019
	21	Mooring H	78,04241	13,81884	2003-2019
Linnébreen	22	ablation stake survey			2004-2013
	23	glacier margin GPS track			2004-2019
Kongressvatnet	24	Deep Hole mooring @ 55 meters	78,02126	13,96078	2003-2019

Kapp Linné Strandflat	25	Borehole KLB1	78,05588	13,63479	2008-2019
	26	Borehole KLB2	78,0544	13,63712	2008-2020
	27	Borehole KLB3	78,05313	13,63982	2008-2021
	41	Solifluction station	78,04522	13,72056	2004-2019
	42	Snowpatch active layer temperature	78,05739	13,74092	2004-2020
	43	Beach Ridge active layer temperature	78,05707	13,67991	2004-2021
	44	Isfjord Radio air temperature logger	78,06222	13,61662	2004-2022
	45	Rock glacier active layer temperature	78,04142	13,72658	2004-2023
Aldegondabreen	28	Snow cover survey	77,96976	14,05857	2001-2014 irregular 2015-2019 regular
		Chemical composition of snow	77,96976	14,05857	2015-2019
		glacier stake survey			2011-2019
	29	weather station A1	77,97991	14,10218	2015-2019
	30	weather station A2	77,96483	14,03276	2016-2019
Aldegonda river	31	water level	77,98707	14,18475	2001-2012
		water level; water temperature	77,98707	14,18475	2013-2014
		water level; water temperature	77,98707	14,18475	2015-2019
		water discharge	77,98707	14,18475	2001-2013 irregular, 2014-2019 regular
		sediment discharge	77,98707	14,18475	2001-2013 irregular, 2014-2019 regular
		Chemical composition of water	77,98707	14,18475	2015-2019
Bryde valley	32	Snow cover survey	78,00006	14,06926	2016-2019
		Chemical composition of snow	78,00006	14,06926	2016-2019
Bryde river	33	water level; water temperature	78,00371	14,1533	2016-2019
		water discharge	78,00371	14,1533	2003-2015 irregular, 2016-2019 regular

		sediment discharge	78,00371	14,1533	2003-2015 irregular, 2016-2019 regular
		Chemical composition of water	78,00371	14,1533	2015-2019
Kongressdalen	34	Snow cover survey	78,02422	14,03085	2016-2019
		Chemical composition of snow	78,02422	14,03085	2016-2019
Kongresselva	35	water level; water temperature	78,02833	14,12969	2016-2019
		water discharge	78,02833	14,12969	2003-2015 irregular, 2016-2019 regular
		sediment discharge	78,02833	14,12969	2003-2015 irregular, 2016-2019 regular
		Chemical composition of water	78,02833	14,12969	2015-2019
Vasstak river	36	water level; water temperature	78,0493	14,0724	2019
		water discharge	78,0493	14,0724	2019
		sediment discharge	78,0493	14,0724	2019
		Chemical composition of water	78,0493	14,0724	2019
Kongressvatnet	37	water level, temp.,chemistry, CTD	78,02092	13,95959	2017-2018 irregular, 2019
Stemmevatnet	38	water level, temp.,chemistry, CTD	78,0548	13,96539	2017-2018 irregular, 2019
Linnévatnet	39	CTD-measuments, chemical oomp.	78,04354	13,81572	2018 March
Kapp Linné small lakes	40	CTD-measuments, chemical oomp.			2016-2019; 2019 July

New data, new techniques and new challenges for updating the state of Svalbard glaciers (SvalGlac)

Thomas V Schuler[1,2], Andrey Glazovsky[3], Jon Ove Hagen[1], Andrew Hodson[4], Jacek Jania[5], Andreas Kääb[1], Jack Kohler[6], Bartłomiej Luks[7], Jakub Malecki[8], Geir Moholdt[6], Veijo Pohjola[9], Ward Van Pelt[9]

1 Dept Geosciences, University of Oslo, Norway
2 Dept Arctic Geophysics, University Centre on Svalbard UNIS, Norway
3 Inst Geography, Russian Academy of Sciences, Russia
4 Dept Arctic Geology, University Centre on Svalbard UNIS, Norway
5 Centre for Polar Studies, University of Silesia, Poland
6 Norwegian Polar Institute, Fram Centre, Tromsø, Norway
7 Inst of Geophysics, Polish Academy of Sciences, Poland
8 Adam Mickiewicz University, Poznań, Poland
9 Dept of Earth Sciences, Uppsala University, Sweden

Corresponding author: Thomas Vikhamar Schuler, t.v.schuler@geo.uio.no, ORCID 0000-0003-0972-3929

Keywords: Arctic glaciers, mass balance, calving, surges, glacier-climate relationship

1. Introduction

Svalbard is among the fastest warming regions on Earth (Nordli et al. 2014; Isaksen et al. 2016). Ongoing climate change alters the energy and mass balances of its glaciers, which in turn affects global sea level, and which has further implications on regional scales. Glacier retreat leads to significant topographic changes, such as increases in fjord length and the area of glacier forefields (e.g. Błaszczyk et al. 2013; Grabiec et al. 2018). Moreover, glaciers temporarily store water on a range of time scales, with its release controlling the hydrology of most Svalbard catchments, as well as influencing terrestrial and marine ecosystems and fjord circulation.

The climate of Svalbard is characterized by strong gradients, ranging from milder and more humid conditions in the South and West, to the colder and drier conditions in the Northeast. These gradients are reflected in the spatial pattern of glacier mass balance, and therefore also in the distribution of glacier-covered area. The largest glaciers are found in the colder northeast, whereas glacier coverage is much less in the milder and drier area of central Spitsbergen.

Glacier monitoring programs have so far been mostly located near the permanent settlements (Ny-Ålesund, Hornsund, Longyearbyen, Barentsburg, see Figure 1), due to the ease of access, but these sites may not optimally represent conditions across Svalbard. However, gaps in survey design and representativeness issues can be addressed using modelling and remote sensing, to optimally link with adjacent disciplines in an Earth System perspective.

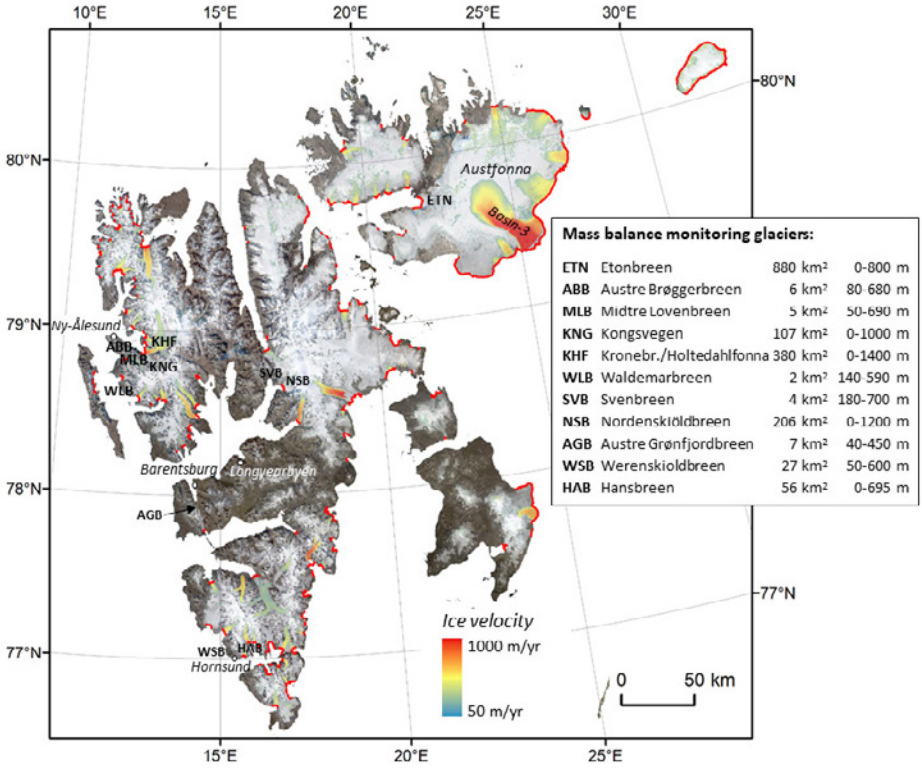

Figure 1: Overview map of Svalbard, showing glacier-covered areas (white) with color-shaded surface velocities for 2018 in cases where glaciers moved faster than 50 m a^{-1}. **Surface velocities** have been retrieved from Gardner et al. 2019: ITS_LIVE Regional Glacier and Ice Sheet Surface Velocities. Data archived at National Snow and Ice Data Center; doi:10.5067/6II6VW8LLWJ7. The red coastal lines show termini of tidewater glaciers from 2018. The background image is a Landsat-mosaic from toposvalbard.npolar.no. Abbreviated labels show the location of present mass balance monitoring glaciers on Svalbard, along with glacier area and elevation range.

To address the overarching, strategic question of "What next in Svalbard glacier studies?", we review the current state of Svalbard glaciers and update previous assessments (Hagen et al. 2003 a, b). Starting from available long-term observations, we discuss new technologies and data that have become available in the past 20 years. We further highlight the important knowledge gaps and outline future research that is needed to close them (including but not limited to ways how SIOS could contribute).

2. Overview of existing knowledge

About 34000 km^2, i.e. 60% of the land area of Svalbard is covered by glaciers (Nuth et al. 2013), corresponding to ~10% of the glacier area in the Arctic, outside the Greenland ice sheet. The more than 1000 individual glaciers larger than 1 km^2 comprise a wide range of glacier types from small cirque glaciers and valley glaciers that mainly terminate on land to large ice fields and ice caps (up to ~8000 km^2) each feeding several outlet glaciers. About 15% of all glaciers on Svalbard by number and as much as 60% by area (Błaszczyk et al. 2009) are tidewater glaciers, which terminate into fjord or ocean water. Tidewater glaciers introduce freshwater at depth into the marine waters, both from subglacial channels and submarine melting, as well as icebergs, which calve off of the glacier fronts. Svalbard's total ice volume has been assessed using different methods, with estimates ranging from 4000 km^3 to 9600 km^3 but most studies (Hagen et al. 1993; Martín-Español et al. 2015; Fürst et al. 2018) more closely agree on a value of around 6200 km^3, corresponding to a sea-level equivalent of 1.5 cm. Most Svalbard glaciers are polythermal (Hagen et al. 1993), they consist of both cold and temperate ice (temperate ice is at the melting point, thus permitting the presence of liquid water in the glacier body even during the cold winter period).

Annual mass balance surveys of Svalbard glaciers have been conducted since 1966 (Hagen and Liestøl 1990). Traditionally, regular measurements have been performed on glaciers in the vicinity of settlements, but also dedicated measurement campaigns have been conducted on the less accessible ice caps in the eastern parts of Svalbard (e.g. Ahlmann 1933; Schytt 1964; Pinglot et al. 2001). At some locations, these measurements have been maintained on a regular basis, and now provide invaluable data for assessing the climate-glacier interaction. Hagen et al. (2003 a, b) reviewed the data available at that time and used different approaches to assess the Svalbard-wide glacier mass balance. More than 15 years have passed since these reviews, and measurements have been continued, new series from formerly under-represented areas have been initiated and new techniques have become available.

Here, we give a new account of the recent development of glacier mass balance for all of Svalbard. We also highlight the activities and recent developments and discuss the intersection with other disciplines; where relevant, these points are coordinated with other SESS reports (Köhler et al. 2020; Gallet et al. 2019).

2.1 New mass balance data

The *glaciological mass balance* is obtained from repeated field visits, and comprises end-of-winter snow-depth sounding and repeated height measurements of an array of stakes. Balance estimates are extrapolated over the entire glacier basin by determining the balance terms as functions of elevation, and averaging them applying weights determined from the distribution of glacier area as a function of elevation. This method quantifies the surface mass balance (SMB), i.e. the mass changes at the surface of the glacier, exposed to the atmosphere, but does not comprise frontal ablation (calving and sub-marine melting at the front of tidewater glaciers).

The *geodetic mass balance* is computed by differencing elevation data from two or more different times. Elevation data can be from a variety of sources: surface surveys; contours from older maps; digital elevation models made photogrammetrically from aerial photographs or satellite imagery; or satellite altimeters. This balance estimate accounts for frontal ablation, hence represents the total mass balance.

Mass balance models, forced either by meteorological observations or output from regional climate models, evaluate the surface energy balance to reveal the climatic mass balance (CMB). The most complete models contain a subsurface routine to account for the impact of water storage and refreezing on the mass and energy budgets. Field data are used to calibrate model parameters and to validate model output. The CMB differs from the measured SMB in that it more accurately accounts for subsurface mass changes that are difficult to measure.

A direct method for estimating mass change by *gravimetry* comes from the GRACE (Gravity Recovery and Climate Experiment) satellites, which mapped the time-varying gravity field of the Earth over the period 2002-2017. However, the values still need to be disentangled from crustal changes due to long-term isostatic rebound. Regional gravitation change is also prone to "leakage" from regions outside of the area of interest. Furthermore, there are certain technical challenges to the data analysis.

2.1.1 Northwest-Spitsbergen

Austre Brøggerbreen (ABB) and **Midtre Lovénbreen** (MLB) are both small glaciers (ca. 5-6 km^2), and neither reach higher than ca. 700 m a.s.l. Both have had consistently negative net balances since measurements started in 1966 (Figure 2), due to their relatively low-lying and small accumulation areas. Mass balance on MLB[1] is less negative than on neighboring

1 https://wgms.ch/products_ref_glaciers/midtre-lovenbreen-svalbard/

ABB[2], in part due to its slightly higher elevation and steeper valley sides, both of which contribute to more accumulation on MLB. The time series for **Kongsvegen** (KNG) is shorter, starting in 1986 (Figure 2). KNG is a larger glacier (ca. 107 km^2), with elevations up to 850 m a.s.l. Because of its higher elevation, it has a larger accumulation area, and therefore its net balance record is higher than that of the lower-lying ABB and MLB. The same is true for the larger (ca. 380 km^2) and higher elevation (up to 1400 m a.s.l.) neighboring glacier system **Holtedahlfonna/ Kronebreen** (KHF), with measurements since 2003.

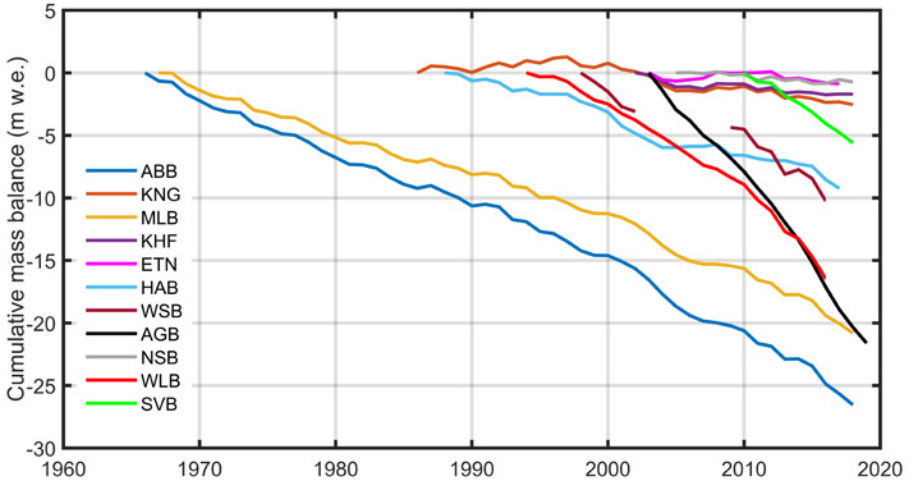

Figure 2: Cumulative surface mass balance (excluding frontal ablation) from in-situ measurements at selected Svalbard glaciers

Waldemarbreen (WLB) is a 3 km^2, low-elevation (up to ca. 600 m a.s.l.) land-terminating glacier, 27 km south of Ny-Ålesund. It has been monitored since 1995, with average 1995-2016 mass balance of -0.75 m w.e. a^{-1}, and an acceleration in mass loss after 2011, leading to its ELA above the glacier top (Sobota et al. 2016).

2.1.2 Central Spitsbergen

Central Spitsbergen is characterized by relatively dry conditions, due to precipitation shadowing. **Svenbreen** (SVB) is a small (4 km^2) valley glacier, north of Billefjorden, whose elevation ranges from 180-700 m a.s.l. Geodetic measurements show that SVB has been losing volume since at least the 1960s, with an apparent acceleration after 1990 (Małecki 2013, 2015, 2016). The mean geodetic balance of the glacier over the period 1990-2009

2 https://wgms.ch/products_ref_glaciers/austre-broeggerbreen-svalbard/

was -0.58 m w.e. a^{-1}. Annual mass balance measurements of the glacier started in 2010, and show that the glacier has been steadily losing mass, including in its high-elevation cirque, in agreement with the geodetic data.

Mass balance measurements on **Nordenskiöldbreen** (NSB), an outlet glacier of the Lomonosovfonna ice cap in central Svalbard, have been performed annually since 2006. NSB is ~25 km long, has an area of 206 km^2, and elevation ranges from 0-1200 m a.s.l. The mean glacier-wide net climatic mass balance for 2006-2018 is -0.06 m w.e. a^{-1}. The mass balance data have contributed to a range of studies on the glacier's climatic mass balance, dynamics, and snow/firn conditions (e.g. Marchenko et al. 2017a, b; Van Pelt et al. 2012, 2018; Vega et al. 2016), and to Svalbard-wide climatic mass balance modelling experiments (e.g. Aas et al. 2016; Østby et al. 2017; Van Pelt et al. 2019).

2.1.3 Southern Spitsbergen

Glaciers in this region have undergone strong mass losses in the last two decades, with rates of annual ice surface lowering nearly twice as much as in previous decades. For the period 2004-2011 mass losses were -1.25 m w.e. a^{-1} for Vøringbreen, -1.08 m w.e. a^{-1} for Aldegondabreen, -0.8 m w.e. a^{-1} for Vestre Grønfjordbreen, and -1.35 mw.e. a^{-1} for **Austre Grønfjordbreen** (AGB) (Mavlyudov et al. 2012). Geodetic measurements supported with some stake measurements on Aldegondabreen shows that in 2015-2018 its mean balance was -1.83 m w.e. a^{-1} (Terekhov et al. 2020).

AGB is nearly 7 km^2, with elevations from 40-450 m a.s.l. Annual mass balance surveys have been performed each autumn. Winter snow accumulation has not been measured regularly, so for some years the winter and summer balance components were not measured directly, but estimated using empirical relationship with air temperature (Chernov et al. 2019).

Hansbreen (HAB) is a medium-sized (56 km^2) tidewater glacier located in the southern part of Wedel Jarlsberg Land, close to the Polish Polar Station in the fjord Hornsund. The glacier is ~16 km long, and elevations extend up to 550 m a.s.l. Surface mass balance monitoring started in 1988/89. Over the period of 1989-2017 the net surface mass balance has been continuously decreasing (Figure 2), with a mean of -0.36 m w.e. a^{-1}. Frontal ablation, measured along the c. 1.5 km long ice cliff shows that mass loss by calving contributes substantially to the total mass loss (23-50%, i.e. additional ablation by an equivalent of c. -0.7 m w.e. a^{-1} on average) and varies interannually.

Werenskioldbreen (WSB) is a medium-sized (27 km^2) land-terminating valley glacier to the west of HAB, with elevations from 50-600 m a.s.l., and has been monitored with some interruptions since 1999. The average mass balance is -0.57 m w.e. a^{-1}.

2.1.4 Northeast-Svalbard

In 2004, the University of Oslo and the Norwegian Polar Institute established a network of mass balance stakes along several profiles crossing the **Austfonna** ice cap (~8000 km^2), by far the largest ice body in Svalbard. Since then, annual measurements of surface elevation changes (Moholdt et al. 2010a; Gray et al. 2015), mass balance (Schuler et al. 2007), surface velocities (Dunse et al. 2012; 2015), snow distribution (Taurisano et al. 2007; Dunse et al. 2009), near-surface meteorology and energy balance (Schuler et al. 2014; Østby et al.. 2013) have been conducted. These activities have been based mainly on research project funding and their focus has varied. Nevertheless, mass balance has been measured each year on **Etonbreen** (ETN, ~880 km^2), and is a part of the MOSJ database[3]. The net mass balance has typically been close to zero, except for an exceptionally positive year in 2008 and two very negative years in 2004 and 2013. The surface mass balance of Etonbreen is representative for the Austfonna ice cap as verified by some years of mass balance surveys over the entire ice cap. Calving and marine melting at the terminus of Etonbreen cause a small additional mass loss. However, for the entire ice cap calving loss is important and gives a mass loss of ca. 2 Gt a^{-1} and for periods surging glaciers may have a very important impact on the overall mass balance as shown by the surge in Basin3 when the surge almost tripled the calving loss of the ice cap to about 5.5 Gt a^{-1} (Dunse et al. 2015). The data from Austfonna have proved valuable for Svalbard-wide glacier models (Aas et al. 2015; Østby et al. 2017; Van Pelt et al. 2019) since they are the only data from a glacier of significant size and from the heavily glacier-covered, but logistically more challenging eastern part of Svalbard.

3 http://www.mosj.no/en/climate/land/mass-balance-glaciers.html

2.2 New technologies

The most striking evolution since the Hagen et al. (2003 a, b) assessments is the more widespread availability of different remotely sensed measurements. Since the 2000's, the number of sensors and platforms has grown considerably, and the resolution, accuracy and frequency of measurements have increased. Access to these data has become easier for a growing number of glacier-relevant measurements, such as surface elevation changes, DEMs as well as land-surface temperatures, albedo, and glacier facies (e.g. Nuth et al. 2010; Moholdt et al. 2010b; Gray et al. 2015). Spaceborne gravimetry allows monitoring mass changes, which, if corrected for a range of other gravitational effects, can provide information on regional glacier-related mass changes (Wouters et al. 2008, 2019; Matsuo and Heki 2013; Gardner et al. 2013).

The availability of global atmospheric reanalyses at improved spatial and temporal resolution, and improved consistency with available observations (e.g. Schuler and Østby 2019), has sparked the application of gap-free meteorologically-forced glacier mass balance models that cover the entire archipelago (e.g. Østby et al. 2017; Van Pelt et al. 2019). These models either directly incorporate local measurements or have been optimized to ensure agreement between simulated and observed values and therefore play an important role in synthesizing the wealth of information that became available.

In addition to increases in the number of stake measurements, and more extensive availability of satellite products around Svalbard since 2003, we are now collecting a broader set of on-glacier data; GPSs (velocities and surface height) Automatic Weather Stations (AWS), wireless-sensor networks (WSN), radar, seismology, time-lapse photography, Terrestrial Laser Scanning (TLS), Structure from Motion (SfM) applied on imagery from unmanned vehicles (UAV), and smart tracers (e.g. Alexander et al. 2019).

There has been a great increase in the use of UAVs, for high-resolution remote sensing tasks. Glaciological applications have focused on optical sensors to make digital elevation models (e.g. Girod et al. 2017), detect changes in surface properties, and resolve ice speed. Submarine UAVs are used to measure oceanic properties and mapping submarine hypsometry in glaciated fiords. The ongoing miniaturization of sensors helps overcoming payload limitations of UAVs and enables multi-sensor measurements over glaciated terrain. One promising example is the development of UAV radar systems that may soon be operational.

Low-cost, autonomously recording and transmitting systems (SIOS project SWAG-Net RiS ID 11214) improve coverage of basic meteorological and glaciological measurements in areas of difficult or even dangerous access. When set up in a communication network, these systems can be enhanced to conduct more specialized and individually tailored measurements.

2.3 New synthesis

2.3.1 Mass balance modelling

Relative to 2003, numerical modelling now plays an increasingly prominent role in glacier studies on Svalbard. Stimulated by the growing availability of observational data for model optimization, models have been increasingly used to simulate climatic mass balance (e.g. Lang et al. 2015; Aas et al. 2016; Østby et al. 2017; Möller and Kohler 2018; Van Pelt et al. 2019) and ice flow (e.g. Gladstone et al. 2014; Schäfer et al. 2014; Vallot et al. 2017; Gong et al. 2018). The climatic mass balance (CMB) refers to mass changes at the glacier surface and in snow/firn, but does not include frontal ablation (calving and sub-marine melting) of tidewater glaciers. Modelled mass balance is spatially complete and covers the entire glacierized area of Svalbard, providing information at relatively high temporal resolution (sub-daily to hourly), depending on the meteorological forcing (Figure 3; Table 1). These products can therefore be understood as spatial-temporal interpolators and have great potential to synthesize a large amount of individual measurements for regional assessments.

CMB models have been used both inline, coupled to regional climate models (Lang et al. 2015; Aas et al. 2016), and offline, forced by downscaled meteorological variables. Offline applications have used an entire spectrum of downscaling procedures, ranging from statistical relations (Möller and Kohler, 2018), intermediate-complexity methods (Østby et al. 2017; Van Pelt et al. 2019), and dynamical downscaling (Hanssen-Bauer et al. 2019). Temporal coverage varies and is either limited by computational cost (Aas et al. 2016; Hanssen-Bauer et al. 2019) or by availability of atmospheric reanalysis data. For instance, ERA-interim (Dee et al. 2011) reanalysis data are available since 1979, ERA-40 (Uppala et al. 2005) start in 1957, allowing longer-term simulations (Østby et al. 2017; Van Pelt et al. 2019), and the ERA-20C reanalysis dataset (Poli et al. 2016) pushes the limit even back to 1900 (Möller and Kohler 2018).

Table 1: Comparison of several Pan-Svalbard estimates of glacier mass balance using different methods. The "flux" method refers to a combination of remotely sensed velocity fields and frontal area changes. "dh" refers to differencing elevation measurements by ground-based GPS profiling, air- and spaceborne photogrammetry, laser and radar altimetry. "Gravimetry" refers to estimates derived from GRACE measurements. The estimates refer to different components of the total mass balance, calving and climatic mass balance (CMB) and are marked in the table, where Total = CMB + Calving.

Reference	Period	Method	Specific B_n (m w.e. a^{-1})	B_n (Gt a^{-1})	Balance component
Hagen et al. 2003a	~1970-1999	Interpolation 1	-0.38 ± 0.33 -0.11	-14 ± 12 -4	Total Calving
Hagen et al. 2003b	~1970-1999	Interpolation, 2	-0.12 ± 0.03	-4.5 ±1	Total
Błaszczyk et al. 2009	1999-2006	Flux	-0.18 ± 0.05	-6.75 ± 1.7	Calving
Dunse et al. 2015	2013 (Basin-3)	Flux		-4.2 ± 1.6	Calving
Nuth et al. 2010	1965/90-2003/7	dh	-0.36 ± 0.02	-9.7 ± 0.55	Total
Moholdt et al. 2010b	2003-2008	dh	-0.12 ± 0.04	-4.1 ± 1.4	Total
Lang et al. 2015	1979-2013	Model (10 km)	-0.04	-1.6	CMB
Aas et al. 2016	2003-2013	Model (3km)	-0.26	-8.7	CMB
Østby et al. 2017	1957–2014	Model (1km)	0.08	2.7	CMB
Möller and Kohler 2018	1900-2010	Model (0.25 km)	-0.002	-0.07	CMB
Hanssen-Bauer 2019	2004-2017	Model (2.5km)	-0.26	-8.7	CMB
Van Pelt et al. 2019	1957-2018	Model (1km)	0.09	3.0	CMB
Wouters et al. 2008	2003-2008	Gravimetry	-0.26 ± 0.09	-8.8 ± 3	Total
Jacob et al. 2012	2003-2010	Gravimetry	-0.09 ± 0.06	-3 ± 2	Total
Mémin et al. 2011	2003-2009	Gravimetry 1 Gravimetry 2	-0.27 ± 0.03 -0.46 ± 0.07	-9.1 ± 1.0 -15.5 ± 2.4	Total Total
Matsuo & Heki 2013	2004-2012	Gravimetry	-0.11 ± 0.09	-3.7 ± 3.0	Total
Gardner et al. 2013	2003-2009	Gravimetry 1 Gravimetry 2	-0.20 ± 0.06 -0.13 ± 0.12	-6.8 ± 2.0 -4.4 ± 4.1	Total
Wouters et al. 2019	2002-2016	Gravimetry 1 Gravimetry 2	-0.21 ± 0.04 -0.27 ± 0.21	-7.2 ± 1.4 -9.1 ± 4.1	Total

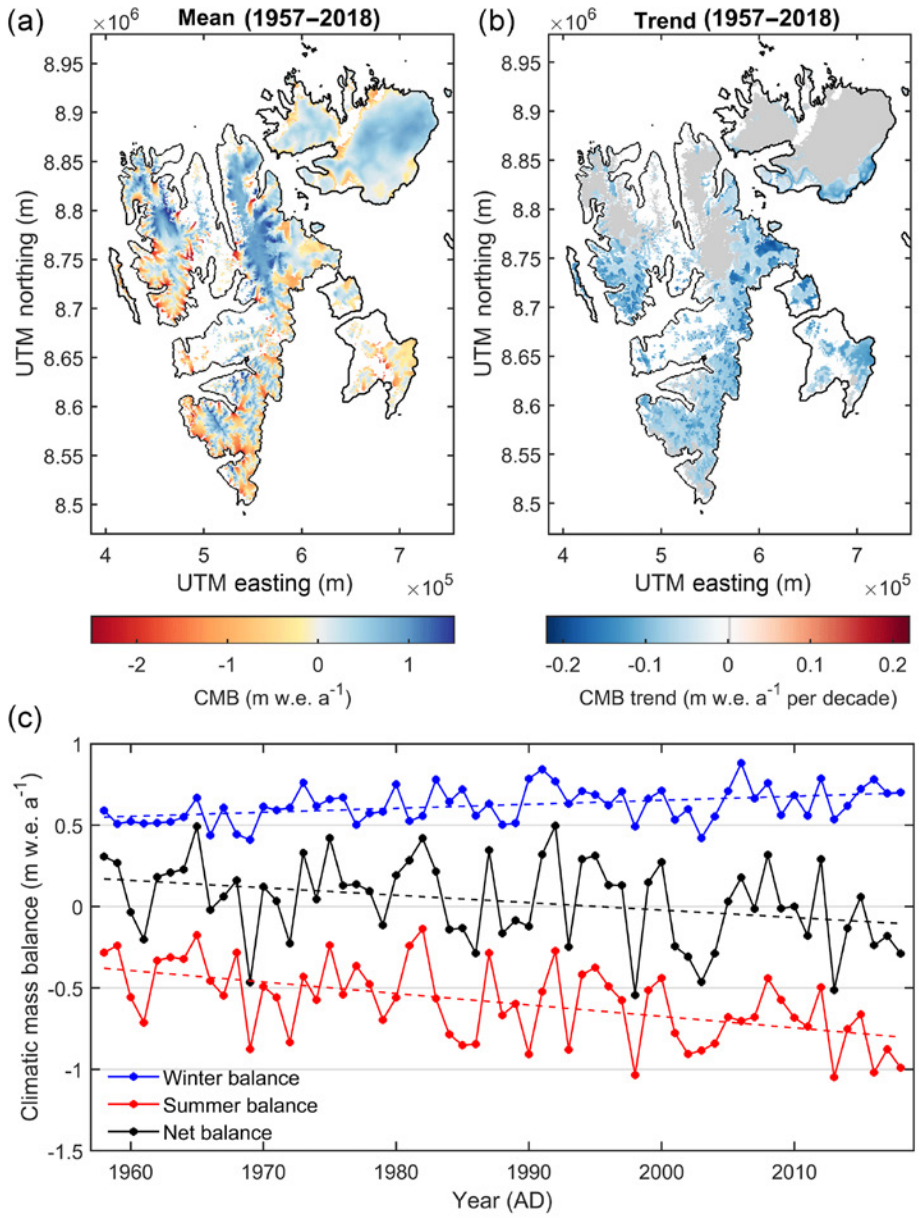

Figure 3: Simulated long-term CMB distribution (a) and trends (b). In (c) time series of area-averaged summer, winter and annual (Sep – Aug) net CMB are shown, along with corresponding linear trends. Figure from Van Pelt et al. (2019). Glacier outlines were extracted from A digital glacier database for Svalbard (chapter in Global Land Ice Measurements from Space by König et al. 2014): https://doi.org/10.21334/npolar.2013.89f430f8.

To various degrees, all model studies made use of an extensive set of measurements from mass balance stakes, AWSs, and firn cores across Svalbard for calibration and validation. Table 1 provides an overview over the different applications, their temporal coverage as well as spatial resolution. All models reveal a distinctive pattern, ranging from negative CMB in southern Spitsbergen to more positive values in northeast Svalbard (Figure 3a), reflecting the gradient of air temperature (Hanssen-Bauer et al. 2019). Over the long-term (>50 years), all studies indicate a slightly positive CMB, but all show clearly negative CMB for more recent periods, especially after 2000 (Figure 3c). The results by Van Pelt et al. (2019) shown in Figure 3 agree with the other model-based assessments, with record negative years in 2004 and 2013, and a close to zero balance for the period 2005-2012, before mass balance turns consistently negative. Although there is agreement on a tendency towards more negative CMB, trend analysis reveals its significance is restricted to southern Svalbard (Figure 3b) with a trend of -0.06 m w.e. a^{-1} $decade^{-1}$. Both Van Pelt et al. (2019) and Østby et al. (2017) find that increased melt and reduced refreezing leads to doubling in glacier runoff over the simulation period. In addition, Østby et al. (2017) find a strong correlation between mass balance and summer temperature.

2.3.2 Frontal ablation

When the only available estimate of ice discharge from Svalbard glacier calving (Błaszczyk et al. 2009) of nearly 7 Gt a^{-1} is added to the different CMB results, the overall Svalbard mass balance becomes clearly negative (Table 1, Figure 4). The Błaszczyk et al. (2009) calving estimate is based on glacier flow velocities and front position changes extracted from ASTER images acquired from 2000–2006. However, due to its close dependence on glacier dynamics and ocean temperature (Luckman et al. 2015), frontal ablation varies over many time scales: seasonal, annual and especially, from irregularly occurring surges. For example. Dunse et al. (2015) quantified the sea-level effect of a single surge in Austfonna over the period 2012-2013, and found that the surge contributed 7 Gt a^{-1}, approximately matching the Błaszczyk et al. (2009) estimate, hence doubling the sea-level contribution per year of entire Svalbard during the surge period.

Because of reduction in ice discharge, marine termini can quickly retreat. Many areas around Svalbard are experiencing rapid ice cliff recessions (10s to 100s m a^{-1}), which significantly affects the marine physical environment and ecosystem. One special case is Hornsund: bed elevations for the Hornbreen – Hambergbreen glacier system have been found approximately 40 m below sea level, such that a new strait between the Greenland Sea and the Barents Sea is expected within the next 2-3 decades, once the glacier termini have retreated (Grabiec et al. 2018).

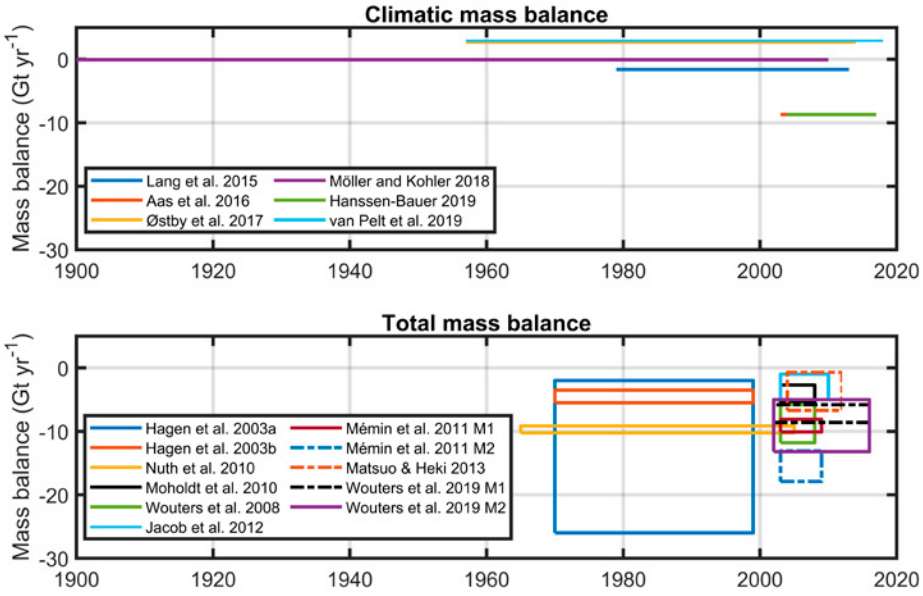

Figure 4: Graphical representation of the mass balance estimates for glaciers on Svalbard (Table 1). The top panel compares the estimates of climatic mass balance, derived from several model studies. The bottom panel compares total mass balance estimates derived from extrapolation of direct, geodetic and gravimetric measurements.

2.3.3 Geodetic mass balance

Nuth et al. (2010) compared satellite altimetry data from the ICESat mission for the period 2003–2007 to older topographic maps and digital elevation models for different epochs (1965–1990). Because the ICESat tracks are relatively sparse, they extrapolated along-track changes to the larger regions using glacier hypsometry. Significant thinning was detected at the lower elevations of most glaciers, and either slight thinning or thickening in the accumulation areas, except for glaciers that surged during the observation period; these glaciers showed thickening in the ablation area and thinning in the accumulation areas. However, the overall balance was very negative at -0.36 m w.e. a^{-1}, corresponding to -9.7 Gt a^{-1} (Table 1). As with the modelling results, the most negative geodetic balances are found in the South and the least negative balances in the Northeast.

Moholdt et al. (2010b) determined elevation changes along the ICESat tracks for the period 2003-2008, extrapolating these changes to the remaining glacier area using the same hypsometric approach as Nuth et al. (2010) to yield a Svalbard-wide estimate of -0.12 m w.e. a^{-1}, or -4.3 Gt a^{-1}. They found that most regions experienced low-elevation thinning and high-elevation balance or thickening, and that the largest ice losses occurred in the West and South, while northeastern Spitsbergen and the Austfonna ice cap slightly gained mass.

This general pattern, however, does not apply for central Spitsbergen, with its mostly small alpine glaciers. Małecki (2016) demonstrated that glacier thinning here has been occurring at all elevation up to 1000 m a.s.l., for the period 1990-2011.

Analysis of older maps and modern DEMs (Kohler et al. 2007) shows that mass loss rates at MLB and Slakbreen, near Svea, appears to have accelerated. For MLB, thinning rates for 2003–2005, were more than four times the average for the first measurement period 1936–1962. On Slakbreen, thinning rates for the period 1990–2003 were more than four times that of the period 1961–1977. James et al. (2012) and Małecki (2013) found a similar increase in thinning rates for other glaciers around Svalbard, particularly in high-elevation areas. More pronounced thinning has been noted for HAB and Hornbreen for two recent periods 2011-2015 and 2015-2017 based on differencing elevations obtained by photogrammetry using high-resolution satellite images (Błaszczyk et al. 2019). This increasingly negative mass balance trend is consistent with both worldwide glacier trends as well as developments in the Arctic (Kaser et al. 2006).

2.3.4 Gravimetry

While satellite gravimetry provides an absolute measure of the total mass change in the region the spatial resolution of GRACE is typically in the order of 0.5°-1° (Wouters et al. 2019) and determination of glacier mass balance is challenging. A number of studies (Wouters et al. 2008; Jacob et al. 2012; Mémin et al. 2011; Matsuo and Heki 2013; Gardner et al. 2013) working with the same dataset but covering slightly different periods, and using different data filtering methods, obtain a range of values for the total mass loss (Table 1). However, the main conclusion one can reach from the body of GRACE analyses is that all find a negative mass balance for the Svalbard archipelago, with values ranging from -0.46 to -0.09 m w.e. a^{-1}, or -15.5 to -3.0 Gt a^{-1} (Table 1), even if the error range for some of the estimates extends into the positive territory. The most recent regional estimate, covering the entire GRACE mission from 2002-2016, indicates an average mass balance of -7 Gt a^{-1} (Wouters et al. 2019).

2.3.5 Summary

Figure 4 shows some variation between the different estimates due to different periods covered and different methods employed. Nevertheless, the different results are consistent in that the surface mass balance of glaciers is negative in general and significantly more negative when frontal ablation at tidewater glaciers (Figure 1) is accounted for. The latter can cause drastic recession and thinning of marine terminating glaciers and extension of new branches of fjords. Analysis of time series indicates that there is a tendency towards increased mass loss over time.

Available long-term mass balance observations (Figure 2) reveal a complex picture of different glacier evolutions. These clearly demonstrate differences between small glaciers (<10 km^2) that are rapidly losing mass (ABB, MLB, WLB, SVB, AGF) and larger glaciers (>50 km^2) like KNG, KHF, NSB, ETN and HAB. These are typically outlets of larger contiguous ice masses (ice fields and ice caps). The steeper slope of the cumulative mass balances shows that glaciers in southern and central Spitsbergen (WSB, SVB, AGF) have more negative mass balances than those located in NW Svalbard (ABB, MLB). Similarly, larger glaciers such as HAB are losing mass more rapidly than at KNG, KHF, NSB or ETN. The latter is an outlet from Austfonna and shows surface mass balance conditions close to zero with little variability, though with a tendency towards more negative values after 2012.

The in-situ measurements (Figure 2) align well with model results (Figure 3). The simulated CMB distribution in Figure 3a shows a pronounced gradient from higher CMB in NE-Svalbard to lower values in S-Svalbard, where trends are significantly negative (Figure 3b). This spatial distribution is equally reproduced in the remotely-sensed geodetic mass balance estimates. The simulated time series support the view that most of the variability of net mass balance is largely due to variability in summer mass balance whereas winter mass balance is more stable (Figure 3c).

The spatial coverage of available mass balance measurements has improved over the past 20 years, especially with the inclusion of data from Austfonna, NSB and SVB, filling gaps both in terms of glacier types and location. Therefore, the presently available data are more representative for Svalbard than the pre-2000 record that was heavily biased towards smaller glaciers in the vicinity of settlements in western Spitsbergen. For a representative picture of Svalbard glacier mass balance, it is therefore imperative to have adequate spatial sampling and include records from the logistically more challenging eastern parts of Svalbard. Mass balance modelling is a valuable tool to link these measurements and to provide a gap-free product with high spatial and temporal resolution.

The total mass balance of Svalbard glaciers consists of two main parts, the climatic mass balance and the frontal ablation (calving and submarine melting). The only available estimate of current ice discharge from Svalbard glaciers (Błaszczyk et al. 2009) is a composite of snapshots in the period 2000-2006 and amounts to 5.0-8.4 Gt a^{-1} (mean 6.75 Gt a^{-1}), hence, ice discharge is roughly equivalent to the mass loss by climatic mass balance in the same period. This work urgently needs to be updated, especially in light of several large glacier surges which discharged large volumes of ice into the ocean over short periods. There are some suggestions that increased melt hastens the triggering effect on surges (Dunse et al. 2015) and a number of other large-scale surges events have been reported in Svalbard (Sund et al. 2014) as well as other Arctic regions (e.g. Willis et al. 2018). These events affect the total ice discharge and have the potential to considerably increase the sea-level contribution from land ice over short time periods.

2.4 New challenges

In concert with warming of the atmosphere, glaciers experience more surface melting. However, due to the polythermal nature of Svalbard glaciers, they have a considerable retention capacity and huge amounts of meltwater refreeze in the porous snow and firn areas. Model estimates described above account for this process (in simplified ways), and all agree that this retention capacity has considerably decreased due to general warming and a reduction in the size of firn areas (Østby et al. 2017; Van Pelt et al. 2019). Analysis of satellite data of Hansbreen, Storbreen and Hornsbreen showed a significant decrease in the firn area between 2013 and 2018, by 30% - 40% (Barzycka et. al. 2019). Consequently, refreezing capacity in the firn is depleted, and more surface meltwater will exit the glacier as runoff, although some of this water may be temporarily stored in surficial lakes or within perennial firn aquifers (Christianson et al. 2015). Due to their potential to release large amounts of water, for instance when intercepted by a crevasse, firn aquifers are of considerable interest for glacier dynamics and hydrology. Furthermore, these aquifers may promote microbial production (e.g. Anesio et al. 2017), and are the focus of ongoing research on glacier ecology (Hodson et al. 2015). In general, a more sophisticated model of drainage system for Svalbard polythermal glaciers has to be developed to follow the novel approach of discrete recharge of an aquifer (outside of the firn zone) via moulins (Gulley et al. 2012; Decaux et al. 2019). However, our understanding of processes that control the vertical percolation of surface meltwater and associated firn warming needs to be refined, and studies of horizontal water motion are largely absent

Changes in the size and volume of temperate ice bodies in polythermal glaciers is important for understanding their hydrothermal regime, potential dynamic instability, and therefore, their response to climate change. Data analysis of ground-based radio-echo sounding of 16 glaciers at Nordenskiöld Land in Spitsbergen shows that 11 of them are polythermal type (Macheret et al. 2019). The volume fraction of temperate ice in total volume of these glaciers varies from 1 % to 74 %. Repeated GPR surveys on selected polythermal glaciers along the same tracks serve as a useful tool in long-term glacier observation projects.

As mentioned above, several major surges have been observed since 2000 (Dunse et al. 2015; Sund et al. 2014; Nuth et al. 2019; Sund et al. 2009), despite earlier prognoses of a decline with ongoing warming (Dowdeswell et al. 1995). Instead, there is an apparent increase in the number of surges, although it is still unclear whether this is due to more frequent surging or to improved observation capabilities (cf. Farnsworth et al. 2016). A related issue is the seasonal dynamical adjustment of ice speed during the start of the ablation period, due to the decrease of basal friction. The use of continuous GPS on Svalbard glaciers has shown a relation between water availability and ice speed-ups (Vieli et al. 2004; Van Pelt et al. 2018; Dunse et al. 2012; Vallot et al. 2017). Even though the ice discharge has been assessed for a number of glaciers, an observational regional assessment

is not yet available. Due to the large mass fluxes involved in these events, such a Svalbard-wide assessment of ice discharge is urgently needed to get a reliably updated view on total mass losses.

Measurements of surging glaciers on Svalbard (e.g. Nuth et al. 2019) have led to recent theoretical progress in understanding the mechanics of destabilisation and surge propagation (Thøgersen et al. 2019; Sevestre et al. 2018) and climatic controls on the global distribution of surging glaciers (Sevestre et al. 2015; Benn et al. 2019). While frequent surging in Svalbard imposes a challenge in determining the mass flux to the ocean, it also represents an opportunity for improving our understanding of dynamic instabilities and potential links to climate warming. Svalbard is an ideal field laboratory for advancing our understanding of these processes, given the relative ease of access and an already existing knowledge and research infrastructure. Better understanding of glacier flow instabilities will provide important insights into the stability of the larger ice sheets of Greenland and Antarctica in a warming climate. The underlying processes could be studied on Svalbard not only at considerably lower logistical efforts but also under actually ongoing warming that may anticipate what the ice-sheets yet have to face.

2.5 New relevance

Glaciers represent a long-term storage element in the **water balance**, hence, in regions with considerable glacier cover, such as Svalbard where almost 60% of the land surface is covered by ice, glaciers have a dominant role in hydrology which in turn links the glaciers to a plethora of other fields such as **hydrology, oceanography and ecology**. For instance, meltwater runoff from glaciers strongly **influences downstream ecosystems** both from marine-terminating (plume, fjord circulation, ecological hotspot) and well as land-terminating glaciers (dominance/modulation of surface runoff). Meltwater migrating through both paths are reaching fjords causing significant freshening of their waters (e.g. Błaszczyk et al. 2019). On the other hand, en- and subglacial drainage have **implications for glacier dynamics** through effects on the thermal regime and glacier sliding and hence is tightly related to instabilities (surges). A recent assessment of climate change on Svalbard and its related impacts (Hanssen-Bauer et al. 2019) demonstrated the close linkage between glaciers and hydrology on Svalbard, with present-day glacier runoff about four times larger than the runoff from ice-free land (Van Pelt et al. 2019).

Seismological measurements by the existing operational seismic network have been successfully used to monitor glacier calving (Köhler et al. 2016) and surges (Nuth et al. 2019). However, the geometry of the network has deficiencies with respect to detecting and locating events in the Eastern part of Svalbard (Köhler et al. 2020).

Furthermore, specially tailored, temporarily installed seismometer arrays have proved valuable in a number of glacier-related projects to detect and quantify calving (Köhler et al. 2019a) and to collect unprecedented on-glacier data that gave new insights into details of glacier motion and meltwater drainage (Gajek et al. 2017; Köhler et al. 2019b). While present-day satellite remote sensing allows measurements of velocity fields at time intervals of about 10 days, GNSS systems on the glacier surface can record hourly displacements (depending on overall flow speed). However, theory suggests that short-lived (seconds-minutes) motion events may have significance. With scanning rates of several Hz, cryoseismology hence fills this observational gap and opens the pathway for better process understanding.

3. Unanswered questions

The ultimate, overarching question concerns **the future evolution of the land-based ice mass on Svalbard and the related release of freshwater to the terrestrial (streamflow) and marine (fjord circulation) systems and associated impacts on ecosystems and socio-economy**. We break this question into more specific parts that address knowledge gaps related to the current status and the future evolution.

Current status:

- How large is the **frontal ablation**? How much does it vary on different time scales (seasonal, interannual, decadal)? How large are the relative contributions of the two components calving and submarine melting? What are the governing processes?
- What is the importance of **surges** for the mass balance? What are the mechanisms that trigger instability and how does it propagate? Does climate change have an influence on surging?
- How large is the **retention capacity** of Svalbard glaciers? How does it change and what is the partitioning between refreezing and liquid water storage? What are the implications of firn aquifers and supraglacial lakes for biogeochemistry and glacier dynamics?

Process understanding and quantification of these components is imperative for reliably assessing the **future evolution**:

- How will glacier **melt, refreezing and runoff** evolve in the future?
- How do **dynamics and geometry** of Svalbard glaciers respond to climate change?
- What are the **impacts** on calving, surging and frontal ablation?

4. Recommendations for the future

Above, we have identified a number of important knowledge gaps, and to resolve them, the consortium requests a number of research projects. We recognize that funding research projects falls outside the scope of SIOS, but we believe that **concerted efforts regarding networking and research infrastructure** can pave the road towards implementation of these urgently needed research projects.

Specifically, we identified **research needs** concerning:

1. Process studies of **unstable glacier flow** and its potential relationship to surface meltwater
2. Development of a **coupled glacier mass balance-glacier dynamics model** that can be applied to investigate the effects of different climate scenarios
3. Detailed measurements to quantify and understand **frontal ablation and its drivers** and to separate its components submarine melting and calving and their relative importance related to surface mass balance.
4. Geophysical characterization of **firn aquifers** and changes thereof, along with multi-disciplinary efforts to understand their implications for biogeochemistry.

By improving critical infrastructure, providing data services and supporting community efforts, SIOS can significantly contribute to developing Svalbard as a field laboratory for polar glaciology where research projects will address the above listed knowledge gaps.

To that end, we recommend SIOS to:

- Strengthen the **network of Svalbard glaciologists** by supporting more regular, community-wide activities, for instance by workshops to coordinate research efforts and infrastructure needs, conduct comparative studies or collectively attack grand challenges. For instance, the present SvalGlac report brought together scientists dealing with mass changes of Svalbard glaciers, and should serve as a kick-off to a wider collaboration. Seed support from SIOS will nurture the positive ambitions created herein, and would stimulate further development. We recognize that glaciological activity on Svalbard comprises much more and propose **a follow-up report on glacier dynamics and novel field techniques**. These aspects are related to but outside the scope of this report, and their review will involve a different part of the glaciological community.
- Support community efforts to collect **a Svalbard-wide dataset of near-front ice thickness**, for instance by using airborne ground-penetrating radar. Combined with available remotely-sensed velocity, this will immediately enable quantifying calving rates at unprecedented accuracy and serve as a baseline for any further efforts

regarding frontal ablation and its temporal variations.

- Further develop **data services improving cross-disciplinary use of open data**. Many scientists are not aware of already available datasets from other disciplines; this could be alleviated by development of a Svalbard-specific **Data Discovery Tool** within SDMS. Many research datasets are not published in repositories due to high requirements on documentation. This could be alleviated by developing a **Dataset Registration Interface** that interactively aids the scientist to compile metadata complying with standards.
- Stimulate **enhanced communication and cooperation** between the remote sensing and the ground based glaciological groups. The fast development of new sensors increases the potential for assessing key questions stated above.
- Support **homogenization of methods** and improve the collective quality of Svalbard-wide data. This could be achieved through investing in a pool of instruments that are compatible with a common data transmission protocol thus ensuring that all partners can follow the same procedures, for instance when **increasing spatial coverage of mass balance monitoring** to currently underrepresented regions. Having homogenized methods will ultimately increase the value of Svalbard-wide datasets that have been collected by different teams.
- Support development of a **'real-time' (online) database of simulated climatic mass balance**, melt, runoff, etc. across Svalbard to directly reach out to glacier-related disciplines (e.g. marine biology, hydrology, seismology), for instance similar to http://polarportal.dk/en/greenland/mass-and-height-change/.

5. Data availability

Glaciological and glacier-related data from Svalbard are available from different repositories and metadata bases. The most important examples are:

- A **digital elevation model** at https://doi.org/10.21334/npolar.2014.dce53a47 and the **glacier outlines** at https://doi.org/10.21334/npolar.2013.89f430f8 (König et al. 2014), the latter is part of the Randolph Glacier Inventory (RGI consortium 2017).
- **Glacier-wide mass balances** in the database of the World Glacier Monitoring Service (WGMS; https://wgms.ch/), and Environmental monitoring of Svalbard and Jan Mayen (MOSJ): http://www.mosj.no/en/climate/land/mass-balance-glaciers.html,
- The Centre for Polar Studies, University of Silesia data are accessible through the Polish Polar Data Base (www.ppdb.us.edu.pl). **The mass balance data**: http://ppdb.us.edu.pl/geonetwork/srv/eng/catalog.search?node=srv#/home; **the glaciers inventory**: http://ppdb.us.edu.pl/geonetwork/srv/eng/catalog.search#/metadata/fb01ad1f-41d8-47f6-b5a2-2c0833b9e772, http://ppdb.us.edu.pl/geonetwork/srv/eng/catalog.search#/metadata/a0f670ad-0c1e-4cd5-a66d-1366cdfc9428; **the**

positions and velocities of the front: http://ppdb.us.edu.pl/geonetwork/srv/eng/catalog.search#/metadata/05e2c69a-5645-4488-bc88-630beb03a462, http://ppdb.us.edu.pl/geonetwork/srv/eng/catalog.search#/metadata/37a59a98-835f-4f98-ab39-52c8d9cb7290.

- Unrestricted access to the **point stake mass balance**, and the remaining **AWS time series** is provided upon request by contacting the institutes that collected the data.
- **Meteorological records** for Ny-Ålesund, Hornsund and Longyearbyen are accessible through the eKlima portal (http://eklima.met.no/); and Kongsvegen AWS data at https://doi.org/10.21334/npolar.2017.5dc31930 (Kohler et al. 2017).
- **Surface velocities** shown in Figure 1 have been retrieved from Gardner, A. S., M. A. Fahnestock, and T. A. Scambos, 2019: ITS_LIVE Regional Glacier and Ice Sheet Surface Velocities. National Snow and Ice Data Center; DOI: 10.5067/6II6VW8LLWJ7.

Acknowledgements

This work was supported by the Research Council of Norway, project number 251658, Svalbard Integrated Arctic Earth Observing System - Knowledge Centre (SIOS-KC). We appreciate comments and delivery of unpublished data by B. Barzycka, M. Grabiec and D. Ignatiuk (Centre for Polar Studies, University of Silesia). Students of the GEO4420: Glaciology course at the University of Oslo were helpful to design and answer the list of frequently asked questions.

References

Aas KS, Dunse T, Collier E, Schuler TV, Berntsen TK, Kohler J, Luks B (2016) The climatic mass balance of Svalbard glaciers: A 10-year simulation with a coupled atmosphere-glacier mass balance model. The Cryosphere 10:1089-1104. https://doi.org/10.5194/tc-10-1089-2016

Ahlmann HW (1933) Scientific Results of the Swedish-Norwegian Arctic Expedition in the Summer of 1931, Part VIII. Glaciology. Geografiska Annaler 15(2-3):161-216. https://doi.org/10.1080/20014422.1933.11880566

Alexander A, Kruusmaa M, Tuhtan JA, Hodson AJ, Schuler TV, Kääb A (2019) Multi-modal sensing drifters as a tool for repeatable glacial hydrology flow path measurements. The Cryosphere Discuss. https://doi.org/10.5194/tc-2019-132, in review

Anesio AM, Lutz S, Chrismas NAM et al. (2017). The microbiome of glaciers and ice sheets. npj Biofilms Microbiomes 3(10). https://doi.org/10.1038/s41522-017-0019-0

Barzycka B, Grabiec M, Laska M, Ignatiuk D, Błaszczyk M, Hagen JO, Jania JA (2019) Glacier's Facies Changes in the Hornsund Fiord Basin (Svalbard) during the Last Decade. Abstract presented at the 27th International Union of Geodesy and Geophysics General Assembly, Montreal, Canada, 8-18 July 2019. https://www.czech-in.org/cmPortalV15/CM_W3_Searchable/iugg19/normal#!abstractdetails/0000751020

Benn D, Fowler A, Hewitt I, Sevestre H (2019). A general theory of glacier surges. Journal of Glaciology, 65(253):701-716. https://doi.org/10.1017/jog.2019.62

Błaszczyk M, Jania JA, Hagen JO (2009) Tidewater glaciers of Svalbard: recent changes and estimates of calving fluxes. Polish Polar Research 30:85-142. https://doi.org/10.2478/popore−2013−0024

Błaszczyk M, Jania JA, Kolondra L (2013) Fluctuations of tidewater glaciers in Hornsund Fjord (Southern Svalbard) since the beginning of the 20th century. Polish Polar Research 34:327-352. https://doi.org/10.2478/popore−2013−0024

Błaszczyk M, Ignatiuk D, Uszczyk A, Cielecka-Nowak K, Grabiec M, Jania JA, Moskalik M, Walczowski W (2019) Freshwater input to the Arctic fjord Hornsund (Svalbard). Polar Research 38:3506. https://doi.org/10.33265/polar.v38.3506

Błaszczyk M, Ignatiuk D, Grabiec M, Kolondra L, Laska M, Decaux L, Jania J, Berthier E, Luks B, Barzycka B, Czapla M (2019) Quality Assessment and Glaciological Applications of Digital Elevation Models Derived from Space-Borne and Aerial Images over Two Tidewater Glaciers of Southern Spitsbergen. Remote Sensing 11:1121. https://doi.org/10.3390/rs11091121

Chernov RA, Kudikov VA, Vshivtseva TV, Osokin NI (2019) Estimation of the surface ablation and mass balance of Austre Grønfjordbreen (Spitsbergen). Ice and Snow 59(1):59-66. https://doi.org/10.15356/2076-6734-2019-1-59-66 [In Russian]

Christianson K, Kohler J, Alley RB, Nuth C, Van Pelt WJJ (2015) Dynamic perennial firn aquifer on an Arctic glacier. Geophysical Research Letters 42:1418-1426. https://doi.org/10.1002/2014GL062806

Decaux L, Grabiec M, Ignatiuk D, Jania J (2019) Role of discrete water recharge from supraglacial drainage systems in modeling patterns of subglacial conduits in Svalbard glaciers. The Cryosphere 13(3):735-752. https://doi.org/10.5194/tc-13-735-2019

Dee D P, Uppala S M, Simmons A J, Berrisford P, Poli P, Kobayashi S, Andrae U, Balmaseda M A, Balsamo G, Bauer P, Bechtold P, Beljaars A C M, van de Berg L, Bidlot J, Bormann N, Delsol C, Dragani R, Fuentes M, Geer AJ, Haimberger L, Healy SB, Hersbach H, Hólm EV, Isaksen L, Kållberg P, Köhler M, Matricardi M, McNally A P, Monge-Sanz B M, Morcrette J-J, Park B-K, Peubey C, de Rosnay P, Tavolato C, Thépaut J-N and Vitart F (2011), The ERA-Interim reanalysis: configuration and performance of the data assimilation system. Q.J.R. Meteorol. Soc. 137: 553–597. https://doi.org/10.1002/qj.828

Dowdeswell JA, Hodgkins R, Nuttall AM, Hagen JO, Hamilton GS (1995) Mass balance change as a control on the frequency and occurrence of glacier surges in Svalbard, Norwegian High Arctic. Geophysical Research Letters 22 (21):2909- 2912

Dunse T, Schuler TV, Hagen J, Eiken T, Brandt O, Høgda K (2009). Recent fluctuations in the extent of the firn area of Austfonna, Svalbard, inferred from GPR. Annals of Glaciology, 50(50): 155-162. https://doi.org/10.3189/172756409787769780

Dunse T, Schuler TV, Hagen JO, Reijmer CH (2012) Seasonal speed-up of two outlet glaciers of Austfonna, Svalbard, inferred from continuous GPS measurements. The Cryosphere 6:453-466. https://doi.org/10.5194/tc-6-453-2012

Dunse T, Schellenberger T, Hagen J O, Kääb A, Schuler T V, Reijmer C H (2015) Glacier-surge mechanisms promoted by a hydro-thermodynamic feedback to summer melt, The Cryosphere 9:197-215. https://doi.org/10.5194/tc-9-197-2015

Farnsworth WR, Ingólfsson O, Retelle M, Schomacker A (2016) Over 400 previously undocumented Svalbard surge-type glaciers identified. *Geomorphology* 264:52-

60. https://doi.org/10.1016/j.geomorph.2016.03.025

Fürst JJ, Navarro F, Gillet-Chaulet F, Huss M, Moholdt G, Fettweis X, et al. (2018) The ice-free topography of Svalbard. Geophysical Research Letters, 45, 11,760–11,769. https://doi.org/10.1029/2018GL079734

Gallet JC, Björkman MP, Borstad CP, Hodson AJ, Jacobi HW, Larose C, Luks B, Schuler TV, Spolaor A, Urazgildeeva A, Zdanowicz C (2019) Snow research in Svalbard: current status and knowledge gaps. In: Orr et al. (eds): SESS report 2018, Svalbard Integrated Arctic Earth Observing System, Longyearbyen, pp. 82-107. https://sios-svalbard.org/SESS_Issue1

Gardner AS, Moholdt G, Cogley JG, Wouters B, Arendt AA Wahr, J, Berthier E. Hock R, Pfeffer WT, Kaser G, Ligtenberg SRM, Bolch T, Sharp MJ, Hagen JO, van den Broeke MR, Paul F (2013) A Reconciled Estimate of Glacier Contributions to Sea Level Rise: 2003 to 2009. Science 340(6134). https://doi.org/10.1126/science.1234532

Gardner AS, Fahnestock MA, Scambos TA (2019) ITS_LIVE Regional Glacier and Ice Sheet Surface Velocities. Data archived at National Snow and Ice Data Center. https://doi.org/10.5067/6II6VW8LLWJ7

Girod L, Nuth C, Kääb A, Etzelmüller B, Kohler J (2017) Terrain changes from images acquired on opportunistic flights by SfM photogrammetry. The Cryosphere 11:827-840. https://doi.org/10.5194/tc-11-827-2017

Gladstone R, Schäfer M, Zwinger T, Gong Y, Strozzi T, Mottram R, Boberg F, Moore JC (2014) Importance of basal processes in simulations of a surging Svalbard outlet glacier. The Cryosphere 8:1393-1405. https://doi.org/10.5194/tc-8-1393-2014

Gong Y, Zwinger T, Åström J, Altena B, Schellenberger T, Gladstone R, Moore JC (2018) Simulating the roles of crevasse routing of surface water and basal friction on the surge evolution of Basin 3, Austfonna ice cap. The Cryosphere 12:1563-1577. https://doi.org/10.5194/tc-12-1563-2018

Grabiec M, Jania JA, Puczko D, Kolondra L, Budzik T (2012) Surface and bed morphology of Hansbreen, a tidewater glacier in Spitsbergen. Pol. Polar Res. 33:111-138

Grabiec M, Ignatiuk D, Jania JA, Moskalik M, Głowacki P, Błaszczyk M, Budzik T, Walczowski W, (2018) Coast formation in an Arctic area due to glacier surge and retreat: The Hornbreen—Hambergbreen case from Spitsbergen. Earth Surface Processes and Landforms 43:387-400. https://doi.org/10.1002/esp.4251

Gajek W, Trojanowski J, Malinowski M (2017) Automating long-term glacier dynamics monitoring using single-station seismological observations and fuzzy logic classification: a case study from Spitsbergen. Journal of Glaciology 63(240):581-592

Gray L, Burgess D, Copland L, Demuth MN, Dunse T, Langley K, Schuler TV (2015) CryoSat-2 delivers monthly and inter-annual surface elevation change for Arctic ice caps. The Cryosphere 9:1895-1913. https://doi.org/10.5194/tc-9-1895-2015

Gulley JD, Grabiec M, Martin JB, Jania J, Catania G, Głowacki P (2012) The effect of discrete recharge by moulins and heterogeneity in flow-path efficiency at glacier beds on subglacial hydrology. Journal of Glaciology 58(211): 926-940. https://doi.org/10.3189/2012JoG11J189

Hagen JO and Liestøl O (1990) Long term glacier mass balance investigations in Svalbard 1950-1988. Annals of Glaciology 14:102-106

Hagen JO, Liestøl O, Roland E, Jørgensen T (1993) Glacier Atlas of Svalbard and Jan Mayen. Norsk Polarinstitutt Meddelelser no 129:141

Hagen JO, Melvold K, Pinglot F, Dowdeswell JA (2003a) On the net mass balance of the glaciers and ice caps in Svalbard, Norwegian Arctic. Arctic, Antarctic, and Alpine Research 35(2):264-270

Hagen JO, Kohler J, Melvold K, Winther J (2003b) Glaciers in Svalbard: mass balance, runoff and freshwater flux. Polar Research 22:145-159. doi:10.1111/j.1751-8369.2003.tb00104.x

Hanssen-Bauer I, Førland E, Hisdal H, Mayer S, Sandø A, Sorteberg A, Adakudlu M, Andresen J, Bakke J, Beldring S, Benestad R, van der Bilt W, Bogen J, Borstad C, Breili K, Breivik Ø, Børsheim K, Christiansen H, Dobler A, Engeset R, Frauenfelder R, Gerland S, Gjelten H, Gundersen J, Isaksen K, Jaedicke C, Kierulf H, Kohler J, Li H, Lutz J, Melvold K, Mezghani A, Nilsen F, Nilsen I, Nilsen J, Pavlova O, Ravndal O, Risebrobakken B, Saloranta T, Sandven S, Schuler T, Simpson M, Skogen M, Smedsrud L, Sund M, Vikhamar-Schuler D, Westermann S, Wong W (2019) Climate in Svalbard 2100 - a knowledge base for climate adaptation. vol. 1/2019, Norwegian Environment Agency (Miljødirektoratet), Norwegian Centre for Climate Services. https://cms.met.no/site/2/klimaservicesenteret/climate-in-svalbard-2100/_attachment/14428?_ts=169fd13ff23

Hodson A, Brock B, Pearce D, Laybourn-Parry J, Tranter M (2015) Cryospheric ecosystems: a synthesis of snowpack and glacial research. Environmental Research Letters 10(11):110201

Isaksen K, Nordli Ø, Førland EJ, Łupikasza E, Eastwood S, Niedźwiedź T (2016) Recent warming on Spitsbergen—Influence of atmospheric circulation and sea ice cover. J. Geophys. Res. Atmos. 121:11913-11931. https://doi.org/10.1002/2016JD025606

Jacob T, Wahr J, Pfeffer WT, Swenson S (2012) Recent contributions of glaciers and ice caps to sea level rise. Nature 482:514-518. https://doi.org/10.1038/

nature10847

James TD, Murray T, Barrand NE, Sykes HJ, Fox AJ, King MA (2012) Observations of enhanced thinning in the upper reaches of Svalbard glaciers. The Cryosphere 6: 1369-1381. https://doi.org/10.5194/tc-6-1369-2012

Kaser G, Cogley JG, Dyurgerov MB, Meier MF, Ohmura A (2006), Mass balance of glaciers and ice caps: Consensus estimates for 1961–2004, Geophysical Research Letters 33, L19501. https://doi.org/10.1029/2006GL027511

Kohler, J., Hudson, S. R., Obleitner, F., & Innsbruck, U (2017). Automatic weather station data from Kongsvegen, Ny-Ålesund [Data set]. Norwegian Polar Institute. https://doi.org/10.21334/npolar.2017.5dc31930

Kohler J, James TD, Murray T, Nuth C, Brandt O, Barrand NE, Aas HF, Luckman A (2007), Acceleration in thinning rate on western Svalbard glaciers. Geophysical Research Letters 34: L18502. https://doi.org/10.1029/2007GL030681

Köhler A, Nuth C, Kohler J, Berthier E, Weidle C, Schweitzer J (2016) A 15 year record of frontal glacier ablation rates estimated from seismic data. Geophysical Research Letters 43:12155-12164. https://doi.org/10.1002/2016GL070589

Köhler A, Maupin V, Nuth C, Van Pelt WJJ (2019a) Characterization of seasonal glacial seismicity from a single-station on-ice record at Holtedahlfonna, Svalbard. Annals of Glaciology60(79):23-36. https://doi.org/10.1017/aog.2019.15

Köhler A, Pętlicki M, Lefeuvre PM, Buscaino G, Nuth, C, Weidle C (2019b) Contribution of calving to frontal ablation quantified from seismic and hydroacoustic observations calibrated with lidar volume measurements. The Cryosphere Discuss. https://doi.org/10.5194/tc-2019-75, in review

Köhler A, Gajek W, Malinowski M, Schweitzer J, Majdanski M, Geissler W, Chamarczuk M, Wuestefeld A (2020) Seismological monitoring of Svalbard's cryosphere: current status and knowledge gaps. In: Van den Heuvel et al. (eds): SESS report 2019, Svalbard Integrated Arctic Earth Observing System, Longyearbyen, 136 – 159 . https://sios-svalbard.org/SESS_Issue2

König M, Nuth C, Kohler J, Moholdt G, Pettersen R (2014) A digital glacier database for Svalbard. In: Kargel J, Leonard G, Bishop M, Kääb A, Raup B (eds) Global Land Ice Measurements from Space. Springer Praxis Books. Springer, Berlin, Heidelberg

Lang C, Fettweis X, Erpicum M (2015) Stable climate and surface mass balance in Svalbard over 1979–2013 despite the Arctic warming. The Cryosphere 9:83-101. https://doi.org/10.5194/tc-9-83-2015

Laska M, Luks B, Budzik T (2016) Influence of snowpack internal structure on snow metamorphism and melting intensity on Hansbreen, Svalbard. Pol. Polar Res. 37(2):193-218

Luckman A, Benn DI, Cottier F, Bevan S, Nilsen F, Inall M (2015) Calving rates at tidewater glaciers vary strongly with ocean temperature. Nature Communications 6:8566

Macheret YY, Glazovsky AF, Lavrentiev II, Marchuk IO (2019) Distribution of cold and temperate ice in glaciers on the Nordenskiöld Land, Spitsbergen, from ground-based radio-echo sounding. Ice and Snow 59(2):149-166. https://doi.org/10.15356/20766734-2019-2-430 [in Russian]

Małecki J (2013) Elevation and volume changes of seven Dickson Land glaciers, Svalbard, 1960-1990-2009. Polar Research 32:18400. https://doi.org/10.3402/polar.v32i0.18400

Małecki J (2015) Snow accumulation on a small high-Arctic glacier Svenbreen: variability and topographic controls. Geografiska Annaler: Series A. Physical Geography 97:809-817. https://doi.org/10.1111/geoa.12115

Małecki J (2016) Accelerating retreat and high-elevation thinning of glaciers in central Spitsbergen. The Cryosphere 10:1317-1329. https://doi.org/10.5194/tc-10-1317-2016

Marchenko S, Pohjola VA, Pettersson R, van Pelt WJJ, Vega CP, Machguth H, Boggild CE, Isaksson E (2017a) A plot-scale study of firn stratigraphy at Lomonosovfonna, Svalbard, using ice cores, borehole video and GPR surveys in 2012–14. Journal of Glaciology 63(237):67-78. https://doi.org/10.1017/jog.2016.118

Marchenko S, van Pelt WJJ, Claremar B, Pohjola V, Pettersson R, Machguth H, Reijmer C (2017b) Parameterizing deep water percolation improves subsurface temperature simulations by a multilayer firn model. Frontiers in Earth Science 5:16. https://doi.org/10.3389/feart.2017.00016

Martín-Español A, Navarro F, Otero J, Lapazaran J, Błaszczyk M (2015) Estimate of the total volume of Svalbard glaciers, and their potential contribution to sea-level rise, using new regionally based scaling relationships. Journal of Glaciology 61(225):29-41. https://doi.org/10.3189/2015JoG14J159

Matsuo K and Heki K (2013) Current ice loss in small glacier systems of the Arctic Islands (Iceland, Svalbard, and the Russian High Arctic) from satellite gravimetry. Terr. Atmos. Ocean. Sci. 24:657-670. https://doi.org/10.3319/TAO.2013.02.22.01

Mavlyudov BR, Savatyugin LM, Solovyanova IY (2012) Reaction of Nordenskiöld Land glaciers, Spitsbergen, on climate change. Arctic and Antarctic Research / Problemy Arktiki i Antarktiki 1(91):67-77, http://www.

aari.ru/misc/publicat/paa/PAA91/PAA91-07(67-77).pdf [in Russian]

Mémin A, Rogister Y, Hinderer J, Omang OC, Luck B (2011) Secular gravity variation at Svalbard (Norway) from ground observations and GRACE satellite data. Geophysical Journal International 184:1119-1130. https://doi.org/10.1111/j.1365-246X.2010.04922.x

Moholdt G, Hagen JO, Eiken T, Schuler TV (2010a) Geometric changes and mass balance of the Austfonna ice cap, Svalbard. The Cryosphere 4:21-34. https://doi.org/10.5194/tc-4-21-2010

Moholdt G, Nuth C, Hagen JO, Kohler J (2010b) Recent elevation changes of Svalbard glaciers derived from ICESat laser altimetry. Remote Sensing of the Environment, 114 (2010), pp. 2756-2767. https://doi.org/10.1016/j.rse.2010.06.008

Möller M, Kohler J (2018) Differing climatic mass balance evolution across Svalbard glacier regions over 1900-2010. Frontiers in Earth Science 6:128. https://doi.org/10.3389/feart.2018.00128

Nordli Ø, Przybylak R, Ogilvie AE, Isaksen K (2014) Long-term temperature trends and variability on Spitsbergen: the extended Svalbard Airport temperature series, 1898–2012, Polar Research, 33:1. https://doi.org/10.3402/polar.v33.21349

Nuth C, Kohler J, Aas H, Brandt O, Hagen JO (2007) Glacier geometry and elevation changes on Svalbard (1936–90): A baseline dataset. Annals of Glaciology 46:106-116. https://doi.org/10.3189/172756407782871440

Nuth C., MoholdtG,Kohler J, Hagen JO, Kääb A (2010), Svalbard glacier elevation changes and contribution to sea level rise. Journal of Geophysical Research 115: F01008. https://doi.org/10.1029/2008JF001223.

Nuth C, Kohler J, König M, von Deschwanden A, Hagen JO, Kääb A, Moholdt G, Pettersson R (2013) Decadal changes from a multi-temporal glacier inventory of Svalbard. The Cryosphere 7:1603-1621. https://doi.org/10.5194/tc-7-1603-2013

Nuth C, Gilbert A, Köhler A, McNabb RW, Schellenberger T, Sevestre H, Weidle C, Girod LMR, Luckman A, Kääb A (2019) Dynamic vulnerability revealed in the collapse of an Arctic tidewater glacier. Scientific Reports 9. https://doi.org/10.1038/s41598-019-41117-0

Pinglot J, Hagen JO, Melvold K, Eiken T, Vincent C (2001) A mean net accumulation pattern derived from radioactive layers and radar soundings on Austfonna, Nordaustlandet, Svalbard. Journal of Glaciology 47(159):555-566. https://doi.org/10.3189/172756501781831800

Poli P, Hersbach H, Dee DP, Berrisford P, Simmons AJ, Vitart F, Laloyaux P, Tan DG, Peubey C, Thépaut J, Trémolet Y, Hólm EV, Bonavita M, Isaksen L, Fisher M (2016) ERA-20C: An Atmospheric Reanalysis of the Twentieth Century. Journal of Climate 29(11):4083-4097. https://doi.org/10.1175/JCLI-D-15-0556.1

RGI Consortium (2017). Randolph Glacier Inventory – A Dataset of Global Glacier Outlines: Version 6.0: Technical Report, Global Land Ice Measurements from Space, Colorado, USA. Digital Media. https://doi.org/10.7265/N5-RGI-60

Schäfer M, Gillet-Chaulet F, Gladstone R, Pettersson R, Pohjola V, Strozzi T, Zwinger T (2014) Assessment of heat sources on the control of fast flow of Vestfonna ice cap, Svalbard, The Cryosphere 8:1951-1973. https://doi.org/10.5194/tc-8-1951-2014

Schuler TV, Loe E, Taurisano A, Eiken T, Hagen JO, Kohler J (2007) Calibrating a surface mass-balance model for Austfonna ice cap, Svalbard. Annals of Glaciology 46:241-248. https://doi.org/10.3189/172756407782871783

Schuler TV, Dunse T, Østby TI, Hagen JO (2014) Meteorological conditions on an Arctic ice cap - 8 years of automatic weather station data from Austfonna, Svalbard. International Journal of Climatology 34:2047-2058. https://doi.org/10.1002/joc.3821

Schuler TV and Østby TI (2019) Sval_Imp_v1: A gridded forcing dataset for climate change impact research on Svalbard. Earth System Science Data Discussion https://doi.org/10.5194/essd-2019-180, in review

Schytt V (1964) Scientific Results of the Swedish Glaciological Expedition to Nordaustlandet, Spitsbergen, 1957 and 1958. Geografiska Annaler 46(3):242-281. https://doi.org/10.2307/520382

Sevestre H and Benn D (2015) Climatic and geometric controls on the global distribution of surge-type glaciers: Implications for a unifying model of surging. Journal of Glaciology 61(228):646-662. https://doi.org/10.3189/2015JoG14J136

Sevestre H, Benn DI, Luckman A, Nuth C, Kohler J, Lindbäck K, Pettersson R (2018) Tidewater glacier surges initiated at the terminus. Journal of Geophysical Research: Earth Surface 123:1035- 1051. https://doi.org/10.1029/2017JF004358

Sobota I, Nowak M, Weckwerth P (2016) Long-term changes of glaciers in north-western Spitsbergen. Global and Planetary Change 144:182-197. https://doi.org/10.1016/j.gloplacha.2016.07.006

Sund M, Eiken T, Hagen J, Kääb A (2009) Svalbard surge dynamics derived from geometric changes. Annals of Glaciology 50(52):50-60. https://doi.org/10.3189/172756409789624265

Sund M, Lauknes TR, Eiken T (2014) Surge dynamics in the Nathorstbreen glacier system, Svalbard. The Cryosphere 8:623-638. https://doi.org/10.5194/tc-8-

623-2014.

Taurisano A, Schuler TV, Hagen JO, Eiken T, Loe E, Melvold K, Kohler J (2007) The distribution of snow accumulation across the Austfonna ice cap, Svalbard: direct measurements and modelling. Polar Research 26:7-13. https://doi.org/10.1111/j.1751-8369.2007.00004.x

Thøgersen K, Gilbert A, Schuler TV, Malthe-Sørensen A (2019) Rate-and-state friction explains glacier surge propagation. Nature Communications 10:2823. https://doi.org/10.1038/s41467-019-10506-4

Terekhov AV, Tarasov GV, Sidorova OR, Demidov VE, Anisimov MA, Verkulich SK (2020) The estimation of mass balance of Aldegondabreen (Spitsbergen) in 2015-2018 based on topographic survey and ArcticDEM, verified by glaciological measurements. Ice and Snow 60(1), in press, [In Russian]

Uppala SM, Kållberg PW, Simmons AJ, Andrae U, da Costa Bechtold V, Fiorino M, Gibson JK, Haseler J, Hernandez A, Kelly GA, Li X, Onogi K, Saarinen S, Sokka N, Allan RP, Andersson E, Arpe K, Balmaseda MA, Beljaars ACM, van de Berg L, Bidlot J, Bormann N, Caires S, Chevallier F, Dethof A, Dragosavac M, Fisher M, Fuentes M, Hagemann S, Hólm E, Hoskins BJ, Isaksen L, Janssen PAEM, Jenne R, McNally AP, Mahfouf JF, Morcrette JJ, Rayner NA, Saunders RW, Simon P, Sterl A, Trenberth KE, Untch A, Vasiljevic D, Viterbo P, Woollen J (2005) The ERA-40 re-analysis. Quart. J. R. Meteorol. Soc. 131:2961-3012. https://doi.org/10.1256/qj.04.176

Vallot D, Pettersson R, Luckman A, Benn DI, Zwinger T, van Pelt WJJ, Kohler J, Schäfer M, Claremar B, Hulton NR (2017) Basal dynamics of Kronebreen, a fast-flowing tidewater glacier in Svalbard: non-local spatio-temporal response to water input. Journal of Glaciology 63:1012-1024. https://doi.org/10.1017/jog.2017.69

Van Pelt WJJ, Oerlemans J, Reijmer CH, Pohjola VA, Pettersson R, van Angelen JH (2012) Simulating melt, runoff and refreezing on Nordenskiöldbreen, Svalbard, using a coupled snow and energy balance model. The Cryosphere 6:641-659. https://doi.org/10.5194/tc-6-641-2012

Van Pelt WJJ, Pohjola VA, Pettersson R, Ehwald LE, Reijmer CH, Boot W, Jakobs CL (2018) Dynamic response of a High Arctic glacier to melt and runoff variations. Geophysical Research Letters 45:4917:4926. https://doi.org/10.1029/2018GL077252

Van Pelt WJJ, Pohjola VA, Pettersson R, Marchenko S, Kohler J, Luks B, Hagen JO, Schuler T V, Dunse T, Noël B, Reijmer C (2019) A long-term dataset of climatic mass balance, snow conditions and runoff in Svalbard (1957-2018). The Cryosphere 13:2259-2280. https://doi.org/10.1594/tc-13-2259-2019

Vega CP, Pohjola VA, Beaudon E, Claremar B, van Pelt WJJ, Pettersson R, Isaksson E, Martma T, Schwikowski M, Bøggild CE (2016) A synthetic ice core approach to estimate ion relocation in an ice field site experiencing periodical melt: a case study on Lomonosovfonna, Svalbard. The Cryosphere 10:961-976. https://doi.org/10.5194/tc-10-961-2016

Vieli A, Jania J, Blatter H, Funk M (2004) Short-term velocity variations on Hansbreen, a tidewater glacier in Spitsbergen. Journal of Glaciology 50: 389–398. https://doi.org/10.3189/172756504781829963

Willis MJ, Zheng W, Durkin WJ, Pritchard ME, Ramage JM, Dowdeswell JA, Benham TJ, Bassford RP, Stearns LA, Glazovsky AF, Macheret YY, Porter CC (2018) Massive destabilization of an Arctic ice cap. Earth and Planetary Science Letters 502. https://doi.org/10.1016/j.epsl.2018.08.049

Wouters B, Chambers D, Schrama EJO (2008) GRACE observes small-scale mass loss in Greenland. Geophysical Research Letters 35:L20501. https://doi.org/10.1029/2008GL034816

Wouters B, Gardner AS, Moholdt G (2019) Global Glacier Mass Loss During the GRACE Satellite Mission (2002-2016). Frontiers in Earth Sciences 7:96. https://doi.org/10.3389/feart.2019.00096

Østby T, Schuler TV, Hagen JO, Hock R, Reijmer C (2013) Parameter uncertainty, refreezing and surface energy balance modelling at Austfonna ice cap, Svalbard, 2004-08. Annals of Glaciology 54(63):229-240. https://doi.org/10.3189/2013AoG63A280

Østby TI, Schuler TV, Hagen JO, Hock R, Kohler J, Reijmer CH (2017) Diagnosing the decline in climatic mass balance of glaciers in Svalbard over 1957-2014. The Cryosphere 11:191-215. https://doi.org/10.5194/tc-11-191-2017

Seismological monitoring of Svalbard's cryosphere: current status and knowledge gaps (CRYOSEIS)

Author names
Andreas Köhler[1], Wojciech Gajek[2], Michal Malinowski[2], Johannes Schweitzer[1], Mariusz Majdanski[2], Wolfram H. Geissler[3], Michal Chamarczuk[2], Andreas Wuestefeld[1]

Institution affiliations
1 NORSAR, Kjeller, Norway
2 Institute of Geophysics Polish Academy of Sciences, Warsaw, Poland
3 Alfred Wegener Institute, Bremerhaven, Germany

Corresponding author: Michal Malinowski, michalm@igf.edu.pl
ORCID number 0000-0002-7190-3683

Keywords: Seismology, glaciology, calving, monitoring, ice-quake, permafrost

1. Introduction

Seismology is the science of studying earthquakes and the material properties in the solid Earth by analyzing observations of elastic waves, which had been radiated by seismic sources and propagated through the Earth. The new research field of environmental seismology studies vibrations and temporal variations in the shallow sub-surface that are caused by non-tectonic sources, such as cryospheric processes or atmospheric forcings (Larose et al. 2015). In particular, seismic signals originating from glaciers and ice sheets have been recently extensively studied in various regions around the globe using either dedicated temporary or permanent seismic stations, making cryoseismology a rapidly developing frontier research topic in Earth Sciences. An excellent overview of the background and existing studies is given in the recent review articles of Podolskiy and Walter 2016 and Aster and Winberry 2017. The popularity of cryoseismology is also recognized in an increasing number of dedicated sessions and workshops at various international conferences and special journal issues devoted to this emerging field (see e.g. special issue of Annals of Glaciology entitled “Progress in Cryoseismology”).

While cryoseismological research has a long history at the Polish research station in Hornsund (southern Spitsbergen, Lewandowska and Teisseyre 1964), it was just within the past 5 – 10 years that an increasing number of studies systematically analyzing glacier seismicity have been carried out in Svalbard. In view of these developments and the benefit of using cryoseismology as a tool complementing well-established methods for monitoring the cryosphere and related changes in the Arctic, it is essential to further advance and promote this new field of research in Svalbard. In contrast to popular study regions like Antarctica, Greenland, Alaska and the Alps, relatively few studies have been conducted in Svalbard, and the full potential of cryoseismology has not been explored yet. Moreover, the area of Svalbard has been warming about three times faster than the global estimate over the last 100 years (e.g. Nordli et al. 2014) and accessibility and logistic is much easier compared to other regions in the Arctic or Antarctica, making it a natural laboratory to study changes in the cryosphere induced by climate change. Therefore, this report has the objective to briefly introduce the reader into cryoseismology within a global context, to highlight the recent research activity in Svalbard, and to recommend directions for future research.

2. Overview of existing knowledge

2.1 Cryoseismology

Passive seismic monitoring is a powerful method for better understanding glacial dynamic

processes and inferring englacial and subglacial conditions in previously inaccessible areas, complementing traditional glaciological observations from field or remote sensing due to its independence from visibility conditions, spatial extent beyond single observation points (boreholes), and unique high temporal resolution (sub-second scale) also during polar nights. Another key opportunity of using continuous seismic records of permanent stations is the systematic analysis of long-term trends and changes in seasonal patterns of cryo-seismicity or sub-surface structures (e.g. permafrost) over a time period of several years or decades, which allows assessing potential effects of climate change.

Strong cryogenic seismic signals, such as those generated by large iceberg calving at glaciers and icestreams, are observed at ranges up to regional (about 100 – 2000 km) or even teleseismic distances (>2000 km) (Ekström et al. 2003). Local glacier microseismicity (i.e., icequakes), mainly related to brittle ice failure (crevasse opening) and basal processes (e.g. stick-slip motion), is best monitored with stations installed on the ice surface or in shallow boreholes (see Podolskiy and Walter 2016; Aster and Winberry 2017, and references therein). However, in Antarctica, tidal triggering of cryoseismicity not related to calving but representing stick-slip motion events can be also observed at distances up to 300 km (Pirli et al. 2018). Moreover, passive seismic records allow studying the state and evolution of the glacier hydraulic system through monitoring either meltwater-related seismic tremors (Bartholomaus et al. 2015a; Helmstetter et al. 2015; Röösli et al. 2016; Köhler et al. 2019a) or transient signals related to hydro-fracturing and fluid resonance (Stuart et al. 2005). Monitoring of iceberg drift is another application of cryoseismology (e.g. Pirli et al. 2015).

Beside studying seismic signals to better understand source processes, cryoseismology also includes structural investigations of the propagation medium of seismic waves, i.e., it allows inferring properties of the ice or shallow subsurface. Records of the background ambient seismic noise wavefield caused by wind, ocean waves, and flowing water are often used for this purpose by applying methods like seismic noise interferometry or Horizontal-To-Vertical Spectral Ratios (HVSR) (Larose et al. 2015). This approach does not only allow studying the state of the internal structure of glaciers, ice sheets and frozen soil (Overduin et al. 2015; Walter et al. 2015; Diez et al. 2016; Picotti et al. 2017; Preiswerk and Walter 2018; Yan et al. 2018), but also allows time-lapse monitoring of subsurface structures, for example the permafrost active layer (Abbott et al. 2016; James et al. 2017, 2019; Kula et al. 2018; Köhler et al. 2019c) and the subglacial drainage system (Gräff et al. 2019; Zhan 2019).

A challenge in cryoseismology is that processes are mostly observed indirectly through seismic waves recorded at a certain distance from the source. Hence, physical models or calibration with direct observations, i.e., actual source parameters or subsurface quantities, using empirical models is required. Such an approach has shown the potential of seismology to assist and advance glaciological or permafrost research in several cases, for example through the study of deep icequakes to uncover stick-slip motion and basal friction laws (see

e.g. Aster and Winberry 2017), through the quantification of calving to better understand mass loss of glaciers (Bartholomaus et al. 2015b; Köhler et al. 2016, 2019b), and through recent experimental studies to improve permafrost active layer monitoring (James et al. 2019).

Seismology is not the only passive, wave propagation-based approach complementing established measurement methods in the cryosphere. For example, infrasound (Asming et al. 2013), hydroacoustic (Glowacki et al. 2015), and water surface waves (Minowa et al. 2019) are well-suitable for monitoring the calving of glaciers. Furthermore, active geophysical methods, such as seismic profiling, ground-penetrating radar (GPR), and electric resistivity tomography (ERT) are well-established methods for ice, snow and permafrost research (Polom et al. 2014; Johansen et al. 2011; Booth et al. 2013; Dow et al. 2013; Church et al. 2019) which can be combined with passive seismology. For example, the glacier's inner structure can be imaged with the highest resolution using a combination of reflection seismic and GPR (King et al. 2008; Church et al. 2019). Those methods can clearly visualize both the bed of the glacier and thermal boundaries between temperate and cold ice. Attempts were made to infer physical basal rock properties using seismic data, e.g. to distinguish between bedrock vs saturated sediments (Dow et al. 2013). Furthermore, refraction seismic can be used to estimate seismic velocities with high precision. Because of seasonal changes in the permafrost active layer, near-surface seismic velocities are changing significantly. Laboratory measurements show (Draebing and Krautblatter 2012) that not only the sediment's but also the low-porosity rock's P-wave velocity increases due to freezing. Such a change can be clearly observed with time-lapse seismic tomography (Hilbich 2010), as water-filled porous rock P-wave velocity will double. This change of near-surface velocities can significantly influence seismological recordings (amplitudes, incidence angles). Moreover, active seismic will result in a 2D or even 3D velocity model of bedrock that is important for precise seismic event localization. To provide such velocity models in areas where active seismic is not permitted or logistically difficult, passive seismology can again come in handy, employing above mentioned ambient noise recordings and seismic interferometry.

State-of-the-art seismological methods and new technologies are expected to further advance cryoseismological research. Automatization of seismic signal detection and classification is mandatory in modern seismology for analyzing the enormous volumes of data obtained from long-term monitoring. Seismic arrays (Schweitzer et al. 2012), which are setups of closely-spaced sensors, allow detection, classification, and location of weak seismic signals and tremors. Detection and classification of various seismic events are nowadays also often performed with machine learning algorithms, which is a rapidly developing field in seismology (Kong et al. 2018; Bergen et al. 2019). Furthermore, developments in seismic measurements using fiber-optic cables (Distributed Acoustic Sensing, DAS) enable time-lapse data acquisition with unprecedented sensor density and spatial sampling down to the meter scale (Jousset et al. 2018, Ajo-Franklin et al. 2019). Such fine sampling, in combination

with long fiber length above 10 km, allows for unprecedented resolution on a local scale. Furthermore, DAS systems measure strain (or strain rate), and very-low frequency analysis allows to monitor deformation in sections along the fiber (Jin and Roy 2017), which may be used to measure glacial deformation with high resolution.

2.2 Seismological infrastructure in Svalbard

Seismological monitoring in Svalbard has a long history with the first temporary station being installed in 1911 in Longyearbyen. Subsequently, several analog seismometers were in operation at Kapp Linne (Isfjord Radio, 1958-1963), in Ny-Ålesund (since 1967), Hornsund (since 1978), Barentsburg (since 1979), and Pyramiden (1982-1989). Furthermore, several temporary seismic deployments for tectonic studies were made between 1976 and 1986 in southern Spitsbergen and in 1982 as well as 1986 on Phippsøya, north of Nordaustlandet.

The current network of permanent (digital) seismometers in Svalbard is the backbone of cryoseismological research in the region (Figure 1). It has been continuously extended and upgraded during the past decades, especially during and after the Fourth International Polar Year (2007-2008). For temporary networks deployed for dedicated studies, we refer to Chapter 2.3. Several seismic broadband stations form a sparse seismic network on Spitsbergen with an average interstation distance of about 100 km (Figure 1, Table 1). The small-aperture Spitsbergen seismic array (SPITS) East of Longyearbyen in Adventdalen has an aperture of about 1 km and presently consists of 9 CMG-3T seismometers. It has been operated by NORSAR since 1992 and was upgraded with three-component broadband stations in 2004. Furthermore, single three-component stations are currently in operation. The Kings Bay seismic station (KBS, STS-2 seismometer) in Ny-Ålesund

Table 1: Permanent seismic stations on Spitsbergen. Access to the Norwegian EIDA node being under construction via http://eida.geo.uib.no/.

Name	Location	Network ID	Operators	Comment	Recording since	Sampling rate	Data access
KBS	Ny-Ålesund	IU/GE	AWI, UiB, GSN, GEOFON	Single, three-component	1994	40 Hz; 100 Hz since 2019	IRIS-DMC
HSPB	Hornsund	PL	IG PAS, NORSAR	Single, three-component	09/2007	100 Hz	IRIS-DMC / EIDA-GFZ
BRBA	Barentsburg	NO	KS GS RAS, NORSAR	Single, three-component	2010	80 Hz	EIDA
BRBB	North of Barentsburg	NO	KB GS RAS, NORSAR	Single, three-component	2012	80 Hz	EIDA 2012 only
SPITS	Jansson-haugen, Advent-dalen	NO	NORSAR	Array of 9 stations, since 2004 6 three-component	1992	40 Hz until 2004; 80 Hz since 2004	EIDA

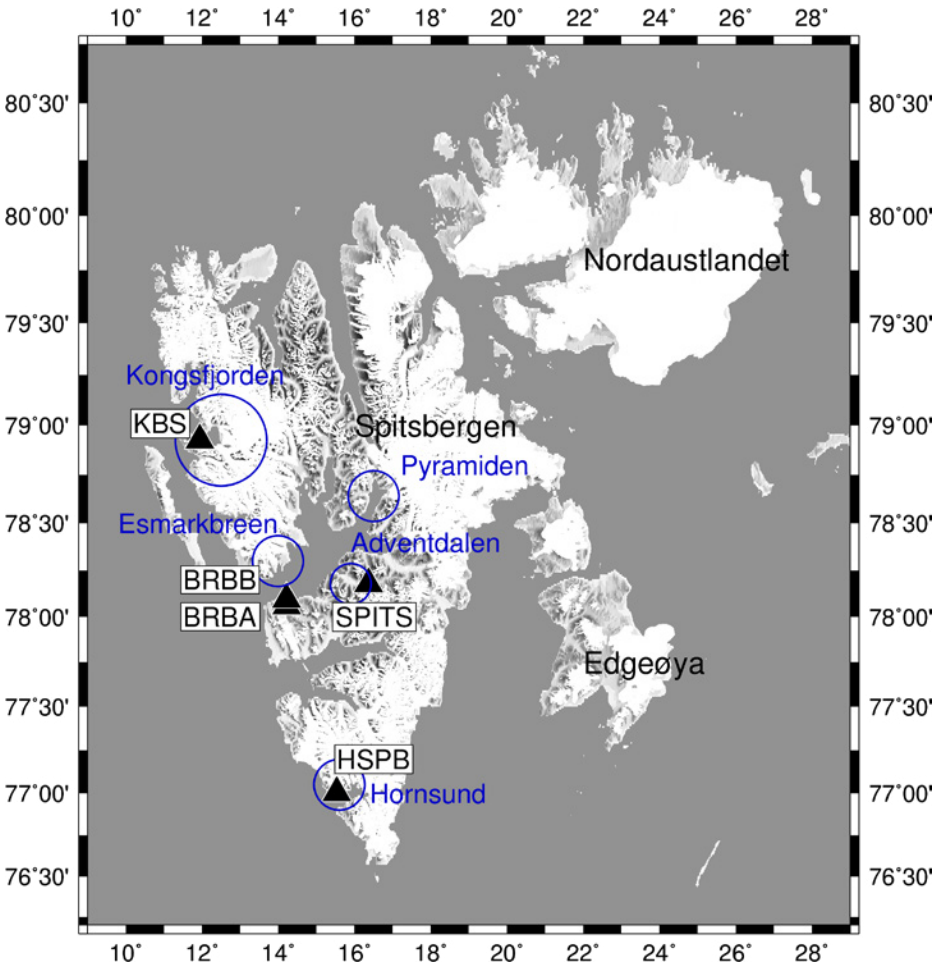

Figure 1: Map of Svalbard showing locations of permanent seismic stations (black triangles, listed in Table 1) and temporary seismic deployments (blue circles, listed in Table 2).

has been in operation as a broadband station of the Global Seismic Network (GSN) and GeoForschungsNetz (GEOFON) seismic network since 1994. After earlier deployments of short-period sensors, for example in 1995 (Górski 2014), an STS-2 broadband seismometer was installed at the Polish research station in Hornsund (HSPB, Figure 2c) in September 2007 by the Institute of Geophysics Polish Academy of Sciences (IGF PAS) and NORSAR (Wilde-Piórko et al. 2009). Since 2010, the Kola Science Centre of the Russian Academy of Sciences has operated a broadband seismometer in Barentsburg (BRBA) in cooperation with NORSAR, and a second seismometer station (BRBB) operated by both partners has

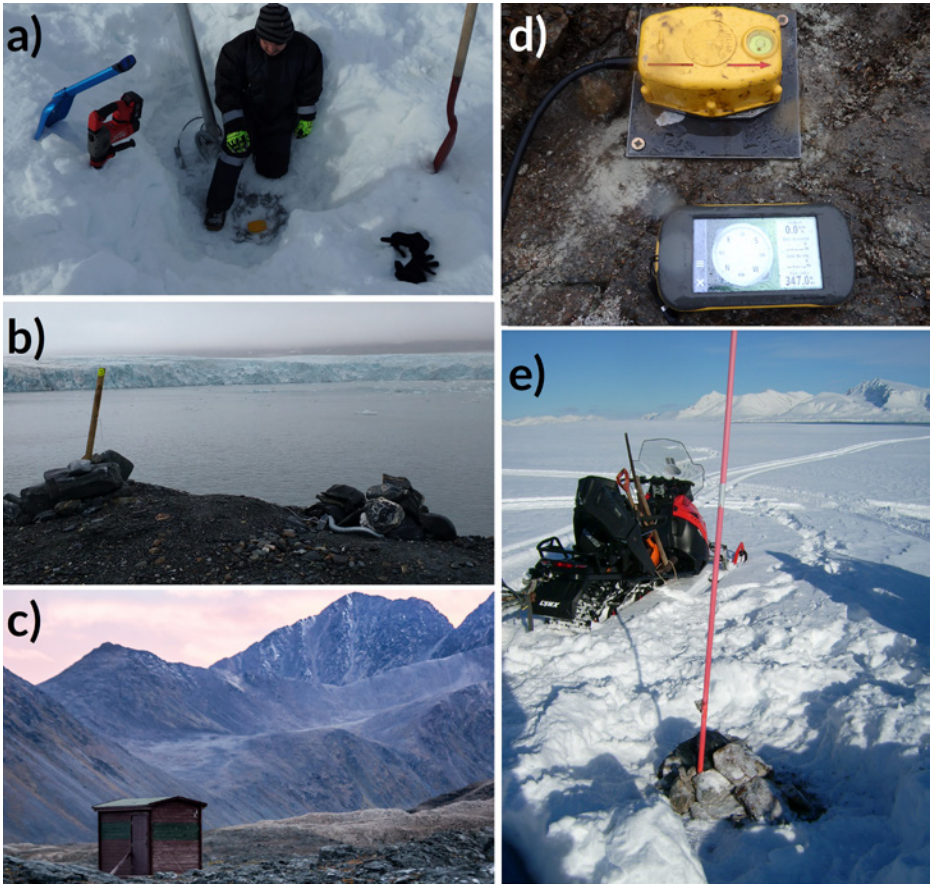

Figure 2: Examples of field installations of seismological equipment. a) on-ice geophone installation in a snow pit (Hansbreen); b) geophone installed like in d), covered with rocks (wind protection) next to the digitizer and power supply. Hansbreen calving front in the background; c) permanent seismological station HSPB next to Polish Polar Station; d) 3-component 4.5 Hz geophone on the metal pad screwed to the rock; e) completed geophone installation deployed on frozen soil close to Ny-Ålesund covered with stones. Photos by courtesy of Wojciech Gajek (a,b,d), Joanna Perchaluk (c), Andreas Köhler (e).

been deployed 4 km north of BRBA in 2012, co-located with a three-site infrasound array. Seismometers are recording with sampling rates of 40 Hz (KBS, SPITS prior to August 2004), 100 Hz (HSPB) and 80 Hz (SPITS after August 2004, BRBA/B). Except for some data gaps during the upgrading and maintenance of seismometers, all stations have been recording continuously since their dates of installation, and data are transferred for analysis to the hosting institutions in near-real-time.

Seismic broadband stations are also located on the island of Hopen since 2007 and Bjørnøya since 1996, both operated by the University of Bergen (UiB). Most recently, on August 2019, NORSAR installed a small aperture seismic array on Bjørnøya. However, due to their distance to glaciated areas, the stations on both islands have not been used for glacier seismological studies, while potential application for permafrost research and monitoring calving at Edgeøya exists. The array deployed on Bjørnøya has been funded through the RCN financed EPOS-Norway infrastructure project, which supplements the European EPOS (European Plate Observing System) infrastructure. More single stations along the coasts of Svalbard and a small aperture seismic array deployment near Hornsund are anticipated using instruments available through EPOS-Norway in 2020.

Seismicity in the Svalbard region is monitored routinely through the automatic processing of SPITS array data by NORSAR (Schweitzer et al. 2012). Due to the high amount of data, only larger events are manually reviewed and re-located by NORSAR analysts, employing also the other seismic stations in the region. However, since the automatic procedure was specifically designed to detect and locate tectonic earthquakes and artificial explosions, the preliminary assigned locations for weak seismic events of a different origin (e.g. icequakes) in the event catalogue can be spurious or biased and give only a rough overview about the spatial-temporal distribution of glacier events.

2.3 Cryoseismological studies in Svalbard

For our review of past cryoseismological studies in Svalbard we distinguish between local studies using mostly temporary sensor deployments, for example, dedicated to monitor calving, icequakes, or tremors at a single glacier, and regional studies utilizing mainly the permanent seismometer network with a focus on detecting and mapping regional glacier seismicity generated by calving and surging. Figure 2 shows field photos of both temporary and permanent installations, while Figure 3 shows examples of cryoseismological signals recorded by such instruments. However, it should be noted that there is an overlap between both approaches, as stations of the permanent network are also used to study local seismicity and sub-surface structures, and temporary stations are used to calibrate, i.e., to constrain the source, of regional seismic event observations. Note also that for logistical reasons and limited station coverage, all local studies as well as regional monitoring efforts so far focused on the main island Spitsbergen.

The first local studies in Svalbard have been carried out at Hornsund by Polish researchers from IG PAS starting already in the ‘60s, particularly focusing on glacier seismicity at Hansbreen. Lewandowska and Teisseyre (1964), Górski (1975), and Czajkowski (1977) investigated ice microtremors and icequakes and their relation to glacier dynamics. This work was continued by IG PAS in the ‘80s and ’90 with a focus on the properties of

seismic signals generated by crevassing and glacier motion (Cichowicz 1983; Górski and Teisseyre 1991; Górski 1997, 1999, 2003, 2004). Górski (2014) provides a summary of all findings from past seismic experiments that took place in Hornsund. Recently, IG PAS deployed a new temporary seismic network at Hansbreen (2017-2018) to follow up on previous works and to continue with the long tradition of cryoseismological research in Hornsund (Table 2). The new experiment consisted of two mini-arrays located on both sides of the Hansbreen calving front supplemented by two on-ice stations and was aimed at monitoring seismic activity at the calving front from autumn to spring and calibrating detections of cryogenic events at the nearby HSPB station. The calving front area is also a natural polygon for applying advanced passive seismic processing techniques like the double beamforming technique (Nakata et al. 2016), which allows to identify and separate the

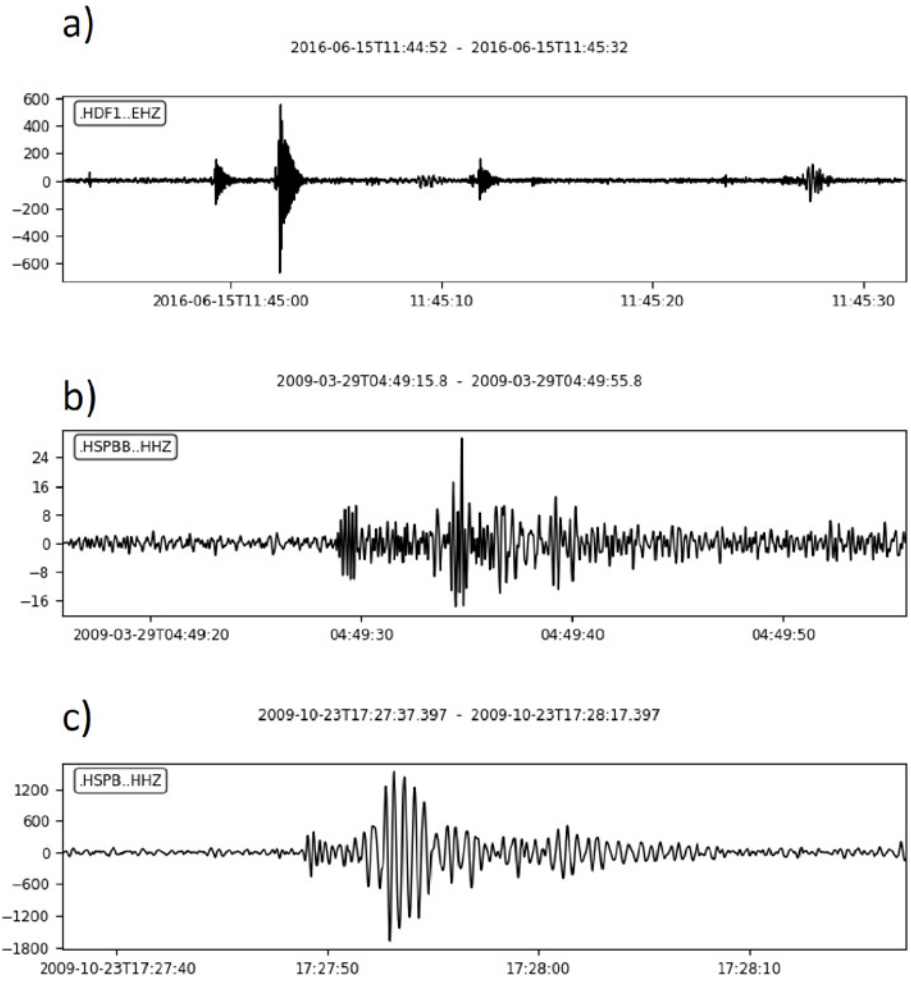

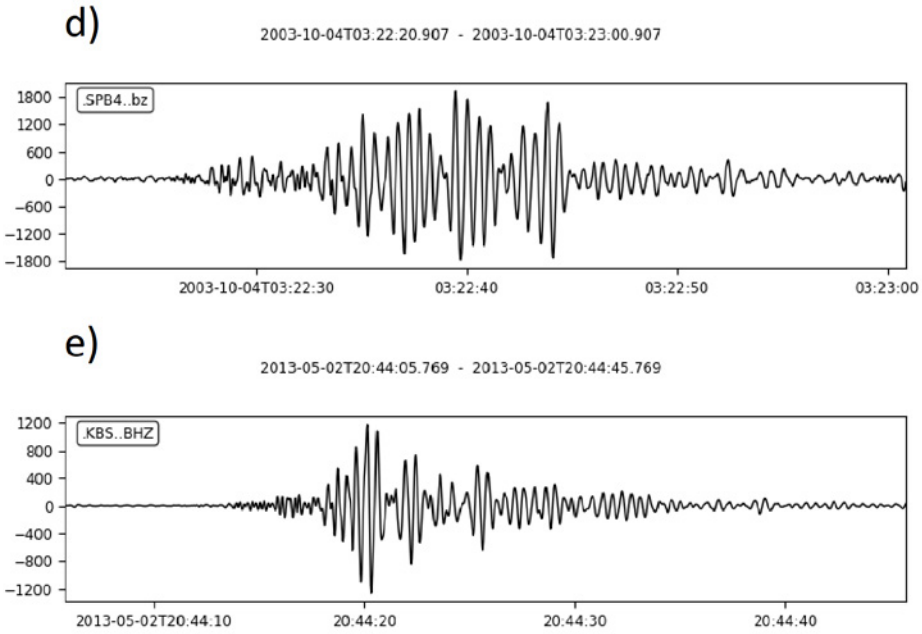

Figure 3: Examples of seismic signals detected on a temporary installation on Holtedalfonna (HDF1) and permanent stations in Svalbard. a) local icequakes, b) a signal of the Nathorstbreen surge, c) calving events at Hansbreen, d) Tunabreen, and e) Kronebreen (Köhler et al. 2015).

specific waves travelling between arrays of sensors and may be used to extract the seismic waves generated, e.g. by calving. Aside from passive seismic studies at Hornsund, also hydroacoustic monitoring of calving at Hansbreen using a single hydrophone temporarily deployed in the fjord has been carried out which allowed distinguishing different types of calving signals (Glowacki et al. 2015).

Another early study has been carried out at Bakaninbreen (SE Spitsbergen) during its surge in 1987 by British researchers presenting for the first time evidence for local seismic emission of a glacier surge in Svalbard (Stuart et al. 2005). Different types of icequakes have been identified on a temporary seismometer network that helped to better understand the progressing of the surge front.

In 2009 and 2010, researchers of the University of Oslo deployed a single-channel geophone at Kronebreen (Kongsfjord, NW Spitsbergen) to record seismic signals generated by calving (Köhler et al. 2012). This pilot study initiates a series of research projects (SEISMOGLAC, NFR grant no. 213359/F20; CalvingSEIS, NFR grant no. 244196/E10)

Table 2: Recent temporary seismic deployments in Svalbard.

Location	Operator	Time period	No. of sensors	Project / Purpose / Comments	Data access, DOIs
Adventdalen	NORSAR	05/2014-09/2014	12	SafeCO2 / SEISVAL	EIDA RESIF, 10.15778/RESIF.Y22014
Kronebreen, Kongsfjorden	UiO, Uni Kiel	05/2013-09/2013	20	SEISMOGLAC	GIPP GFZ, 10.5880/GIPP.201303.1 10.2312/GFZ.b103-17094
Ny Ålesund / Kronebreen / Holtadalfonna	UiO	04/2016-09/2016	24	CalvingSEIS	GIPP GFZ, 10.5880/GIPP.201604.1 10.2312/GFZ.b103-19038
Hansbreen	IG PAS	10/2017-04/2018	11	3-seasons long calving front obs.	Unprocessed dataset, to be available from 1.5.2020, 10.5281/zenodo.3377402
Kongsbreen	UiO, Uni Kiel	04/2018-01/2019	5	Surge and lake drainage obs.	Unprocessed dataset, not openly available yet
Pyramiden / Norden-skiöldbreen	KB GS RAS	2015-??	1	seismic station + infrasound array	unknown
Esmarkbreen	KB GS RAS	06/2012-09/2012	1	Single, three-component	unknown

including local temporary seismic deployments in the Kongsfjord area in 2013 (Kronebreen), 2016 (Kronebreen, Holtedalfonna, and Ny-Ålesund; included hydrophone measurements in Kongsfjord), and 2018/2019 (Kongsvegen) (Figure 1, Table 2) which were carried out in collaboration between the Universities of Oslo and Kiel. These datasets were used to constrain the origin and type of regional glacier seismicity (Köhler et al. 2015), to calibrate and develop methods for seismic quantification of frontal ablation and calving ice loss at Kronebreen (Köhler et al. 2016, 2019b), and to study the sources and seasonal distribution of icequakes and tremors at Holtedalfonna (Köhler et al. 2019a). Outcomes of the CalvingSEIS project were a continuous time series of ice loss at Kronebreen obtained with two different approaches. Seismic calving signals detected at the close station KBS (~15 km from glacier terminus) were calibrated with satellite remote sensing observations of frontal ablation to produce weekly ablation rate estimates between 2001 and 2015 (Köhler et al. 2016). The second method provides ice volumes for individually-observed calving events using calving signals at KBS and was calibrated with LIDAR volume measurements and time-lapse camera images at Kronebreen (Köhler et al. 2019b). While most seismic deployments of UiO were arranged in small-scaled arrays on solid ground, a single on-ice station was installed in a shallow borehole on Holtedalfonna in 2016. This record revealed a complex distribution of icequakes with remarkable correlation with glacier velocity, clear relation to glacier runoff, and evidence for seismic sources at the base of the glacier (Köhler et al. 2019a).

The Kola Branch of the Geophysical Service of the Russian Academy of Sciences (KB

GS RAS) in Apatity, Russia, conducted several studies combining seismic and infrasonic measurement of signals of glacial origin. The seismic station BRBB in Barentsburg was complemented by an infrasound station and a temporary station at the northern bank of Isfjorden which allowed detecting and locating glacier seismic events from Esmarkbreen and Nansenbreen (Asming et al. 2013; Vinogradov et al. 2015). Recently, KB GS RAS has started operating a seismic-infrasound station in Pyramiden with a special focus on monitoring signals originating from Nordenskiölbreen (Vinogradov et al. 2016).

Several studies were carried out focusing on regionally-observed glacier seismicity. Köhler et al. (2015) for the first time systematically detected and located cryogenic seismic signals on Spitsbergen. Clusters of seismic events were identified at several tidewater glaciers which showed a clear seasonal variability and were found to be mainly caused by calving. Based on these findings, regional calving event observations at KBS and SPITS were used to estimate frontal ablation rates at Kronebreen (Köhler et al. 2016). Furthermore, exceptional temporal patterns related to surges were observed for two glaciers (Köhler et al. 2015). Increasing seismic activity at Tunabreen in central Spitsbergen was a result of higher calving activity after the surge in 2003. The initial phase of the recent surge of Nathorstbreen in winter 2009 went along with icequake emissions related to ice failure when the change in back-stress up-glacier led to a sudden increase in basal shear stress and started a dynamic instability (Nuth et al. 2019). Analysis of the seismicity helped to constrain the timing of that process.

Different automatic techniques have been suggested to detect and map regional glacier seismicity in Svalbard using long-term seismological observations. While Köhler et al. (2015, 2016) used a combination of single station STA/LTA triggers (KBS, HSPB), waveform polarization, and array analysis (SPITS), Asming and Fedorov (2015) developed a three-component station detector and locator (HSPB) based on a STA-LTA trigger, P-S phase association, and joint polarization analysis. Gajek et al. (2017) also employed single station detection motivated by the presence of weak seismic events that are difficult to record due to the sparse seismological network in Svalbard. They developed an automatic procedure to distinguish between glacial and non-glacial signals using a fuzzy logic algorithm based on the signal frequency and energy flow analysis. The method was applied to HSPB and KBS to study glacier seismicity providing multi-annual catalogs of monthly-binned cryogenic events for Hornsund and Kongsfjorden regions.

A common finding of all long-term cryoseismological studies (Köhler et al. 2015, 2016; Gajek et al. 2017) is an increase in glacier-related seismicity mainly due to calving activity in recent years (Figure 4), for example a doubling of the number of seismic events in the Hornsund area over the years 2013-2014 (Gajek et al. 2017). Furthermore, those studies showed that the seasonal event distribution shows a time lag of about one month with respect to air temperatures, which suggests a relation between calving activity and fjord-water temperatures. The increase in the number of calving events in the Kongsfjorden

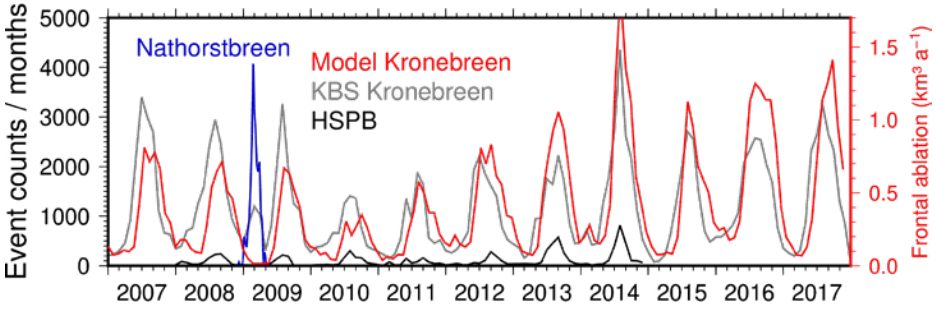

Figure 4: Example of the temporal distribution of cryoseismicity in Svalbard. Detections were made at KBS (Köhler et al. 2019b) and HSPB (Gajek et al. 2017) and include dominantly calving events (in summer/fall), except for surge signals originating from Nathorstbreen in 2009 (blue). An empirical model calibrated with satellite remote sensing observations of frontal ablation is used to estimate ice loss at Kronebreen from seismic data (red).

area since 2013 (Köhler et al. 2016, 2019b) is mainly related to the dramatic retreat of Kronebreen.

Pioneering research focusing on sub-surface structures in the cryosphere using ambient seismic noise has been conducted in the Kongsfjord region within the framework of the CalvingSEIS project and at the Hornsund research station. The potential of the single station HVSR method for monitoring seasonal permafrost active layer variability was explored in Hornsund (Kula et al. 2018) and Ny-Ålesund (Köhler et al. 2019c) with promising results. The HVSR technique will require further studies for calibrating measurements to permafrost parameters and for optimization of the best-suitable seismic network. The method has also been used to infer the (1D) internal seismic velocity structure of Holtedalfonna which allowed modeling of synthetic icequake signals (Köhler et al. 2019a). Results of seismic noise interferometry for active permafrost layer studies (James et al. 2017, 2019) are not yet available in Svalbard. However, a temporary seismic network was deployed in Adventdalen by NORSAR together with French colleagues in 2014 for monitoring a CO2 storage experiment (SafeCO2 project). The goal was to detect microseismicity and to use seismic noise interferometry to investigate the potential of measuring changes in the sub-surface as a result of the CO2 injection. Data are freely available and can be reused in future studies focusing on permafrost for example (Table 2).

Apart from the passive methods, active seismic methods have been successfully used to study the permafrost structure and properties in Svalbard. Rossi et al. (2018) performed a comprehensive test of active seismic methods over a pingo system in Adventdalen. In 2017-18 two active seismic measurements were performed by IG PAS at Hornsund. Initial results (Marciniak et al. 2019ab) show the successful application of active seismic methods

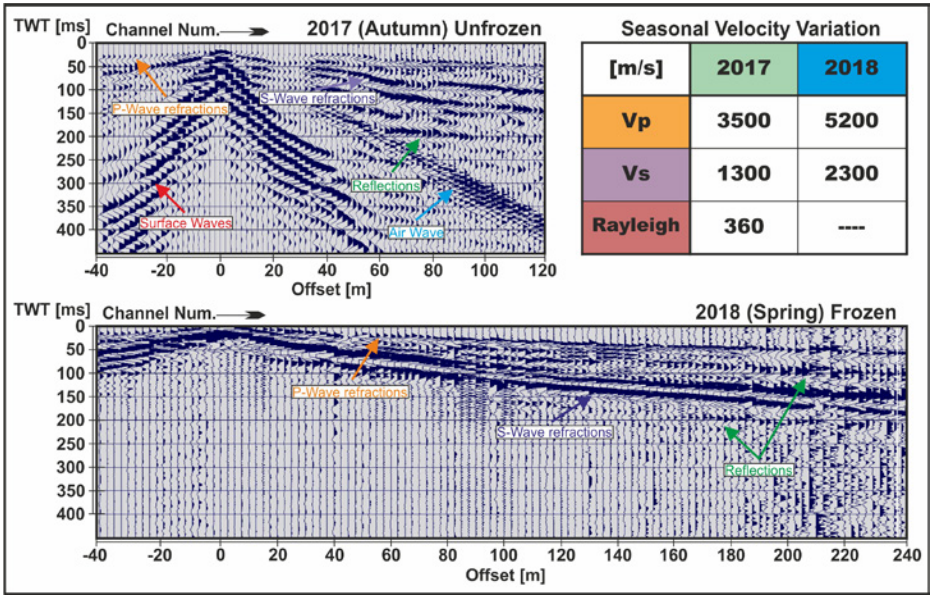

Figure 5: Active seismic wavefield recorded in Hornsund during two seasons: unfrozen (Autumn 2017) and frozen (Spring 2018). Note the significant change in apparent velocities and recorded wavefield due to freezing of the permafrost active layer (Marciniak et al. 2019b).

in the form of surface wave analysis (MASW) for near-surface S-wave velocity structure, refraction seismic tomography for time-lapse P-wave velocity variations (Figure 5), and reflection seismic imaging for geological structures and continuity of permafrost. Those seismic results have been combined with shallow borehole temperature profiles, GPR and ERT images showing clear compatibility.

3. Unanswered questions

3.1 Regional spatial-temporal distribution of glacier seismicity

What is the event distribution beyond the already monitored areas and how can we improve locations of detected events?

There is relatively good knowledge about glacier seismic sources in the Kongsfjord region, Hornsund area, and parts of central Spitsbergen where dedicated studies have been carried out in recent years thanks to the vicinity to permanent seismic stations and other research infrastructure, and the availability of direct observations of glacier dynamic processes (see

section 2.3). However, due to lacking station coverage, the spatial-temporal distribution of regional glacier seismicity is still unresolved for large parts of Svalbard, especially in the East of Spitsbergen and the other islands of the archipelago. Of special interest are the tidewater glaciers along the East coast of Spitsbergen and the ice caps of Nordaustlandet, where for example surges have occurred recently and are expected to happen in the future. Using the existing network for mapping sources of glacier seismicity is challenging since larger distances reduce the sensitivity to detect weak seismic signals, i.e., they affect the achievable completeness of event observations. Furthermore, the spatial resolution for discriminating between individual glaciers and tectonic earthquakes suffers from insufficient station coverage. While the ability to use the existing seismic network to study the East of Svalbard is limited, there is still some potential to identify strong events originating from glaciers or ice caps in that region. This has to be further assessed in dedicated studies using, for example, direct and independent observations of strong glacier dynamic events such as glacier surges or large iceberg calving, obtained from satellite remote sensing data. In addition to the seismic network limitation, seismic event locations are biased by unknown structural features in the Earth's crust affecting seismic wave propagation. To obtain reliable location estimates for glacier seismicity, structural investigations on the upper crust are needed by e.g. applying standard seismological methods.

How can we use glacier seismicity to monitor calving and surging?

It is known from previous studies that regional glacier seismicity in Svalbard is dominated by calving (see section 2.3). Calving monitoring with the high temporal resolution is essential but often lacking in glaciological research to better understand the mass loss of glaciers. Furthermore, since glacier seismicity has also shown to be suitable for observing glacier surges in Svalbard, more studies are required to evaluate how efficient this method is for detecting and monitoring future surges in near real-time. For example, it is not yet well-understood which (size) and how surges (mechanisms) generate regionally observable seismicity. It would be also essential for early warning purposes (e.g. for quickly restricting access to active glaciers) to automatize surge detection in seismic records and to define a detection threshold.

How can we produce continuous long-term cryogenic seismic event bulletins?

While dedicated studies have produced catalogues of glacier seismic events for past time periods in particular regions in Svalbard using the entire station network (see section 2.3), there is currently no automatic, real-time system for specifically detecting regional and local glacier seismicity in operation, mainly because those projects had time-limited funding and were not conducted at institutions with a long-term monitoring mandate and suitable infrastructure. Research programs and infrastructures are needed to implement and guarantee continuous, long-term monitoring of glacier seismicity in Svalbard and to produce

glacier seismic event bulletins/catalogs usable for glaciological research. These efforts would be based on the outcomes of the already completed projects and would benefit very much from an extension of the current permanent seismic network as well as the deployment of more temporary networks to identify dominant sources of seismicity.

3.2 Seismic observations vs. source and sub-surface parameters

How can observations be transferred into information useful in interdisciplinarity studies?

Detection, classification, and location of glacier seismic signals, as well as measuring seismic velocity variations with ambient noise, can help to identify trends and relative changes in the seasonality of glacier activity and subsurface properties. While this information is already very valuable for glaciological and permafrost research due to its high temporal resolution and the continuous long-term record, actual quantification methods based on seismic measurements are still lacking for many processes. Seismic observables such as event counts, signal properties, seismic velocity changes have to be transferred into physical, glaciological and permafrost-related parameters or quantities. This can be achieved either by developing empirical or physicals models.

How can quantifying dynamic ice loss from seismic observations be extended and improved?

Calibration using satellite and terrestrial remote sensing has already been used for quantifying frontal ablation and the contribution of calving at Kronebreen directly from seismic data, but the empirical models developed are only valid for this particular glacier. Long-term, continuous, and high-temporal resolution records (frontal ablation, dynamic ice loss, sub-marine melting) are not yet available for many glaciers but are necessary to better understand fine-scale processes and key climatic-dynamic feedbacks between calving, climate, terminus evolution, and marine conditions. Field measurements of seismic calving signals simultaneously with the corresponding ice loss volumes at multiple tidewater glaciers in Svalbard are lacking but needed to develop a more general quantification method. Furthermore, there is currently no seismic source model available to simulate seismic signals for the dominant calving style in Svalbard. Developing a physical model would, therefore, offer an alternative to using empirical models for ice loss quantification.

How can seismic observations be used to better understand mechanisms and processes inside or at the base of glaciers?

Icequake signals and tremors can be analyzed using standards seismological methods to for example infer source mechanisms to study not yet well-understood sub-glacier processes such as stick-slip and basal sliding (friction laws). This approach provides high temporal

resolution and hence insight that cannot be achieved by other techniques (GNSS, remote sensing). Such methods have been successfully applied for example in Antarctica and on Alpine glaciers, however, not yet in Svalbard due to the lack of suitable (temporary) on-ice seismic networks with good spatial coverage deployed in dedicated field campaigns. Similar, for quantifying discharge using observations of seismic meltwater tremors, methods previously applied on Greenland and Alaska should be adapted. To better understand source processes of seismic signals, integrated approaches are required on glaciers combining passive seismic measurements with e.g. borehole measurements (drill cores, downhole pressure, temperature, and deformation sensors, etc.), in-situ GNSS tracking of glacier flow, remote sensing, and other (active) geophysical methods.

How can seismology contribute to improving permafrost monitoring?

Ground temperature measurements in boreholes close to most research stations/ settlements in Svalbard are commonly used to monitor the effects of climate change on permafrost (Christiansen et al. 2019). They offer sufficient temporal resolution (hourly sampling) but the spatial coverage of these points measurements is naturally limited. In addition, regular (manual) probing of the permafrost active layer thickness on spatial grids is performed (CALM sites) but is only possible in fine-grained soils. Simultaneous seismic measurements at these sites are lacking but are key for developing passive methods for permafrost monitoring applicable in arbitrary areas. One important variable to observe with a wider spatial extent is, for example, the timing of the active-layer freeze-back in autumn since later re-freezing in the season promotes permafrost degeneration (Christiansen et al. 2019). This is of particular significance in the lowlands of Svalbard where the degradation can result in subsidence, landslides, and will affect the local ecosystems and hydrology. In particular, calibration studies are required to relate seasonal changes and long-term trends in the permafrost to seismic velocity changes measured from ambient seismic noise. Furthermore, since permafrost is a new application of ambient noise-based methods, a best-practice for these experiments has not been established yet. In contrast to the HVSR methods, ambient noise interferometry for permafrost monitoring as done in Alaska has not yet been performed in Svalbard.

3.3 Best practice in the field and potential of new technologies

What is the best practice for temporary seismic deployments in Svalbard?

Deployment and maintenance of passive seismic networks in the Arctic environment are challenging due to harsh weather conditions, polar night, and remote locations (Figure 2). There are issues related to the continuous, real-time transfer of large data volumes (lacking mobile network), power supply during winter (limited battery capacity, no solar cells) and

instrument coupling to the ground during melt season. Regular maintenance is not always feasible due to remote installations or inaccessibility during certain seasons of the year. Experiences gained during recent field measurements have to be compiled in guidelines and recommendations for future seismic experiments in glacier and permafrost studies. This includes finding and evaluating cost-effective and robust solutions for on-ice and in-ice borehole seismic installations. Borehole instrumentations add the vertical dimension to seismic networks, enhancing the information content of seismological data and providing better insight into the analysis of basal seismicity. However, deployment (drilling, placement) and operation are challenging in moving and deforming ice compared to common seismic borehole installations.

Especially for permafrost monitoring, finding suitable solutions for stable sensor installation during thawed conditions is critical. Questions that have to be addressed in test studies are where the instruments are best placed (surface, within permafrost, borehole), how to keep the sensors from tilting and losing coupling, and what kind of sensors should be used.

Can new technologies improve cryo-seismological measurements?

Advanced and new technologies have to be tested in the field such as DAS recording systems. Also, on-ice seismic arrays can be deployed for detecting and locating weak icequakes and tremors and observing crevassing and its correlation with ice flow, as already exploited in the Alps (e.g. Lindner et al. 2019) and Antarctica (e.g. Smith et al. 2017), but not yet in Svalbard. It is important to determine the common standard and best practices of instrument deployment and optimal layouts of seismic network and array for different applications and purposes in Svalbard (icequake detection, location, structural imaging, noise interferometry, etc.).

Which methods should be combined in the field?

Integrated approaches are essential to advance cryoseismological research (see section 3.2). Different methods complement each other; for example, while active methods have a higher depth resolution (e.g. to measure the thickness of permafrost, the active layer, or glaciers), passive methods allow time-lapse monitoring with high resolution and borehole measurements guarantee high precision but sample a very limited area. Integrated approaches proved to be effective in, e.g. Alpine applications (Gräff et al. 2019), however, the potential of combining passive seismic measurements with active or borehole geophysical measurements is still to be explored in Svalbard.

4. Recommendations for the future

Based on previous cryoseismological studies carried out in Svalbard and in view of the existing knowledge gaps, we provide the following recommendations for related future research and for improving as well as better exploiting the existing research infrastructure. They are also aligned with the previous and current priorities stated in the SESS reports (Christiansen et al. 2019, Schuler et al. 2020):

1. The permanent seismic station network in Svalbard should be extended with long-term deployments to improve detectability and location of glacier seismicity, especially along the east coast of Spitsbergen and in Nordaustlandet. This can be accomplished by deploying single-stations at existing meteorological observation sites or other SIOS monitoring infrastructure, for instance at the depot at Oxford peninsula, in close vicinity to Austfonna and Vestfonna with ongoing glacier monitoring and occurrence of several surges. We also recommend upgrading current single stations to seismic arrays, for example in Hornsund and Ny-Ålesund, where the necessary infrastructure (power supply, internet connection, whole year maintenance possibilities) is already available without additional environmental impact, and which would result in a considerably improved detection capability in combination with the existing SPITS array.

2. Existing and routinely recorded seismic data volumes should be used to extend regional seismic glacier monitoring to so far unstudied regions and unconsidered time periods by implementing a continuous automatic near-real-time event detection system. This system should be based on template events from locally identified sources (calving events, surges, etc.), may adopt machine-learning and advanced seismic array methods to distinguish for example between tectonic and glacier seismicity, and should deliver a sharable, routinely updated bulletin of glacier seismic events in Svalbard findable in the SIOS data access point which allows extracting information about variability of activity (trends and seasonality) in a form usable also for non-seismologists. This effort will benefit from making available legacy seismic datasets.

3. To improve the location of glacier seismicity, structural investigation on crustal scales should be performed which will benefit from network extensions (see point 2) and temporal seismic deployments for structural and/or cryoseismological studies.

4. Multi-disciplinary, integrated field campaigns should be carried out combining passive and active seismic and other geophysical methods with direct observations of cryosphere processes such as calving, meltwater discharge, sub-glacier dynamics, and permafrost thaw depths. These experiments are mandatory to infer physical

cryospheric parameters and quantities from seismic measurements as well as to develop seismic source models. In particular, we recommend to (i) extend the calving quantification method developed for Kronebreen to other tidewater glaciers, (ii) to deploy temporary, purpose-built seismic networks close to existing and to-be-established permafrost observation sites (e.g. Ny-Ålesund, Adventdalen, Barentsburg, Hornsund, Kapp Linné) to calibrate seismic methods, e.g. to monitor the freeze-back in areas not being represented by the existing sites (Christiansen et al. 2019), and (iii) to combine on-ice seismic networks with glacier in-situ measurements to study subglacial drainage and basal processes. These efforts would benefit from establishing a multidisciplinary instrument pool (including seismometers, drilling equipment, borehole sensors, GNSS, etc.) that can also be used for urgent deployments (e.g. an ongoing glacier surge) (Schuler et al. 2020).

5. New technologies and methods have been successfully applied in seismology in recent years such as fiber-optic cables (DAS), seismic noise interferometry, and machine learning. These approaches should be used in Svalbard for cryoseismological research. DAS measurements on glaciers will not only allow analyzing seismicity with high spatial resolution but also inferring slow, aseismic glacier deformation. Noise interferometry has a huge potential for monitoring changes in the permafrost active layer. Machine learning can assist in analyzing large seismic data volumes.

5. Data availability

Table 1 lists information about all permanent seismic broadband stations in Svalbard. There is unrestricted data access to all raw seismic records. All metadata including links to landing sites can be found in the SIOS data access point (referenced there as "seismological station records"). While these datasets might currently be mainly useful for seismologists, we recommend in this report to produce data products useful for cryosphere research in general. We anticipate that the outcomes of future studies will be integrated into the SIOS data access point.

Continuous seismic waveform data are available through different data centres. The most common access is through ORFEUS EIDA nodes (Datacentres of the European Integrated Data Archive, https://www.orfeus-eu.org/data/eida/nodes). Data can be accessed via web-interfaces (ORFEUS or data centres of individual nodes, e.g. GFZ, GEOFON) or different application programming interfaces (e.g. ObsPy). In Table 1, "EIDA" refers to the common Norwegian EIDA node hosted at the University of Bergen, while "IRIS-DMC" means that data are available through the IRIS (Incorporated Research Institutions for Seismology) data centre. The Norwegian EIDA node is under construction within the EPOS-Norway project. Note, that not all seismic datasets have DOIs yet, but European efforts are underway to

complete the missing identifiers (see https://www.orfeus-eu.org/data/eida/networks). In Svalbard, only KBS has a registered DOI (https://doi.org/10.7914/SN/IU) today.

Table 2 gives an overview of recent seismic datasets recorded during temporary measurements in Svalbard. Data access status is either open, free on request, or not (yet) available.

Acknowledgments

This work was supported by the Research Council of Norway, project number 251658, Svalbard Integrated Arctic Earth Observing System - Knowledge Centre (SIOS-KC). We thank Dr. Myrto Pirli and Prof. Thomas Vikhamar Schuler for critically reading through this report and suggesting improvements.

References

Abbott R, Knox HA, James S, Lee R, Cole C (2016) Permafrost Active Layer Seismic Interferometry Experiment (PALSIE), Tech. rep., Sandia National Laboratories (SNL-NM), Albuquerque, NM (United States), available at: https://prod.sandia.gov/techlib/access-control.cgi/2016/160167.pdf (last access: 7 January 2019)

Ajo-Franklin JB, Dou S, Lindsey NJ, Monga I, Tracy C, Robertson M, Rodriguez Tribaldos V, Ulrich C, Freifeld B, Daley T, Li X (2019) Distributed Acoustic Sensing Using Dark Fiber for Near-Surface Characterization and Broadband Seismic Event Detection. Sci. Rep. 9(1):1328

Asming V, Baranov S, Vinogradov YA, Voronin A (2013) Seismic and infrasonic monitoring on the Spitsbergen Archipelago. Seis. Instr. 49:209–218

Asming V, Fedorov A. (2015) Possibility of using a single three-component station automatic detector–locator for detailed seismological observations, Seis. Instr. 51(3):201– 208

Aster RC, Winberry JP (2017) Glacial seismology. Rep on Progress in Phys 80:126801

Bartholomaus TC, Larsen CF, West ME, O'Neel S, Pettit EC, Truffer M (2015a) Tidal and seasonal variations in calving flux observed with passive seismology. J. Geophys. Res: Earth Surface 120(11):2318-2337

Bartholomaus TC, Amundson JM, Walter JI, O'Neel S, West ME, Larsen CF (2015b) Subglacial discharge at tidewater glaciers revealed by seismic tremor. Geophys. Res. Lett. 42(15):6391–6398

Bergen KJ, Johnson PA, de Hoop MV, Beroza GC (2019) Machine learning for data-driven discovery in solid Earth geoscience. Science 363:6433

Booth AD, Mercer A, Clark R, Murray T, Jansson P, Axtell C (2013). A comparison of seismic and radar methods to establish the thickness and density of glacier snow cover. Ann. Glac, 54:73-82

Christiansen HH, Gilbert GL, Demidov N, Guglielmin M, Isaksen K, Osuch M, Boike J (2019) Permafrost thermal snapshot and active-layer thickness in Svalbard 2016-2017. In: Orr et al (eds): SESS report 2018, Svalbard Integrated Arctic Earth Observing System, Longyearbyen, 26–47. https://sios-svalbard.org/SESS_Issue1

Church G, Bauder A, Grab M, Rabenstein L, Singh S, Maurer H (2019). Detecting and characterising an englacial conduit network within a temperate Swiss glacier using active seismic, ground penetrating radar and borehole analysis. Ann. Glac. 60:193-205

Cichowicz A (1983) Icequakes and glacier motion: The Hans glacier, Spitsbergen. Pure and App. Geophys. 121(1):27-38

Czajkowski R (1977) The results of investigations into microquakes on the Hans Glacier. Acta Univ. Wratisl. 387

Diez A, Bromirski PD, Gerstoft P, Stephen RA, Anthony RE, Aster RC, Cai C, Nyblade A, Wiens DA (2016) Ice shelf structure derived from dispersion curve analysis of ambient seismic noise, Ross Ice Shelf, Antarctica. Geophys J Int 205(2):785–795

Dow CF, Hubbard A, Booth AD, Doyle SH, Gusmeroli A, Kulessa B. (2013) Seismic evidence of mechanically weak sediments underlying Russell Glacier, West Greenland. Ann Glac, 54:135-141

Draebing D, Krautblatter M (2012) P-wave velocity changes in freezing hard low-porosity rocks: a laboratory-based time-average model. Cryosphere 6:1163-1174

Ekström G, Nettles M, Abers GA (2003) Glacial earthquakes. Science 302:622-624

Gajek W, Trojanowski J, Malinowski M (2017) Automating long-term glacier dynamics monitoring using single-station seismological observations and fuzzy logic classification: a case study from Spitsbergen. J. Glaciol 63(240):581-592

Glowacki O, Deane GB, Moskalik M, Blondel PH, Tegowski J, Blaszczyk M (2015) Underwater acoustic signatures of glacier calving. Geophys Res Let 42:804-812

Górski M (1975) Observations of natural ice-micro-tremors of the Hans glacier. Acta Univ Wratisl 251:95-100

Górski M, Teisseyre R (1991) Seismic events in Hornsund, Spitsbergen, Polish Polar Res. 12:345-352

Górski M (1997) Seismicity of the Hornsund region, Spitsbergen: icequakes and earthquakes, Publs. Inst. Geophys. Pol. Acad. Sci. B-20 (308), 77 pp.

Górski M (1999) Seismic wave velocities in the Hans Glacier. In: J. Repelewska-Pękalowa (ed.), Polish Polar Studies, 26th Intern. Polar Symposium, UMCS Press, Lublin, 77-81. Acta Geophys. Pol. 51:399-407

Górski M (2003) Icequakes in Hans Glacier, Spitsbergen: source parameters of icequake series. Acta Geophys Pol 51(4):399-407

Górski M (2004) Predominant frequencies in the spectrum of ice-vibration events. Acta Geophys Pol 52(4)

Górski M (2014) Seismic events in glaciers. Springer, ISBN 978-3-642-31851-1

Gräff D, Walter F, Lipovsky B (2019) Crack wave resonances within the basal water layer. Ann Glac 60(79)

Helmstetter A, Moreau L, Nicolas B, Comon P, Gay M (2015) Intermediate-depth icequakes and harmonic tremor in an alpine glacier (glacier d'Argentière, France): evidence for hydraulic fracturing? J. Geophys. Res. Earth Surf. 120(3):402–416

Hilbich C (2010) Time-lapse refraction seismic tomography for the detection of ground ice degradation. Cryosphere 4:243-259

James SR, Knox H, Abbott RE, Screaton EJ (2017) Improved moving window cross-spectral analysis for resolving large temporal seismic velocity changes in permafrost, Geophys. Res. Lett. 44:4018–4026

James SR, Knox HA, Abbott RE, Panning MP, Screaton EJ (2019) Insights into Permafrost and Seasonal Active-Layer Dynamics from Ambient Seismic Noise Monitoring, J. Geophys. Res. Earth Surf, published online

Johansen TA, Ruud BE, Bakke NE, Riste P, Johannessen EP, Henningsen T (2011) Seismic profiling on Arctic glaciers. First Break 29(2): 65-71

Jin G, Roy B (2017) Hydraulic-fracture geometry characterization using low-frequency DAS signal. The Leading Edge 36(12):962-1044

Jousset P, Reinsch T, Ryberg T, Blanck H, Clarke A, Aghayev R, Hersir GP, Henninges J, Weber M, Krawczyk CM (2018) Dynamic strain determination using fibre-optic cables allows imaging of seismological and structural features. Nature Comm 9:2509

King EC, Smith AM, Murray T, Stuart GW (2008) Glacier-bed characteristics of midtre Lovenbreen, Svalbard, from high-resolution seismic and radar surveying. J Glac, 54(184):145-156

Köhler A, Chapuis A, Kohler J, Nuth C, Weidle C (2012) Autonomous detection of calving-related seismicity at Kronebreen, Svalbard. The Cryosphere 6:393-406

Köhler A, Nuth C, Kohler J, Berthier E, Weidle C, Schweitzer J (2016) A 15 year record of frontal glacier ablation rates estimated from seismic data. Geophys Res Lett 43:12155-12164

Köhler A, Nuth C, Schweitzer J, Weidle C, Gibbons SJ (2015) Regional passive seismic monitoring reveals dynamic glacier activity on Spitsbergen, Svalbard. Polar Res 34:26178

Köhler A, Maupin V, Nuth C, van Pelt W (2019a) Characterization of seasonal glacial seismicity from a single-station on-ice record at Holtedahlfonna, Svalbard, Ann. Glac. https://doi.org/10.1017/aog.2019.15

Köhler A, Petlicki M, Lefeuvre PM, Buscaino G, Nuth C, Weidle C (2019b) Contribution of calving to frontal ablation quantified from seismic and hydroacoustic observations calibrated with lidar volume measurements. The Cryosphere Disc. https://doi.org/10.5194/tc-2019-75

Köhler A, Weidle, C (2019c) Potentials and pitfalls of permafrost active layer monitoring using the HVSR method: a case study in Svalbard. Earth Surf Dyn 7:1-16

Kong Q, Trugman TD, Ross ZE, Bianco MJ, Meade BJ, Gerstoft P (2018) Machine Learning in Seismology: Turning Data into Insights. Seismol. Res. Lett. 90:3–14

Kula D, Olszewska D, Dobiński W, Glazer M. (2018) Horizontal-to-vertical spectral ratio variability in the presence of permafrost. Geophys. J. Int. 214:219–231

Larose E, Carrière S, Voisin C, Bottelin P, Baillet L, Guéguen P, Walter F, Jongmans D, Guillier B, Garambois S, Gimbert F, Massey C (2015) Environmental seismology: What can we learn on earth surface processes with ambient noise? J Appl Geophys 116:62–74

Lewandowska H, Teisseyre R (1964) Investigations of the ice microtremors on Spitsbergen in 1962, Biul. Inf. Komisji Wypraw Geof. PAN, 37:1– 5

Lindner F, Laske G, Walter F, Doran AK (2019) Crevasse-induced Rayleigh-wave azimuthal anisotropy on Glacier de la Plaine Morte, Switzerland. Ann Glac 60(79): 96-111

Marciniak A, Owoc B, Wawrzyniak T, Nawrot A, Glazer M, Osuch M, Dobiński W, Majdański M (2019a) Recognition of the varying permafrost condidions in the SW Svalbard by multiple geophysical methods. EGU General Assembly 2019 21:EGU2019-377

Marciniak A, Owoc B, Wawrzyniak T, Nawrot A, Glazer M, Osuch M, Dobiński W, Majdański M (2019b) Near-surface geophysical imaging of the permafrost - initial results of two high Arctic expeditions to Spitsbergen. EAGE Near Surface Geoscience, Hague. 5pp

Minowa M, Podolski, EA, Jouvet G, Weidmann Y, Sakakibara D, Tsutaki S, Genco R, Sugiyama S (2019) Calving flux estimation from tsunami waves, Earth and Planet Sci Lett 515:283--290

Nakata N, Boué P, Brenguier F, Roux P, Ferrazzini V, Campillo M (2016) Body and surface wave reconstruction from seismic noise correlations between arrays at Piton de la Fournaise volcano. Geophys Res Lett 43

Nordli Ø, Przybylak R, Ogilvie AE, Isaksen K (2014) Long-term temperature trends and variability on Spitsbergen: the extended Svalbard Airport temperature

series, 1898-2012. Polar Res 33:21349

Nuth C, Gilbert A, Köhler A, McNabb R, Schellenberger T, Sevestre H, Weidle C, Girod L, Luckman A, Kääb A (2019) Dynamic vulnerability revealed in the collapse of an Arctic tidewater glacier. Sci Rep 9:5541

Overduin PP, Haberland C., Ryberg T, Kneier F, Jacobi T, Grigoriev M, Ohrnberger M. (2015) Submarine permafrost depth from ambient seismic noise, Geophys. Res. Lett. 42:7581–7588

Picotti S, Francese R, Giorgi M, Pettenati F, Carcione JM (2017) Estimation of glacier thicknesses and basal properties using the horizontal-to-vertical component spectral ratio (HVSR) technique from passive seismic data. J. Glac 63(238):229–248

Polom U, Hofstede C, Diez A, Eisen O (2014) First glacier-vibroseismic experiment - results from cold firn of Colle Gnifetti. Near Surface Geophys 12:493-504

Pirli M, Matsuoka K, Schweitzer J, Moholdt G (2015) Seismic signals from large, tabular icebergs drifting along the Dronning Maud Land coast, Antarctica, and their significance for iceberg monitoring. J. Glac 61(227):481-492

Pirli M, Hainzl S, Schweitzer J, Köhler A, Dahm T (2018) Localised thickening and grounding of an Antarctic ice shelf from tidal triggering and sizing of cryoseismicity. Earth and Planet Sci Lett, 503:78-87

Podolskiy EA, Walter F (2016) Cryoseismology. Rev Geophys 54:708-758

Rossi G, Accaino F, Boaga J, et al. (2018) Seismic survey on an open pingo system in Adventdalen Valley, Spitsbergen, Svalbard. Near Surface Geophys 16:89–103

Röösli C, Walter F, Ampuero JP, Kissling E (2016) Seismic moulin tremor. J. Geophys. Res.: Solid Earth 121(8):5838–5858

Preiswerk LE, Walter F (2018) High-Frequency (>2 Hz) Ambient Seismic Noise on High-Melt Glaciers: Green's Function Estimation and Source Characterization. J. Geophys. Res.: Earth Surf. 123(8):1667–1681

Smith EC, Baird AF, Kendall JM, Martín C, White RS, Brisbourne AM, Smith AM (2017) Ice fabric in an Antarctic ice stream interpreted from seismic anisotropy. Geophys. Res. Lett. 44(8):3710-3718

Schuler TV, Glazovsky A, Hagen JO, Hodson A, Jania J, Kääb A, Kohler J, Luks B, Malecki J, Moholdt G, Pohjola V, van Pelt W (2020), SvalGlac: New data, new techniques and new challenges for updating the state of Svalbard glaciers. In: Van den Heuvel et al. (eds): SESS report 2019, Svalbard Integrated Arctic Earth Observing System, Longyearbyen, **108 – 135**. **https://sios-svalbard.org/SESS_Issue2**

Schweitzer J, Fyen J, Mykkeltveit S, Gibbons S, Pirli M, Kühn D, Kværna T (2012) Seismic arrays. In P. Bormann (ed.): New manual of seismological observatory practice 2 (NMSOP-2). 2nd edn. Potsdam: German Research Centre for Geosciences

Stuart G, Murray T, Brisbourne A, Styles P, Toon S (2005) Seismic emissions from a surging glacier: Bakaninbreen, Svalbard. Ann. Glac. 42:151-157

Vinogradov YA, Asming VE, Baranov SV, Fedorov AV, Vinogradov AN (2015) Seismic and infrasonic monitoring of glacier destruction: a pilot experiment on Svalbard. Seis Instr 51:1–7

Vinogradov A, Asming VE, Baranov SV, Fedorov AV, Vinogradov Y (2016) Joint seismo-infarsound monitoring of outlet glaciers in the Arctic: case study of the Nordenskiold outlet glacier terminus near Pyramiden (Spitsbergen). International Multidisciplinary Scientific GeoConference: SGEM: Surveying Geology & mining Ecology Management 3: 521--528

Yan P, Zhiwei L, Fei L, Yuande Y, Weifeng H, Feng B (2018) Antarctic ice sheet thickness estimation using the horizontal-to-vertical spectral ratio method with single-station seismic ambient noise. Cryosphere 12:795–810

Walter F, Roux P, Roeoesli C, Lecointre A, Kilb D, Roux PF (2015) Using glacier seismicity for phase velocity measurements and Green's function retrieval. Geophys J Int, 201(3):1722–1737

Wilde-Piórko M, Grad M, Wiejacz P, Schweitzer J (2009): HSPB seismic broadband station in Southern Spitsbergen: First results on crustal and mantle structure from receiver functions and SKS splitting. Polish Polar Res 40(4):301-316

Zhan Z (2019) Seismic noise interferometry reveals transverse drainage configuration beneath the surging Bering Glacier. Geophys Res Lett 46(9):4747--4756

Long-term monitoring of landfast sea ice extent and thickness in Kongsfjorden, and related applications (FastIce)

6

Sebastian Gerland[1], Olga Pavlova[1], Dmitry Divine[1], Jean Negrel[1], Sandro Dahlke[2], A. Malin Johansson[3], Marion Maturilli[2], and Maximilian Semmling[4]

1 Norwegian Polar Institute, Fram Centre, Tromsø, Norway
2 Alfred Wegener Institute, Helmholtz Centre for Polar and Marine Research, Potsdam, Germany
3 UiT The Arctic University of Norway, Tromsø, Norway
4 German Research Centre for Geosciences (GFZ), Department of Geodesy, Potsdam, Germany

Corresponding author: Sebastian Gerland, gerland@npolar.no
ORCID number 0000-0002-2295-9867

Keywords: Kongsfjorden, Svalbard, sea ice, fast ice, time series, climate change

1. Introduction

Landfast sea ice covers the inner parts of Kongsfjorden, Svalbard, for a limited time in winter and spring months, being an important feature for the physical and biological fjord systems (Figure 1). Systematic fast-ice monitoring for Kongsfjorden, as a part of a long-term project at the Norwegian Polar Institute (NPI) was started in 2003, with some more sporadic observations from 1997 to 2002. It includes the ice extent mapping and in situ measurements of ice and snow thickness, and freeboard at several sites in the fjord. The permanent presence of NPI personnel in Ny-Ålesund Research Station enables regular in situ fast-ice thickness measurements as long as the fast ice is accessible. Further, daily visits to the observatory on the mountain Zeppelinfjellet close to Ny-Ålesund, allow regular ice extent observations (weather, visibility, and daylight permitting). Data collected within this standardized monitoring programme have contributed to a number of studies. Monitoring of the sea-ice conditions in Kongsfjorden can be used to demonstrate and investigate phenomena related to climate change in the Arctic.

Figure 1: Landfast sea ice in Kongsfjorden in spring 2009, with an iceberg in some distance. (Photo: S. Gerland)

2. State of fast-ice monitoring for the period 2003-2019

2.1 Method

Conception and methodology of the systematic fast-ice monitoring in Kongsfjorden are described in Gerland and Hall (2006), Gerland and Renner (2007) and Pavlova et al. (2019). The fast-ice extent observations are based on visual observations for days with sufficient daylight, and, accordingly, no data are available for days when there is limited visibility (low clouds, fog and darkness). The maps are drawn by hand visually assessing the ice edge, and photographs are taken from Zeppelinfjellet. In maps and from photographs, we classify the ice as "fast ice" and "drift ice". Ice thickness and freeboard are measured conventionally from drill holes on up to five sites in the inner fjord, using a 2" auger and a Kovacs thickness-gauge tape measure or a measurement stick with a notch. The snow thickness is measured with a metal stake.

2.2 Fast-ice extent

The fast-ice coverage reached its maximum (120 km^2) within the defined observation area in the years 2003-2006 and 2011 (Pavlova et al. 2019, their Figure 3). The period after 2006 was characterised by relatively little sea-ice cover and shorter ice cover season, except 2011. The lowest ice extent (21%) was observed in 2012. The time series of maximum fast-ice coverage for each of five months (February-June) in the period 2003-2019 shows alternating periods of extensive and little ice cover (Figure 2). Maximum fast-ice coverage values (100% of the surveyed area in the fjord) in February were reached in the years 2004-2006 and 2011. For 2003, no ice-cover information is available prior to March, and in 2004 the entire observation area was ice-covered with fast ice in mid-January (not shown) and also registered in February. In March, only the years 2003-2005 had 100% fast-ice coverage, while in April, the two largest maximal fast-ice cover values (93% and 80.5% of ice-covered area) were observed in 2004 and 2011, respectively. In the two other months (May-June), in the years when fast ice was observed then, the maximum fast-ice coverage was below 50%, except for the period 2003-2005. Maximum fast-ice coverage of 50% and higher was reached in the years 2003–2006 and 2009–2011 between February/March and April. During the periods 2007-2008 and 2012-2019, fast ice covered less than 50% of the study area, except for February 2008 and 2015, and for March 2018 and 2019. Based on available visual observations, late ice growth, low coverage and short seasons of fast ice were observed in the years 2012, 2014, 2016 and 2017. Despite the lowest February ice coverage (during the monitoring period) observed in 2018 (2.5%), ice extent in March 2018 was relatively high (66.7%). Finally, also the year 2019 can be counted among years with a rather short sea ice season, but with relatively high per cent of fast-ice coverage in February

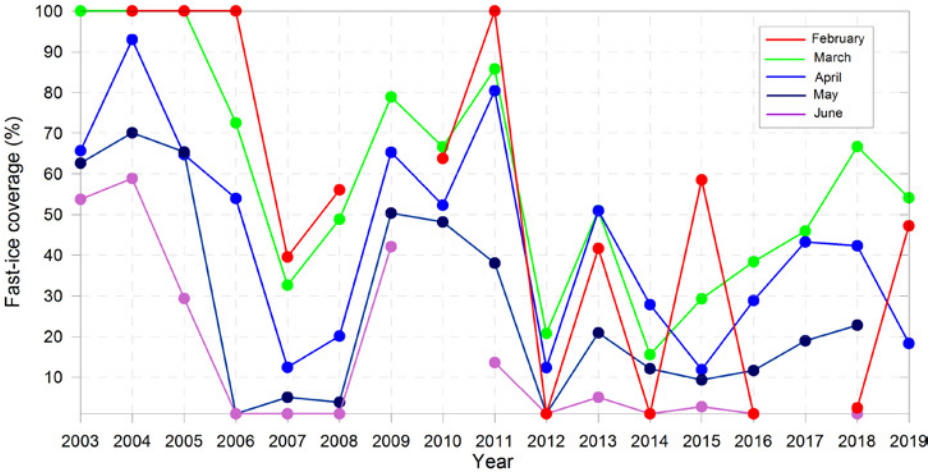

Figure 2: Maximum fast-ice coverage for each month from February to June (2003-2019). Gaps in the lines are related to years/months where no data are available.

and March (near 50%). Based on conditions from 2003-2019, the fast-ice evolution in Kongsfjorden during this period showed that i) fast-ice formation scenarios varied annually, but with intervals (2-3 years or more) of relatively high and low sea-ice cover; and ii) most years after 2006 had low ice extent and short seasons of fast ice.

Over the last 30 years, the coastline has changed due to glacier retreat, and therefore the observation area has increased. This does not only increase the available area for ice formation, it also alters conditions for ice formation through creation of new areas/bays protected from swell and waves.

2.3 Ice and snow thickness

Both fast ice and snow thickness have experienced negative trends over the observation period 1997-2016, towards thinner ice and snow cover (Pavlova et al. 2019). Before 2006 the ice was usually at least 0.6 m thick. In recent years until 2016, except for 2011, values decreased to around 0.2 m. The linear trend of that change for the period 1997-2016 is -24.7% per decade. However, the inter-annual variation in ice thickness appears to be substantial. In parallel to this development, snow thickness decreased in the same period from around 0.2 m to < 0.05 m, exhibiting an even larger negative trend in relative values with -41.7% per decade.

After 2016, in most areas ice thickness was still at low levels, with the exception of the

wave-protected area of Raudvika (a bay in inner Kongsfjorden, which is increasing in size due to glacier retreat), where sea ice well over 0.2 m thick was observed.

The snow cover on sea ice slows down ice growth (relative to sea ice without a snow cover), but it also can, under specific conditions, contribute to the sea ice growth. From observations (Gerland et al. 1999, 2004; Nicolaus et al. 2003) and modelling (Nicolaus et al. 2006; Wang et al. 2015), it is known that snow ice and superimposed ice do contribute to ice and snow thickness evolution in Kongsfjorden. Air temperature and precipitation are critical factors for snow ice and superimposed ice formation, and the total ice formation at the ice surface are more sensitive to precipitation than to air temperature (Wang et al. 2015).

2.4 Related applications

The sea ice monitoring in Kongsfjorden represents additional value beyond what it contributes to climate research. A larger number of process- and validation studies with links to the role of sea ice in the fjord has been conducted in Kongsfjorden since the late 1990s. Here, we discuss a few examples of such studies conducted in recent years. Advantages of using the landfast sea ice in the fjord for a number of applications are: (i) the fact that the fast ice is not mobile, giving the opportunity to install measurement equipment that can relative easy be retrieved later, and it helps for connecting satellite imagery to features on the ice observed with a small time difference; and (ii) the fact that most of the fast ice properties are largely homogeneous in horizontal dimensions, which means it can serve as a 1-D case for testing process models, and findings from one site can be extended within some (limited) area around the observation site.

Sea ice in Kongsfjorden was used for two studies validating SAR (Synthetic Aperture Radar) satellite remote sensing products (Negrel et al. 2018, Johansson et al. in press). It could be demonstrated, that under certain circumstances, the edge of the fast ice can be reasonably well mapped using SAR products, however, limitations of this method were visible, for example, when the sea ice is less than 0.1 m thick, SAR methods were not able to distinguish sea ice from open water. This is important when further developing satellite methods in order to aid or even replace direct observations.

Another validation study focused on the remote sensing application of Global Navigation Satellite System (GNSS). Such GNSS, like the US-operated Global Positioning System (GPS), provide signals with global coverage initially meant for navigation. The study conducted at Kongsfjorden examines the reflected GNSS signals for remote sensing of the sea surface and the adjacent glaciers (Peraza et al. 2017). Under certain conditions, sea ice properties, e.g. its concentration, can be derived from the reflected signals (Semmling et al. 2019). A

challenge for the setup at Kongsfjorden is that in recent years, the fjord area in immediate vicinity of Ny-Ålesund was usually free of ice also in winter.

Interesting scientific questions, when looking at environmental changes, address the couplings (e.g. energy fluxes) between atmosphere, sea ice and ocean, including fjords. Ultimately these processes control how much and which type of sea ice is present in a region. In a recent study (Dahlke et al. unpublished data) the coupling of atmospheric properties and sea ice extent is investigated, with a focus on the Svalbard region. Comparing information on surface air temperature (SAT) and sea ice extent (SIE) in Svalbard fjord systems led to the conclusion that, on time scales of a few months, changes in SAT affect SIE more than the other way around. This is an important finding for improving the understanding of the Arctic system, and how the system is changing, from local to larger scales.

2.5 Conclusions

Fast ice and ice and snow thickness in Kongsfjorden have been monitored regularly since 2003. This study is ongoing, and a major aim is to identify and quantify connections between the fast-ice evolution in Kongsfjorden and climate variability, in particular atmosphere and ocean related drivers. Consistent monitoring of sea ice is challenging because of changing observation area settings. Changes in glacier fronts present a challenge for fast-ice monitoring in Kongsfjorden. For long-term monitoring, changing (retreating) glacier fronts lead to (i) change (increase) in the total surface area of the fjord, and (ii) new coastline and hydrographic conditions, which might be both less and more favourable for fast-ice formation.

Sea-ice monitoring in Kongsfjorden is not only used for climate change research, it also contributes to past, ongoing and future process and validation studies in many disciplines conducted at the Ny-Ålesund Research Station. For the future, *in situ* and visual measurements are planned to be regularly complemented or even (partly) substituted by satellite observations. Satellite remote sensing with a higher resolution and more frequent coverage (e.g. with the new ESA Sentinel satellites) promotes development of more accurate methods and tools to describe the sea-ice regime in Kongsfjorden.

3 Unanswered questions

Current monitoring is limited in temporal and spatial resolution. Local information on atmospheric and oceanic forcing is also limited. Further changes of the fast-ice evolution might lead to new and not yet observed scenarios, where new processes and feedbacks could play a role.

The sea ice evolution in Kongsfjorden has been modelled with a 1-D process model (Wang et al. 2015), but not yet with a coupled regional model. Such work could improve the understanding of the observed changes.

4 Recommendation for future

The monitoring presented here started in 2003 and has resulted in a much better understanding of the seasonal evolution of landfast sea ice in Kongsfjorden, and how it varies and changes over time. Results have also contributed to several (partially interdisciplinary) process studies. The value of the time series is increasing the longer the series becomes. We recommend to continue the monitoring as a robust and affordable initiative. While keeping consistency in the methods, it can also help and improve the monitoring programme to introduce modern and autonomous technology. For example, experiments with automatic time-laps cameras have successfully been implemented. We further recommend to continue developing tools based on optical and radar satellite remote sensing for supporting the established monitoring methods. Finally, further development of a sea ice component in a coupled regional model could improve the understanding of changes and variability observed, and in return the observations may help to improve modelling of sea ice.

5 Data availability

Data from the described monitoring initiative are planned to be made available on data.npolar.no.

Acknowledgements

We are grateful to the personnel of the Norwegian Polar Institute in Ny-Ålesund Research Station for conducting ice observation and fast-ice thickness measurements in Kongsfjorden. Fast-ice monitoring in Kongsfjorden is a part of Norwegian Polar Institute's Svalbard programme. Validation experiments related to SAR satellite products were a part of "CIRFA" (Center for Integrated Remote Sensing and Forecasting for Arctic operations) funded by partners and the Research Council of Norway (CIRFA SFI grant no. 237906), OIBSAR (RCN project no. 280616) and the Fram Centre project "Mapping Sea Ice Characteristics relevant for Arctic Coastal Systems" in the Fram Centre Fjord and Coast Flagship. The combined atmosphere-sea ice study is a part of the work in the Transregional Collaborative Research Center "ArctiC Amplification: Climate Relevant Atmospheric and SurfaCe Processes, and Feedback Mechanisms (AC)³", funded by the Deutsche Forschungsgemeinschaft (DFG, German Research Foundation) – Projektnummer 268020496 – TRR 172.

References

Gerland S, Winther J-G, Ørbæk JB, Ivanov BV (1999) Physical properties, spectral reflectance and thickness development of first year fast ice in Kongsfjorden, Svalbard. Polar Res 18:275–282

Gerland S, Haas C, Nicolaus M, Winther J-G (2004) Seasonal development of structure and optical surface properties of fast ice in Kongsfjorden, Svalbard. Reports on Polar and Marine Research 492:26–34

Gerland S, Hall R (2006) Variability of fast-ice thickness in Spitsbergen fjords. Ann Glaciol 44:231-239.

Gerland S, Renner AHH (2007) Sea-ice mass balance monitoring in an Arctic fjord. Ann Glaciol 46:435-442

Johansson AM, Malnes E, Gerland S, Cristea A, Doulgeris AP, Divine D, Pavlova O, Lauknes TR (in press) Consistent ice and open water classification combining historical synthetic aperture radar satellite images from ERS-1/2, Envisat ASAR, RADARSAT-2, and Sentinel-1A/B. Ann Glaciol. https://doi.org/10.1017/aog.2019.52.

Negrel J, Gerland S, Doulgeris AP, Lauknes TR, and Rouyet L (2018) On the potential of hand-held GPS tracking of fjord ice features for remote-sensing validation. Annals of Glaciology. http://doi.org/10.1017/aog.2017.35

Nicolaus M, Haas C, Bareiss J (2003) Observations of superimposed ice formation at melt-onset on fast ice on Kongsfjorden, Svalbard. Phys Chem Earth 28:1241–1248

Nicolaus M, Haas C, Bareiss J, Willmes S (2006) A model study of differences of snow thinning on Arctic and Antarctic first-year sea ice during spring and summer. Ann Glaciol 44:147–153.

Pavlova O, Gerland S, Hop H (2019) Changes in Sea-Ice Extent and Thickness in Kongsfjorden, Svalbard (2003–2016). In: Hop H., Wiencke C. (eds.) The Ecosystem of Kongsfjorden, Svalbard. Advances in Polar Ecology 2. Springer, Cham

Peraza L, Semmling M, Falck C, Pavlova O, Gerland S, Wickert J (2017) Analysis of grazing GNSS reflections observed at the Zeppelin mountain station, Spitsbergen. Radio Science. 52, 1352–1362

Semmling M, Rösel A, Divine D, Gerland S, Stienne G, Reboul S, Ludwig M, Wickert J, Schuh H (2019) Sea Ice concentration derived from GNSS reflection measurements in Fram Strait. IEEE Trans. Geosci. Remote Sens. 57, 10350-10361

Wang C, Cheng B, Wang K, Gerland S, Pavlova O (2015) Modelling snow ice and superimposed ice formation on landfast sea ice in Kongsfjorden, Svalbard. Polar Research 34, 20828, http://dx.doi.org/10.3402/polar.v34.20828

Multidisciplinary research on biogenically driven new particle formation in Svalbard (SVALBAEROSOL)

Mikko Sipilä[1], Clara J. M. Hoppe[2], Angelo Viola[3], Mauro Mazzola[4], Radovan Krejci[5], Paul Zieger[5], Lisa Beck[1], Tuukka Petäjä[1]

1 Institute for Atmospheric and Earth System Research (INAR), University of Helsinki, Helsinki, Finland
2 Alfred Wegener Institute, Helmholtz Centre for Polar and Marine Research, Am Handelshafen 12, 27570 Bremerhaven, Germany
3 Institute of Polar Sciences, National Research Council of Italy, Via Fosso del Cavaliere 100, 00133 Rome, Italy
4 Institute of Polar Sciences, National Research Council of Italy, Via P. Gobetti 101, 40129 Bologna, Italy
5 Stockholm University, Svante Arrhenius väg 8, SE-11418 Stockholm, Sweden

Corresponding author: Mikko Sipilä, mikko.sipila@helsinki.fi,
ORCID-0000-0002-8594-7003

Keywords: Phytoplankton, dimethyl sulphide, secondary aerosol formation, cloud condensation nuclei, marine biology, atmospheric research

1. Introduction

1.1 Arctic change, clouds and climate

The climate and environment in the Arctic are changing faster than anywhere else on this planet (e.g. Mauritsen 2016). The warming climate is reflected in the decrease in snow cover, thawing of permafrost, changes in flora and fauna and decay and thinning of Arctic sea ice (e.g Overland and Wang 2013; Stroeve and Notz 2018). Sea ice loss further accelerates warming since the Arctic sea ice plays an important climatic role by reflecting solar light back into space. There is a positive feedback: when the ice melts, solar radiation is absorbed into and thereby heats the (darker) seawater and leads to increased melting. Melting of sea ice and other climate change effects influence also the marine ecosystem, including phytoplankton and their productivity (Wassmann and Reigstad 2011). As phytoplankton are also emitting biogenic vapours into the atmosphere (Levasseur 2013, Galí et al 2019), these changes may have consequences to atmospheric chemistry, secondary aerosol formation and clouds. An increase in phytoplankton productivity may thus lead to another feedback (negative or positive) that could mitigate or accelerate Arctic warming. The idea of increasing phytoplankton productivity with increasing temperature leading to a negative feedback via perturbations of cloud properties was first presented by Charlson et al. (1987). This so-called CLAW-hypothesis has also been strongly criticized (Quinn and Bates 2011). However, the Arctic system is highly complex and the sign of the feedback depends on many more variables (see below). Nevertheless, much more data are required before final conclusions on these mechanisms can be drawn.

Low-level clouds above Arctic sea ice and open waters play an important climatic role that is connected to the characteristics of the sea ice. Above highly reflecting ice surfaces, low-level clouds decrease the radiative cooling of the surface which keeps the ice warmer than it would be without clouds. This process reverses above dark surfaces, such as open seawater, where the reflectance of solar radiation by clouds cools the surface whenever the radiation intensity is sufficient (Tjernström et al. 2014). The formation of clouds depends on the prevailing meteorological conditions, but the optical properties of clouds are determined by both their micro- and macro-physical characteristics. The optical properties of clouds depend, among other variables, on the amount and properties of cloud condensation nuclei (CCN), which are aerosol particles with diameters larger than 20 nm. Cloud droplets are formed by water condensation on CCN. If the CCN concentrations are high, little water remains for each droplet leading to small but numerous cloud droplets, which makes the cloud highly reflective (Twomey et al. 1974). Small droplet size also increases the lifetime of the cloud (Albrecht et al. 1989). The sign and magnitude of any cloud feedback depends not only on aerosol properties and CCN concentrations but also on the height and geographical location of the cloud, time of the year and day, availability of water vapour, surface albedo

etc. Arctic clouds, in general, produce a cooling effect at the surface only in the summer while warming the Arctic surface for the rest of the year (Alterskjaer et al. 2010; Sedlar et al. 2011; Doscher et al. 2014; Intrieri et al. 2002; Shupe and Intrieri 2004). Addition of cloud nuclei can thus lead to cooling or warming of surface temperatures and therefore the overall effects of aerosol – cloud interactions in the Arctic currently remain highly uncertain. This report does not aim at describing the details of aerosol – cloud – climate interactions. However, these interactions and associated feedbacks – including those driven by sea ice loss – cannot be reliably solved, unless the mechanisms of how these CCN end up in the Arctic atmosphere are known. So, what is known?

1.2 Aerosols

Atmospheric aerosol particle diameters range from nanometers to micrometers. When particles are in the few nanometers scale, supersaturated water vapor cannot condense on them. When particles are larger than ~20 - 100 nm, water vapor (RH>100%) may condense on them, thereby growing the particles into cloud droplets. The lower end of the size range of CCN is not fixed, as it depends on atmospheric humidity and particle chemical composition as well as on concentration (availability) of potential CCN. In the clean Arctic environment particles as small as ~20 nm may act as CCN (Beck et al. unpublished data).

The sources of polar CCN are both natural and anthropogenic. In the High Arctic, anthropogenic particles are long-range transported from Europe, North America and East Asia (Stohl 2006). The main source of natural aerosols is the ocean. Marine aerosols constitute one of the most important natural aerosol systems, which contributes significantly to the Earth's radiative budget and biogeochemical cycling (O'Dowd and de Leeuw 2007). The primary particles released from the sea surface (as sea spray) mainly consist of sea salt by mass but contain also biogenic organic matter. The secondary marine aerosol is suggested to originate from phytoplankton-emitted dimethyl sulphide (DMS). Over ice covered oceans, secondary aerosol formation is connected also to iodine emissions. The role of oceanic biota in modifying marine aerosol formation remains one of the most important questions in estimating the climate forcing by aerosols (O'Dowd and de Leeuw 2007). In the Arctic, around the Svalbard Archipelago, frequent new particle formation (NPF) events have been linked to biogenic precursors released by open water and melting of sea ice regions (Dall'Osto et al. 2017). NPF from gas phase vapours is an important topic, since up to 90% of Arctic CCN are suggested to belong to this fraction (Merikanto et al. 2009). Anthropogenic pollution, mainly SO_2, may contribute to new particle production especially in the early spring during the transition from the Arctic haze period to clean, natural conditions. However, in this report we will limit our assessment to non-anthropogenic biogenic processes.

1.3 New particle formation (NPF) mechanisms in the Arctic

Atmospheric NPF is, in general, connected to a) emission of several precursor vapours, b) ionization of air by radon or galactic cosmic radiation, c) adiabatic cooling of airmasses during updraft leading to increased supersaturation of precursor vapours and d) the surface area of pre-existing aerosols which serve as a sink for precursor vapours needed for new particle formation. NPF starts with homogeneous nucleation of vapours where gas phase molecules stick to each other, or heterogenous ion-induced nucleation of vapours where gas phase vapours condense on top of an air ion (usually HSO_4^- - ion) due to ion-dipole interactions. In presence of sufficient amounts of supersaturated vapours, these approx. 1 nm clusters can grow up to CCN sizes in time scales of hours to days. While growing, these small particles suffer from continuous threat to be scavenged by pre-existing larger aerosol particles and therefore only a small fraction of the formed clusters ever reaches the CCN size. CCN formation is therefore highly sensitive to the availability of condensing vapours, as well as the surface area of pre-existing particles.

To understand the present and predict the future CCN concentrations and properties, the exact secondary aerosol formation pathways must be known. In many mid- or low latitude continental environments, secondary aerosol formation is likely driven by a cocktail of sulphuric acid (H_2SO_4) (Kulmala et al. 2013), ammonia (NH_3) (Kirkby et al. 2011), amines (Almeida et al. 2013, Yao et al. 2018), and highly oxidized organic molecules (HOM) (Ehn et al. 2014) from natural or anthropogenic VOC (Volatile Organic Compound) sources. In coastal areas, local aerosol formation from iodine oxyacids, especially iodic acid HIO_3 originating from macroalgae iodine emissions, produces vast concentrations of new particles (Sipilä et al. 2016). But what is known about Arctic polar aerosol formation?

1.3.1 Arctic aerosol formation and the role of phytoplankton DMS and bird colony NH_3

One of the first datasets on Arctic aerosol size distributions was recorded in late summer and early autumn 1991 during the International Arctic Ocean Expedition (IAOE-91) onboard the Swedish icebreaker Oden (Wiedensohler et al. 1996; Covert et al. 1996). Those datasets are the first to report the existence of a “nucleation” mode aerosol (<20 nm) indicating active NPF in the Arctic atmosphere. These studies also connect the appearance of these nucleation mode particles to oceanic emissions, potentially DMS. Since then several reports on observations of NPF have been published.

Giardi et al. (2016) used data collected at the Gruvebadet laboratory in Ny-Ålesund and found NPF to be frequent during spring and summertime. While in early spring, anthropogenic sulphur was observed in bulk aerosol, late spring and early summertime observations of aerosol phase methane sulphonate (MSA) suggested a strong influence of biogenic marine DMS emissions (MSA is a proxy for DMS, the oxidation of which leads to

the formation of H_2SO_4) in NPF or at least in particle growth to detectable sizes.

The role of DMS in secondary aerosol and NPF is generally well established. Ghahremaninezhad et al. (2016) performed measurements in the Arctic ocean and concluded that fine particles were mainly made of sulphate of biological origin showing the critical role of marine organisms, e.g. phytoplankton, for the formation of new particles in the summertime Arctic. Mungal et al. (2017) measured fluxes of DMS in the summertime Arctic (Baffin Bay between Greenland and Canada). As a result of airmass and chemical transport modelling, they concluded that though marine sources were dominant, there is a possibility that non-marine sources (e.g. lakes, melt ponds and tundra) could make additional contributions to atmospheric DMS concentrations. Further DMS data both from the atmosphere and from the sea water with larger spatial and temporal resolution are needed to resolve this issue. Park et al. (2017) analyzed atmospheric DMS concentrations, aerosol particle size distribution and aerosol chemical composition in Ny-Ålesund, Svalbard. They showed that the formation of submicron (secondary) aerosols was strongly correlated with the atmospheric DMS mixing ratio during the phytoplankton bloom period.

Besides availability of aerosol precursor vapours or gases, such as DMS, the formation of new particles is strongly connected to properties of pre-existing aerosols. Data collected from Alert (Nunavut, northern Canada) shows that NPF is frequent in the summertime Arctic and associated with a low condensation sink (pre-existing aerosol surface) (Leaitch et al. 2013). Tunved et al. (2013), based on data taken at the Zeppelin station, Ny-Ålesund, also showed that NPF events associated with marine airmasses are a rather common phenomen on in the Arctic during summer, which result from both photochemical production of particle precursor vapours and low condensation sinks. Furthermore, Croft et al. (2016) confirmed that NPF during summer time in the Arctic is associated with efficient wet removal of larger pre-existing aerosol allowing the condensable vapour concentrations to reach the levels needed for efficient NPF and growth. Authors call for further research on cloud scavenging and wet removal of aerosols as well as NPF to reduce uncertainties in aerosol-cloud-climate coupling in the Arctic.

Dall'Osto et al. (2017) investigated the role of sea ice extent NPF by analysing 11 years of aerosol size distribution data from the Zeppelin observatory next to Ny-Ålesund. They found that NPF occurred in 18% of the days with a peak of 51% during the summer months. They suggested that these events are connected to biogenic precursors gases released from regions with open water and/or melting sea ice. They also showed that NPF is anti-correlated with sea ice extent, suggesting the open ocean as a primary source of new particle precursor gases. Furthermore, they demonstrate a more than 20% increase in CCN concentrations due to NPF and suggest that melting sea ice via accelerated new particle and CCN formation may have already accelerated Arctic warming (i.e. they assume positive feedback). In a follow-up work, Dall'Osto et al. (2019) analysed simultaneously collected

data from Zeppelin and two additional high Arctic sites during a 3-year period (2013–2015) – Gruvebadet in Ny-Ålesund and Villum Research Station at Station Nord, Greenland. Their analysis shows that NPF occurred in 16% - 32% of the days. The authors suggest that lower ultrafine aerosol concentrations at the Greenland site in comparison to the Svalbard sites are indicative of less efficient NPF due to longer time periods of consolidated pack ice in Greenland. Conclusions regarding the role of sea ice in suppressing aerosol formation are highly convincing but authors still state that it is imperative to continue strengthening international scientific cooperation to address these research questions beyond a singular station or measurement events. Data collected from Alert, Nunavut, northern Canada also shows that NPF is frequent in the summertime Arctic and associated with a low condensation sink (Leaitch et al. 2013). The authors show that NPF is connected with the presence of MSA, which points toward emissions of DMS, and possibly other organic precursors as a primary driver of NPF.

Leaitch et al. (2013) assessed the increase in CCN and cloud droplet number concentrations (CDNC) due DMS-related new particle formation. They show that increases in CDNC can be as high as 23–44 cm^{-3}, which would remarkably modify the Arctic summer shortwave cloud albedo. Their study unambiguously shows that secondary aerosol formation is a highly important phenomenon in the clean summertime Arctic environment. All in all, DMS clearly seems to be important for Arctic aerosol formation, CCN concentrations and cloud properties. But how?

In the atmosphere, DMS is oxidized by OH-radicals to MSA and SO_2. SO_2 further reacts with OH to produce H_2SO_4, which is known to be responsible for particle formation in multiple environments over the globe. H_2SO_4 molecules, however, do not stick to each other and any clusters would evaporate immediately, therefore stabilizing compounds are required for nucleation. Water can stabilize nucleating clusters in cold temperatures (Kirkby et al. 2011) relevant for the upper troposphere, but unlikely in close to zero degrees Celsius temperatures of summertime Arctic. Ammonia, on the other hand, would stabilize small clusters far better than water and minute, sub-100 pptv concentrations can enhance the rate of NPF by several orders of magnitude (Kirkby et al. 2011; Dunne et al. 2016). Ammonia measurements in the concentrations required to catch the particularly low Arctic levels are, however, almost non-existent. Wentworth et al. (2016), measured ammonia in Baffin Bay and the eastern Canadian Arctic Archipelago and found concentrations between 40 - 870 pptv. Such concentrations would be sufficient to enhance particle formation rates by a factor of approx. 100 (40 pptv) – up to over 1000 (870 pptv) in H_2SO_4-limited conditions (H_2SO_4 < few 10^7 molecules cm^{-3}), which is the case in most parts of the world (in Antarctica, the closest point of comparison, the maximum recorded values are in the range of 2×10^7 molecules cm^{-3}, Jokinen et al. 2018). Wentworth et al. (2016) suggest sea-bird colonies as a primary source of ammonia. Simulations that account for colonies suggest ammonia concentrations from few pptv to few hundreds of pptv that contribute strongly to new

particle and CCN formation around the Svalbard archipelago (Croft et al. 2016). However, due to sparseness of data and difficulties related to ammonia measurement techniques, a proper assessment would require more data on ammonia concentrations with better spatial and temporal resolutions around the whole Arctic.

Another open question concerns the role of MSA in the formation and growth of sub-CCN aerosols. MSA is found in bulk aerosol samples (e.g. Park et al. 2017), but analysis of bulk hardly tells anything about the composition of particles in the sub-50 nm size range. As the measurements of chemical composition of Arctic low concentrations of sub-50 nm particles are either extremely challenging or impossible, concurrent measurements of gas phase MSA and particle growth rate, or the measurement of aerosol hygroscopicity or volatility would provide indirect evidence of whether MSA contributes to the growth of small particles or not.

1.3.2 Phytoplankton, DMSP production and DMS emissions

Arctic DMS (dimethylsulphide) emissions increased by 33% in the past decade (Galí et al. 2019). This trend is mostly explained by the reduction in sea-ice extent and the extrapolation to an ice-free Arctic summer could imply up to 3.6-fold increase in DMS emissions compared to present emissions (Galí et al. 2019). Such a change, if reflected in H_2SO_4 and MSA concentrations, would largely influence new particle and CCN production in the Arctic. DMS, which represents the main source of biogenic sulphur emissions (Liss et al. 1997), is produced by the degradation of dimethylsulfoniopropionate (DMSP). DMSP itself is produced by marine algae for osmoregulation, and may also have other important cellular functions (e.g. as an antioxidant or cryoprotectant; Sunda et al. 2002; Stefels et al. 2007). DMSP is released from the algae primarily as a result of grazing or virus-induced lysis of the cells, and cleaved to DMS via bacterial degradation (Curson et al. 2011). After its release, DMSP is consumed by bacteria, depending on the degradation pathway either via the release of DMS or the usage of both carbon and sulphur (Kiene et al. 2000). Thus, the interplay of microbial production and consumption rates together with air-sea exchange processes influence the measurable DMS and DMPS concentrations in seawater.

A number of studies have shown the general correspondence of DMS/DMSP and chlorophyll-a in the marine environment (Challenger and Simpson 1948; Trevena and Jones 2006 and 2012; Uhlig et al. 2019; Jarníková et al. 2018). However, not all marine algae are capable of producing DMSP and production varies between taxonomic groups. Dinoflagellates as well as prymnesiophytes (e.g. the important colony-forming *Phaeocystis* spp.) producing the highest, and diatoms as well as prasinophytes (e.g. the picoplankter *Micromonas* spp.) producing rather low amounts of DMSP (Keller et al. 1989; Stefels et al. 2007). In polar regions, also sea ice algae make an important contribution (Kirst et al. 1991; Uhlig et al. 2019). The quantification of the contribution of different marine algae and their

associated bacteria to DMSP and DMS emissions are key in understanding the factors affecting DMS emissions in the Arctic. Despite differences between taxonomic groups, also physiological adjustments have an impact on microalgal DMSP production. As reviewed by Stefels et al. (2007), potential stressful conditions such as a strong increase in salinity or irradiance or very cold temperatures have been found to increase cellular DMSP levels in different phytoplankton, while effects of nutrient limitation are complex and still not fully understood. Therefore, impacts of the multiple drivers that are concurrently changing under climate change are not straight-forward to predict. There is evidence that DMS production by phytoplankton decreases with ongoing ocean acidification (Hussherr et al. 2017) even though Arctic phytoplankton species composition and primary production have been shown to be rather resistant towards acidification (Hoppe et al. 2018). Understanding how the interplay of processes affecting the timing, taxonomic composition and physiological state of phytoplankton blooms around Svalbard (Hegseth et al. 2019; Hoppe et al. (unpublished data)) will affect DMS emissions and aerosol formation will require coordinated oceanographic, biological and atmospheric observations. The Ny-Ålesund research station provides ideal conditions for such an endeavour.

1.3.3 Recent update: Iodine emissions and aerosol formation

Besides DMS, iodine emissions have been recently identified as a source of aerosol precursor vapours. Iodine chemistry in general plays important roles in atmospheric chemistry, including ozone and mercury depletion in the polar troposphere (Saiz-Lopez and von Glasow 2012; Simpson et al. 2015). Very recently, Sipilä et al. (2016) measured high concentrations (up to 10^8 molecules cm^{-3}) of iodic acid (HIO_3) in spring time northern Greenland (Villum Research station) associated with NPF events. By direct measurements of the chemical composition of the nucleating clusters, they suggested that particle formation proceeds via sequential addition of HIO_3 molecules, i.e. homogenous unimolecular nucleation of HIO_3, possibly followed by subsequent conversion to I_2O_5 in clusters and recycling of water. However, the exact formation pathways of HIO_3 in the atmosphere are not known, and neither are the iodine-containing precursors. The primary candidate here is I_2, which is photolyzed to two iodine radicals which subsequently react with ozone, leading to the formation of IO. Pathways from IO to HIO_3 are under intensive research with no conclusion yet. But where does iodine come from?

Due to limited knowledge, we now need to have a wider perspective to understand the possible sources and focus not only on the Arctic but both polar areas. Studies have shown that inorganic iodine compounds (i.e. iodide monoxide (IO) and molecular iodine (I_2)) are abundant in the ice-covered polar regions; especially during spring. Saiz-Lopez et al. (2007a) measured a peak of 20 ppt of IO during the springtime in Halley station, Antarctica. Satellite observations confirmed the presence of widespread IO, with the highest concentration observed over the ice-covered seas around Antarctica (Saiz-Lopez et al. 2007b; Schönhard

et al. 2012; Atkinson et al. 2012). Atkinson et al. (2012) suggested that I_2 is most likely the precursor for IO, as they concurrently observed significant levels of I_2 (up to 31 ppt) above the surface snow and sea ice in Antarctica. In the Arctic, Mahajan et al. (2010) reported IO concentrations up to 3.4 ppt at a sea ice edge site in Hudson Bay, Canada and Raso et al. (2017) measured 0.3-1.0 ppt of I_2 in the Arctic atmosphere during spring time. Although there is a clear indication of iodine chemistry in the polar atmosphere, the source of inorganic iodine has not been clarified yet. Also, there is a significant difference in iodine emission between Antarctic and Arctic sea ice. This is probably associated with the fact that Antarctic ice is thinner, while in the Arctic multiyear thick ice is still more abundant. Thick ice prevents solar radiation to penetrate underneath the ice, and disables phytoplankton to bloom and produce significant amounts of iodine compounds (Nicolaus et al. 2012). Besides losing its areal coverage, Arctic sea ice is also thinning fast and losing multiyear ice, iodine emission rates therefore may increase in the future (Cuevas et al. 2018).

It is widely known that inorganic iodine can be produced by photochemical reactions of biogenic iodocarbons emitted from the ocean and ozone deposition to the open sea surface (Vogt et al. 1999, O'Dowd et al. 2002, Carpenter et al. 2012; MacDonald et al. 2014). Recent studies have highlighted the relationship between inorganic iodine compounds and polar sea ice as well as snow/ice covered regions in Antarctica (Spolaor et al. 2013; Granfors et al. 2014; Vallelonga et al. 2017), which may occur also in the Arctic. It was suggested that iodine emissions are attributed to the production of iodide (I^-) and hypoiodous acid (HOI) by microalgae (e.g. pennate diatoms, dinoflagellates, flagellates) growing underneath or within the sea ice, and then being emitted to the atmosphere by permeation through the porous ice or fractures in the thin sea ice pack or due to melting of sea ice during the summer (Atkinson et al. 2012; Saiz-Lopez et al. 2015).

The snowpack can be another source of iodine emissions. High concentrations of iodine were found to be confined within the snowpack during wintertime and being released to the atmosphere through the photochemistry-induced re-mobilisation of iodine from the snowpack in the summer in Antarctica (Frieß et al. 2010; Spolaor et al. 2014). The emission mechanism is currently unclear, but could be potentially due to the accelerated (photo-)oxidation of iodide in ice/snow (Kim et al. 2016; Watanabe et al. 2019) and/or the photolysis of iodate in frozen salt (Gálvez et al. 2016). In the Arctic, whether the iodine compounds are primarily emitted from the open ocean (Mahajan et al. 2010) or from ice/snow covered regions still remains an open question, although a recent field observation by Raso et al. (2017) points out that the snowpack can be a source of I_2 to the Arctic boundary layer.

Despite many open questions related to the sources and the exact chemical nature of iodine emissions, iodine is likely becoming more and more important in atmospheric chemistry and especially for understanding aerosol formation. Measurements from the RECAP ice-

core (East Greenland) show that concentrations of atmospheric iodine have tripled (!) in the northern hemisphere within the past decades (Cuevas et al. 2018). They suggest that this increase is driven by anthropogenic ozone pollution and the thinning of Arctic sea ice, the latter resulting in enhanced phytoplankton productivity underneath the ice. Systematic measurements of gas phase iodine species would be required to resolve this question.

1.3.4 What is the role of volatile organic compounds (VOC) in Arctic aerosol formation?

As stated earlier, highly oxidized organic molecules (HOM, e.g. Ehn et al. 2014) from natural or anthropogenic VOC sources are highly important constituents and drivers of NPF and globally main constituents of secondary aerosol (Jimenez et al. 2009). In certain conditions and concentrations, HOM may even nucleate without H_2SO_4 or other inorganic species (Kirkby et al. 2016). Whether that is the case in Svalbard, or Arctic in general, is not known. At a coastal Antarctic site, more than a thousand kilometres away from the nearest macroscopic land vegetation, peat lands or thawing permafrost (i.e. Sandwich islands), no indication of HOM was obtained (Jokinen et al. 2018). However, Arctic tundra flourishes in summertime, vegetation forms peat, and soils are in places rich in organic matter. Arctic tundra has been thus recognized as a source of VOC (Lindwall et al. 2016). Further, field measurements in Greenland indicates that thawing permafrost releases VOCs (Kramshøj et al. 2018).

The sea surface microlayer has also been recognized as source of Arctic VOC (Mungal et al. 2017). Another, surprising source of (oxidized) VOC is the photochemically active snowpack. OVOCs like acetaldehyde and acetone have been measured in the snowpack of Alert, Nunavat, Canada (Guimbaud et al. 2002; Houdier et al. 2002). Styrene fluxes have also been measured in the snow pack in Alert, indicating it to be a potential contributor of VOCs (Kos et al. 2014). Formic and acetic acid fluxes have also been measured in the snowpack of Greenland and the South Pole (Dibb and Arsenault 2002). These VOC, may or may not be converted to HOM in the gas phase oxidation reactions with potential consequences to Arctic NPF and especially to growth to CCN. Experimental evidence is, however, largely lacking, though studies have also been extended from the mere quantification of VOCs to the measurement of the oxidation products of biogenic volatile organic compounds (isoprene, monoterpenes, and sesquiterpene) in the Canadian High Arctic (Fu et al. 2009).

Figure 1 summarizes the known and speculated sources of volatile species, their oxidation processes, resulting aerosol precursors, the conversion of these precursors to small clusters by nucleation, and further growth to climatically relevant CCN sizes by condensation.

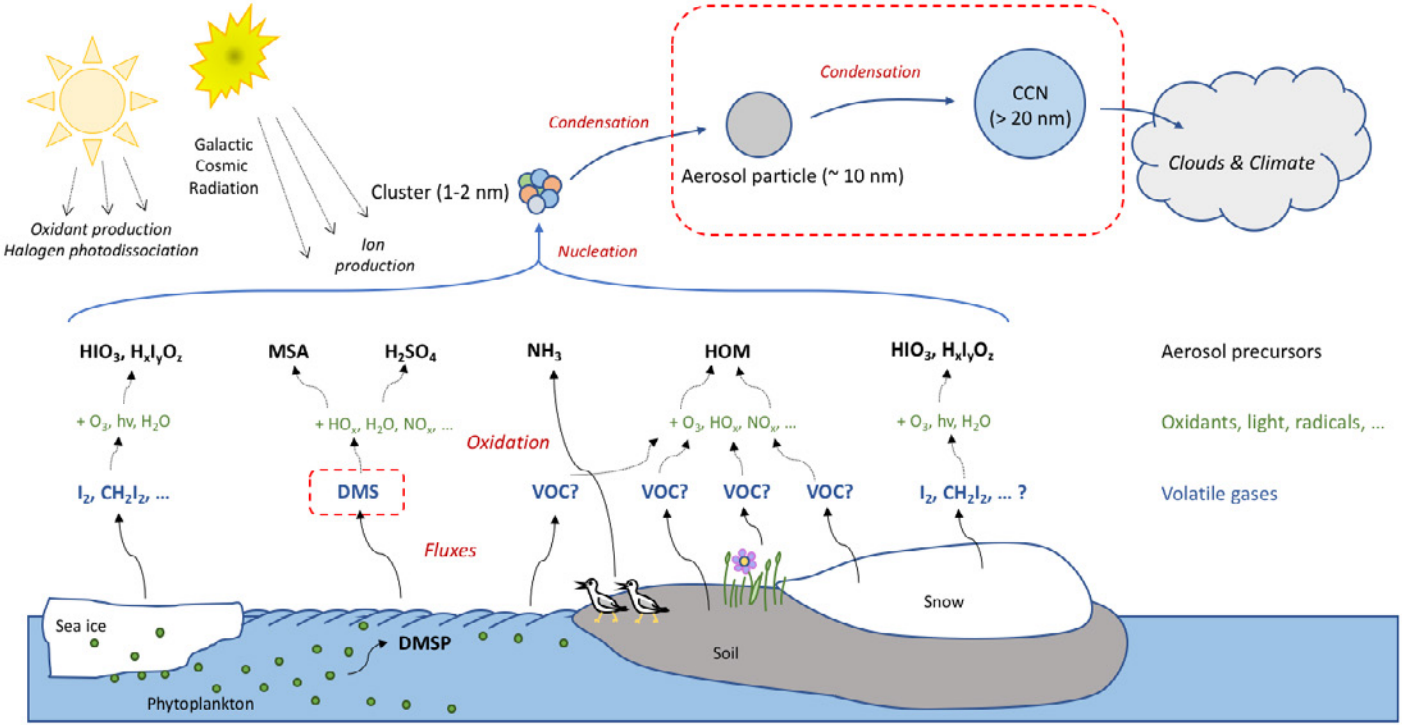

Figure 1: Simplified scheme of potential processes leading to secondary aerosol formation in Svalbard. Almost none of the relevant quantities and compounds – including all condensable aerosol precursor vapours – are systematically measured today.

1.4 Novel technology that allows resolving and monitoring NPF processes

1.4.1 Atmospheric monitoring of vapours and small particles

In this chapter, we discuss a novel measurement technology with which a deep insight in aerosol formation in Svalbard and elsewhere in the Arctic could be obtained and with which a systematic long-term monitoring programme, necessary for observing the changes in highly sensitive processes associated with NPF, could be carried out. This type of technology and methods are also suggested among others in chapter 4 "Recommendations" to be promoted for long-term monitoring in Svalbard.

Since there are no data available from Svalbard that we could use in this report for enlightening the potential of these methods, we discuss the technology in light of exemplary data collected from the other side of the planet, the Finnish Antarctic Research Station Aboa, Queen Maud Land, eastern Antarctica. Out of all sites where freely available data exist, Aboa is climatically the most similar to Svalbard. Like Svalbard, the Aboa station is in the vicinity of a plankton-rich ocean, as well as sea ice and coastal bird colonies (in this case primarily penguins). Result from this site therefore may, to some extent, reflect also the atmospheric processes in the Svalbard region. The main difference between Aboa and Svalbard is that there is no macroscopic vegetation nearby Aboa, and that the flora is only represented by some cyanobacteria and other unicellular species in the summertime meltwater ponds. Climate at Aboa is colder, even though Aboa is located further away from the pole at 73°03′S while Svalbard (Ny-Ålesund) lays at 78°55′N. In general, the surroundings of Svalbard are becoming more and more marine, while the same is not true for the Aboa region. Summertime UV-radiation at Aboa is also much stronger due to the ozone hole and ubiquitous reflecting glaciers. Despite the differences, Aboa is still climatically the closest point of comparison where data exist and the processes observed there may provide indications on processes taking place in Svalbard. Data were collected in 2014-2015 summer season and are partly published by Jokinen et al. (2018).

The core of the measurement setup comprised a Differential Mobility Particle Sizer (DMPS) – which is essentially the same instrument as a Scanning Mobility Particle Sizer (SMPS) currently operated at the Gruvebadet laboratory and Zeppelin Observatory in Svalbard, a Neutral cluster and Air Ion Spectrometer (NAIS, manufactured by Airel Ltd, Asmi et al. 2009), a Particle Size Magnifier (PSM, manufactured by Airmodus Oy/Ltd, Finland, Vanhanen et al. 2011), an Atmospheric Pressure interface - Time-of-Flight mass spectrometer (APi-TOF, manufactured by TofWerk A.G. Switzerland, Junninen et al. 2010) and a nitrate ion Chemical Ionization APi-TOF (CI-APi-TOF, Jokinen et al. 2012). The DMPS was used to measure aerosol size distribution between 7 nm and 800 nm. The NAIS was used for recording the size distribution of naturally charged ion clusters and particles in the size range of 0.8 to

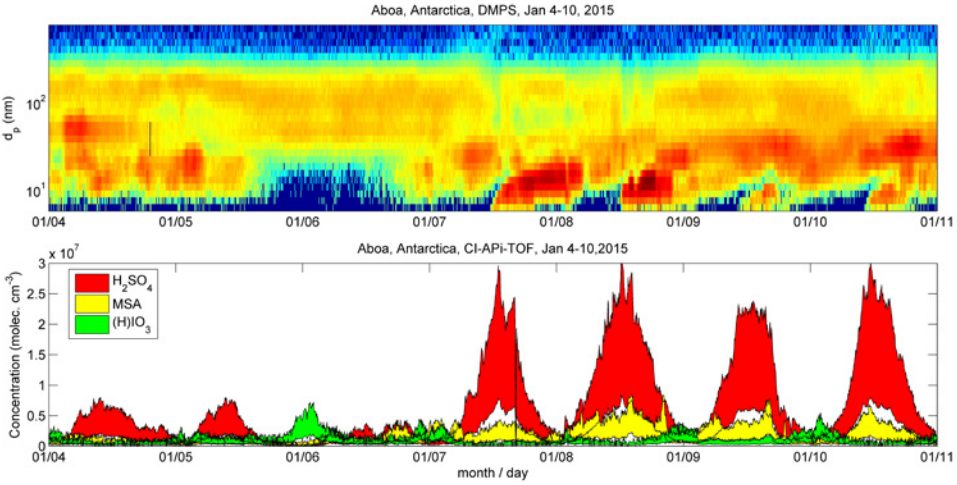

Figure 2: The upper panel shows a 1-week time series of aerosol size distribution data collected by a differential mobility particle sizer at the Finnish Antarctic Research Station Aboa. Aerosol formation in this case coincides with very high sulphuric acid (H_2SO_4) concentrations. Also, MSA concentrations are elevated in comparison to non-event time periods. Iodic acid (HIO_3), which is an important aerosol precursor at least in northern Greenland, next to sea ice, shows no correlation with particle formation at Aboa. Simultaneous measurements of aerosol size distributions and particle precursor vapours are the first step towards understanding the formation mechanisms of new particles.

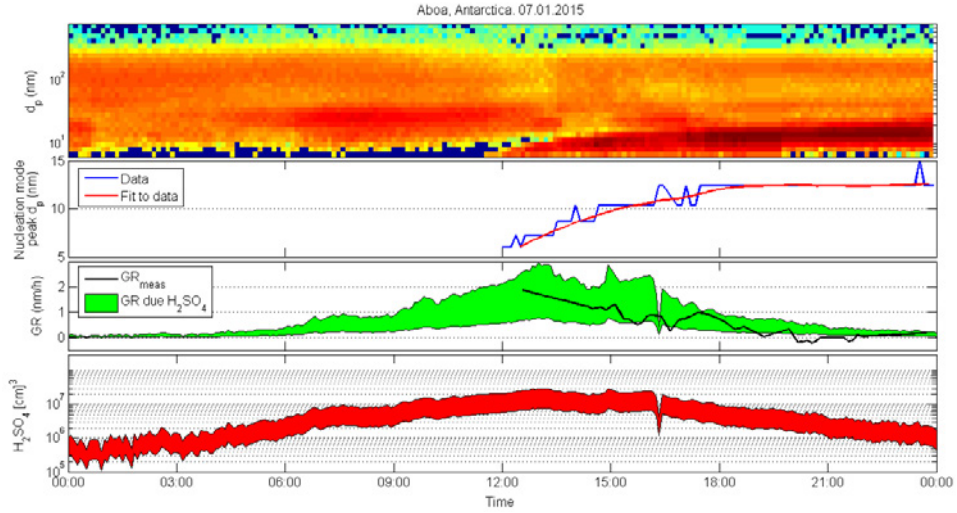

Figure 3: Measurements of condensable precursor vapours and aerosol growth rate enables conceptually resolving the aerosol growth mechanism. Here, the peak of nucleation mode is measured from the DMPS data (2nd panel) and from the time evolution of the peak, the growth rate is derived (3rd panel). Condensation due to sulphuric acid can be calculated (Nieminen et al. 2010) from measured sulphuric acid concentrations (4th panel) assuming irreversible condensation (typically a well justified assumption in case of sulphuric acid (Kirkby et al. 2011)). In this case, measured and calculated growth rates agree well (3rd panel) suggesting that sulphuric acid is the primary condensing species.

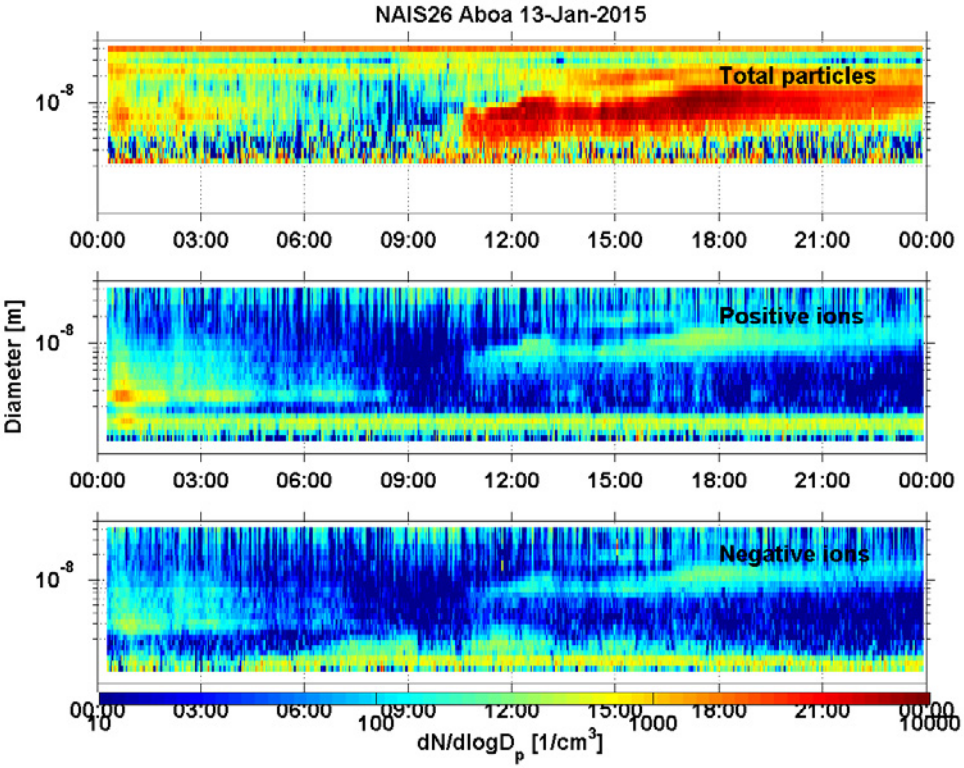

Figure 4: More insight in the initial steps of new particle formation, the nucleation process, can be obtained by measurements of negative and positive ion size distributions, together with the total aerosol size distribution by means of the Neutral cluster and Air Ion Spectrometer (NAIS). It should be noted that NAIS is capable of detecting neutral (total) particles reliably only above diameters of approx. 2-3, while ion detection can be extended down to molecular ~1 nm sizes. The figure illustrates that in the morning with increasing radiation, small negative omnipresent cluster ions start to grow. This is seen as an increased signal in the size range of 1.5 – 2.5 nm. Positive cluster ions do not grow, suggesting that, in this case, particles form by negative ion – induced nucleation (Kirkby et al. 2011).

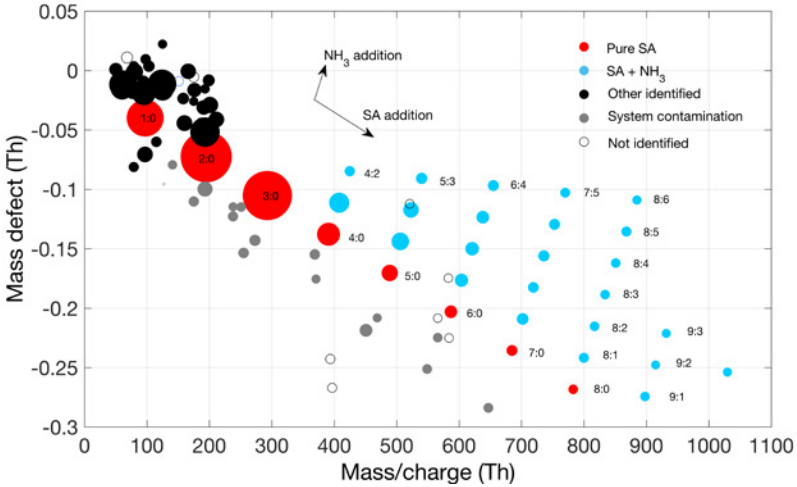

Figure 5: If initial clusters form by ion-induced nucleation, their chemical composition can be determined using an Atmospheric Pressure interface – Time-Of-Flight mass spectrometer (APi-TOF). This example has been recorded during intensive particle formation and depicts an observed mass spectrum. The mass defect is the difference between the measured (exact) mass and the integer mass defined by the sum of protons and neutrons in the atomic nuclei of molecules in the cluster and it's used together with the isotopic distribution for an accurate identification of the atomic composition. Here, both pure sulphuric acid (SA) clusters (red) and sulphuric acid – ammonia (SA-NH_3) clusters (blue) are dominating the mass spectrum during the event, together with above discussed data, suggesting that aerosol nucleation takes place via ternary sulphuric acid – ammonia – water negative ion-induced nucleation. Water is lost from the clusters in the sampling process, but laboratory experiments suggest that water contributes to cluster formation (Kirkby et al. 2011).

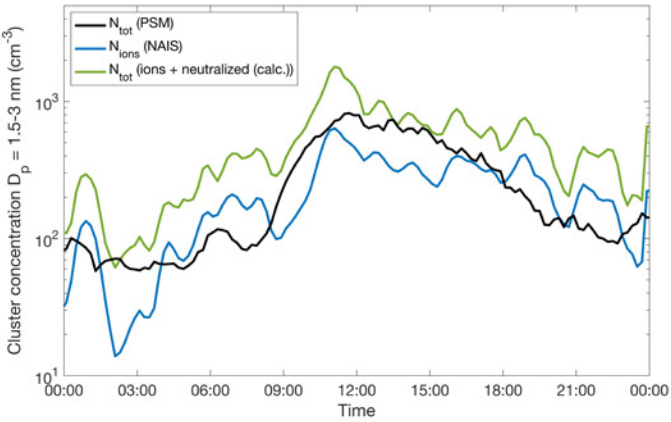

Figure 6: Simultaneous measurements of ion (blue, NAIS) and total cluster concentrations (black, PSM) suggest that, in this case, particle formation is dominated by ion induced nucleation. From the measured ion cluster concentrations, the fraction of ion clusters that are neutralized during the cluster growth by collisions with the ions of opposite polarity can be accounted for by assuming the resulting neutral clusters are stable (green). In environments where neutral nucleation mechanism dominates (e.g. Kulmala et al. 2013; Sipilä et al. 2016), total concentration is typically clearly higher.

40 nm and neutral particles from approx. 3 to 40 nm. The PSM was used for measuring the total concentration of clusters/particles between 1.5 and 3 nm in diameter. The APi-TOF recorded the mass spectrum of naturally charged ion clusters (negative/positive) in the mass range of 50 to 1200 Th while the CI-APi-TOF was deployed to measure concentrations of potential particle precursor vapours, including H_2SO_4, MSA, HIO_3 and a variety of extremely low vapour pressure HOM. Out of potential aerosol precursors, concentrations of bases (ammonia, amines) were not measured, because sensitive enough technology for measuring predicted low concentrations of relevant bases does not exist. H_2SO_4, MSA, HIO_3 and HOM can be measured by CI-APi-TOF with high sensitivity, with lowest limit of detection (LOD) below 10^5 molecules cm^{-3} (1 part per quadtrillion, 0.001 ppt, Jokinen et al. 2012). Typical methods for e.g. ammonia detection can hardly reach 100 ppt, which is not sufficient in pristine clean environments. However, the presence of ammonia can be confirmed from ion cluster chemical composition measurements by APi-TOF and concentration can be indirectly estimated e.g. by comparison of measured cluster distribution to cluster distributions obtained from laboratory experiments (e.g. Kirkby et al. 2011).

Data collected from Aboa are summarized in Figures 2-6. Figure 2 depicts a 1-week time series of aerosol size distribution data. Aerosol formation in this case coincides with very high H_2SO_4 concentrations. Also, MSA concentration is elevated in comparison to non-event time periods. HIO_3, which is an important aerosol precursor at least in northern Greenland, next to sea ice, shows no correlation with particle formation at Aboa. Simultaneous measurements of the aerosol size distribution and particle precursor vapours are the first step toward understanding the formation mechanisms of new particles. Measurements of condensable precursor vapours and aerosol growth rate enable conceptually resolving the growth mechanism of aerosols as shown in Figure 3. Here, the peak of nucleation mode is measured from the DMPS data (2nd panel), and the growth rate is derived from the time evolution of the peak (3rd panel). Condensation due H_2SO_4 can be calculated (3rd panel) (Nieminen et al. 2010) from measured H_2SO_4 concentrations (4th panel) assuming irreversible condensation (typically a well justified assumption in case of H_2SO_4 (Kirkby et al. 2011)). In this case, measured and calculated growth rates agree well (3rd panel) suggesting that H_2SO_4 is the primary condensing species.

More insight in the initial steps of NPF, i.e. the nucleation process, can be obtained by measuring negative and positive ion size distributions, together with the total aerosol size distribution by NAIS (Figure 4). It should be noted that NAIS is capable of detecting neutral (total) particles reliably only above approx. 2-3 nm in diameter, while ion detection can be extended down to molecular ~1 nm sizes. The figure illustrates that in the morning with increasing radiation, small negative omnipresent cluster ions start to grow. This is seen as an increased signal in the size range of 1.5 – 2.5 nm. Positive cluster ions do not grow, suggesting that, in this case, particles form by negative ion – induced nucleation (Kirkby et al. 2011). If initial clusters form by ion-induced nucleation, their chemical composition

can be determined using an APi-TOF. The example shown in Figure 5 was recorded during intensive particle formation and depicts an observed mass spectrum. The mass defect is the difference between the measured (exact) mass and the integer mass defined by the sum of protons and neutrons in atomic nuclei of molecules in the cluster, which are used together with the isotopic distribution for accurate identification of atomic composition. Here, both pure H_2SO_4 (SA) clusters (red) and H_2SO_4– ammonia (SA-NH_3) clusters are dominating the mass spectrum during the event, together with above discussed data suggesting that aerosol nucleation takes place via ternary H_2SO_4 – ammonia – water negative ion-induced nucleation. Water is lost from the clusters in the sampling process, but laboratory experiments suggest that water contributes to the cluster formation (Kirkby et al. 2011).

To draw conclusions on whether the ion-induced pathway dominates the new particle formation, simultaneous measurement of the concentrations of ion (blue, NAIS) and total clusters (black, PSM) are needed. The result of such measurements is shown in Figure 6, suggesting that in this case particle formation is dominated by ion induced nucleation since the total cluster concentration does not significantly exceed ion cluster concentrations. From the measured ion cluster concentration, the fraction of ion clusters that are neutralized during the cluster growth by collisions with the ions of opposite polarity can be accounted for by assuming the resulting neutral clusters are stable (green). In environments where the neutral nucleation mechanism dominates (e.g. Kulmala et al. 2013; Sipilä et al. 2016), the total concentration is typically much higher.

The above discussed measurements are needed also in Svalbard in order to resolve and monitor the mechanisms of NPF in the Arctic.

1.4.2 Monitoring of phytoplankton

However, despite the capacity to resolve and monitor the concentrations of aerosol precursor vapours and detailed molecular steps of new particle formation, atmospheric measurements alone are insufficient for an holistic understanding of the associated biosphere – atmosphere interactions. In order to increase our understanding on the controls of microalgal composition and productivity, we depend on observational long-term monitoring projects such as the moorings deployed in Kongsfjorden (Cottier et al. 2018) in combination with a mechanistic understanding of certain key processes that can only be investigated by carefully designed campaigns and experimental approaches (e.g. Hoppe et al. 2018). In the future, optimized algorithms for Arctic coastal retrieval of remote sensing-based ocean colour may provide a powerful tool to increase our understanding of temporal and spatial dynamics in aerosol production by Arctic microalgae.

Furthermore, investigations on emissions of biogenic vapours from terrestrial ecosystems - soil and tundra vegetation - would be required to understand the role of volatile organic

compounds in the processes leading to new particle and, in general, secondary aerosol formation.

2. Overview of existing research and knowledge in Svalbard

Only few key measurements relevant for understanding NPF and monitoring quantities connected with secondary aerosol formation are systematically recorded in Svalbard. Aerosol size distribution and new, >10 nm, particle formation is currently measured on a long-term basis by SMPS systems at the Gruvebadet laboratory and Zeppelin Observatory

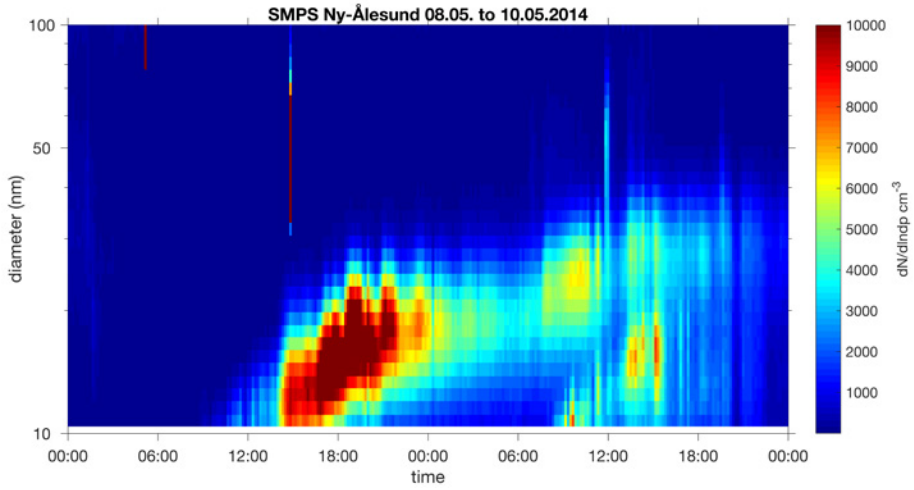

Figure 7: Typical aerosol formation event as measured by SMPS system in Gruvebadet, Ny-Ålesund during the phytoplankton bloom period in May.

in Ny-Ålesund. Simplified, SMPS is an instrument that charges sampled aerosol particles and classifies them according to their electrical mobility (which can be converted to particle diameter) and counts the classified particles one by one by means of a condensation particle counter (CPC). In a CPC, particles are exposed to supersaturated (usually) butanol vapour. Vapour condenses on particles growing them to optically detectable sizes after which they are counted based on the signals from scattered light of a laser beam.

Figure 7 shows an example of aerosol size distribution data collected in Gruvebadet laboratory during the phytoplankton bloom period. In this case, the measurements are performed from 10 nm up to 450 nm. Aerosol formation starts from molecular sizes of approx. 1 nm, therefore the SMPS system is blind to the initial steps of particle production

and weaker formation events, when particles do not reach the 10 nm detection threshold, are not recorded. At the Zeppelin observatory, aerosol measurements start from 3 nm sizes, but no long-term measurements on <3 nm particles, that would be critical for understanding the initial steps of new particle formation, are carried out in a systematic manner. Figure 2 depicts data from a longer period (1st April to 15th August 2014). Here, anthropogenic air pollution, Arctic haze, is seen as an abundancy of 100-300 nm particles during April. Intense NPF starts in the beginning of May and continues at least until the end of the measurement period. Earlier reports that focus on NPF in Svalbard utilizing data collected in Zeppelin and Gruvebadet include those by Ström et al. (2003), Ström et al. (2009), Tunved et al. (2013), Giardi et al. (2016), Lupi et al. (2016), Dall'Osto et al. (2017) and Dall'Osto et al. (2019), discussed above.

Out of the atmospheric vapours and gases responsible for the production of aerosol or aerosol precursor vapours, DMS is monitored on a semi-continuous manner in Zeppelin observatory by The Korea Polar Research Institute (KOPRI) and ozone is monitored by NILU. Neither DMS nor ozone is measured at Gruvebadet. None of the potential aerosol precursor vapours – H_2SO_4, MSA, HIO_3, HOMs (hundreds of compounds) and ammonia (NH_3) – has

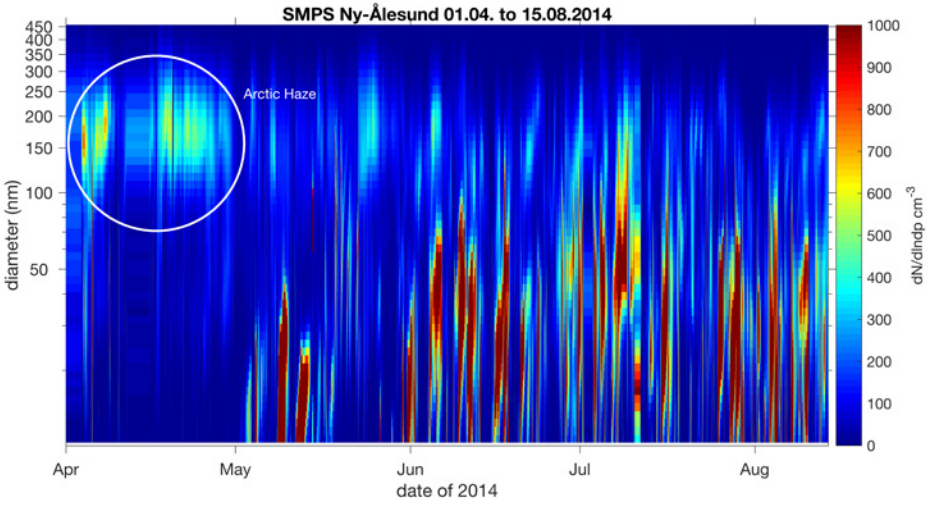

Figure 8: Aerosol formation continues intensely until the end of the measurement period in mid-August suggesting that besides phytoplankton activity, other sources of particle precursor vapours exist. Only measurement of gas phase vapours would reveal the nature of condensing species and give hints regarding the potential source of these vapours.

been monitored anywhere in Svalbard before recent proof-of-concept experiments at Gruvebadet laboratory, conducted in collaboration with the University of Helsinki and CNR, Italy in March – August 2017. The study deployed APi-TOF, NO_3^- -CI-APi-TOF, NAIS, PSM and SMPS sensors. The study has continued with a limited setup since April 2018. Those experiments are also the first deploying instrumentation for sub-3 nm particles in Svalbard. Data from these studies are not yet available though, and cannot be analysed or discussed here. Nevertheless, these are campaign type measurements and will not serve as a long-term monitoring program unless continued.

It is notable that, while the high phytoplankton biomass from the spring bloom in the Arctic ocean and North Atlantic usually starts to decay in May or June (Hegseth et al. 2019), particle formation events continue occurring at least until mid-August (Figure 8). This observation may suggest that phytoplankton activity and DMS emission rates may still be high, even though biomass build-up is balanced by grazing pressure from higher trophic levels as usually occurring in stratified post-bloom situations (Behrenfeld and Boss 2018). Alternatively, there could also be another source of aerosol precursor vapours in the area. The identity of relevant aerosol precursors, their sources and temporal variability remain unknown without gas phase measurements of the most relevant possible precursor. Measurements of particle precursor vapours and <10 nm particles are, however, necessary to get more insight in the formation process. Long-term data are required to see trends associated with the warming of the Arctic as well as changes in the extent and properties of sea ice.

3. Unanswered questions

Figure 1 shows a simplified scheme on the potential sources of primary volatile compounds, and their conversion to aerosol precursors. As already discussed above, currently systematic long-term observations are performed only for aerosol particles above approx. 10 nm in diameter (Gruvebadet/CNR, Zeppelin/SU), CCN properties (Zeppelin/SU) and solar radiation (Zepplin / NPI and Ny-Ålesund / AWI). Cosmic radiation, the primary source of ions which are potentially highly important for aerosol formation, is monitored, though aerosol formation is not sensitive to small variations in cosmic radiation intensity. Some studies have been performed on phytoplankton and related marine DMSP measurements (Kongsfjorden; Hoppe unpublished data) as well as gas phase DMS (Zeppelin/KOPRI). For other quantities, including VOC emissions and concentrations, measurements of all aerosol precursors expect ammonia, 1-3 nm molecular clusters and cluster growth to and above 10 nm have only been performed in a preliminary field campaign (UH+CNR). Important oxidant, hydroxyl radical (OH), is not recorded in Ny-Ålesund at all. This indicates that there is a massive gap in systematic, long-term high-quality measurements of almost all of the quantities relevant for secondary aerosol formation, which needs to be filled. In the next section, we discuss some of the technology that would help in filling the gaps.

4. Recommendations for the future

We suggest following instrument upgrades on permanent atmospheric measurements in Svalbard:

Mass spectrometer systems capable of measuring aerosol precursors vapours (H_2SO_4, MSA, all low volatile HOM-species, HIO_3, $H_xI_yO_z$), primary volatile compounds (VOCs, iodine-species, DMS) and naturally charged ion clusters. This can be achieved by nitrate- or bromide-ion CI-APi-TOF, APi-TOF and PTR-TOF/VOCUS instruments. A system capable of switching between ionization methods would enable the detection of wider range of required compounds with a single instrument (Manufacturers providing the necessary technology include at least Tofwerk A.G Switzerland; Karsa Oy/Ltd, Finland; Aerodyne Research Inc USA and Ionicon Analytic GmbH, Austria).

An instrument for recording size distribution of naturally charged ion-clusters and aerosol particles (commercially available instruments are NAIS and Balanced Scanning Mobility Analyzer, BSMA, both delivered by Airel Ltd Estonia).

An instrument for recording neutral 1-3 nm clusters (commercially available instruments are PSM, manufactured and delivered by Airmodus Oy, Finland and the Diethylene Glycol – Condensation Particle Counter, DEG-CPC, manufactured by TSI Inc. USA).

These instruments should be located in Gruvebadet or Zeppelin station in Ny-Ålesund, preferably in both. Since Kongsfjorden and the ocean nearby Ny-Ålesund experiences mostly absent sea ice, measurements should ideally be performed also along the coasts surrounded by ice. However, as this is not likely to be feasible in Svalbard, a logistically more meaningful location would be e.g. the Villum research station in Greenland. This suggestion calls for deep collaboration with other Arctic sites. To get a comprehensive picture of the consequences of sea ice decline and thinning, measurements in both environments – ice free and ice covered – are strongly needed. Data series from the above detection instrumentation would preferably have a time resolution of approximately one minute.

If long-term measurements of VOCs are not feasible, due to the current lack of sensitive enough instrumentation within the scientific community working in Svalbard, we suggest a 6-month measurement campaign in spring-summer season utilizing a VOCUS to resolve the concentrations and chemical nature of VOCs and long-term monitoring of VOC concentrations using offline analysis methods, such as Tenax tubes and off-line gas chromatography. Offline VOC flux measurements from the ocean, soil and snow would help in pointing out the primary sources of VOCs in the area.

It would be desirable to establish a systematic long-term monitoring program of

phytoplankton populations and associated DMSP production in Kongsfjorden, which would also support gas phase measurements performed in Ny-Ålesund. While spring-bloom monitoring has been conducted regularly since 2014 (Hoppe et al. unpublished data) and a pilot study on year-round sampling has been initiated this year (Hop and Assmy, unpublished data), there are currently no capacities for sophisticated biochemical measurements (e.g. for DMS and DMSP).

A problematic, but important issue, for which we currently do not have a feasible solution, are the gas phase ammonia measurements. As discussed above, there is currently no technology for reliable ammonia quantification in presumably very low ammonia concentrations (maybe <100 ppt) around Svalbard. If such measurement could be performed, such activity should be strongly promoted.

Besides these above suggested amendments, it is absolutely imperative to guarantee the continuation of existing DMS and aerosol measurements – located in Gruvebadet and Zeppelin stations – in Svalbard.

Future collaboration between the institutes and stations working on the topics discussed in this report should be promoted. To our knowledge, phytoplankton studies in Kongsfjorden are currently primarily performed (occasionally) by AWI and NPI, aerosol measurements are carried out by CNR-Italy and Stockholm University, gas phase measurements of precursor vapours and clusters are (occasionally) conducted by University of Helsinki and DMS measurements by KOPRI. These institutes have already established collaboration over the past years. Other institutes working with a connection to topics discussed here, should be encouraged to join efforts with existing collaborations.

5. Data availability

Data collected from Svalbard, Ny-Ålesund and presented in Figure 7-8 are owned by CNR-Italy and available on request from mikko.sipila@helsinki.fi.

Acknowledgements

This work was supported by the Research Council of Norway, project number 251658, Svalbard Integrated Arctic Earth Observing System - Knowledge Centre (SIOS-KC).

References

Albrecht BA (1989) Aerosols, Cloud Microphysics, and Fractional Cloudiness. Science 245:1227-1230. https://doi.org/10.1126/science.245.4923.1227

Almeida J, Schobesberger S, Kürten A, Ortega IK, Kupiainen-Määttä O, Praplan AP, et al. (2013) Molecular understanding of sulphuric acid-amine particle nucleation in the atmosphere. Nature 502(7471), 359–363. https://doi.org/10.1038/nature12663

Alterskjaer K, Kristjánsson JE, Hoose C (2010) Do anthropogenic aerosols enhance or suppress the surface cloud forcing in the Arctic? J Geophys Res, 115:D22204. https://doi.org/10.1029/2010JD014015

Asmi E et al. (2009) Results of the first air ion spectrometer calibration and intercomparison workshop. Atmos Chem Phys 9:141–154. https://doi.org/10.5194/acp-9-141-2009

Atkinson HM, Huang R-J, Chance R, Roscoe HK, Hughes C, Davison B, Schönhardt A, Mahajan AS, Saiz-Lopez A, Hoffmann T (2012) Iodine emissions from the sea ice of the Weddell Sea. Atmos Chem Phys 12:11229-11244. https://doi.org/10.5194/acp-12-11229-2012

Behrenfeld MJ and Boss ES (2018) Student's tutorial on bloom hypotheses in the context of phytoplankton annual cycles. Glob Change Biol 24(1): 55-77. https://doi.org/10.1111/gcb.13858

Carpenter LJ, Archer SD, Beale R (2012) Ocean-atmosphere trace gas exchange, Critical Review. Chem Soc Rev 41:6473-6506. https://doi.org/10.1039/C2CS35121H

Challenger F and Simpson MI (1948) Studies on biological methylation. Part XII. A precursor of the dimethyl sulphide evolved by Polysiphonia fastigiata. dimethyl-2-carboxyethylsulphonium hydroxide and its salts. J Chem Soc 320:1591-1597. https://doi.org/10.1039/JR9480001591

Charlson RJ, Lovelock JE, Andreae MO, Warren SG (1987) Oceanic phytoplankton, atmospheric sulphur, cloud albedo and climate. Nature 326:655–661. https://doi.org/10.1038/326655a0

Cottier F, Skogseth R, David D, Berge J (2019) Temperature time-series in Svalbard fjords. A contribution from the "Integrated Marine Observatory Partnership". In: Orr et al. (eds): SESS report 2018, Svalbard Integrated Arctic Earth Observing System, Longyearbyen, pp. 108-118. https://sios-svalbard.org/SESS_Issue1

Covert DS, Wiedensohler A, Aalto P, Heintzenberg J, Mcmurry PH, Leck C (1996) Aerosol number size distributions from 3 to 500 nm diameter in the arctic marine boundary layer during summer and autumn. Tellus B 48(2):197-212. https://doi.org/10.3402/tellusb.v48i2.15886

Croft B et al. (2016) Processes controlling the annual cycle of Arctic aerosol number and size distributions. Atmos Chem Phys 16:3665–3682. https://doi.org/10.5194/acp-16-3665-2016

Cuevas CA et al. (2018) Rapid increase in atmospheric iodine levels in the North Atlantic since the mid-20th century. Nat Commun 9:1452. https://doi.org/10.1038/s41467-018-03756-1

Curson ARJ et al. (2011) Catabolism of dimethylsulphoniopropionate: microorganisms, enzymes and genes. Nat Rev Microbiol 9: 849-859. https://doi.org/10.1038/nrmicro2653

Dall'Osto M et al. (2019) Simultaneous measurements of aerosol size distributions at three sites in the European high Arctic. Atmos Chem Phys 19:7377–7395. https://doi.org/10.5194/acp-19-7377-2019

Dall'Osto M et al. (2017) Arctic sea ice melt leads to atmospheric new particle formation. Sci Rep 7: 3318. https://doi.org/10.1038/s41598-017-03328-1

Dibb JE and Arsenault M (2002) Shouldn't snowpacks be sources of monocarboxylic acids? Atmos Environ 36:2513–2522. https://doi.org/10.1016/S1352-2310(02)00131-0

Doscher R, Vihma T, Maksimovich E (2014) Recent advances in understanding the Arctic climate system state and change from a sea ice perspective: A review. Atmos Chem Phys 14(24):13571-13600. https://doi.org/10.5194/acp-14-13571-2014

Dunne EM et al. (2016) Global atmospheric particle formation from CERN CLOUD measurements. Science 354(6316):1119-1124. https://doi.org/10.1126/science.aaf2649

Ehn M et al. (2014) A large source of low-volatility secondary organic aerosol. Nature 506(7489):476. https://doi.org/10.1038/nature13032

Frieß U, Deutschmann T, Gilfedder BS, Weller R, Platt U (2010) Iodine monoxide in the Antarctic snowpack. Atmos Chem Phys 10:2439-2456. https://doi.org/10.5194/acp-10-2439-2010

Fu P, Kawamura K, Chen J, Barrie LA (2009) Isoprene, Monoterpene, and Sesquiterpene Oxidation Products in the High Arctic Aerosols during Late Winter to Early Summer. Environ Sci Technol 43(11):4022-4028. https://doi.org/10.1021/es803669a

Galí M, Devred E, Babin M, Levasseur M (2019)

Decadal increase in Arctic dimethylsulfide emission. P Natl Acad Sci USA 116(39):19311-19317. https://doi.org/10.1073/pnas.1904378116

Gálvez Ó, Baeza-Romero MT, Sanz M, Saiz-Lopez A (2016) Photolysis of frozen iodate salts as a source of active iodine in the polar environment. Atmos Chem Phys 16:12703-12713. https://doi.org/10.5194/acp-16-12703-2016

Ghahremaninezhad R, Norman AL, Abbatt JPD, Levasseur M, Thomas JL (2016) Biogenic, anthropogenic and sea salt sulfate size-segregated aerosols in the Arctic summer. Atmos Chem Phys, 16(8), 5191–5202. https://doi.org/10.5194/acp-16-5191-2016

Giardi F et al. (2016) Size distribution and ion composition of aerosol collected at Ny-Ålesund in the spring-summer field campaign 2013. Rend Fis Acc Lincei 27(1):47. https://doi.org/10.1007/s12210-016-0529-3

Granfors A, Ahnoff M, Mills MM, Abrahamsson K (2014) Organic iodine in Antarctic sea ice: A comparison between winter in the Weddell Sea and summer in the Amundsen Sea. J Geophys Res 119:2276-2291. https://doi.org/10.1002/2014JG002727

Guimbaud C et al. (2002) Snowpack processing of acetaldehyde and acetone in the Arctic atmospheric boundary layer. Atmos Environ 36(15–16): 2743-2752, https://doi.org/10.1016/S1352-2310(02)00107-3

Hegseth EN et al. (2019) Phytoplankton seasonal dynamics in Kongsfjorden, Svalbard and the adjacent shelf. In: Hop H., Wiencke C. (eds) The Ecosystem of Kongsfjorden, Svalbard. Advances in Polar Ecology, vol 2. Springer, Cham. https://doi.org/10.1007/978-3-319-46425-1_6

Hoppe CJM, Wolf KKE, Schuback N, Tortell PD, Rost B (2018) Compensation of ocean acidification effects in Arctic phytoplankton assemblages. Nat Clim Change 8:529–533. https://doi.org/10.1038/s41558-018-0142-9

Houdier S, Perrier S, Domine, F, Cabanes A, Legagneux L, Grannas AM, Guimbaud C, Shepson PB, Boudries H, Bottenheim JW (2002) Acetaldehyde and acetone in the Arctic snowpack during the ALERT2000 campaign. Snowpack composition, incorporation processes and atmospheric impact. Atmos Environ 36(15–16):2609-2618. https://doi.org/10.1016/S1352-2310(02)00109-7

Hussherr R et al. (2017) Impact of ocean acidification on Arctic phytoplankton blooms and dimethyl sulfide concentration under simulated ice-free and under-ice conditions. Biogeosciences 14(9):2407-2427. https://doi.org/10.5194/bg-14-2407-2017

Intrieri JM, Fairall CW, Shupe MD, Persson, POG, Andreas EL, Guest PS, Moritz RE (2002) An annual cycle of Arctic surface cloud forcing at SHEBA. J Geophys Res 107(C10):8039. https://doi.org/10.1029/2000JC000439

Jarníková T et al. (2018) The distribution of methylated sulfur compounds, DMS and DMSP, in Canadian subarctic and Arctic marine waters during summer 2015. Biogeosciences 15(8):2449-2465. https://doi.org/10.5194/bg-15-2449-2018

Jimenez J et al. (2009) Evolution of organic aerosols in the atmosphere. Science 326:1525-1529. https://doi.org/10.1126/science.1180353

Jokinen T et al. (2012) Atmospheric sulphuric acid and neutral cluster measurements using CI-APi-TOF. Atmos Chem Phys 12(9):4117-4125. https://doi.org/10.5194/acp-12-4117-2012

Jokinen T et al. (2018) Ion-induced sulfuric acid-ammonia nucleation drives particle formation in coastal Antarctica. Science Advances 4(11): 9744. https://doi.org/10.1126/sciadv.aat9744

Junninen H, Ehn M, Petäjä T, Luosujärvi L, Kotiaho T, Kostiainen R, Rohner U, Gonin M, Fuhrer K, Kulmala M, Worsnop DR (2010) A high-resolution mass spectrometer to measure atmospheric ion composition. Atmos Meas Tech 3:1039–1053. https://doi.org/10.5194/amt-3-1039-2010

Keller MD et al. (1989) Dimethyl Sulfide Production in Marine Phytoplankton. In Biogenic Sulfur in the Environment. American Chemical Society 393: 167-182. https://doi.org/10.1021/bk-1989-0393.ch011

Kiene RP et al. (2000) New and important roles for DMSP in marine microbial communities. J Sea Res 43(3):209-224. https://doi.org/10.1016/S1385-1101(00)00023-X

Kim K, Yabushita A, Okumura M, Saiz-Lopez A, Cuevas CA, Blaszczak-Boxe CS, Min DW, Yoon H-I, Choi W (2016) Production of Molecular Iodine and Tri-iodide in the Frozen Solution of Iodide: Implication for Polar Atmosphere. Environ Sci Technol 50:1280-1287. https://doi.org/10.1021/acs.est.5b05148

Kirkby J et al. (2011) Role of sulphuric acid, ammonia and galactic cosmic rays in atmospheric aerosol nucleation. Nature 476: 429-433. https://www.nature.com/articles/nature10343

Kirkby J et al. (2016) Ion-induced nucleation of pure biogenic particles. Nature 533(7604):521. https://doi.org/10.1038/nature17953

Kirst GO et al. (1991) Dimethylsulfoniopropionate (DMSP) in icealgae and its possible biological role. Mar Chem 35(1):381-388. https://doi.org/10.1016/S0304-4203(09)90030-5

Kos G, Kanthasami V, Adechina N, Ariya PA (2014) Volatile organic compounds in Arctic snow:

concentrations and implications for atmospheric processes. Environ Sci-Proc Imp 16:2592-2603. https://doi.org/10.1039/C4EM00410H

Kramshøj M, Albers CN, Holst T, Holzinger R, Elberling B, Rinnan R (2018) Biogenic volatile release from permafrost thaw is determined by the soil microbial sink. Nature Communications, 9(1). https://doi.org/10.1038/s41467-018-05824-y

Kulmala M et al. (2013) Direct Observations of Atmospheric Aerosol Nucleation. Science 339(6122):943-946. https://doi.org/10.1126/science.1227385

Leaitch WR, Sharma S, Huang L, Toom-Sauntry D, Chivulescu A, Macdonald AM, et al. (2013) Dimethyl sulfide control of the clean summertime Arctic aerosol and cloud. Elem Sci Anth 1:000017. https://doi.org/10.12952/journal.elementa.000017

Levasseur M (2013) Impact of Arctic meltdown on the microbial cycling of Sulphur. Nat Geosci 6:691-700. https://doi.org/10.1038/ngeo1910

Lindwall R, Schollert M, Michelsen A, Blok D, Rinnan R (2016) Fourfold higher tundra volatile emissions due to arctic summer warming. J Geophys Res-Biogeo 121(3):895-902. https://doi.org/10.1002/2015JG003295

Liss PS et al. (1997) Marine sulphur emissions. Philos T Roy Soc B 352(1350):159-169. https://www.jstor.org/stable/56558

Lupi A et al. (2016) Multi-seasonal ultrafine aerosol particle number concentration measurements at the Gruvebadet observatory, Ny-Ålesund, Svalbard Islands. Rend Fis Acc Lincei 27(1):S59–S71. https://doi.org/10.1007/s12210-016-0532-8

MacDonald SM, Gómez Martín JC, Chance R, Warriner S, Saiz-Lopez A, Carpenter LJ, Plane JMC (2014) A laboratory characterisation of inorganic iodine emissions from the sea surface: Dependence on oceanic variables and parameterisation for global modelling. Atmos Chem Phys, 14(11), 5841–5852. https://doi.org/10.5194/acp-14-5841-2014

Mahajan AS, Shaw M, Oetjen H, Hornsby KE, Carpenter LJ, Kaleschke L, Tian-Kunze X, Lee JD, Moller SJ, Edwards P, Commane R, Ingham T, Heard DE, Plane JMC (2010) Evidence of reactive iodine chemistry in the Arctic boundary layer. J Geophys Res-Atmos 115:D20303. https://doi.org/10.1029/2009JD013665

Mauritsen T (2016) Arctic climate change: Greenhouse warming unleashed. Nat Geosci 9:271-272. https://doi.org/10.1038/ngeo2677

Merikanto J, Spracklen DV, Mann GW, Pickering SJ, Carslaw KS (2009) Impact of nucleation on global CCN. Atmos Chem Phys 9:8601–8616. https://doi.org/10.5194/acp-9-8601-2009

Mungal EL et al. (2017) Microlayer source of oxygenated volatile organic compounds in the summertime marine Arctic boundary layer. P Natl Acad Sci USA 114:6203-6208. https://doi.org/10.1073/pnas.1620571114

Nicolaus M, Katlein C, Maslanik J, Hendricks S (2012) Changes in Arctic sea ice result in increasing light transmittance and absorption. Geophys Res Lett, 39(24), 1–6. https://doi.org/10.1029/2012GL053738

Nieminen T, Lehtinen KEJ, Kulmala M (2010) Sub-10 nm particle growth by vapor condensation-effects of vapor molecule size and particle thermal speed. Atmos Chem Phys, 10(20), 9773–9779. https://doi.org/10.5194/acp-10-9773-2010

O'Dowd C, Jimenez JL, Bahreini R, Flagan RC (2002) Marine aerosol formation from biogenic iodine emissions. Nature 417:632-636. https://doi.org/10.1038/nature00775

O'Dowd C, de Leeuw G (2007) Marine aerosol production: A review of the current knowledge. Philos T Roy Soc A 365:1753–1774. https://doi.org/10.1098/rsta.2007.2043

Overland JE and Wang M (2013) When will the summer Arctic be nearly sea ice free? Geophys Res Lett 40(10):2097-2101. https://doi.org/10.1002/grl.50316

Park K-T, Jang S, Lee K, Yoon YJ, Kim M-S, Park K, Cho H-J, Kang, J-H, Udisti R, Lee B-Y, Shin, K-H. (2017) Observational evidence for the formation of DMS-derived aerosols during Arctic phytoplankton blooms. Atmos Chem Phys 17:9665-9675. https://doi.org/10.5194/acp-17-9665-2017

Quinn PK and Bates TS (2011) The case against climate regulation via oceanic phytoplankton sulphur emissions. Nature 480:51–56. https://doi.org/10.1038/nature10580

Raso ARW, Custard KD, May NW, Tanner D, Newburn MK, Walker L, Moore RJ, Huey LG, Alexander L, Shepson PB, Pratt KA (2017) Active molecular iodine photochemistry in the Arctic. P Natl Acad Sci USA 114:10053-10058. https://doi.org/10.1073/pnas.1702803114

Saiz-Lopez A, Blaszczak-Boxe CS, Carpenter LJ (2015) A mechanism for biologically induced iodine emissions from sea ice. Atmos Chem Phys 15:9731-9746. https://doi.org/10.5194/acp-15-9731-2015

Saiz-Lopez A, Chance K, Liu X, Kurosu TP, Sander SP (2007a) First observations of iodine oxide from space. Geophys Res Lett 34:L12812. https://doi.org/10.1029/2007GL030111

Saiz-Lopez A, Mahajan AS, Salmon RA, Bauguitte SJ-B, Jones AE, Roscoe HK, Plane JMC (2007b) Boundary Layer Halogens in Coastal Antarctica. Science 317:348-351. https://science.sciencemag.org/

content/317/5836/348

Saiz-Lopez A, von Glasow R (2012) Reactive halogen chemistry in the troposphere. Chem Soc Rev 41:6448-6472. https://doi.org/10.1039/C2CS35208G

Schönhardt A, Begoin M, Richter A, Wittrock F, Kaleschke L, Gómez Martín JC, Burrows JP (2012) Simultaneous satellite observations of IO and BrO over Antarctica. Atmos Chem Phys, 12(14), 6565–6580. https://doi.org/10.5194/acp-12-6565-2012

Sedlar J, Tjernström M, Mauritsen T, Shupe MD, Brooks IM, Persson POG, Birch CE, Leck C, Sirevaag A, Nicolaus M (2011) A transitioning Arctic surface energy budget: The impacts of solar zenith angle, surface albedo and cloud radiative forcing. Climate Dynamics 37(7–8), 1643–1660. https://doi.org/10.1007/s00382-010-0937-5

Shupe MD, Intrieri JM (2004) Cloud radiative forcing of the Arctic surface: The influence of cloud properties, surface albedo, and solar zenith angle. J Climate 17(3):616–628.

Simpson WR, Brown SS, Saiz-Lopez A, Thornton JA, Glasow RV (2015) Tropospheric halogen chemistry: Sources, cycling, and impacts. Chem Rev 115:4035-4062. https://doi.org/10.1021/cr5006638

Sipilä M, Sarnela N, Jokinen T, Henschel H, Junninen H, Kontkanen J, Richters S, Kangasluoma J, Franchin, A, Peräkylä O, Rissanen MP, Ehn M, Vehkamäki H, Kurten T, Berndt T, Petäjä T Worsnop D, Ceburnis, D, Kerminen V-M, Kulmala M, O'Dowd C (2016) Molecular scale evidence of new particle formation via sequential addition of HIO3. Nature 537: 532-534. https://doi.org/10.1038/nature19314

Spolaor A, Vallelonga P, Gabrieli J, Martma T, Björkman M, Isaksson E, Cozzi G, Turetta C, Kjær H, Curran M (2014) Seasonality of halogen deposition in polar snow and ice. Atmos Chem Phys 14:9613-9622. https://doi.org/10.5194/acp-14-9613-2014

Spolaor A, Vallelonga P, Plane J, Kehrwald N, Gabrieli J, Varin C, Turetta C, Cozzi G, Kumar R, Boutron C (2013) Halogen species record Antarctic sea ice extent over glacial–interglacial periods. Atmos Chem Phys 13:6623-6635. https://doi.org/10.5194/acp-13-6623-2013

Stefels J et al. (2007) Environmental constraints on the production and removal of the climatically active gas dimethylsulphide (DMS) and implications for ecosystem modelling. Biogeochemistry 83(1): 245-275. https://doi.org/10.1007/s10533-007-9091-5

Stohl A (2006) Characteristics of atmospheric transport into the Arctic troposphere. J Geophys Res 111:D11306. https://doi.org/10.1029/2005JD006888

Stroeve JC and Notz D (2018) Changing state of Arctic sea ice across all seasons. Environ Res Lett 13:103001. https://doi.org/10.1088/1748-9326/aade56

Ström J, Engvall A-C, Delbart F. Krejci R, Treffeisen R (2009) On small particles in the Arctic summer boundary layer: Observations at two different heights near Ny-Ålesund, Svalbard. Tellus B 61(2):473-482. https://doi.org/10.1111/j.1600-0889.2008.00412.x

Ström J, Umegard J, Torseth K, Tunved P, Hansson HC, Holmen K, Wismann V, Herber A, Konig-Langlo G (2003) One year of particle size distribution and aerosol chemical composition measurements at the Zeppelin Station, Svalbard, March 2000–March 2001. Phys Chem Earth 28:1181-1190. https://doi.org/10.1016/j.pce.2003.08.058

Sunda W et al. (2002) An antioxidant function for DMSP and DMS in marine algae. Naturem 418(6895): 317-320. https://doi.org/10.1038/nature00851

Tjernström M et al. (2014) The Arctic Summer Cloud Ocean Study (ASCOS): overview and experimental design. Atmos Chem Phys 14:2823-2869. https://doi.org/10.5194/acp-14-2823-2014

Trevena AJ and Jones GB (2006) Dimethylsulphide and dimethylsulphoniopropionate in Antarctic sea ice and their release during sea ice melting. Mar Chem 98(2):210-222. https://doi.org/10.1016/j.marchem.2005.09.005

Trevena A, Jones G (2012) DMS flux over the Antarctic sea ice zone. Mar Chem, 134–135, 47–58. https://doi.org/10.1016/j.marchem.2012.03.001

Tunved P et al. (2013) Arctic aerosol life cycle: linking aerosol size distributions observed between 2000 and 2010 with air mass transport and precipitation at Zeppelin station, Ny-Ålesund, Svalbard. Atmos Chem Phys 13:3643-3660. https://doi.org/10.5194/acp-13-3643-2013

Twomey S (1974) Pollution and the planetary albedo. Atmos Environ 8:1251-1256. https://doi.org/10.1016/0004-6981(74)90004-3

Uhlig C et al. (2019) Sea Ice and Water Mass Influence Dimethylsulfide Concentrations in the Central Arctic Ocean. Front Earth Sci 7:179. https://doi.org/10.3389/feart.2019.00179

Vallelonga P, Maffezzoli N, Moy AD, Curran MA, Vance TR, Edwards R, Hughes G, Barker E, Spreen G, Saiz-Lopez A, Corella JP, Cuevas CA, Spolaor A (2017) Sea-ice-related halogen enrichment at Law Dome, coastal East Antarctica. Clim Past 13:171. https://doi.org/10.5194/cp-13-171-2017

Vanhanen J et al. (2011) Particle Size Magnifier for Nano-CN Detection. Aerosol Sci Tech 45(4):533-542. https://doi.org/10.1080/02786826.2010.547889

Vogt R, Sander R, von Glasow R, Crutzen PJ (1999) Iodine Chemistry and its Role in Halogen Activation and Ozone Loss in the Marine Boundary Layer: A

Model Study. J Atmos Chem 32:375-395. https://doi.org/10.1023/A:1006179901037

Wassmann P and Reigstad M. (2011) Future Arctic Ocean seasonal ice zones and implications for pelagic-benthic coupling. Oceanography 24(3):220–231. https://doi.org/10.5670/oceanog.2011.74

Watanabe K, Matsuda S, Cuevas CA, Saiz-Lopez A, Yabushita A, Nakano Y (2019) Experimental Determination of the Photooxidation of Aqueous I– as a Source of Atmospheric I2. ACS Earth Space Chem 3(4):669-679. https://doi.org/10.1021/acsearthspacechem.9b00007

Wentworth GR (2016) Ammonia in the summertime Arctic marine boundary layer: sources, sinks, and implications. Atmos Chem Phys 16:1937–1953. https://doi.org/10.5194/acp-16-1937-2016

Wiedensohler A, Covert DS, Swietlicki E, Aalto P, Heizenberg J, Leck C (1996) Occurrence of an ultrafine particle mode less than 20 nm in diameter in the marine boundary layer during Arctic summer and Autumn. Tellus B 48(2):213-222. https://doi.org/10.3402/tellusb.v48i2.15887

Yao L, Garmash O, Bianchi F, Zheng J, Yan C, Kontkanen J, Junninen H, et al. (2018) Atmospheric new particle formation from sulfuric acid and amines in a Chinese megacity. Science 361(6399), 278 LP – 281. https://doi.org/10.1126/science.aao4839

Atmospheric black carbon in Svalbard (ABC Svalbard)

Stefania Gilardoni[1], Angelo Lupi[1], Mauro Mazzola[1], David Michele Cappelletti[2], Beatrice Moroni[2], Luca Ferrero[3], Piotr Markuszewski[4], Anna Rozwadowska[4], Radovan Krejci[5], Paul Zieger[5], Peter Tunved[5], Linn Karlsson[5], Stergios Vratolis[6], Konstantinos Eleftheriadis[6], Angelo Pietro Viola[7]

1 Institute of Polar Sciences, National Research Council of Italy, Via P. Gobetti 101, 40129 Bologna, Italy
2 University of Perugia, Department of Chemistry, Biology and Biotechnology, Via Elce di Sotto 8, 06123 Perugia, Italy
3 University of Milano-Bicocca, Piazza della Scienza 1 - 20126 Milan, Italy
4 Institute of Oceanology, Polish Academy of Sciences, Powstancow Warszawy 55, 81-712, Poland
5 Stockholm University, Svante Arrhenius väg 8, SE-11418 Stockholm, Sweden
6 National Center for Scientific Research, Demokritos, Ag. Paraskevi, Attiki - GR-15310, Greece
7 Institute of Polar Sciences, National Research Council of Italy, Via Fosso del Cavaliere 100, 00133 Rome, Italy

Corresponding author: Stefania Gilardoni, **stefania.gilardoni@cnr.it**,
ORCID number 0000-0002-7312-5571

Keywords: Black carbon, light absorption coefficient, radiative forcing, BC vertical profiles, climate change

1. Introduction

Black carbon (BC) is a component of submicrometer aerosol particles, characterized by atmospheric residence times of a few days up to a week. This relative longer life-time, compared to coarse particles, allows BC transport from source regions to remote locations. Once in the Arctic, BC impacts the regional radiation balance by absorbing incoming solar radiation (direct effect), altering cloud distribution and their radiative properties, and reducing snow and ice surface albedo after deposition. In addition, BC at mid-latitudes can still warm the Arctic, affecting the transport of heat towards higher latitudes, with the strongest impacts in summer and in the upper troposphere (Sand et al. 2013).

BC radiative direct effect in the Arctic is enhanced compared to mid-latitude impacts, due to the prolonged solar light exposure during summer and the high reflectivity of lower atmosphere and surface, characterized by low level clouds and snow/ice cover, respectively (Quinn et al. 2011). The top of the atmosphere radiative forcing due to BC direct effect calculated using different modelling tools and approaches ranges between +0.12 and +0.80 W m^{-2} (Quinn et al. 2011; Quinn et al. 2015 and references therein). Differences among results are mainly driven by BC atmospheric burden (Quinn et al. 2011), particle atmospheric residence time (Wang et al. 2014), cloud distribution, and treatment of radiative processes (Quinn et al. 2015). In addition, current model uncertainties are strongly affected by lack of constraints on BC vertical distribution and a simplified description of the BC radiative properties (Koch and Del Genio, 2010; Boucher et al. 2013).

In addition to direct radiative forcing, BC aerosol particles can alter the Earth's energy budget participating to cloud formation. Although freshly emitted BC particles are hydrophobic, atmospheric processing promotes BC particle coating by soluble components, that eventually make BC particles hydrophilic enough to act as cloud condensation nuclei (CCN) (Park et al. 2005). Promoting cloud nuclei formation, BC might increase cloud thickness and cloud residence time, leading to a negative radiative forcing (Boucher et al. 2013). On the other side, atmospheric heating induced by cloud interstitial BC can favour cloud evaporation (Jacobson et al. 2010), suppressing precipitation and thus reducing BC wet removal. Conversely, the ability of BC particle to act as ice nuclei (IN) is still under debate (Xu et al. 2019). Climate response driven by BC-cloud interaction is characterized by large uncertainties, mainly driven by limited number of modelling studies and limited observational constraints (Bond et al. 2013; Xu et al. 2019).

After removal from the atmosphere through wet and dry deposition, BC can still affect the climate by darkening snow and ice surface (albedo reduction) and promoting their melting. Even a small number of BC particles has a significant impact on snow and ice, since BC has a mass absorption cross-section up to five times higher than snow. In addition, ice and snow crystals reflect solar radiation, increasing the light optical path, and enhancing the probability

of interaction between light and BC embedded in snow and ice (Quinn et al. 2011). Finally, snowpack warming promotes metamorphism, which leads to larger snow crystal formation and thus further albedo reduction (Ginot et al. 2014; Hadley and Kirchstetter 2012). These effects can trigger a feedback mechanism: earlier snow melting during the warm season decreases the surface albedo and increases the fraction of solar energy trapped by the atmosphere. To estimate BC albedo forcing, models need to simulate BC concentration and light absorption in the upper layers of the snow surface. BC concentration in snow depends on BC concentration in snowfall, BC settled through dry deposition, snow melting/sublimation, and BC runoff (Doherty et al. 2014). In addition, the BC mass absorption cross section in snow depends on particle age (Schwartz et al. 2013). Using a multi-model approach and BC observations, Jiao et al. (2014) calculated that the regional BC albedo forcing was equal to +0.17 W m^{-2} (Jiao et al. 2014). Based on direct observations of BC in snow samples, Dang et al. (2017) drew comparable results, with BC albedo forcing in the Arctic ranging between 0.06 and 0.5 W m^{-2} considering old and fresh snow, respectively.

Although recent improvements, models that are used to quantify BC climate impacts and related temperature changes in the Arctic often underestimate the actual BC concentrations and fail in reproducing the amplitude of its seasonal variation (Winiger et al. 2017). Actual sources of BC in the Arctic are still characterized by some degree of uncertainty. The integration of chemical transport models and aircraft observations indicated that anthropogenic sources dominated BC in the Arctic lower troposphere, with Russian emission accounting for the largest BC share (Wang et al. 2011; Popovicheva et al. 2017). Sand et al. (2016) calculated that BC is responsible for the increase of Arctic temperature by 0.48 K, with the highest impacts from domestic emissions from Asia and flaring from Russia, while observations in the Siberian Arctic would suggest an overestimation of flaring emissions (Winiger et al. 2017). Finally, radiocarbon characterization of carbonaceous aerosol indicated that the actual emission inventories tend to underestimate the contribution of biomass burning (Winiger et al. 2017; Winiger et al. 2019). Future BC emission scenarios are even more unclear, since projections depend on changing local anthropogenic activities in the Arctic and on changing transportation pattern of BC from low-latitudes (Winiger et al. 2017). Future changes in wildfires frequency in warming climate are also undetermined.

To summarize, the description of BC impacts on climate and air quality in the Arctic requires an accurate understanding of BC optical and microphysical properties, BC aerosol-cloud interaction, wet and dry deposition, and sources (Mahmood et al. 2016; Winiger et al. 2017). The analysis of BC spatial and temporal variability can help to understand how changes in climate and anthropogenic activities affect BC concentration and can support the analysis of BC climate-relevant properties. The specific aims of this chapter are: i) to quantitatively describe temporal variability of BC concentrations at different altitude sites based on long-term measurements, ii) and to deploy available short-term observations to describe horizontal and vertical variability of BC concentrations.

2. Overview of existing data

2.1 Long-term observations at Svalbard

BC is defined operationally, based on the measurement techniques employed for its quantification (Lack et al. 2014). Long-term observations at Svalbard deploy optical techniques to infer BC concentration: aerosol particles are deposited on a filter and change in light transmission through the filter is measured. These techniques allow the quantification of equivalent black carbon (eBC), namely the amount of strongly light absorbing carbon, with optical properties similar to those of soot, that would lead to the same absorption signal (Andreae and Gelencser, 2006). eBC mass concentration is then derived by multiplying the measured light absorption coefficient by an appropriate mass absorption cross section (MAC), which needs to be specified when eBC is reported (Petzold et al. 2013).

The quantification of eBC through filter-based optical measurements relies on a few assumptions. First, light absorption is assumed to be due exclusively to BC particles, ignoring the contribution of organic aerosol (brown carbon) and dust. Observations indicate that brown carbon and dust absorptions have a stronger wavelength dependence than BC, and are higher in the UV and visible part of the spectrum (Bergstrom et al. 2007; Russell et al. 2010). As a consequence, this report focuses on measurements at wavelength larger than 600nm, where BC light absorption dominates over other species (Kirchstetter et al. 2004). In addition, liquid-like organic aerosol can spread across the filter substrate after collection, altering filter optical properties and particle morphology, and consequently decreasing accuracy of eBC quantification (Subramanian et al. 2007; Lack et al. 2008). Such a bias depends on the type of sampled air masses and can be relevant (larger than 10%) in polluted environments (Lack et al, 2008). This artefact is likely negligible in the Arctic. Finally, to convert absorption into eBC concentration, an accurate MAC value is required. MAC of BC depends on the particles' diameter, morphology (fractal or compact shape), and coating by non-absorbing materials, thus it varies while the particles reside in the atmosphere and is higher far from the source regions (Sharma et al. 2004; Bond et al. 2006). Measurements of BC MAC in the Arctic are consistently higher than those of bare BC particles (Sharma et al. 2017; Zanatta et al. 2016; Zanatta et al. 2018), and range between 7.5 and 9.9 $m^2\ g^{-1}$ at 550 nm. Due to the variability of MAC with aerosol age, here we compare long-term measurements of light absorption coefficients without converting them into eBC concentration.

Long-term light absorption measurements at Svalbard are performed at Gruvebadet and Zeppelin. Gruvebadet observatory (78.918°N, 11.895°E; 61m above sea level) is located 800m south-west of the Ny-Ålesund research village. The Zeppelin observatory (78.908°N, 11.881°E; 474 m above sea level) is located at the top of the Zeppelin mountain, about 10

km from the coast and 5 km from Gruvebadet observatory. The Zeppelin Observatory is owned and managed by the Norwegian Polar Institute and is part of the Global Atmospheric Watch network.

At Zeppelin aerosol light absorption measurements were performed with a single wavelength aethalometer AE-9 in 1998 and in 1999, operating at 880 nm. Starting from 2001, light absorption has been measured continuously at seven wavelengths, ranging from 370 nm to 950 nm, with a multi-wavelength aethalometer AE-31. Both instruments worked at 30-minute time resolution (Eleftheriadis et al. 2009). Light attenuation measurements were corrected for filter transmissions according to Backamn et al. (2017) and using a multiple scattering correction factor C equal to 3.25. Light absorption at 525 nm has been measured with a Particles Soot Absorption Photometer (PSAP) since 2002. Since June 2015 an Aethalometer AE33 is running in parallel with the AE31. Work is currently in progress to evaluate the performance of the two instruments, with respect to other parallel absorption measurements. It is aimed to consolidate the use of loading and multiple scattering correction factors and provide quality assured absorption coefficient time series at the Arctic sites. At Gruvebadet aerosol light absorption is measured at three wavelengths with a Radiance Research PSAP at 1-minute time resolution (Bond et al. 1999), since 2010. Data are then averaged over 1-hour period. Absorption coefficients are measured at 467 nm, 530 nm, and 660 nm, with a precision ranging between 20 and 25%. Measurements are performed generally from April to September, with a limited number of data during the winter season. Measurements are corrected according to Bond et al. (1999) for filter transmission, flow, and sampling filter area. Data are not corrected for aerosol scattering, while shadowing effect is considered negligible due to the low aerosol loading. At both sites absorption coefficients are normalized at standard pressure and temperature conditions (1 atm and 0 °C).

Figure 1 (panels a and c) shows the time series of daily-averaged Zeppelin and Gruvebadet aerosol absorption coefficients at 660 nm, while panels 1b and 1d report the seasonal capture of light absorption at the two sites. The wavelength of 660 nm is chosen to minimize the interference of brown carbon and dust, and since it is a common wavelength to aethalometer and PSAP instruments. Although the variability range of the two time-series is comparable, Gruvebadet shows often short episodes of high absorption coefficient values, likely due to the influence of local emission sources at Ny-Ålesund village and harbour, constrained in the lower layers of the troposphere and not affecting the high-altitude site. The annual average absorption coefficient at Zeppelin from 2005 to 2018 was 0.13 Mm^{-1}. Over the period 1998-2007 Eleftheriadis et al. (2009) measured an annual average eBC concentration of 39 ng m^{-3}. Assuming a MAC at 660 nm in the range of 6.2-8.2 (extrapolated at 660 nm from Zanatta et al. 2018 and assuming an absorption angstrom exponent of 1), the average eBC observed during the period 2005-2018 is equivalent to 16-20 ng m-3, in agreement with the decreasing tendency during the 2000s reported by

Stone et al. (2014) for multiple sites in the Arctic. The average absorption coefficient over spring and summer, when measurements are representative of both sites, were 0.15 Mm^{-1} and 0.28 Mm^{-1} at Zeppelin and Gruvebadet, respectively, indicating higher concentration of BC at the lower altitude observatory.

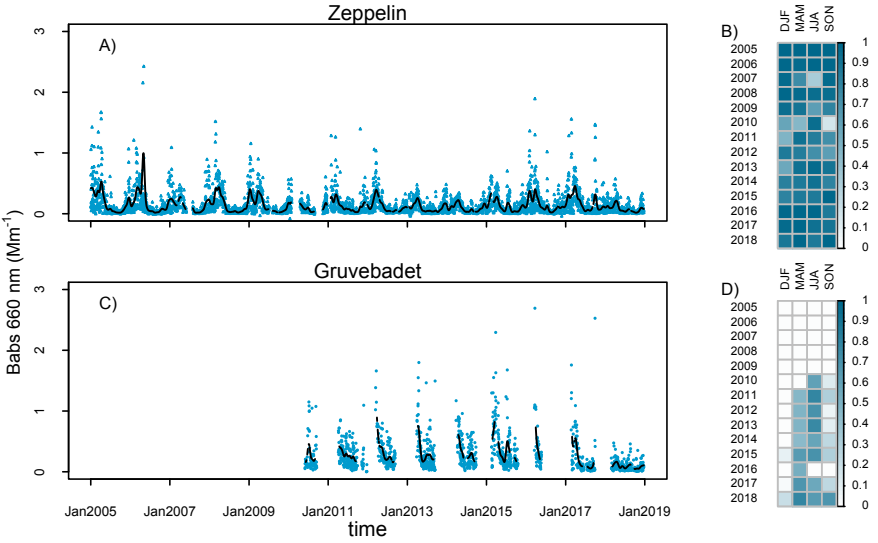

Figure 1. Time series of daily average aerosol light absorption coefficients at 660 nm from aethalometer measurements at Zeppelin (A) and PSAP measurements at Gruvebadet (C); the black line in each panel indicates the seasonal trend from the application of a Kolmogorov-Zurbenko filter. On the right, the seasonal data coverage of hourly light absorption coefficient measurements at Zeppelin (B) and Gruvebadet (D) is shown.

The black lines in Figure 1 indicate the seasonal trend of the light absorption coefficient at 660 nm, calculated with the Kolmogorov-Zurbenko (KZ) filter on daily average data. $KZ_{(m,p)}$ filter is a low-pass filter obtained by applying a moving average with a window length of m days repeated for p iterations (Wise and Comrie, 2005). To isolate the seasonal trend, m and p were here set equal to 15 and 5, respectively. Aerosol absorption coefficients show a clear seasonality, with the highest values in spring, and the lowest records in summer and fall. The observed trend is due to the enhanced transport of pollution from mid-latitudes in winter and spring (Sharma et al. 2004) and higher efficiency of wet removal in summer (Shen et al. 2017). The Gruvebadet seasonal trend showed maxima that were synchronized with those observed at Zeppelin, although with values up to 3 times higher. Notably in 2018, when both sites were characterized by significant lower concentrations of eBC compared to previous years, the seasonal trends overlapped well.

2.2. eBC Spatial variability

A climatological approach to BC and eBC distribution within Svalbard is difficult because of scarcity of long-term measurements. Nevertheless, short-term observations have been reported for several locations across the islands. eBC measurements were performed during cruises (ship measurements, e.g. Ferrero et al. 2019) and short-term intensive field campaigns (e.g. Zhan and Gao 2014; Chen et al. 2016; Ferrero et al. 2016, Lisok et al. 2016). Existing observations indicate the importance of local sources to explain spatial variability of eBC at local scale. Major land-based anthropogenic sources are located in the central part of the Spitsbergen. They are related to the settlements of Barensburg, Longyearbyen, Sveagruva, Ny-Ålesund and mining activities at Barensburg (up to 2007), Longyearbyen and Sveagruva. Occasionally, local dust storms can also be a source of absorbing aerosols (Dörnbrack et al, 2010), although it is not clear if they play a significant role in the overall aerosol characteristics of the Svalbard area.

Results of eBC (photoacoustic extinctiometer) observations in Longyearbyen, carried out within the iAREA2014 campaign (the Impact of Absorbing aerosols on Radiative forcing in the European Arctic) in spring 2014, indicate a significant impact of the local anthropogenic pollutions (Lisok et al. 2016). The absorption coefficient showed a distinct diurnal cycle with the day time maximum about 3-4 times larger than the background night values, which implies local emissions between 05:00 and 21:00 UTC. The values measured during night-time (0.6 ± 1.2 Mm^{-1}, 26 Mar - 14 Apr) were close to Ny-Ålesund levels (0.8 ± 0.4 Mm^{-1}).

The research vessel r/v Oceania (Institute of Oceanology Polish Academy of Sciences) has carried out atmospheric aerosol measurements along Svalbard every summer since 1987. In the years 2011 and 2012 (Ferrero et al. 2019), 2014, 2015, 2016, 2018, and 2019 measurements of eBC and/or EC were also performed. The EC concentrations measured in 2011-2012 (35±1 and 25±1 ng m^{-3}, respectively) were close to the eBC concentrations measured during the AREX2018 (ARctic EXperiment) cruise (Ferrero et al. 2019). The data from 2014-2016 AREX campaigns need correction for elevated relative humidity of filter samples (40-60%). Measurements which allow to estimate the impact of relative humidity on the eBC values and to optimize a correction algorithm are planned for AREX2020. During AREX2018 a considerable increase in eBC concentration near Svalbard was measured at latitudes 76-78° N (about 60-100 ng m^{-3}) when compared to seas north and south of these latitudes (10-20 ng m^{-3}), with the largest concentration near the southern coast of the archipelago (75.5-76.5 ° N). The most elevated concentrations located south of Svalbard suggest that the Black Carbon emission from marine transport may be one of the main sources. Ship emission impact on eBC is most probably limited to coastal regions and should not influence the interior of Svalbard.

The contribution of local sources, both land-based and ship emissions to the mean concentration of atmospheric eBC over Svalbard is still an open question. However, the observed east–west gradient of elemental carbon (EC) concentrations in snow over Spitsbergen (Forsström et al. 2009) suggests that the impact of the long-range transport on the atmospheric BC concentration is dominant. The snow EC gradient is the outcome of a combination of the elevated BC in air masses advected to Svalbard from the eastern sector, "the orographic effect of the archipelago, and the efficient scavenging of the carbonaceous particles through precipitation".

Recently new techniques have been developed to study the spatial distribution of eBC in local scales. Spolaor et al. (2017) presented an innovative approach to characterize concentration of atmospheric aerosol particles and air mass layering along the elevation profile of glaciers. This methodology has been employed during the BC-3D campaign (Cappelletti et al. 2019) in the Spitzbergen and Hornsund regions at Svalbard. The general observed phenomenology points at an accumulation of eBC in the lower sectors of the glaciers. Low weight and fast response sensors (microaethalometers) and a miniature Diffusion Size Classifier (miniDisc) deployed on a snowmobile were used. Measurements by means of small unmanned aerial system (UAS) carrying microaethalometers are also promising in fjord/local scales (e.g. Chiliński et al. 2019).

2.3 eBC vertical distribution

Only few experimental data on eBC vertical distribution are reported in the literature. These results have been obtained mainly with remote techniques (sun-photometers) or by in-situ observation (soot photometers and microaethalometers) deployed on aircraft, helicopters, or tethered balloons (Schwarz et al. 2010; Spackman et al. 2010; Kupiszewski et al. 2013; Bates et al. 2013; Ferrero et al. 2016; Mazzola et al. 2016; Markowicz et al. 2017).

The springtime PAM-ARCMIP (Stone et al. 2010) and HIPPO (Schwarz et al. 2010) campaigns showed high BC concentrations close to the ground, below the thermal inversion, but also dense pollution and BC at high altitudes over the Arctic. Interestingly, the PAM-ARCMIP results show a decrease of eBC compared to past measurements (i.e., AGASP; Hansen and Novakov, 1989). In addition, the HIPPO campaign revealed that in the lower troposphere the eBC vertical gradient can change seasonally from positive to negative (Schwarz et al. 2013). Spackman et al. (2010) reported eBC located mainly in the Arctic free troposphere with a positive gradient in the lower troposphere.

Regular campaigns of aerosol vertical profiles have been conducted at Ny-Ålesund at the Gruvebadet observatory in the periods 2011-2012 and 2014-2018 and at the AWIPEV observatory in the period 2015-2017 by deploying aerosol instrumentation on tethered

balloons that are able to sound the Arctic troposphere continuously at high resolution up to about 1.5 km (Moroni et al. 2015; Ferrero et al. 2016; Moroni et al. 2016; Mazzola et al. 2016; Markowicz et al. 2017). The field campaigns were manly performed in spring, and in fall in 2014 (Mazzola et al. 2016). Recently, the first winter vertical profiles in the Arctic have been reported (Nakoudi et al. 2019). eBC measurements were mainly based on the AE51 Magee Microaethalometer, a light, single wavelength (880 nm) filter-based instrument. In the 2019 winter campaign a PSAP was also deployed on the AGAP payload and intercompared with the AE51.

Spring and summer eBC profiles were compared for the period 2011-2012 (Ferrero et al. 2016). Homogeneous profiles have been observed only for 15% of the cases in spring, while they dominate (37%) in summertime. 20% of the spring profiles showed an increase of the eBC concentration with elevation, with frequent layers of BC observed around and above 1 km of altitude and attributed to long-range transport during the Arctic Haze. Averaged spring eBC concentrations exceed 5 times the summer ones. When big ships were present in the Kongsfjord strong increases (up to 40-fold) have been observed for BC concentration. This increase was observed mainly at lower altitude and for short times, i.e. before ship plume dispersion took place (Ferrero et al. 2016).

3. Unanswered questions

Long-term trends of atmospheric BC concentration show a clear seasonality, associated with long (years) and short time-scale (hours) variability. The dynamics of BC entrainment in the Arctic boundary layer is still a poorly understood process and may have a wide variability depending on local conditions. The differences in light absorption observed between Gruvebadet and Zeppelin can help to investigate such a dynamic. The two sites are located at different altitudes, but at close distance. A deeper analysis of BC (or light absorption) variability on short and long time scale, together with vertical profile measurements of BC, meteorological variables and particle number concentration (Mazzola et al. 2020) can help to better understand the impact of local sources and long-range transport on BC vertical structure. Cyclonic disturbances, low clouds dynamics and orographic effects may be some of the important factors to be studied in order to reduce the overall large uncertainties. In addition, extending the data coverage at Gruvebadet to the winter months would be beneficial for this analysis.

The year-to-year variability of light absorption observed at the two long-term monitoring sites can support a deeper investigation of all the factors affecting BC variability at Svalbard, and in the Arctic in general. BC atmospheric concentration in the Arctic region is controlled by BC emissions at high and middle latitudes, local meteorology and large-scale circulation, and BC removal efficiency through wet and dry deposition, which in turn are controlled by BC microphysical properties and meteorology. A better understanding of all the factors controlling BC atmospheric concentration and vertical distribution is a key element to improve the model ability to describe BC climate impact and reduce uncertainty of future climate scenarios.

Emission inventories indicate that implementation of climate and air quality policies in Europe and United States have efficiently contributed to fossil fuel BC emission reductions over the last 40 years. At the same time, emissions of BC from wood burning from residential heating in winter and exceptionally high emissions of BC from forest fires in summer have increased over the last 20 years due to a larger use of biofuels and increased frequency of wildfires (Chin et al. 2014). Although these changes are expected to translate non-linearly into changes in atmospheric concentration, the limited temporal and spatial coverage of existing atmospheric BC measurements cannot track these trends, specifically relevant for atmospheric and climate model validation. Sediments and ice are historical archives of atmospheric composition changes. The use of such archives requires an accurate knowledge of the BC deposition fluxes and all the mechanisms able to modify BC concentration in snow, including melting-freezing cycles and wind scouring of surface winter snow. BC long-term measurements, together with glaciers and snow monitoring activities (Schuler et al. 2020) are extremely valuable tools to better understand the link between atmosphere and cryosphere composition.

In addition to primary or processed combustion particles, secondary particles from nucleation events represent a potentially increasing source of particles in the Arctic, triggered by the sea ice melting. Long-term BC monitoring could be useful to identify the presence of anthropogenically influenced air masses during the year, linking the analysis of new particle formation events with air mass origin (Sipilä et al. 2020).

4. Recommendations for the future

- Improving the comparability and accuracy of atmospheric BC measurements, by understanding the differences among different monitoring methods (PSAP, MAAP, aethalometer, SP2) and by improving the existing correction algorithm for aerosol light absorption measurements with optical techniques. The development of a correction algorithm specifically designed and tested in the Arctic conditions, i.e. low aerosol loading and high single scattering albedo, is advisable. Experiments where different measurement techniques are co-located will support the achievement of these goals.
- Increasing space and time coverage of BC vertical profile measurements, especially during winter. Developing efficient methodology for continuous monitoring of the vertical profiles of optical properties of aerosols on a global and regional scale would improve the knowledge of BC climate impact in the Arctic.
- Promoting dry and wet deposition measurements of BC on snow surface and supporting simultaneous and long-term BC measurements in the atmosphere and cryosphere to develop reliable parameterizations of BC wet and dry deposition, BC impacts on snow and ice albedo, and to support the use of historical BC records in snow and ice to reconstruct atmospheric BC trends. The development of common discussion platforms and integrated database is recommended.
- BC-cloud interaction is a key factor affecting BC climate impact. Starting from 2015 light absorption coefficient of eBC at Zeppelin is measured with a Multi-Angle Absorption Photometer (MAAP) both inside cloud droplets and in the cloud interstitial aerosol. Similar measurements able to quantitatively describe the ability of BC particles to act as cloud condensation nuclei and ice nuclei, together with the analysis of atmospheric processes altering such ability in the Arctic, are needed.

5. Data availability

Data discussed in this report include: long-term measurements of aerosol light absorption coefficients measured at Zeppelin and provided by NCSR Demokritos (http://ebas.nilu.no/), and long-term measurements of aerosol light absorption coefficients at Gruvebadet and provided by ISP-CNR (Italian Arctic Data Centre IADC database).

Dataset	Parameters	Period	Location or area	Dataset landing page	Comment
Gruvebadet time series	Light absorption coefficients	2010-07-01 2018-12-31	Svalbard, Gruvebadet observatory	http://iadc.cnr.it/cnr/metadata_view.php?id=75	Data are available upon request. Contact: stefania.gilardoni@cnr.it
Zeppelin time series	Light absorption coefficients	2005-01-01 2018-12-31	Svalbard, Zeppelin observatory	http://ebas.nilu.no/	

Acknowledgements

This work was supported by the Research Council of Norway, project number 251658, Svalbard Integrated Arctic Earth Observing System - Knowledge Centre (SIOS-KC).

References

Andreae MO and Gelencsier A (2006) Black carbon or brown carbon? the nature of light-absorbing carbonaceous aerosols. Atmos. Chem. Phys 6(10):3131-3148.

Backman J, Schmeisser L, Virkkula A, Ogren JA, Asmi E, Starkweather S, Sharma S, Eleftheriadis K, Uttal T, Jefferson A, (2017) On aethalometer measurement uncertainties and an instrument correction factor for the Arctic. Atmos. Meas. Tech 5039–5062.

Bates TS, Quinn PK, Johnson JE, Corless A, Brechtel F J, Stalin SE, Meinig C, and Burkhart J (2013) Measurements of atmospheric aerosol vertical distributions above Svalbard, Norway, using unmanned aerial systems Atmos. Meas. Tech. 6:2115–2120.

Bergstrom RW, Pilewskie P, Russell PB, Redemann J, Bond TC, Quinn P K, and Sierau B (2007) Spectral absorption properties of atmospheric aerosols. Atmos. Chem. Phys. 7:5937-5943.

Bond TC and Bergstrom RW (2006) Light absorption by carbonaceous particles: An investigative review. Aerosol Sci. and Tech 40(1):27-67.

Bond TC, Anderson TL, and Campbell D (1999) Calibration and intercomparison of filter-based measurements of visible light absorption by aerosols. Aerosol Sci. and Tech. 30(6): 582-600.

Bond TC, Doherty SJ, Fahey DW, Forster PM, Berntsen T, DeAngelo BJ, Flanner MG, Ghan S, Kärcher B, Koch D, Kinne S, Kondo Y, Quinn PK, Sarofim MC, Schultz MG, Schulz M, Venkataraman C, Zhang H, Zhang S, Bellouin N, Guttikunda SK, Hopke PK, Jacobson MZ, Kaiser JW, Klimont Z, Lohmann U, Schwarz JP, Shindell D, Storelvmo T, Warren SG, and Zender CS (2013) Bounding the role of black carbon in the climate system: A scientific assessment.J. Geophys. Res.-Atmos 118:5380-5552.

Boucher O, Randall D, Artaxo P, Bretherton C, Feingold G, Forster P, Kerminen V, Kondo Y, Liao H, Lohmann U, Rasch P, Satheesh SK, Sherwood S, Stevens B, and Zhang X (2013) Clouds and aerosols. In Climate change 2013: the physical science basis. Contribution of Working Group I to the Fifth Assessment Report of the Intergovernmental Panel on Climate Change571-657. Cambridge University Press.

Cappelletti D, Petroselli C, Moroni B, Gallet JC, Hudson S, Isaksson E, Luks B, Nawrot A, Maturilli M, Ritter Ch, Neuber R, Mazzola M, Viola A, Barbaro E, Spolaor A, Larose C (2019) Spatial distributions of black carbon and mineral dust in air and snow surface layers upon Svalbard glaciers: the BC-3D project (a Svalbard Strategic Grant) final report, Svalbard Science Conference, Oslo, 5-6 November 2019.

Chen L, Li W, Zhan J, Wang J, Zhang Y, and Yang X (2016) Increase in aerosol black carbon in the 2000s over Ny-Alesund in the summer. J. Atmos. Sci, 73(1):251-262.

Chilinski MT, Markowicz KM, Zawadzka O, Stachlewska IS, Lisok J, and Makuch P (2019) Comparison of columnar, surface, and uas profiles of absorbing aerosol optical depth and single scattering albedo in south-east Poland. Atmosphere 10(8):446.

Chin M, Diehl T, Tan Q, Prospero J, Kahn R, Remer L, Yu H, Sayer A, Bian H, Geogdzhayev I, et al. (2014) Multi-decadal aerosol variations from 1980 to 2009: a perspective from observations and a global model. Atmos. Chem. Phys. 14:3657-3690.

Dang C, Warren SG, Fu Q, Doherty SJ, Sturm M, and Su J (2017) Measurements of light-absorbing particles in snow across the Arctic, North America, and China: Effects on surface albedo. J. Geophys. Res.-Atmos 122(19):10-149.

Doherty S, Bitz C, and Flanner M (2014) Biases in modelled surface snow BC mixing ratios in prescribed aerosol climate model runs. Atmos. Chem. Phys 14(21):11697-11709.

Dörnbrack A, Stachlewska I, Ritter C, and Neuber R (2010) Aerosol distribution around Svalbard during intense easterly winds. Atmos. Chem. Phys 10(4):1473-1490.

Eleftheriadis K, Vratolis S, and Nyeki S (2009) Aerosol black carbon in the European Arctic: measurements at Zeppelin station, Ny-Alesund, Svalbard from 1998-2007. Geophys. Res. Lett. 36(2):L02809.

Ferrero L, Cappelletti D, Busetto M, Mazzola M, Lupi A, Lanconelli C, Becagli S, Traversi R, Caiazzo L, Giardi F, et al. (2016) Vertical profiles of aerosol and black carbon in the Arctic: a seasonal phenomenology along 2 years (2011-2012) of field campaigns. Atmos. Chem. and Phys 16(19):12601-12629.

Ferrero L, Sangiorgi G, Perrone MG, Rizzi C., Cataldi M, Markuszewski P, Pakszys P, Makuch P, Petelski T, Becagli S, et al. (2019) Chemical composition of aerosol over the Arctic ocean from summer Arctic expedition (arex) 2011{2012 cruises: Ions, amines, elemental carbon, organic matter, polycyclic aromatic hydrocarbons, n-alkanes, metals, and rare earth elements. Atmosphere 10(2):54.

Forsström S, Ström J, Pedersen C, Isaksson E, and Gerland S (2009) Elemental carbon distribution in Svalbard snow. J. Geophis. Res.- Atmos. 114(D19), 2009.

Ginot P, Dumont M, Lim S, Patris N, Taupin J-D, Wagnon P, Gilbert A, Arnaud Y, Marinoni A, Bonasoni P, et al. (2014) A 10 year record of black carbon and dust from a Mera peak ice core (Nepal): variability and potential impact on melting of Himalayan glaciers. Cryosphere 8 (4):1479-1496.

Hadley OL and Kirchstetter TW (2012) Black-carbon reduction of snow albedo. Nat. Clim. Change 2(6):437.

Hansen A and Novakov T (1989) Aerosol black carbon measurements in the Arctic haze during agasp-ii. J. Atmos. Chem 9(1-3):347-361.

Jacobson MZ (2010) Short-term effects of controlling fossil-fuel soot, biofuel soot and gases, and methane on climate, Arctic ice, and air pollution health. J. Geophis. Res.- Atmos.115(D14).

Jiao C, Flanner M, Balkanski Y, Bauer S, Bellouin N, Berntsen T, Bian H, Carslaw K, Chin M, De Luca N, et al. (2014) An Aerocom assessment of black carbon in Arctic snow and sea ice. Atmos. Chem. Phys. 14(5):2399-2417.

Kirchstetter TW, Novakov T, and Hobbs PV (2004) Evidence that the spectral dependence of light absorption by aerosols is affected by organic carbon. J. Geophys. Res. 109:D21208.

Koch D and Del Genio AD (2010) Black carbon semi-direct effects on cloud cover: review and synthesis. Atmos. Chem. Phys 10(16):7685-7696.

Kupiszewski P, Leck C, Tjernström M, Sjogren S, Sedlar J, Graus M, Müller M, Brooks B, Swietlicki E, Norris S et al. (2013) Vertical profiling of aerosol particles and trace gases over the central Arctic ocean during summer. Atmos. Chem. Phys 13(24):12405-12431.

Lack DA, Cappa CD, Covert DS, Baynard T, Massoli P, Sierau B, Bates TS, Quinn PK, Lovejoy ER, and Ravishankara A. (2008) Bias in filter-based aerosol light absorption measurements due to organic aerosol loading: Evidence from ambient measurements. Aerosol Sci. Tech.42(12):1033-1041.

Lack DA, Moosmüller H, McMeeking GR, Chakrabarty RK, and Baumgardner D (2014) Characterizing elemental, equivalent black, and refractory black carbon aerosol particles: a review of techniques, their limitations and uncertainties. Anal. Bioanal. Chem. 406(1): 99-122.

Lisok J, Markowicz K, Ritter C, Makuch P, Petelski T, Chilinski M, Kaminski J, Becagli S, Traversi R, Udisti R, et al. (2016) 2014 Iarea campaign on aerosol in Spitsbergen-part 1: Study of physical and chemical properties. Atmos. Env 140:150-166.

Mahmood R, von Salzen K, Flanner M, Sand M, Langner J, Wang H, and Huang L (2016) Seasonality of global and Arctic black carbon processes in the Arctic monitoring and assessment programme models. J. Geoph. Res.-Atmos 121(12):7100-7116.

Markowicz K, Ritter C, Lisok J, Makuch P, Stachlewska I, Cappelletti D, Mazzola M, and Chilinski M (2017) Vertical variability of aerosol single-scattering albedo and equivalent black carbon concentration based on in-situ and remote sensing techniques during the Iarea campaigns in Ny- Ålesund. Atmos. Env. 164:431-447.

Mazzola M, Busetto M, Ferrero L, Viola AP, and Cappelletti D (2016) Agap: an atmospheric gondola for aerosol profiling. Rendiconti Lincei, 27(1):105-113.

Mazzola M, Viola AP, Cappelletti DM, Ritter C, Storvold R (2020) Probing of the Vertical Structure of the lower Atmosphere over Svalbard. In: Van den Heuvel et al. (eds): SESS report 2019, Svalbard Integrated Arctic Earth Observing System, Longyearbyen, 212 - 235 . https://sios-svalbard.org/SESS_Issue2

Moroni B, Becagli S, Bolzacchini E, Busetto M, Cappelletti D, Crocchianti S, Ferrero L, Frosini D, Lanconelli C, Lupi A, et al. (2015) Vertical profiles and chemical properties of aerosol particles upon Ny-Ålesund (Svalbard islands). Adv. Meteorol 292081.

Moroni B, Cappelletti D, Ferrero L, Crocchianti S, Busetto M, Mazzola M, Becagli S, Traversi R, and Udisti R (2016) Local vs. long-range sources of aerosol particles upon Ny-Ålesund (Svalbard islands): mineral chemistry and geochemical records. Rendiconti Lincei 27(1):115-127.

Nakoudi K, Ritter C, Mazzola M, Cappelletti D, Böckmann C, Maturilli M, Neuber R (2019) Synergistic Investigation of Arctic Aerosol in the darkness: remote sensing and in-situ observations, Svalbard Science Conference, Oslo, 5-6 November 2019.

Park RJ, Jacob DJ, Palmer P, Clarke A., Weber RJ., Zondlo M, Eisele F, Bandy A, Thornton D, Sachse G, and Bond TC (2005) Export efficiency of black carbon aerosol in continental outflow: Global implications. J. Geophys. Res.-Atmos. 110(D11).

Petzold A, Ogren JA, Fiebig M, Laj P, Li S-M, Baltensperger U, Holzer-Popp T, Kinne S, Pappalardo G, Sugimoto N, et al. (2013) Recommendations for reporting" black carbon" measurements. Atmos. Chem. Phys. 13(16):8365-8379.

Popovicheva OB, Evangeliou N, Eleftheriadis K, Kalogridis AC, Sitnikov N, Eckhardt S, and Stohl A (2017) Black carbon sources constrained by observations in the Russian high Arctic. Environ. Sci. Technol 51(7):3871-3879.

Quinn PK, Stohl A, Arneth A, Berntsen T, Burkhart JF, Christensen J, Flanner MG, Kupiainen K,Lihavainen H, Shepherd M, Shevchenko V, Skov H, and Vestreng V (2011) The impact of black carbon on Arctic climate. Technical report, Arctic Monitoring and Assessment Programme 2011.

Quinn PK, Stohl A, Arnold S, Baklanov A, Berntsen T, Christensen J, Eckhardt S, Flanner MG, Klimont Z, Korsholm S, Kupiainen K, Langner J, Law K, Monks S, von Salzen K, Sand M, Schmale J, and Vestreng V (2015) Black carbon and ozone as Arctic climate forcers. Technical report, Arctic Monitoring and Assessment Programme 2015.

Russell P, Bergstrom R, Shinozuka Y, Clarke A, DeCarlo P, Jimenez J, Livingston J, Redemann J, Dubovik O, and Strawa A (2010) Absorption Angstrom Exponent in Aeronet and related data as an indicator of aerosol composition. Atmos. Chem. Phys 10(3):1155-1169.

Sand M, Berntsen T K, Kay J E, Lamarque J F, Seland Ø, Kirkevåg A (2013) The Arctic response to remote and local forcing of black carbon. Atmos. Chem. Phys., 13, 211–224.

Sand M, Berntsen T, Von Salzen K, Flanner M, Langner J, and Victor D (2016) Response of Arctic temperature to changes in emissions of short-lived climate forcers. Nat. Clim. Change 6(3): 286.

Schwarz JP, Spackman JR, Gao RS, Watts LA, Stier P, Schulz M, Davis SM, Wofsy SC, and Fahey DW (2010) Global-scale black carbon profiles observed in the remote atmosphere and compared to models. Geophys. Res. Lett. 37(18): L18812.

Schwarz J, Gao R, Perring A, Spackman J, and Fahey D. (2013) Black carbon aerosol size in snow. Sci.Rep 3:1356.

Schuler TV, Glazovsky A, Hagen JO, Hodson A, Jania J, Kääb A, Kohler J, Luks B, Malecki J, Moholdt G, Pohjola V, van Pelt W (2020), SvalGlac: New data, new techniques and new challenges for updating the state of Svalbard glaciers. In: Van den Heuvel et al. (eds): SESS report 2019, Svalbard Integrated Arctic Earth Observing System, Longyearbyen, **108 - 135** . **https://sios-svalbard.org/SESS_Issue2**

Sharma S, Lavoué D, Cachier H, Barrie LA, and Gong SL (2004) Long-term trends of the black carbon concentrations in the Canadian Arctic. J. Geophys. Res., 109(D15):D15203.

Sharma S, Leaitch WR, Huang L, Veber D, Kolonjari F, Zhang W, Hanna SJ, Bertram AK,

and Ogren JA (2017). An evaluation of three methods for measuring black carbon in Alert, Canada. Atmos. Chem. Phys 17(24): 15225–15243.

Shen Z, Ming Y, Horowitz LW, Ramaswamy V, and Lin M (2017) On the seasonality of Arctic black carbon. J. Clim 30(12):4429-4441.

Sipilä M, Hoppe CJM, Viola A, Mazzola M, Krejci R, Zieger P, Beck L, Petäjä T (2020) Multidisciplinary research on biogenically driven new particle formation in Svalbard. In: Van den Heuvel et al. (eds): SESS report 2019, Svalbard Integrated Arctic Earth Observing System, Longyearbyen, **168 - 195** . **https://sios-svalbard.org/SESS_Issue2**

Spackman J, Gao R, Neff W, Schwarz J, Watts L, Fahey D, Holloway J, Ryerson T, Peischl J, and Brock C. (2010) Aircraft observations of enhancement and depletion of black carbon mass in the springtime Arctic. Atmos. Chem. Phys., 10(19):9667-9680.

Spolaor A, Barbaro E, Mazzola M, Viola AP, Lisok J, Obleitner F, Markowicz KM, and Cappelletti D (2017) Determination of black carbon and nanoparticles along glaciers in the Spitsbergen (Svalbard) region exploiting a mobile platform. Atmo. Environ. 170:184-196.

Stone RS, Herber A, Vitale V, Mazzola M, Lupi A, Schnell R, Dutton E, Liu P, Li S.-M, Dethlo K, et al. (2010) A three-dimensional characterization of Arctic aerosols from airborne sun photometer observations: Pam-Arcmip, April 2009. J. Geophys. Res.-Atmos, 115:D1320.

Stone RS, Sharma S, Herber A, Eleftheriadis K, Nelson DW (2014) A characterization of Arctic aerosols on the basis of aerosol optical depth and black carbon measurements. Elem Sci Anth, 2: 000027.

Subramanian R, Roden CA, Boparai P, and Bond TC (2007) Yellow beads and missing particles: Trouble ahead for filter-based absorption measurements. Aerosol Sci. Tech. 41(6): 630-637.

Wang H, Rasch PJ, Easter RC, Singh B, Zhang R, Ma P-L, Qian Y, Ghan SJ, and Beagley N (2014) Using an explicit emission tagging method in global modelling of source-receptor relationships for black carbon in the Arctic: Variations, sources, and transport pathways. J. Geophys. Res.-Atmos. 119(22):12,888-12,909.

Wang Q, Jacob DJ, Fisher JA, Mao J, Leibensperger E, Carouge C, Sager PL, Kondo Y, Jimenez J, Cubison M, et al. (2011) Sources of carbonaceous aerosols and deposited black carbon in the Arctic in winter-spring: implications for radiative forcing. Atmos. Chem. Phys 11(23):12453-12473.

Winiger P, Andersson A., Eckhardt S, Stohl A, Semiletov IP., Dudarev OV, Charkin A, Shakhova N, Klimont Z, Heyes C, et al. (2017) Siberian Arctic black carbon sources constrained by model and observation. Proc Natl Acad Sci U S A 114(7):E1054-E1061.

Winiger P, Barrett T, Sheesley R, Huang L, Sharma S, Barrie LA, Yttri KE, Evangeliou N, Eckhardt S, Stohl A, et al. (2019) Source apportionment of circum-Arctic atmospheric black carbon from isotopes and modelling. Sci. Adv. 5(2):eaau8052.

Wise EK and Comrie AC (2005) Extending the Kolmogorov-Zurbenko filter: application to ozone, particulate matter, and meteorological trends. J Air Waste Manag Assoc 55(8):1208-1216.

Xu J, Zhang J, Liu J, Yi K, Xiang S, Hu X, Wang Y, Tao S, and Ban-Weiss G (2019) Influence of cloud microphysical processes on black carbon wet removal, global distributions, and radiative forcing. Atmos. Chem. Phys. 19(3):1587-1603.

Zanatta M, Gysel M, Bukowiecki N, Müller T, Weingartner E, Areskoug H, Fiebig M, Yttri KE, Mihalopoulos N, Kouvarakis G, et al. (2016) A European aerosol phenomenology-5: Climatology of black carbon optical properties at 9 regional background sites across Europe. Atmos. Environ. 145:346-364.

Zanatta M, Laj P, Gysel M, Baltensperger U, Vratolis S, Eleftheriadis K, Kondo Y, Dubuisson P, Winiarek V, Kazadzis S, et al. (2018) Effects of mixing state on optical and radiative properties of black carbon in the European Arctic. Atmos. Chem. Phys. 18(19):14037-1405.

Zhan J, Gao Y (2014) Impact of summertime anthropogenic emissions on atmospheric black carbon at Ny-Ålesund in the Arctic. Polar Research, 33, 1, 21821.

Probing of the Vertical Structure of the lower Atmosphere over Svalbard (ProVeSAS)

Mauro Mazzola[1], Angelo Pietro Viola[2], David Michele Cappelletti[3], Christoph Ritter[4], Rune Storvold[5]

1 Institute of Polar Sciences, National Research Council of Italy, Via P. Gobetti 101, 40129 Bologna, Italy
2 Institute of Polar Sciences, National Research Council of Italy, Via Fosso del Cavaliere 100, 00133 Rome, Italy
3 University of Perugia, Department of Chemistry, Biology and Biotechnology, Via Elce di Sotto 8, 06123 Perugia, Italy
4 Alfred Wegener Institute, Telegrafenberg, Gebäude A43-45, Potsdam, Germany
5 Norwegian Research Centre AS, SIVA Innovasjonssenter, Sykehusvn 21, Tromsø, Norway

Corresponding author: Mauro Mazzola, mauro.mazzola@cnr.it,
ORCID number 0000-0002-8394-2292

Keywords: Atmospheric profiles, meteorology, aerosol, clouds, radiosonde, tethered balloon, remote sensing, UAV, drones

1. Introduction

Atmospheric measurements in the Arctic are still considered scarce in number and geographical cover. For in situ measurements, this is due to the harsh conditions that need to be faced out and to the low population that is living at these latitudes. Even remote sensing from satellite is limited to the sunny season for some of the atmospheric parameters and detection techniques (e.g. passive remote sensing of aerosol and gases). This shortage is even more evident if one wants to go beyond the ground level measurements and obtain information on the vertical structure of the atmosphere. Existing records of upper-air measurements are insufficient for studying the climate change, as they mainly lack continuity, homogeneity and representativeness of data.

Historically, the vertical profiles of meteorological parameters such as temperature, humidity, wind speed and direction, i.e. meteorological soundings, were the first to be obtained on large scale and they constitute a fundamental input for meteorological forecast models (Ingleby et al. 2018). Before that, it had to be deduced from surface charts, a few scattered balloon and meteorograph ascents and mountain observations. It became very soon a standard for meteorology, considered that a code for the international exchange of radiosonde data was already adopted in 1946. For what concerns other measurements, such as those regarding atmospheric constituents, airborne campaigns remained for long time the only possibility, despite its very high cost. Other techniques that were developed already some decades ago make use of remote sensing, optical and acoustic, to infer some of the properties of the atmosphere through inversion of the measured echoes. Thanks to the technological improvements of the last years that permitted to realize very small and light devices able to measure many atmospheric parameters, new probing techniques are emerging, such as the use of tethered balloon and drones which can host an increasing number of sensing devices.

In this contribution, we review the existing techniques suitable for atmospheric profiling. In Section 2 they are briefly described, defining pros and cons for each of the considered ones. In Section 3 the results obtained by using such techniques in Svalbard and surroundings are reported and summarized, providing references to the relevant literature. This contribution is ideally an extension of Viola et al. (2019) in the SESS report 2018, with the aim to be more specific on studies about the atmospheric vertical column. The techniques illustrated here can be applied for studies described in two chapters of the current issue: 'Atmospheric Black Carbon at Svalbard' (Gilardoni et al. 2020), and 'Multidisciplinary research on biogenically driven new particle formation in Svalbard (Sipilä et al. 2020). Vertical measurements can be useful to understand how local emissions diffuse on the column, or to study the long-range transport of pollution from lower latitudes during the Arctic haze. Ferrero et al. (2016) reported on both these two processes for black carbon in Ny-Ålesund using tethered balloon measurements. Furthermore, in the scientific community is not clear which is the

role of black carbon in the formation and evolution of clouds: are they good condensation nuclei or not? Example of studies of new particle formation and ice nuclei on the vertical column can be found in Hoppel et al. (1973), Clarke and Kapustin (2010) and Kontkanen et al. (2016).

2. Overview of existing knowledge

2.1 Existing techniques: history, pros and cons

While there are advantages and disadvantages employing all of the measurement platforms, data can be combined synergistically to build a more comprehensive picture of the lower atmosphere. For example, aircraft measurements that cover a large spatial area can be integrated with the column model provided by a tethered balloon to improve comparisons with simulations. Remote sensing measurements need to be analysed with inverse methods, in order to retrieve actual atmospheric parameters, and hence, direct measurements from unmanned aerial vehicles (UAVs) or balloons are of help in checking the results.

2.1.1 Radiosonde, ozonesonde, dropsonde, driftsonde, controlled balloons

Radiosondes were invented in 1930 by aerologist Pavel Molchanov, as well as the method for using it to study the atmosphere. The next year he was invited by German scientists to join an expedition to the Arctic with the dirigible Graf Zeppelin to operate radiosondes at Polar latitudes. Twelve probes were successfully launched and is surprising that the first observations were conducted in the Arctic. The technological development permitted to obtain miniaturized devices that weigh less than 200 g, instead of the first prototypes weighing about two kilograms, and they can take measurements up to 40 km, drifting for thousand kilometres. Sensors are raised by helium-filled latex balloons that expand gradually, till explosion. Very recently, the use of corn balloons has been introduced in order to reduce the environmental impact. Modern radiosondes can even determine the intensity of radiation, cosmic rays and ozone concentrations. Other supplemental measurements in use today include optical backscattering by particles, electric field, and video imaging of particles and hydrometeors. The same sensors can be adopted by dropsondes, devices designed to be released from aircraft in order to measure atmospheric parameters as the device falls to the surface, slowed by a parachute. They are suitable to be used over remote areas such as the oceans, polar regions, and sparsely inhabited landmasses; they also provide a means to obtain soundings in and around severe weather systems, such as hurricanes. A similar concept is used in the driftsonde system, in this case the sondes are released from a gondola attached to a specially designed balloon platform. An approach that is halfway between radiosonde and tethered balloon is that of the so called controlled meteorological

(CMET) balloons. They can fly for several days in the troposphere with altitude controlled via satellite link (Voss et al. 2013). Altitude control (0-3500 m) is achieved by a dual balloon design (high-pressure inner and low-pressure outer balloon) between which helium is transferred by a pump–valve system.

In general, pros of this kind of measurement techniques are: they provide direct in-situ measurement of many atmospheric parameters; near real-time information are available for the entire globe; 1-2 times per day a snapshot of the global atmosphere (radiosonde); good vertical resolution (about 10 m); they can measure in any meteorological condition. On the other hand, the cons to be considered are: indirect measurement of wind speed and direction; not continuous over long periods; the sensors, as well as the balloons, are lost for each launch (cost and pollution).

2.1.2 Tethered balloons

Alfred Wegener was the first, in 1906, to use tethered balloons (TB) and kites for studying the Polar atmosphere during an expedition in Greenland. Since Wegener, TB have been employed in many locations to study in-situ microphysical parameters of the atmosphere (Morris et al. 1975; Duda et al. 1991; Argentini et al. 1999; Tjernström et al. 2004; Maturilli et al. 2008; Maturilli et al. 2009; Sikand et al. 2010 and 2013; Becker et al. 2018; Egerer et al. 2019), gaseous air pollution (Rankin et al. 2002; Armstrong et al. 1981; Davis et al. 1994; Pisano et al. 1997; Johnson et al. 2008) and aerosol properties (Maletto et al. 2003; Ferrero et al. 2007 and 2012; Hara et al. 2013; Li et al. 2015). A TB system has also been employed in 2007/2008 during the 35th Russian North Pole Ice drifting station (NP-35) to study the dynamics and the structure of the boundary layer (Maturilli et al. 2008). The advantage of in-situ measurements is that they are usually very specific and accurate and do not require a precise understanding of the radiative or acoustic properties of the atmosphere, such as are needed for remote sensing. An important concern of in-situ measurements is insuring the sample is not altered as it is being brought into the measuring device. In general, a TB system is capable of making repeated vertical profiles at high spatial resolution of particle concentrations, meteorological parameters, microphysical and radiative properties of boundary layer clouds. Typical maximum altitudes sounded by a TB system are in the range of 1-2 km.

Pros of TB platforms are: they can stay aloft and collect data for long periods (hours); vertical profiles are possible continuously from ground to about 2 km all the way up and down; profiles are nearly vertical (if wind speed is moderate); the relatively slow ascending/descending speed (typically between 30 and 80 m/min) maximize the spatial resolution and minimize sampling artefacts at the instrument inlets; the cost of operation of a TB is a relatively low if compared with other devices. Cons of a TB include: the payload can't be too heavy; operation is restricted to moderate wind conditions (<10 m/s); operation inside

clouds could be subject to icing of the balloon and possibly sudden falls.

2.1.3 Remote sensing: radiometers, SODAR, LIDAR

Remote sensing instruments are by definition not in direct contact with the object, which is to be measured. Hence, by remote sensing instruments, which are ground based or looking downwards from satellites and planes, one can obtain information of (a part of) the atmospheric column without the need of flying in all individual layers. They are further subdivided into "active" and "passive" instruments, depending on whether they emit directly signals (light or sound) or whether they only passively detect natural emissions. Typically, active remote sensing instruments allow for a higher vertical resolution for the price of a more complicated, expensive instruments and the need of a more elaborate data evaluation. Generally, remote sensing instruments got mature in technology. Many environmental quantities like humidity, wind, temperature, trace gas concentration, aerosol and clouds can be measured by dedicated instruments. However, the evaluation of data requires sometimes a complicated physical model or even inverse techniques. An example for easy remote sensing measurement is a wind LIDAR that only requires knowledge of the spectral Doppler shift. Contrary, the derivation of aerosol microphysical properties from remote sensing relies on a scattering theory (for the irregularly shaped aerosol). For this reason, aerosol properties from remote sensing instrument will not have the same precision as in-situ instruments and fully equipped supersites are needed in all climate zones to calibrate the remote sensing instruments by in situ measurements. Microwave radiometers (MWR) measure thermal electromagnetic radiation emitted by atmospheric gases at millimetre-to-centimetre wavelengths. As the atmosphere is semi-transparent in this spectral range, including cloudy sky, they can operate under nearly all weather conditions, continuously and autonomously. They allow to derive important meteorological quantities such as vertical temperature and humidity profile, columnar water vapour amount, or columnar liquid water path with a high temporal resolution in the order of seconds to minutes. First developments of MWR were dedicated to the measurement of radiation of extra-terrestrial origin in the 1930s, but the first application to the study of the atmosphere appeared in the 60s of the same century. Atmospheric LIDAR (acronym for LIght Detection And Ranging) is a class of instruments that uses laser light to study atmospheric properties from the ground up to the top of the atmosphere. Such instruments have been used to study, among other, atmospheric gases, aerosols, clouds, wind and temperature. The basic concepts to study the atmosphere using light were first developed by E.H. Synge in the 1930s to study the density of the upper atmosphere using a searchlight beam. During the first experiments, light scattering patterns observed in the troposphere were not compatible with a pure molecular atmosphere. This incompatibility was attributed to suspended haze particles. After the development of lasers, the LIDAR technique made an enormous step over and by the end of the 1960s, over 20 lasers were already in use by meteorologists in the United States for various applications. SOnic Detection And Ranging (SODAR) is a simple and economically effective device for the

ground-based remote sensing of the lower troposphere. The principal physics of acoustic sounding was given by A.M. Obukhov in the 40s of the nineteenth century. The theory of operation is based on the reflection of acoustic pulses at temperature inhomogeneities in the air with subsequent Doppler effect analysis. Minimum height level for the measurements can be as low as 30 m, while the maximum height depends on the atmospheric conditions, during calm days reaching up to 800 m while during windy days not even surpassing 300 m. Using SODARs, a vast amount of knowledge about the structure and dynamics of the atmospheric boundary layer (ABL) can been obtained.

Pros: the observed atmospheric target is not disturbed; operation can be continuous and automatic. Cons: a theory for interpretation of data and retrieving the final information is needed; some kind of instrumentation are sophisticated and hence costly; some observations depend on weather conditions (wind speed, cloudiness); there could be some "blind" layers, for example some hundreds meters above the surface.

2.1.4 Unmanned aerial vehicles

The development of UAVs (or aerial drones or simply drones) technology is rapid and their use is increasing fast. They are being used to collect data in a wide range of scientific disciplines. Their capabilities, with regard to available sensors reliability and performance are increasing rapidly and reduced costs make them more feasible. The main advantages with drones as a measurement platform is that they provide a way to gather data in form of profiles and transects from local to regional scale, bridging point measurements and satellite measurements and allowing for both remote sensing type of sensors as well as in-situ techniques. Compared to manned aircraft, the coverage is usually much more limited but the footprint of the operation is much smaller, and usually emission free, with the exception of the larger long range systems today. Drones have usually less payload capacity than manned aircraft but can to a larger extent be optimized to the payload needs in regard to size and range and be more affordable. Drones also reduce the risk for personnel and can be flown in conditions when manned aircraft could not be used. There are designed drones that can be dropped by weather balloons from up to 40 km altitude and glide back to the starting position, hence securing vertical profiles and reusable payloads, allowing advanced in situ gas and aerosol measurements through the stratosphere and troposphere at an affordable cost. Some of the challenges with using aircraft and drones for atmospheric measurements is that the vehicle is a part of the sensor so care must be taken in integration, calibration and validation of sensors in particular for in-situ measurements. Further, certain types of measurements would require the establishment of a temporal danger area to ensure segregation to other air traffic when flying beyond visual line of sight and above 120 m of the ground. This is a process that could take up to 4 months under current regulations. Initiatives for the developing, fielding, and evaluating of integrated small unmanned aircraft systems for enhanced atmospheric physics measurements exists (Jacob et al. 2018).

2.2 Measurements taken in Svalbard and surroundings: scientific results and knowledge

2.2.1 Radiosonde, ozonesonde, dropsonde, driftsonde, controlled balloon

Routine daily radiosonde launches started in Svalbard during October 1991 from the AWI observatory in Ny-Ålesund. The sondes are launched daily at 11 a.m. UTC while, occasionally and during special programs, multiple launches are made per day. Collected data have been used by many publications as a result of specific campaigns or studies. Treffeisen et al. (2007) used fifteen years of data (1991-2006, 5718 launches in total) to retrieve the key characteristics of the vertical relative humidity evolution in the troposphere over Ny-Ålesund. They found that supersaturation with respect to ice is observed all year round, with a clear seasonal trend, from 19% of occurrence during winter, 12% during spring and 9% during summer. The ice-supersaturation layers were found between 6 and 9 km during winter, while they shift higher during summer. This is in accordance with the results obtained from the SAGE II experiment for sub-visible clouds, indicating that this phenomenon is diffused over the Arctic. A shorter subset (1993-2006) of the above mentioned data was used by Dahlke and Maturilli (2017) to quantify the contribution of the advection to the observed atmospheric warming over Svalbard, showing a strong dependence on the synoptic flow. Analysing FLEXPART back-trajectories, they found that the recent change in the atmospheric circulation favours an increased advection of moist and warm air from the lower latitude Atlantic region. This is valid not only for surface temperatures, but for the entire troposphere. A temperature increase of about 0.45 K per decade over the estimated 2 K for the entire Arctic is attributable to this phenomenon. The difference in tropospheric temperature for airmasses coming from south to that coming from north can reach up to 8 K. Maturilli and Kayser (2017) compiled a homogenized dataset from Ny-Ålesund radiosondes for the period from 1993 to 2014. They found a strong increase in atmospheric temperature and humidity, in particular during winter and below 1 km, as a consequence of a change on the atmospheric circulation[1]. Radiosondes have been launched form the R/V Polarstern, managed by AWI, during cruises around the Arctic and Svalbard in particular. Yamazaki et al. (2015) used observations from radiosondes launched twice per day during the ARK-XXVII/1 and /2 cruises (13 to 29 July 2012) to determine the impact of such additional information on the forecast of an intense Arctic cyclone. They were found to be essential for the prediction, even if the observation were taken far from the actual location of the cyclone, thanks to the reproducibility of the large-scale upper tropospheric circulation pattern. This is not usually possible only relying on the information given by drifting buoys at the surface. Kayser et al. (2017) studied the vertical thermodynamic structure of the troposphere during the Norwegian young sea ICE expedition (N-ICE2015). During the cruise (January to June 2015) radiosondes were launched twice per day. They provided

1 The resulting record is available at http://doi.pangaea.de/10.1594/PANGAEA.845373.

statistics of temperature inversion, stability, and boundary layer extent. Radiative cooling is more effective during winter, when also the strongest impact of synoptic cyclones was found. In spring radiative fluxes warm the surface, leading to lifted temperature inversions and a statically unstable boundary layer.

Weekly ozonesonde profiling started in Ny-Ålesund even earlier, during 1988, by the same institution, the launches being always in tandem with the meteorological ones (Schrems 1992). The ozone sensor measures the ozone partial pressure by means of an electrochemical concentration cell, from which the ozone volume mixing ratios can be calculated with a vertical resolution of about 150 m. Wessel et al. (1998) studied the vertical extent of tropospheric ozone minima (detected by continuous surface ozone measurements) increasing the number of launches up to two times per day. During those periods, they determined the following common situations: the depleted layers were restricted to the planetary boundary layer (PBL), where the relative humidity was above 80% and the surface temperature generally decreased by 5–20 K during the event. Usually, temperature inversion coincided with the top of the ozone poor air mass, preventing vertical intrusion from above. The inversion layer height varied between 100 m and 600 m, while a stable stratification was found within the ozone depleted layer. Rex and von der Gathen (2004) analysed data for 10 winters between 1991 and 2003 applying a method (Match) developed to quantify the vertical distribution of the ozone loss. They found that chemical ozone loss indeed occurs in the Arctic and that periods of strong loss were associated with very cold periods and polar stratospheric clouds (PSC) formation. On the contrary, during warm winters, e.g. 1998-1999, no significant loss was detected. Kivi et al. (2007) studied the inter-annual variability and recent trends in Arctic ozone profiles from seven Arctic stations, including Ny-Ålesund, from 1989 to 2003, using a statistical model. Long-term changes have been identified during late winter/spring period for both the stratosphere and troposphere. Negative trends in the lower stratosphere prior to 1997 can be attributed to the combined effect of dynamical changes, the impact of aerosols from the Mt. Pinatubo eruption and winters of relatively large chemical ozone depletion. Since 1996–1997 the observed increase in lower stratospheric ozone can be attributed primarily to dynamical changes. In the free troposphere, a statistically significant increase over the 15 years' period, can likely be attributed to the effects of changes in the Arctic oscillation. Ozone amounts in the stratosphere were found to highly correlate with proxies for the stratospheric circulation, Polar ozone depletion and tropopause height. Petkov et al. (2018) studied the main characteristics of the joint meteorological (temperature and wind speed) and ozone vertical profiles over 1992-2016 (2207 profiles), using a statistical approach. They identified two main subsets, one corresponding to intra-seasonal variations (periods between 30 and 60 days) and another one corresponding to inter-annual variations (period longer than 1 year). Peculiarly, the first two components of the infra-seasonal variations seem to be influenced by phenomena like ozone depletion and solar eclipses. In the inter-annual subset, the three parameters presented harmonics that correspond to large-scale periodic phenomena like

Quasi-Biennial, El Niño-Southern, North Atlantic and Arctic oscillations.

Barstad and Adakudlu (2011) compared model simulations with observations from dropsondes as well as wind and water vapour LIDAR taken by a Falcon aircraft. Five dropsondes were released during the flight of 27 February 2008 in the Hinlopen Strait (which separates Spitsbergen from Nordaustlandet Island) in order to study an episode with significant local disturbances, that caused gap flow and wake formation phenomena. The model simulations have effectively reproduced the observed episodes. Other studies employing dropsondes data are reported in Lüpkes and Schlünzen (1996), Lampert et al. (2012), Kristjánsson et al. (2011), and Tetzlaff et al. (2014). Roberts et al. (2016) analysed observations from five controlled meteorological balloon launches in order to provide insights into tropospheric meteorological conditions around Svalbard. The balloons were launched from the AWIPEV observatory in Ny-Ålesund between 5 and 12 May 2011. One notable flight achieved a suite of 18 continuous soundings that probed the Arctic marine ABL over a period of more than 10 h. They compared acquired data with outputs from two different models, one with moderate and one with high resolution. In one case, the observed stable boundary layer with temperature inversion was reproduced only by the high-resolution model. In another case, presenting strong wind shear, the increasing temperature and humidity profiles were broadly reproduced by both models, but again the high-resolution one captured the wind shear phenomenon[2]. To not forget to cite stratospheric balloons, it is worth to mention the experiments conducted by La Sapienza University (Italy), with launches from Longyearbyen and Ny-Ålesund, mostly devoted to cosmic ray studies, but in some cases aimed at stratospheric solid particles collection (Della Corte et al. 2011).

2.2.2 Tethered balloons

In order to characterize the wind field profile in the Kongsfjorden, Argentini et al. (2003) used a tethersonde system consisting of a 5 m^3 balloon, properly shaped to facilitate orientation upwind, and a winch with 1000 m rope. The payload included dry and wet bulb thermometers, pressure, wind speed and wind direction sensors. Data were sent to the receiving station every 6 seconds. The same TB system described in Maturilli et al. (2008, 2009) is in use since many years by AWI in Ny-Ålesund during multiple campaign periods. In the 2008, a TB system was deployed at Ny-Ålesund (Lawson et al. 2011) for microphysics and radiative measurements in mixed-phase clouds. Measurements at Ny-Ålesund, were compared to those at the South Pole. The stratus clouds at Ny-Ålesund ranged in temperature from 0°C to -10°C and were mostly mixed phase with heavily rimed ice particles. Conversely, mixed-phase clouds at the South Pole contained regions with only water drops at temperatures as cold as -32°C and were often composed of pristine ice

2 Information on these and other flights are available at http://www.science.smith.edu/cmet/flight.html.

crystals. Air temperature and specific humidity inversions and low-level jets were studied over two Svalbard fiords, Isfjorden and Kongsfjorden, applying three tethersonde systems (Vihma et al. 2011) in March and April 2009. The same group compared the tethered balloon soundings with simulations of the vertical structure of the atmospheric boundary layer, performed with the mesoscale model Weather Research and Forecasting (WRF) as well as with its polar optimized version Polar WRF model (Kilpelainen et al. 2012). Mayer et al. (2012) compared the performances of a TB system with those of an unmanned aerial system SUMO (Small Unmanned Meteorological Observer) for the observation of the structure and behaviour of the atmospheric boundary layer above the Advent Valley, Svalbard. During a two-week period in early spring 2009, temperature, humidity and wind profiles measured by the SUMO system have been compared with measurements of a small TB system that was operated simultaneously. It is shown that both systems complement each other. Above 200m, the SUMO system outperformed the tethered balloon in terms of flexibility and the ability to penetrate strong inversion layers of the Arctic boundary layer. Below that level, the tethered balloon system provided atmospheric profiles with higher accuracy, mainly due to its ability to operate at very low vertical velocities.

Over 200 aerosol vertical profiles were recorded since spring 2011 in Ny-Ålesund from the Gruvebadet laboratory (Moroni et al. 2015, Ferrero et al. 2016) exploiting a TB system. The first instrumental payload (2011-2012) included two optical particle counters (dry and wet), a black carbon monitor, a total nanoparticle counter, and an ozone monitor. Four main types of profiles were found and their behaviour was related to the main aerosol and atmospheric dynamics occurring at the measuring site. Homogeneous profiles have been observed only for 15% of the cases in spring 2011 while they dominate (37%) in summertime 2012. Aerosol particles were also sampled on filters and characterized by SEM (Scanning Electron Microscopy) analysis (Moroni et al. 2015). The results pointed at a significant role of long-range transport on the aerosol mineralogy in the upper parts of the profiles. The payload has been improved in the 2014 campaign, by including a radio transmitting system and a nephelometer (Mazzola et al. 2016a). Since then, spring aerosol profiles were regularly recorded in Ny-Ålesund in the 2015, 2016, 2017 and 2018, also in the framework of the iAREA campaign (Markowitz et al. 2017). In 2019 the first winter aerosol profiles by TB systems have been measured by the same team and compared with LIDAR profiles (Nakoudi et al. 2019). The TB system and an example of the aerosol absorption coefficient and black carbon concentration measured are shown in Figure 1.

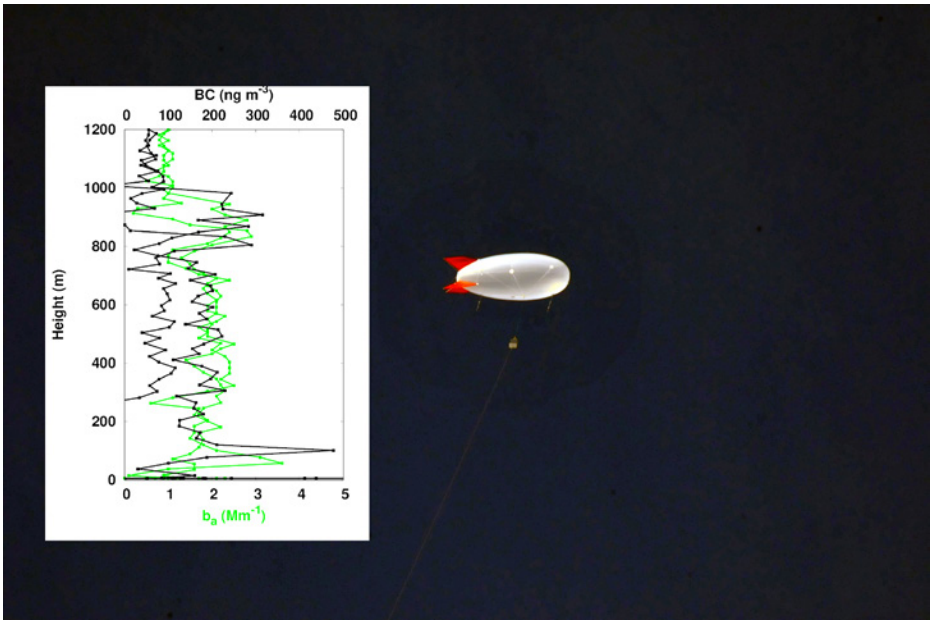

Figure 1: The TB system used by CNR and UniPG during January 2019 in Ny-Ålesund. The payload box and the tether are visible. The graph shows the profiles of aerosol absorption coefficient (b_a) and black carbon (BC) concentration measured on January 22, 2019.

2.2.3 Remote sensing

The remote sensing of temperature is currently done in Ny-Ålesund by microwave radiometers (at the AWIPEV station and at Gruvebadet by NCPOR, India). This evaluation generally requires plane-parallel stratified atmospheric conditions which are only a rough assumption below 2 km altitude in the Kongsfjorden. While the temperature profiles from microwave radiometers below 2 km altitude can be used to judge atmospheric stability (Schulz 2017) and the advection of different air masses in the free troposphere, the humidity profiles of this class of instrument are not very precise. Two radiometers for ozone (GROMOS-C for University of Bern and OZORAM from University of Bremen) and one for water vapour (MIAWARA-C again from University of Bern) are also installed at the AWIPEV station in Ny-Ålesund. Schranz et al. (2017) reported on the diurnal cycle of ozone and its tertiary maximum at an altitude of 70 km. Water vapour data show two and five-day wave activity and a descent rate within the polar vortex.

Remote sensing of clouds by radars has started a few years ago in Ny-Ålesund. A first statistics of cloud occurrences and properties has been published by Nomokonova et al. (2019). They used a combined dataset (14 months) obtained from a ceilometer, a 94 GHz cloud radar, and a microwave radiometer. A cloud occurrence of ~81 % was obtained (45 % multilayer, 36 % single-layer). The dataset has been analysed using the Cloudnet algorithm, obtaining outputs such as cloud target classification and microphysical properties, e.g. ice and liquid water content[3].

Figure 2: The triaxial SODAR and wind LIDAR installed in the proximity of the CCT in Ny-Ålesund.

The remote sensing of wind is currently performed in Ny-Ålesund by SODAR, managed by CNR and in operation since this year at the Amundsen-Nobile Climate Change Tower (CCT, see Mazzola et al. 2016b) and wind LIDAR, active since 2012 at the AWIPEV observatory and since 2017 at CCT (managed by KOPRI). Wind LIDARs gained reliability over the last years but cannot penetrate thick clouds and on overcast days their range is limited. Currently, authors are not aware of publications using this kind of measurements. SODARs were operational temporarily in the past during dedicated campaigns. Figure 2 shows the SODAR and wind LIDAR installed near the CCT at Ny-Ålesund. Beine et al. (2001) reported results for the wind field at different altitudes obtained using a triaxial Doppler SODAR in Ny-Ålesund during the ARTIST campaign, from March to September 1998. Comparing the

3 Near real time data and quick-plots can be seen at http://devcloudnet.fmi.fi/.

distributions of wind at 65 and 170 m a.m.s.l., considered to be representative of the lower and upper boundary layer respectively, show that they vary with season as well as with altitude, in particular during the summer months. While Ny-Ålesund receives predominantly katabatic flow from the Kongsvegen glacier, the field is rotated towards East and then North between 300 and 800 m. Other results of the ARTIST campaign are presented in Argentini et al. (2003). Sarchosidis and Klöwer (2016) studied the influence of low-level wind shear on the surface turbulence kinetic energy (TKE) production in Adventdalen during February 2016 using, beside other instruments, a SODAR measuring wind and turbulence up to 1000 m above the ground. Comparing the vertically averaged TKE as obtained from the SODAR with that measured by two sonic anemometers at two surface stations they found that in most situation the TKE is forced by large scale weather. Conversely, some events of high TKE only observed by the SODAR at higher levels, indicate a decoupling of the surface with the above atmosphere. Tjernström (2005) presented results from the Arctic Ocean Experiment 2001 (AOE-2001, 2–21 August), on-board the Swedish icebreaker Oden in the Central Arctic. The cruise started south–east of Svalbard, continued north, north–west and back again to Svalbard. The measuring package included: wind profiler, cloud radar, scanning microwave radiometer, radiosoundings, two SODARs and a tethered balloon for meteorology, turbulence and aerosol measurements. They found that there are often two inversions, one elevated and one at the surface, while occasionally additional inversions occur. The ABL is generally quite shallow, with depth less than 200 m, where aerosols were trapped. Other results from the same campaign are illustrated in Tjernström et al. (2004), while those from similar campaigns in other years are reported in Tjernström et al. (2012, 2014), Brooks et al. (2017).

The remote sensing of atmospheric parameters by means of LIDAR in Ny-Ålesund started in the late 1980s. The stratospheric ozone concentration and temperature have been measured during the dark season. Neuber and Krüger (1990) reported on ozone profiles by a LIDAR and balloon sondes from January until the end of March 1989. The comparison between LIDAR and sonde profiles revealed good agreement, permitting to create an integrated dataset. They detected no ozone depletion during that period, prevented by the extremely cold situation, with a stable vortex insulating the Arctic from middle latitudes. Two ozone pulses were measured during two distinct periods above 20 km, associated with warm air intrusions.

Only a short time later LIDAR measurements of stratospheric aerosol were started. Neuber et al. (1992) reported PSCs profiles for January 1989 and 1990, showing a good correlation with atmospheric temperature. During August 1991, an aerosol layer was detected, presumably due to the Mt. Pinatubo eruption. Since 2000, aerosol measurements by a Raman LIDAR in the tropo- and stratosphere have been performed regularly during all seasons (Schumacher 2001). During night time and clear sky conditions, also measurements of the absolute humidity are possible. Figure 3 shows the laser beam of the KARL LIDAR

Figure 3: The laser beam of the KARL LIDAR from the AWIPEV observatory in Ny-Ålesund, under northern lights.

emerging from the AWIPEV observatory. Gerding et al. (2004) described the measurements obtained between June 2001 and December 2002. During darkness profiling is possible up to 6–7 km, while daylight limits the profiles to maximum 3 km. During specific events, simultaneous observations of humidity and aerosol extinction show distinct differences at the various altitudes. In the boundary layer, aerosols are poorly affected by the humidity, while in the free troposphere, the LIDAR ratio give evidence for water uptake by the particles. Hoffmann et al. (2010) reported on the detection of aerosol plumes coming to Ny-Ålesund from the Kasatochi eruption of 2008. Information on the morphology of the particles were obtained from the measured depolarization ratio at different heights. Di Liberto et al. (2012) used data from an automated small size LIDAR system installed in Ny-Ålesund to estimate the PBL height by means of a gradient method based on abrupt changes in the vertical aerosol profile and monitor its temporal evolution. The results of this method were successfully compared to those obtained by others using radiosondes and a one-dimensional model based on a parameterization of the turbulent kinetic energy, indicating that in favourable cases it may provide reliable results. Lampert et al. (2012) used an inclined LIDAR with very high resolution (0.4 m) for detailed boundary layer studies above the Kongsfjord. On 29 April 2007, a layer of enhanced backscatter by spherical particles was

observed in the lowest 25 m above the open water surface, disappearing in the afternoon. On the morning of 1 May 2007, the atmosphere up to Zeppelin showed enhanced values of the backscatter coefficient, while, around noon, the top of the layer decreased from 350 to 250 m as confirmed by radiosonde data. Ritter et al. (2016) analysed LIDAR data for the spring 2014 Arctic haze season, providing typical values and probability distributions for aerosol backscatter, extinction and depolarisation, the LIDAR ratio and the colour ratio along the troposphere. Results showed that the 2014 season was only moderately polluted and no clear temporal evolution over the 4-week dataset was seen, except for the extinction coefficient and the LIDAR ratio, which significantly decreased below 2 km altitude by end April. Between 2 and 5 km the haze season lasted longer. Maturilli and Ebell (2018) presented a 25-year (1992-2017) data record of cloud base height measured by a ceilometer in Ny-Ålesund. This information is essential for interpretation of the surface radiation budget and of meteorological processes. It is also useful as complementary to other advanced technologies that provide information on cloud microphysical properties, such as cloud radar. They found that cloud cover conditions are more frequent in summer and the lowest occurrence is in April[4]. Kulla and Ritter (2019) revised the LIDAR water vapour calibration by co-located radiosonde launches in order to obtain highly resolved profiles. They found that small scale variability of the humidity was a large source of error in the comparison. Averaging over several independent measurements increases the quality of the calibration, up to 5% for individual profiles and 1% for the entire season. The calibrated dataset shows high temporal variability up to 4 km and provides additional, independent information to the radiosonde measurements. While current ceilometers struggle to produce reliable aerosol profiles in the generally clean Arctic conditions, a continuous 24/7 LIDAR operation for aerosol and cloud monitoring is provided by a micro pulse LIDAR (MPL) installed by NIPR at the AWI observatory (Shiobara et al. 2003)[5]. These data have been used by Campell and Shiobara (2008) to study the glaciation of mixed-phase boundary layer clouds. Shibata et al. (2018) analysed 4 years (2014-2018) of aerosol backscattering data showing that monthly averaged concentration of aerosols was largest in the lowest free troposphere at about 1 km in altitude and was an order of magnitude smaller at an about 10 km. At the same time, it was larger from late spring to summer and lower from late summer to fall. Maxima in the monthly averaged non-sphericity and size are not coincident with concentration suggesting a seasonal change in the morphology of the particles. With a synergic use of LIDAR, sun-photometer and radiosonde data, Ritter et al. (2018) studied a strong biomass burning transport episode detected over Ny-Ålesund during July 2015. They obtained size distribution, refractive index and single scattering albedo at different relative humidity, finding predominance of particles in the accumulation mode and hygroscopic growth for RH above 80%.

4 Data used for this work are available at https://doi.org/10.1594/PANGAEA.880300.

5 http://polaris.nipr.ac.jp/~dbase/e/300/e/300_data-MPL-NYA.htm

Up to now, Ny-Ålesund is by far the most important centre for vertically resolved remote sensing in Svalbard, but such activities were performed in the past also at other sites, also during specific campaigns, some of them continuing nowadays. A Raman Lidar was in operation from late 2009 until Sep 2016 in Hornsund. It was used for aerosol and water vapour profiling. Furthermore, a ceilometer is in operation at the Polish station since 2015. Karasiński et al. (2014) reported on the detection of aerosol layers over Hornsund after two volcanic eruptions, those of the Eyjafjallajökull (April–May 2010) and Grímsvötn (May 2011), both located in Iceland. Few days after the eruptions, layers of high aerosol concentration have been observed by multi-wavelength LIDAR, as confirmed by backward trajectories showing their paths passing over the location of volcanoes. Bloch & Karasiński (2014) reported on vertical sounding of a water vapour content in the lower and middle troposphere obtained up to 6 km altitude during winter from 2009 to 2012, obtaining results in good agreement with the results obtained from the AIRS satellite instrument. From 1998 to 2001 a LIDAR was operational in Longyearbyen for research of the upper atmosphere. Höffner et al. (2003) installed a potassium LIDAR near Longyearbyen in order to detect noctilucent clouds (NLCs) and to measure temperature in the lower thermosphere (above 100 km). At the same time a series of meteorological rockets were launched to measure temperature from the lower thermosphere to the stratosphere. They found that during the period between 12 June and 12 August the NLC occurrence is 77%, with a mean peak altitude equal to 83.6 km, without any significant variation with season.

2.2.4 Aircraft, unmanned vehicles

Up to 2015, flight permits were issued on a case by case basis based on applications to the Norwegian Civil Aviation Authority and submitted standard procedures and risk assessments for the planned activity. Norway/Svalbard got a national drone (RPAS) regulation in place in 2016 and a common European (EASA) regulation has been approved and will be adopted into Norwegian law in July 2020. This makes it more predictable to plan for the use of drones in the future but also sets stricter requirements to the operators of drones. The first time drones were used on Svalbard for atmospheric research was in 2008 in connection with the International Polar Year (IPY). As a part of the IPY-THORPEX (Kristjánsson et al. 2011) drones were used to profile the atmospheric boundary layer in February-March out of Longyearbyen. During this experiment the DLR Falcon also had multiple transects in the Svalbard region, with dropsondes and profiling LIDARs to measure wind, turbulence, temperature and humidity profiles. Such profiling up to 1000-3000 meters altitude has been done on single campaign basis since, by several research groups. Basic meteorological observations can be obtained with compact and light instrumentation, hence flown with small and inexpensive drones (Reuder 2009). Most work on Svalbard has been done in a collaboration between University of Bergen and UNIS, and an example of data collected in the Advent valley is presented in Mayer et al. (2012). Drones provide a unique platform for in-situ atmospheric sensing allowing for both vertical and horizontal sampling. This makes

drones an interesting platform that support modelling and process studies involving aerosol transport and formation and deposition as well as trace gas chemistry and transport. In 2011 and in 2015 there were larger coordinated campaigns with drones, balloons, ground based and satellite remote sensing with focus on aerosol and black carbon transport and deposition in the Arctic and albedo effects. Drones were operated by AARI, NOAA and Norut (now NORCE). AARI provided meteorological measurements and vertical profiles at different locations over Kongsfjorden. Norut did both meteorological profiles as well as hyperspectral snow reflectance measurements around Ny-Ålesund, Holtedalsfonna and Kongsvegen Glaciers. NOAA flew an advanced aerosol and meteorological instrument package and did profiles from 30 to 3000 meters. Detailed description of drone aerosol instrumentation and results are described in Bates et al. (2013). Snow reflectance measurements are described in Burkhart et al. (2017). Figure 4 shows the team involved in this experiment posing with three drones. In 2018 the University of Braunschweig had an extensive drone campaign investigating aerosol formation and small scale vertical and horizontal variability in the atmospheric boundary layer. This is an ongoing project (RIS 10977) lead by Astrid Lampert.

Figure 4: The CICCI flight teams (NOAA, Norut and AARI) in 2011 on the airstrip of Ny-Ålesund.

3. Unanswered questions

Ny-Ålesund already has a long-lasting competence in aerosol research, both via in-situ and remote sensing techniques via several research institutes. The balloon-borne aerosol measurements (Ferrero et al. 2016) complete and link in an ideal way the ground-based aerosol measurements and the LIDAR observations. Similarly, aerosol in situ measurements on board of UAV will increase the spatial extent of aerosol measurements. However, due to the complexity of aerosol chemical and micro-physical properties and the general missing of a scattering theory for arbitrarily shaped particles such "aerosol closure experiments" (the agreement of aerosol properties derived by different instruments and methods) are difficult and an open task for the near future. Generally, comparing e.g. the various IPCC reports over the last 20 years, our understanding of the radiative impact of aerosol and its contribution to cloud properties has not increases as much as desired. Aerosols still contribute to an unsatisfactory uncertainty in climate models. However, although Ny-Ålesund is a peculiar site with a complicated orography, the suite of aerosol measurements and the used platforms are impressive and quite complete and the main research groups already have a long-lasting cooperation in terms of joint campaigns and publications (e.g. Ritter et al. 2018; Ferrero et al. 2019).

Further, the interaction between aerosol and the boundary layer are a concern for the site of Ny-Ålesund. This is important for the comparison between the different ground-based aerosol in-situ measurements at the site as well as for the comparison between (vertical) remote sensing to either UAV or ground based measurements.

Some important open scientific questions are the aerosol type resolved properties as a function of humidity, the precise pollution pathways into the Arctic, the comparison between aerosol properties on the ground and in the free troposphere, their impact on radiation and cloud microphysics.

4. Recommendations for the future

The joint, international campaigns for atmospheric research, concerning aerosol in particular, in different seasons with different platforms (especially a comparison between balloon- and UAV-borne instruments and LIDAR data) should be continued. For this reason, flight permissions for tethered balloons and UAV, also in dark and cloudy conditions should be facilitated. For the same reason, specific infrastructures devoted to the use of UAVs and tethered balloons should be created. In Ny-Ålesund a facility for UAVs was created in 2015 (coordinated by NORCE). Tethered balloon operations would take advantage from the presence of a dedicated hangar to store the inflated balloons for long periods, with adequate dimension, including the door, and a system (compressor) to recover the helium.

Both these solutions would permit to save a lot of money for buying the gas.

Generally, the link between the various atmospheric measurements in Svalbard and climate modelling on scales from LES (Large Eddy Simulation) to regional modelling could and need to be improved. This would also advance the enormous efforts put into the observational activities by the different countries and institutions. The remote sensing of aerosol could be used to validate aerosol transport into the Arctic. Together with in situ measurements our understanding of life-time, chemical alteration and radiative impact of aerosol could be greatly improved.

Concerning the remote sensing of meteorological quantities, wind LIDARs with a vertical range larger than 2 km become available and have the potential to sound into the free troposphere to give information on the synoptic flow that is no longer influenced by the orography. Lidar-based continuous monitoring of temperature and water vapour (including summer) do not exist yet in Ny-Ålesund. However, at the given rate of technical progress their usage in Arctic conditions may be useful soon. For this reason, a common Ny-Ålesund scientific investment plan for the upcoming years might be discussed within NySMAC.

The efforts on data visibility and sharing, already started by SIOS, should be enforced in order to ameliorate the scientific coordination, to avoid overlapping, and to improve data usage.

5. Data availability

Some of the reported activities regularly contribute to publicly accessible international databases. Table 1 reports the links to these databases, together with referenced publications, the technique used, the site and period of measurements.

On the contrary, most of the collected data are not publicly accessible or easily discovered. They should be requested contacting the corresponding author of the publication.

Acknowledgements

This work was supported by the Research Council of Norway, project number 251658, Svalbard Integrated Arctic Earth Observing System - Knowledge Centre (SIOS-KC).

Table 1: List of datasets publicly available among those cited in the text. The main reference is reported, as well as sites and available periods.

Reference	Technique	Parameters	Site	Period	Link to database or information
Maturilli and Kayser (2017)	Radiosonde	Meteorology	Ny-Ålesund	1993-2014	http://doi.pangaea.de/10.1594/PANGAEA.845373
Roberts et al. (2016)	Controlled balloon	Meteorology	Ny-Ålesund (surroundings)	May 2011	http://www.science.smith.edu/cmet/flight.html
Nomokonova et al. (2019)	Radar	Cloud microphysics	Ny-Ålesund	June 2016 - July 2017	http://devcloudnet.fmi.fi
Maturilli and Ebell (2018)	Ceilometer	Cloud base height	Ny-Ålesund	1992-2017	https://doi.org/10.1594/PANGAEA.880300
Shiobara et al. (2003)	LIDAR	Aerosol backscattering	Ny-Ålesund	2002-2017	https://mplnet.gsfc.nasa.gov/data?s=Ny_Alesund&v=V2
Mazzola et al. (2016a)	Tethered balloon	Aerosol size distribution and optical properties	Ny-Ålesund	2014-2019	http://mainnode.src.cnr.it/cnr/
Kivi et al. (2011)	Ozonesonde	Ozone concentration	Ny-Ålesund	1990-2013	https://woudc.org/data/stations/?id=089
Ritter et al. (2016), Neuber and Krüger (1990), Kulla and Ritter (2019), Schranz et al. (2017)	LIDAR and radiometers	Aerosol, ozone, temperature, water vapour	Ny-Ålesund	1991-present	http://www.ndaccdemo.org/stations/ny-%C3%A5lesund-norway

References

Argentini S, Mastrantonio G, Viola A (1999) Estimation of turbulent heat fluxes and exchange coefficients for heat at Dumont d'Urville, East Antarctica. Antarct Sci, 11(1):93-99. https://doi.org/10.1017/S0954102099000127

Argentini S, Viola AP, Mastrantonio G, Maurizi A, Georgiadis T, Nardino M (2003) Characteristics of the boundary layer at Ny-Ålesund in the Arctic during the ARTIST field experiment. AnnGeophys-Italy, 46(2).

Armstrong JA, Russell PA, Sparks LE, Drehmel DC (1981) Tethered Balloon Sampling Systems for Monitoring Air Pollution. JAPCA J Air Waste Ma, 31(7):735-743. https://doi.org/10.1080/00022470.1981.10465268

Barstad I and Adakudlu M (2011) Observation and modelling of gap flow and wake formation on Svalbard. Q J R Meteorol Soc, 137:1731-1738. https://doi.org/10.1002/qj.782

Bates TS, Quinn PK, Johnson JE, Corless A, Brechtel FJ, Stalin SE, Meinig C, Burkhart, JF (2013) Measurements of atmospheric aerosol vertical distributions above Svalbard, Norway, using unmanned aerial systems (UAS). Atmos Meas Tech, 6:2115-2120. https://doi.org/10.5194/amt-6-2115-2013

Becker R, Maturilli M, Philipona R, Behrens K (2018) In-situ sounding of radiation flux profiles through the Arctic lower troposphere. Atmos Meas Tech Discuss. https://doi.org/10.5194/amt-2018-173

Beine H, Argentini S, Maurizi A et al. (2001) The local wind field at Ny-Ålesund and the Zeppelin mountain at Svalbard. Meteorol Atmos Phys, 78:107-113. https://doi.org/10.1007/s007030170009

Bloch M and Karasinski G (2014) Water Vapour Mixing Ratio Profiles over Hornsund, Arctic. Intercomparison of Lidar and AIRS Results. Acta Geophys, 62(2):290–301. https://doi.org/10.2478/s11600-013-0168-3

Brooks IM, Tjernström M, Persson POG, Shupe MD, Atkinson RA et al. (2017) The turbulent structure of the Arctic summer boundary layer during The Arctic Summer Cloud-Ocean Study. J Geophys Res-Atmos, 122:9685–9704. https://doi.org/10.1002/2017JD027234

Burkhart JF, Kylling A, Schaaf CB, Wang Z, Bogren W, Storvold R, Solbø S, Pedersen CA, Gerland S (2017) Un-manned aerial system nadir reflectance and MODIS nadir BRDF-adjusted surface reflectances intercompared over Greenland. Cryosphere, 11:1575–1589. https://doi.org/10.5194/tc-11-1575-2017

Campell JR and Shiobara M (2008) Glaciation of a mixed-phase boundary layer cloud at a coastal arctic site as depicted in continuous lidar measurements. Polar Sci, 2(2):121-127. https://doi.org/10.1016/j.polar.2008.04.004

Clarke A and Kapustin V (2010) Hemispheric Aerosol Vertical Profiles: Anthropogenic Impacts on Optical Depth and Cloud Nuclei. Science, 329(5998):1488-1492. https://doi.org/10.1126/science.1188838

Dahlke S, Maturilli M (2017) Contribution of Atmospheric Advection to the Amplified Winter Warming in the Arctic North Atlantic Region. Adv Meteorol, 2017. https://doi.org/10.1155/2017/4928620

Davis KJ, Lenschow DH, Zimmerman PR (1994) Biogenic nonmethane hydrocarbon emissions estimated from tethered balloon observations. J Geophys Res-Atmos, 99(D12):25587– 25598. https://doi.org/10.1029/94JD02009

Della Corte V, Palumbo P, De Angelis S, Ciucci A, Brunetto R, Rotundi A, Rietmeijer FJM, Zona E, Bussoletti E, Colangeli L, Esposito F, Mazzotta Epifani E, Mennella V, Peterzen S, Masi S, Ibba R (2011) DUSTER (Dust in the Upper Stratosphere Tracking Experiment and Return): a balloon-borne dust particle collector. Mem S A It Suppl, 16:14-21.

Di Liberto L, Angelini F, Pietroni I, et al. (2012) Estimate of the Arctic Convective Boundary Layer Height from Lidar Observations: A Case Study. Adv Meteorol, 2012:1-9. https://doi.org/10.1155/2012/851927

Duda DP, Stephens GL, Cox SK (1991) Microphysical and Radiative Properties of Marine Stratocumulus from Tethered Balloon Measurements. J Appl Meteor, 30:170–186. https://doi.org/10.1175/1520-0450(1991)030<0170:MARPOM>2.0.CO;2

Egerer U, Gottschalk M, Siebert H, Ehrlich A, Wendisch M (2019) The new BELUGA setup for collocated turbulence and radiation measurements using a tethered balloon: First applications in the cloudy Arctic boundary layer. Atmos Meas Tech Discuss, in review. https://doi.org/10.5194/amt-2019-80

Ferrero L, Bolzacchini E, Petraccone S, Perrone MG, Sangiorgi G, Lo Porto C, Lazzati Z, Ferrini B (2007) Vertical profiles of particulate matter over Milan during winter 2005/2006. Fresen Envion Bull, 16:697–700.

Ferrero L, Cappelletti D, Busetto M, Mazzola M, Lupi A, Lanconelli C, Becagli S, Traversi R, Caiazzo L, Giardi F, Moroni B, Crocchianti S, Fierz M, Močnik G, Sangiorgi G, Perrone MG, Maturilli M, Vitale V, Udisti R, Bolzacchini E (2016) Vertical profiles of aerosol and black carbon in the Arctic: a seasonal phenomenology along 2 years (2011–2012) of field campaigns. Atmos Chem Phys, 16:12601-12629. https://doi.org/10.5194/acp-16-12601-2016

Ferrero L, Cappelletti D, Moroni B, Sangiorgi G, Perrone MG, Crocchianti S, Bolzacchini E (2012) Wintertime aerosol dynamics and chemical composition across the mixing layer over basin valleys. Atmos Environ, 56:143–153. https://doi.org/10.1016/j.atmosenv.2012.03.071

Ferrero L, Ritter C, Cappelletti D, Moroni B, Močnik G, Mazzola M, Lupi A, Becagli S, Traversi R, Cataldi M, Neuber R, Vitale V, Bolzacchini E (2019) Aerosol optical properties in the Arctic: The role of aerosol chemistry and dust composition in a closure experiment between Lidar and tethered balloon vertical profiles. Sci Total Environ, 686:452-467. https://doi.org/10.1016/j.scitotenv.2019.05.399

Gerding M, Ritter C, Neuber R (2004) Tropospheric water vapour soundings by lidar at high Arctic latitudes, Atmos Res, 71:4. https://doi.org/10.1016/j.atmosres.2004.07.002

Gilardoni S, Lupi A, Mazzola M, Cappelletti DM, Moroni B, Ferrero L, Markuszewski P, Rozwadowska A, Krejci R, Zieger P, Tunved P, Karlsson L, Vratolis S, Eleftheriadis K (2020) Atmospheric Black carbon at Svalbard. In: Van den Heuvel et al. (eds): SESS report 2019, Svalbard Integrated Arctic Earth Observing System, Longyearbyen, 196 - 211 . https://sios-svalbard.org/SESS_Issue2

Hara K, Osada K, Yamanouchi T (2013) Tethered balloon-borne aerosol measurements: seasonal and vertical variations of aerosol constituents over Syowa Station, Antarctica. Atmos Chem Phys, 13:9119-9139. https://doi.org/10.5194/acp-13-9119-2013

Hoffmann A, Ritter C, Stock M, Maturilli M, Eckhardt S, Herber A, Neuber R (2010) Lidar measurements of the Kasatochi aerosol plume in August and September 2008 in Ny-Ålesund, Spitsbergen. J Geophys Res-Atmos, 115. https://doi.org/10.1029/2009JD013039

Hoppel WA, Dinger JE, Ruskin RE (1973) Vertical Profiles of CCN at Various Geographical Locations. J Atmos Sci, 30:1410–1420. https://doi.

org/10.1175/1520-0469(1973)030<1410:VPOCAV>2.0.CO;2

Höffner J, Fricke-Begemann C, Lübken F-J (2003) First observations of noctilucent clouds by lidar at Svalbard, 78°N. Atmos Chem Phys, 3: 1101-1111. https://doi.org/10.5194/acp-3-1101-2003

Ingleby B, Isaksen L, Kral T, Haiden T, Dahoui M (2018) Improved use of atmospheric in situ data. ECMWF Newsletter, 155(m): 20-25. https://doi.org/10.21957/cf724bi05s

Jacob JD, Chilson PB, Houston AL, Smith SW (2018) Considerations for Atmospheric Measurements with Small Unmanned Aircraft Systems. Atmosphere-Basel, 9(7):252. https://doi.org/10.3390/atmos9070252

Johnson BJ, Helmig D, Oltmans SJ (2008) Evaluation of ozone measurements from a tethered balloon-sampling platform at South Pole Station in December 2003. Atmos Environ, 42(12):2780-2787. https://doi.org/10.1016/j.atmosenv.2007.03.043

Karasinski G, Posyniak M, Bloch M, Sobolewski P, Malarzewski L, Soroka J (2014) Lidar Observations of Volcanic Dust over Polish Polar Station at Hornsund after Eruptions of Eyjafjallajökull and Grímsvötn. Acta Geophys, 62(2):316–339. https://doi.org/10.2478/s11600-013-0183-4

Kayser M, Maturilli M, Graham RM, Hudson SR, Rinke A, Cohen L, Kim J-H, Park S-J, Moon W, Granskog MA (2017) Vertical thermodynamic structure of the troposphere during the Norwegian young sea ICE expedition (N-ICE2015), J Geophys Res-Atmos, 122:10855–10872. https://doi.org/10.1002/2016JD026089

Kilpeläinen T, Vihma T, Manninen M, Sjöblom A, Jakobson E, Palo T, Maturilli M (2012) Modelling the vertical structure of the atmospheric boundary layer over Arctic fjords in Svalbard. Q J R Meteorol Soc, 138:1867-1883. https://doi.org/10.1002/qj.1914

Kivi R, Kyrö E, Turunen T, Harris NRP, von der Gathen P, Rex M, Andersen SB, Wohltmann I (2007) Ozonesonde observations in the Arctic during 1989–2003: Ozone variability and trends in the lower stratosphere and free troposphere. J Geophys Res-Atmos, 112. https://doi.org/10.1029/2006JD007271

Kontkanen J, Järvinen E, Manninen HE, Lehtipalo K, Kangasluoma J, Decesari S, Gobbi GP, Laaksonen A, Petäjä T, Kulmala M (2016) High concentrations of sub-3nm clusters and frequent new particle formation observed in the Po Valley, Italy, during the PEGASOS 2012 campaign. Atmos Chem Phys, 16:1919–1935. https://doi.org/10.5194/acp-16-1919-2016

Kristjánsson JE, Barstad I, Aspelien T, Føre I, Godøy Ø, Hov Ø, Irvine E, Iversen T, Kolstad E, Nordeng TE, McInnes H, Randriamampianina R, Reuder J, Saetra Ø, Shapiro M, Spengler T, Ólafsson H (2011) THE NORWEGIAN IPY–THORPEX: Polar Lows and Arctic Fronts during the 2008 Andøya Campaign. B Am Meteorol Soc, 92(11):1443-466. http://www.jstor.org/stable/26218601

Kulla BS and Ritter C (2019) Water Vapor Calibration: Using a Raman Lidar and Radiosoundings to Obtain Highly Resolved Water Vapor Profiles. Remote Sens-Basel, 11(6):616. https://doi.org/10.3390/rs11060616

Lampert A, Maturilli M, Ritter C, Hoffmann A, Stock M, Herber A, Birnbaum G, Neuber R, Dethloff K, Orgis T, Stone R, Brauner R, Kässbohrer J, Haas C, Makshtas A, Sokolov V, Liu P (2012) The Spring-Time Boundary Layer in the Central Arctic Observed during PAMARCMiP 2009. Atmosphere-Basel 3(3):320-351. https://doi.org/10.3390/atmos3030320

Lawson RP, Stamnes K, Stamnes J, Zmarzly P, Koskuliks J, Roden C, Mo Q, Carrithers M, Bland GL (2011) Deployment of a Tethered-Balloon System for Microphysics and Radiative Measurements in Mixed-Phase Clouds at Ny-Ålesund and South Pole. J Atmos Oceanic Technol, 28:656–670. https://doi.org/10.1175/2010JTECHA1439.1

Li J, Fu Q, Huo J, Wang D, Yang W, Bian Q, Duan Y, Zhang Y, Pan J, Lin Y, Huang K, Bai Z, Wang S-H, Fu JS, Louie PKK (2015) Tethered balloon-based black carbon profiles within the lower troposphere of Shanghai in the 2013 East China smog. Atmos Environ, 123(B):327-338. https://doi.org/10.1016/j.atmosenv.2015.08.096

Lüpkes C and Schlünzen KH (1996) Modelling the arctic convective boundary-layer with different turbulence parameterizations. Bound-Lay Meteorol, 79:107. https://doi.org/10.1007/BF00120077

Maletto A, McKendry IG, Strawbridge KB (2003) Profiles of particulate matter size distributions using a balloonborne lightweight aerosol spectrometer in the planetary boundary layer. Atmos Environ, 37:661–670. https://doi.org/10.1016/S1352-2310(02)00860-9

Markowicz KM, Ritter C, Lisok J, Makuch P, Stachlewska IS, Cappelletti D, Mazzola M, Chilinski MT (2017) Vertical variability of aerosol single-scattering albedo and equivalent black carbon concentration based on in-situ and remote sensing techniques during the iAREA campaigns in Ny-Ålesund. Atmos Environ, 164:431-447. https://doi.org/10.1016/j.atmosenv.2017.06.014

Maturilli M, Dethloff K, Graeser J, Rinke A, Mielke M (2009) Meteorological Profiling of the Arctic Boundary Layer. Proceedings of the 8th International Symposium on Tropospheric Profiling, ISBN 978-90-6960-233-2, Delft, The Netherlands.

Maturilli M and Ebell K (2018) Twenty-five years of cloud base height measurements by ceilometer in Ny-Ålesund, Svalbard. Earth Syst Sci Data, 10:1451-1456. https://doi.org/10.5194/essd-10-1451-2018

Maturilli M and Kayser M (2017) Arctic warming,

moisture increase and circulation changes observed in the Ny-Ålesund homogenized radiosonde record. Theor Appl Climatol, 130:1. https://doi.org/10.1007/s00704-016-1864-0

Maturilli M, Graeser J, Mielke M, Rinke A (2008) Tethered Balloon Measurements on the North Pole Drifting Ice Station NP-35. 23rd International Polar Meeting, 10 - 14 March 2008, Münster, Germany. https://epic.awi.de/id/eprint/19107/1/Mat2008d.pdf

Mayer S, Sandvik A, Jonassen MO et al. (2012) Atmospheric profiling with the UAS SUMO: a new perspective for the evaluation of fine-scale atmospheric models. Meteorol Atmos Phys, 116:15. https://doi.org/10.1007/s00703-010-0063-2

Mazzola M, Busetto M, Ferrero L, Viola AP, Cappelletti D (2016a) AGAP: an atmospheric gondola for aerosol profiling. Rend Lincei-Sci Fis, 27(1):105. https://doi.org/10.1007/s12210-016-0514-x

Mazzola M, Viola AP, Lanconelli C, Vitale V (2016b) Atmospheric observations at the Amundsen-Nobile Climate Change Tower in Ny-Ålesund, Svalbard. Rend Lincei-Sci Fis, 27(1):7–18. https://doi.org/10.1007/s12210-016-0540-8

Moroni B, Becagli S, Bolzacchini E et al. (2015) Vertical Profiles and Chemical Properties of Aerosol Particles upon Ny-Ålesund (Svalbard Islands). Adv Meteorol, 2015:11p. https://doi.org/10.1155/2015/292081

Morris AL, Call DB, McBeth RB (1975) A small tethered balloon sounding system. B Am Meteorol Soc, 56:964–970. https://doi.org/10.1175/1520-0477(1975)056<0964:ASTBSS>2.0.CO;2

Nakoudi K, Ritter C, Mazzola M, Cappelletti D, Bockmann C, Maturilli M, Neuber R (2019) Synergistic Investigation of Arctic Aerosol in the darkness: remote sensing and in-situ observations. Svalbard Science Conference, Oslo, 5-6 November 2019.

Neuber R and Krüger BC (1990) The stratospheric ozone layer above Spitsbergen in winter 1989, Geophys Res Lett, 17:4. https://doi.org/10.1029/GL017i004p00321

Neuber R, Beyerle G, Schrems O (1992) LIDAR Measurements of Stratospheric Aerosols in the Arctic. Berich Bunsen Gesell, Wiley, 96:350-353. https://doi.org/10.1002/bbpc.19920960322

Nomokonova T, Ebell K, Löhnert U, Maturilli M, Ritter C, O'Connor E (2019) Statistics on clouds and their relation to thermodynamic conditions at Ny-Ålesund using ground-based sensor synergy. Atmos Chem Phys, 9. https://doi.org/10.5194/acp-19-4105-2019

Petkov BH, Vitale V, Svendby TM, Hansen GH, Sobolewski PS, Láska K, Elster J, Pavlova K, Viola A, Mazzola M, Lupi A, Solomatnikova A (2018) Altitude-temporal behaviour of atmospheric ozone, temperature and wind velocity observed at Svalbard. Atmos Res, 207:100-110. https://doi.org/10.1016/j.atmosres.2018.03.005

Pisano JT, McKendry I, Steyn DG, Hastie DR (1997) Vertical nitrogen dioxide and ozone concentrations measured from a tethered balloon in the Lower Fraser Valley. Atmos Environ, 31(14):2071-2078. https://doi.org/10.1016/S1352-2310(96)00146-X

Rankin AM and Wolff EW (2002) Aerosol Profiling Using a Tethered Balloon in Coastal Antarctica. J Atmos Oceanic Technol, 19:1978–1985. https://doi.org/10.1175/1520-0426(2002)019<1978:APUATB>2.0.CO;2

Reuder J, Brisset P, Jonassen M, Müller M, Mayer S (2009) The Small Unmanned Meteorological Observer SUMO: a new tool for atmospheric boundary layer research. Meteorol Z,18(2): 141–147. https://doi.org/10.1127/0941-2948/2009/0363

Rex M and von der Gathen P (2004) Stratospheric ozone losses over the Arctic. In: Wiencke C (ed.) The coastal ecosystem of Kongsfjorden, Svalbard. Synopsis of biological research performed at the Koldewey Station in the years 1991 – 2003. Ber Polarforsch Meeresforsch 492, ISSN 1618 – 3193. Alfred Wegener Institute for Polar and Marine Research, Bremerhaven.

Ritter C, Angeles Burgos M, Böckmann C, Mateos M, Lisok J et al. (2018) Microphysical properties and radiative impact of an intense biomass burning aerosol event measured over Ny-Ålesund, Spitsbergen in July 2015. Tellus B, 70(1):1-23. https://doi.org/10.1080/16000889.2018.1539618

Ritter C, Neuber R, Schulz A, Markowicz KM, Stachlewska IS et.al (2016) 2014 iAREA campaign on aerosol in Spitsbergen – Part 2: Optical properties from Raman-lidar and in-situ observations at Ny-Ålesund. Atmos Environ, 141. https://doi.org/10.1016/j.atmosenv.2016.05.053

Roberts TJ, Dütsch M, Hole LR, Voss PB (2016) Controlled meteorological (CMET) free balloon profiling of the Arctic atmospheric boundary layer around Spitsbergen compared to ERA-Interim and Arctic System Reanalyses. Atmos Chem Phys, 16:12383-12396. https://doi.org/10.5194/acp-16-12383-2016

Sarchosidis C and Klöwer M (2016) The influence of low-level wind shear on the surface turbulence kinetic energy production in Adventdalen, Svalbard. Report AGF-350/850, University Centre in Svalbard, 14pp. http://milank.de/documents/SEB_harrymilan.pdf

Schranz F, Fernandez S, Tschanz B, Kämpfer N, Palm M (2017) Analysis of middle atmospheric ozone and water vapour measurements and SD-WACCM simulations of the last two winters at Ny-Ålesund/Svalbard. Geophysical Research Abstracts, 19. EGU2017-9533

Schrems O (1992) Die Ozonschicht der nordpolaren

Stratosphäre (The Ozone Layer in the Northern Arctic Stratosphere). Global Change Prisma, 3:4-9.

Schulz A (2017) Untersuchung der Wechselwirkung synoptisch-skaliger mit orographisch bedingten Prozessen in der arktischen Grenzschicht über Spitzbergen (Investigation of the interaction of synoptic-scale with orographic processes in the Arctic boundary layer over Spitsbergen). PhD thesis, Univ. Potsdam, urn:nbn:de:kobv:517-opus4-400058

Schumacher R (2001) Messung von optischen Eigenschaften troposphärischer Aerosole in der Arktis (Measurement of optical properties of tropospheric aerosols in the Arctic). PhD thesis, Univ. Potsdam, Berichte zur Polarforschung, 386, ISSN 0176–5027.

Shibata T, Shiraishi K, Shiobara M, Iwasaki S, Takano T (2018) Seasonal Variations in High Arctic Free Tropospheric Aerosols Over Ny-Ålesund, Svalbard, Observed by Ground-Based Lidar. JGeophys Res-Atmos, 123:12353–12367. https://doi.org/10.1029/2018JD028973

Shiobara M, Yabuki M, Kobayashi H (2003) A polar cloud analysis based on micro-pulse LIDAR measurements at Ny-Ålesund, Svalbard and Syowa, Antarctica. Phys Chem Earth, 28:1205-1212. https://doi.org/10.1016/j.pce.2003.08.057

Sikand M, Koskulics J, Stamnes K, Hamre B, Stamnes JJ, Lawson RP (2010) Optical properties of mixed phase boundary layer clouds observed from a tethered balloon platform in the Arctic. JQuant Spectrosc Ra, 111(12–13):1921-1930. https://doi.org/10.1016/j.jqsrt.2010.03.002

Sikand M, Koskulics J, Stamnes K, Hamre B, Stamnes JJ, Lawson RP (2013) Estimation of Mixed-Phase Cloud Optical Depth and Position Using In Situ Radiation and Cloud Microphysical Measurements Obtained from a Tethered-Balloon Platform. J Atmos Sci, 70:317–329. https://doi.org/10.1175/JAS-D-12-063.1

Sipilä M, Hoppe CJM, Viola A, Mazzola M, Krejci R, Zieger P, Beck L, Petäjä T (2020) Multidisciplinary research on biogenically driven new particle formation in Svalbard. In: Van den Heuvel et al. (eds): SESS report 2019, Svalbard Integrated Arctic Earth Observing System, Longyearbyen, 168 - 195 . https://sios-svalbard.org/SESS_Issue2

Tetzlaff A, Lüpkes C, Birnbaum G, Hartmann J, Nygård T, Vihma T (2014) Brief Communication: Trends in sea ice extent north of Svalbard and its impact on cold air outbreaks as observed in spring 2013. Cryosphere, 8:1757-1762. https://doi.org/10.5194/tc-8-1757-2014

Tjernström M (2005) The Summer Arctic Boundary Layer during the Arctic Ocean Experiment 2001 (AOE-2001). Bound-Lay Meteorol, 117(1):5-36. https://doi.org/10.1007/s10546-004-5641-8

Tjernström M, Birch CE, Brooks IM, Shupe MD, Persson POG, Sedlar J, Mauritsen T, Leck C, Paatero J, Szczodrak M, Wheeler CR (2012) Meteorological conditions in the central Arctic summer during the Arctic Summer Cloud Ocean Study (ASCOS). Atmos Chem Phys, 12:6863-6889. https://doi.org/10.5194/acp-12-6863-2012

Tjernström M, Leck C, Birch CE, Bottenheim JW, Brooks BJ, Brooks IM, Bäcklin L, Chang RY-W, de Leeuw G, Di Liberto L, de la Rosa S, Granath E, Graus M, Hansel A, Heintzenberg J, Held A, Hind A, Johnston P, Knulst J, Martin M, Matrai PA, Mauritsen T, Müller M, Norris SJ, Orellana MV, Orsini DA, Paatero J, Persson POG, Gao Q, Rauschenberg C, Ristovski Z, Sedlar J, Shupe MD, Sierau B, Sirevaag A, Sjogren S, Stetzer O, Swietlicki E, Szczodrak M, Vaattovaara P, Wahlberg N, Westberg M, Wheeler CR (2014) The Arctic Summer Cloud Ocean Study (ASCOS): overview and experimental design. Atmos Chem Phys, 14:2823-2869. https://doi.org/10.5194/acp-14-2823-2014

Tjernström M, Leck C, Persson CO, Jensen ML, Oncley SP, Targino A (2004) The Summertime Arctic Atmosphere: Meteorological Measurements during the Arctic Ocean Experiment 2001. B Am Meteorol Soc, 85:1305–1322. https://doi.org/10.1175/BAMS-85-9-1305

Treffeisen R, Krejci R, Ström J, Engvall AC, Herber A, Thomason L (2007) Humidity observations in the Arctic troposphere over Ny-Ålesund, Svalbard based on 15 years of radiosonde data. Atmos Chem Phys, 7:2721-2732. https://doi.org/10.5194/acp-7-2721-2007

Vihma T, Kilpeläinen T, Manninen M et al. (2011) Characteristics of Temperature and Humidity Inversions and Low-Level Jets over Svalbard Fjords in Spring. Adv Meteorol, 2011:14p. https://doi.org/10.1155/2011/486807

Viola AP, Hudson SR, Krecji R, Ritter C, Pedersen CA (2019) The Lower Atmosphere above Svalbard (LAS): Observed long-term trends, small scale processes and the surface exchange. In: Orr et al. (eds): SESS report 2018, Svalbard Integrated Arctic Earth Observing System, Longyearbyen, pp. 108-118. https://sios-svalbard.org/SESS_Issue1

Voss PB, Hole LR, Helbling EF et al. (2013) Continuous In-Situ Soundings in the Arctic Boundary Layer: A New Atmospheric Measurement Technique Using Controlled Meteorological Balloons. J Intell Robot Syst, 70:609. https://doi.org/10.1007/s10846-012-9758-6

Wessel S, Aoki S, Winkler P, Weller R, Herber A, Gernandt H, Schrems O (1998) Tropospheric ozone depletion in polar regions A comparison of observations in the Arctic and Antarctic. Tellus B, 50(1):34-50. https://doi.org/10.3402/tellusb.v50i1.16020

Yamazaki A, Inoue J, Dethloff K, Maturilli M, König-Langlo G (2015) Impact of radiosonde observations on forecasting summertime Arctic cyclone formation. J Geophys Res-Atmos, 120:3249– 3273. https://doi.org/10.1002/2014JD022925

Permafrost temperatures and active layer thickness in Svalbard during 2017/2018 (PermaSval)

Hanne H. Christiansen[1], Graham L. Gilbert[1,2], Nikita Demidov[3], Mauro Guglielmin[4], Ketil Isaksen[5], Marzena Osuch[6], Julia Boike[7]

1 University Centre in Svalbard, UNIS, Arctic Geology Department, Longyearbyen, Norway.
2 Norwegian Geotechnical Institute, Natural Hazards Division, Oslo, Norway.
3 Arctic and Antarctic Research Institute, AARI, Ministry of Natural Resources and Environment, Russia.
4 Insubria University, Department of Theoretical and Applied Science, Varese Italy.
5 Norwegian Meteorological Institute, Research and Development Department, Oslo, Norway.
6 Institute of Geophysics, Polish Academy of Sciences, Poland.
7 Alfred Wegener Institute for Polar and Marine Sciences, Potsdam, & Geography Department, Humboldt-Universität Berlin, Germany.

Corresponding author: Hanne H. Christiansen (hanne.christiansen@unis.no)
ORCID Number: 0000-0002-6218-3493

Keywords: Permafrost, active layer, meteorology, ground temperature, Svalbard

1. Introduction

Permafrost is ground (soil or rock) that remains at or below 0 °C for two or more consecutive years. In Svalbard, changes in permafrost conditions have the potential to impact infrastructure, ecosystems and slope stability. This is because the strength and stability of frozen soil are closely related to its temperature. Globally permafrost is significant due to its role in preserving ancient organic matter and entrapping greenhouse gases. Monitoring permafrost essential climate variables (ECVs) is important for the assessment of local landscape stability and in quantifying the impacts of climate change on cold-region landscapes and their ecosystems. Permafrost data are globally archived in the Global Terrestrial Network on Permafrost (GTN-P).

This report follows up on the report published in the SESS Report 2018 (Christiansen et al. 2019). Since 2018, the Norwegian Environment Agency has released the *Climate in Svalbard 2100* report summarizing observed trends in permafrost conditions over the period of field measurements and a forecast for the future, based on recent climate and permafrost modelling (Hanssen-Bauer et al. 2019). It is well established that the terrestrial cryosphere in Svalbard has changed since modern permafrost monitoring efforts began in the late 1990s. In central Svalbard in the Adventdalen area, ground temperatures have risen by as much as 0.15°C per year (10 m depth) and the thickness of the seasonally-unfrozen active layer increased by 0.6 cm per year since 2000 in sediments and 1.6 cm/year in bedrock (Hanssen-Bauer et al. 2019), while in Ny-Ålesund ground temperatures increased by 0.18°C/year and the thickness of active layer increased by 5 cm/year (Boike et al. 2018). Modern monitoring techniques mean that it is relatively easy to quantify permafrost change in terms of temperature. The visible effects of warming permafrost are, however, more ambiguous. A prolonged thaw season is anticipated to result in a thicker active layer, and increased rainfall intensity can result in more frequent landslides. The strength of frozen soil decreases when warming and permafrost change may expectedly result in infrastructure problems in cases where climate change was not considered during the initial design.

The aims of this part of the State of Environmental Science in Svalbard reporting are to: (1) provide an overview of permafrost data collected during the 2017-2018 hydrological year (1 September 2017 – 31 August 2018), (2) contrast these results with the 2016-2017 hydrological year as presented in Christiansen et al. (2019), (3) summarise developments in permafrost monitoring in Svalbard, and (4) provide recommendations for future permafrost investigations. Understanding the spatial distribution of permafrost conditions is critical to predicting geomorphological change and understanding the variability in climate impacts.

2. The thermal state of permafrost

A summary of air temperature, precipitation, permafrost temperature, and active layer thickness for the 2017-2018 hydrological year, extending from 1 September 2017 and 31 August 2018 is provided in this section. Background information concerning these climate variables and permafrost conditions in Svalbard can be found in Christiansen et al. (2019). Site specific details can be found in Isaksen et al. (2001), Christiansen et al. (2010), Demidov et al. (2016), Boike et al. (2018), Christiansen et al. (2019), and Gilbert et al. (2019). The borehole locations are presented in Figure 1.

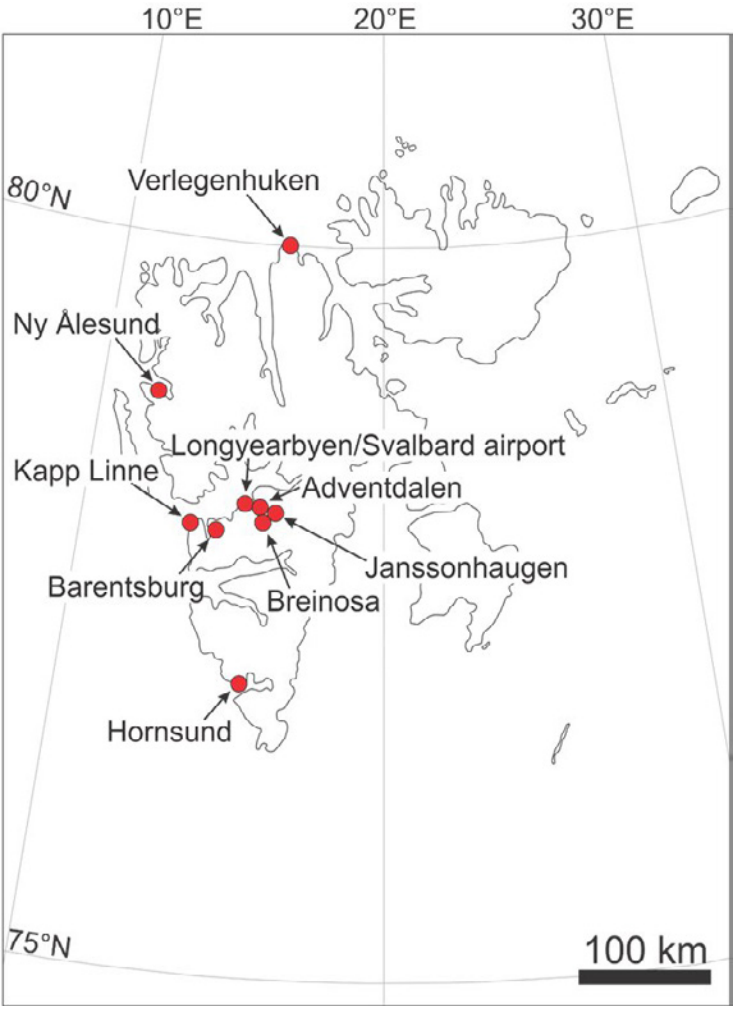

Figure 1: Location of permafrost boreholes and key observation sites mentioned in the text.

2.1 Air temperature, degree days, precipitation, and snow

Average air temperatures near the permafrost borehole locations during the 2017-2018 hydrological year ranged from -0.7°C at Kapp Linné to -3.0°C at Janssonhaugen. For most sites, average air temperatures were near to -1.5°C. In comparison with 2016-2017, conditions during the 2017-2018 hydrological year were markedly warmer (Table 1). Mean air temperatures were higher at all locations, by between 0.9°C (Ny-Ålesund) and 0.1°C (Hornsund).

The magnitude of freezing and thawing conditions is quantified and compared between the two hydrological years by using the thawing-degree days (TDD) and freezing-degree days (FDD) indices (Table 1). In the 2016-2017 hydrological year the thawing season extended relatively late until November 2016 (c.f. Christiansen et al. 2019), however, TDD calculated for both periods are comparable, within ca. 30 of each other (Table 1). This indicates that the total magnitude of the thawing season was relatively similar during the two periods. In contrast, the 2016-2017 hydrological year was significantly colder than the 2017-2018 hydrological year. FDD indices were greater in the 2016-2017 hydrological year (ranging from 1198 at Kapp Linné to 1955 at Janssonhaugen) than in the 2017-2018 hydrological year (ranging from 976 at Kapp Linné to 1678 at Janssonhaugen), indicating that, despite the shorter freezing season, the magnitude of cold temperatures was greater during the former period.

Total annual precipitation ranged from 801 mm (Hornsund) to 239 mm (Svalbard airport). The highest precipitation values were recorded near the west coast and decreased with distance inland. Generally, the total precipitation amounts were much lower than the rather wet hydrological year 2016-2017, with the largest reduction of 307 mm in Barentsburg, while Ny-Ålesund only had a 1 mm increase from the 2016-2017 hydrological year (Table 1).

Maximum snow depths at the monitoring sites varied from ca. 20 cm in Longyearbyen to ca. 140 cm in Barentsburg. In general, these spatial patterns are comparable to those described in Christiansen et al. (2019) and illustrate the effect of continentality moving towards the centre of Svalbard, and with elevation. Snow accumulation started in the end of October (e.g. 25/10/17 in Barentsburg). This is earlier than in 2016 when snow accumulation began in late-November. The timing and thickness of seasonal snow cover are significant for permafrost conditions as snow mediates the exchange of energy between the ground surface and the atmosphere. In general, a thicker snow cover which arrives earlier in the season will contribute to warmer ground conditions.

Table 1: Temperature summary at the permafrost borehole sites for the 2016-2017 and 2017-2018 hydrological years.

Location	Borehole name/ ID	MAT (°C) TDD (°C) *FDD (°C)*		MGST (°C)		MPST (°C)	
		2017	2018	2017	2018	2017	2018
Ny Ålesund	Bayelva	-2.3 701 ***1486***	-1.4 729 ***1232***	-3.6	-2.9	-2.7	-2.9
	DBNyÅlesund			-3.7 (0.3 m)	-3.1 (0.3 m)	-2.7	-3.1
Lower Adventdalen	UNIS East	-1.9 833 ***1514***	-1.3 822 ***1279***	n/a	-1.3	n/a	-2.2
	Old Auroral Station 2			-1.3	-1.1	-3.2	-3.3
	Endalen			n/a	-0.1	-0.5	-1.1
Inner Adventdalen	Breinosa	-3.8 569 ***1955***	-3.0 591 ***1678***	-4.1	-4.1	-4.0	-4.2
	Janssonhaugen/ P10			n/a	n/a	n/a	n/a
	Janssonhaugen/ P11			-3.7 (0.2 m)	-3.3 (0.2 m)	-3.7	-3.5
Kapp Linné	Kapp Linné 1	-1.2 746 ***1198***	-0.7 732 ***976***	-1.6	-1.5	-1.8	-1.8
	Kapp Linné 2			-1.6	-1.4	-1.5	-1.3
Barentsburg	Borehole 12	-2.2 707 ***1506***	-1.7 680 ***1292***	-0.8	-1.5	-1.3	-1.8
Hornsund	Meteo	-1.3 726 ***1210***	-1.2 607 ***1049***	-1.0	-0.7 (0.2 m)	n/a	-0.9

MAT: Mean annual air temperature
TDD: Thawing degree days
FDD: Freezing degree days
MGST: Mean ground surface temperature
MPST: Mean permafrost surface temperature

	MGT (°C) (depth)		Precipitation (mm)		Maximum snow depth (cm)	Active layer thickness (cm)* *Interpolated values* **CALM grid (± std. dev.)**		Duration of active-layer freeze-back (days)	
	2017	2018	2017	2018		2017	2018	2017	2018
	-2.8 (9 m)	-2.6 (9 m)	656	657	>100	*200*	*179*	*49*	*62*
	-3.1 (20 m)	-3.1 (20 m)			50	*148*	*142* **166±20**	*35*	*56*
	n/a	-3.0 (8 m)	305	239	<20	*n/a*	*96*	*n/a*	*63*
	-5.2 (10 m)	-5.1 (10 m)			20	*94* **105±6**	*93* **103±5**	*22*	*53*
	-2.7 (19 m)	-2.6 (19 m)			50	*190*	*204*	*140*	*151*
	-5.1 (10 m)	-5.1 (10 m)	n/a	n/a	<50	*49*	*64*	*18*	*2*
	-5.0 (20 m)	-4.8 (20 m)			<20	n/a	n/a	n/a	n/a
	n/a	n/a			<20	*185*	*187*	*41*	*36*
	-2.6 (20 m)	-2.5 (20 m)	711	427	<10	*300*	*297*	*44*	*72*
	-2.8 (20 m)	-2.7 (20 m)			<10	*190*	*195*	*49*	*72*
	-2.3 (15 m)	-2.3 (15 m)	849	542	ca. 20	*175* **138±10**	*147* **145±10**	*59*	*59*
	-1.1* (12 m)	-1.2 (12 m)	754	801	46	*n/a*	*463*	*n/a*	*113*

2.2 The ground thermal regime

Ground thermal conditions are presented for the five main permafrost observation sites in Svalbard: Ny-Ålesund, Adventdalen, Kapp Linné, Barentsburg, and Hornsund. Borehole locations and instrumentation at each site is detailed in Christiansen et al. (2019) and Gilbert et al. (2019). A summary of the ground thermal regime during the 2017-2018 hydrological year at each site is presented in Figure 2 . A time-series of selected depths in the top active layer and at around 10 m depth as close as possible to the depth of zero annual amplitude, is plotted together with air temperatures in Figure 3 to indicate the seasonal temporal fluctuations in temperatures. Mean hydrological year temperatures at key depths are summarised in Table 1, since 2016.

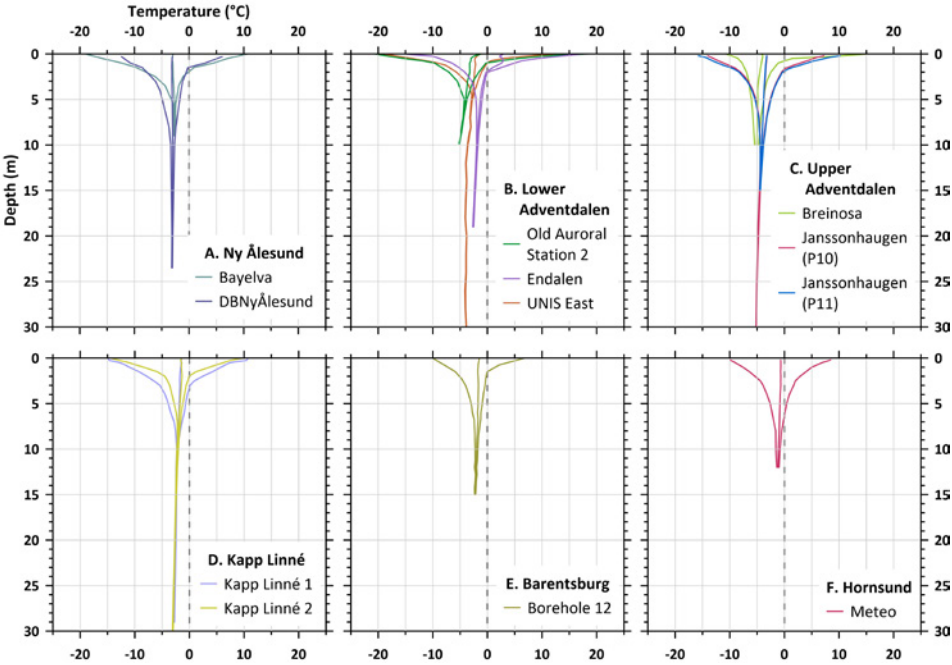

Figure 2: Ground thermal snapshot (minimum, mean, and maximum temperatures) measured in the upper 10 – 30 m of the permafrost observation boreholes in Svalbard during the 2017-2018 hydrological year.

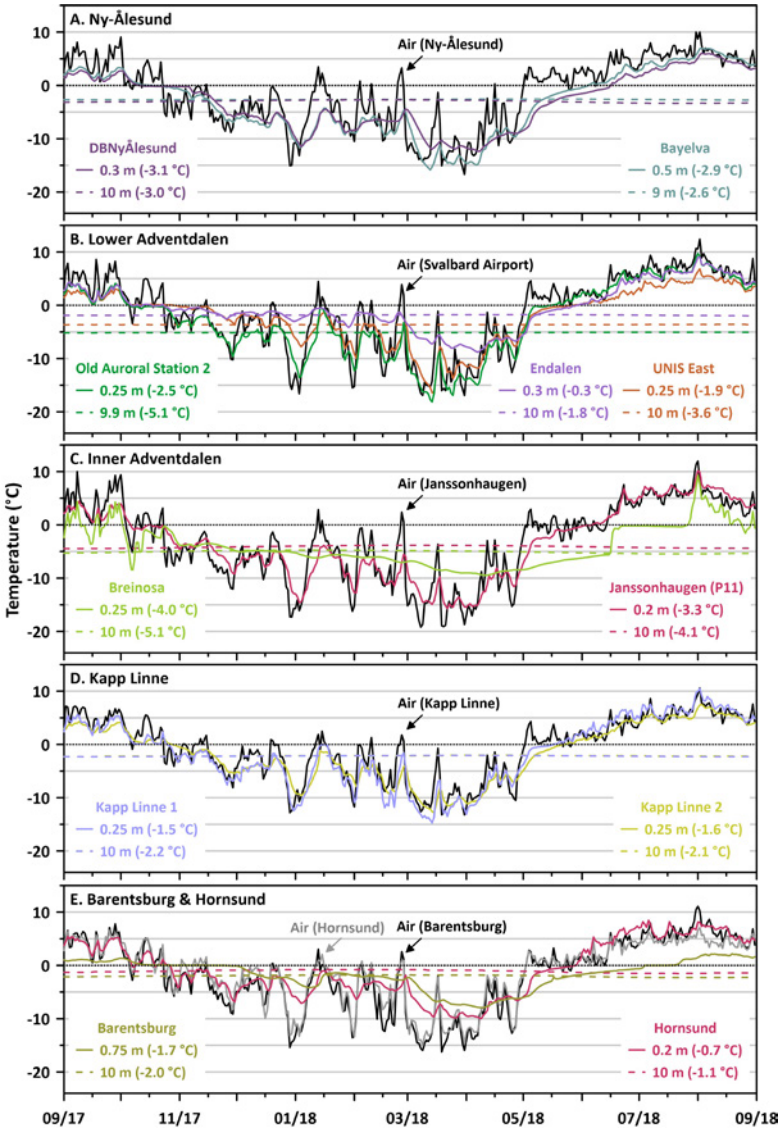

Figure 3: Air and ground temperatures during the 2017-2018 period for the five permafrost observations areas in Svalbard. The presented selected sensors are located near to the ground surface (ca. 0.2 – 0.75 m) and at 10 m depth (where possible). The mean ground temperature, calculated at each depth, is presented in brackets.

The ground is warmest near to the coasts (e.g. Kapp Linne & Hornsund) and in areas with thicker snow cover during winter (e.g. Endalen & Bayelva). Mean annual temperatures at the ground surface (MGST) ranged from - 0.1°C (Endalen) to - 4.1°C (Breinosa). Mean annual temperature near the permafrost surface (MPST) varied from - 0.9°C (Hornsund) to - 4.2°C (Breinosa), see Table 1. Mean annual ground temperatures (MGT), as measured at the depth of zero annual amplitude or lowermost sensor, varied from - 1.2°C (Hornsund at 12 m depth) to - 5.1°C (Breinosa and Old Auroral Station 2 at ca. 10 m depth) Table 1.

The duration of active layer freeze back is a significant parameter which, as an integral of air temperatures, snow conditions (onset and total thickness), soil moisture, and surficial geology, influences permafrost conditions by restricting heat exchange to the atmosphere for its duration. During the 2017-2018 hydrological year, the duration of active layer freeze back varied from 2 days at Breinosa to 151 days at Endalen (Table 1). Breinosa is a mountain top dry block-field site with coarse blocky material (Christiansen et al. 2019). Estimating active layer freeze back at this site is problematic due to convection within the blocky material. In most cases, the active layer freeze back duration was longer during the 2017-2018 hydrological year than in the 2016-2017 hydrological year. The difference is likely due to the smaller number of FDD during the 2017/2018 hydrological year providing less cooling following the transition to freezing air temperatures in autumn.

Aside from proximity to the coast, the temporal distribution of snow and soil moisture appear to be the most significant factors controlling permafrost conditions locally in Svalbard. Temperature presented in this report, including the first full year of ground temperature data from the Hornsund area, indicate that the north-south gradient present in air temperatures is also present in ground temperatures in Svalbard with the warmest permafrost temperatures in Hornsund in the South, intermediate in Barentsburg and Kapp Linne in the central part, and lowest in the Ny-Ålesund area in the northern part. The Endalen site, located on a hillslope in central Spitsbergen exhibits the warmest permafrost conditions in Svalbard. This is likely because of snow conditions coupled with drainage conditions on the slope, which impact permafrost through advective heat transfer and saturation of the active layer – prolonging active layer freeze back and delaying cooling. It appears permafrost is most susceptible to degradation at such locations.

2.3 Active layer thickness

The thickness of the active layer is either recorded directly through probing in CALM sites or calculated by interpolating the depth of the 0°C isotherm using borehole thermal measurements (Burn, 1998). Interpolation is used towards the end of the thawing season to calculate active layer thickness in the borehole temperature data. From the three Circumpolar Active Layer Monitoring (CALM) sites in Svalbard, in Adventdalen (UNISCALM),

near Barentsburg, and in Ny Ålesund (Christiansen & Humlum 2008; Shiklomanov et al. 2012; Christiansen et al. 2019) thaw progression measured by probing is provided as a value recorded towards the end of the thawing season (Table 1).

Active layer thickness varied in summer 2018 between 64 cm (Breinosa) and 463 cm (Hornsund). The thinnest active layer is reported from a block field. Sites with sediment typically report active layer thicknesses of between 90 cm and ca. 180 cm. At bedrock sites, active layer thickness exceeded 185 cm. Comparing the results from this period with the 2016-2017 hydrological year (Christiansen et al. 2019), there is no clear pattern in change. Based on borehole interpolation, active layer thickness appears to have decreased in Ny-Ålesund and at selected sites in Adventdalen, Kapp Linné, and Barentsburg, while increasing at Janssonhaugen and a few other sites. Data measured in the CALM grids indicate a reduction in mean active layer thickness in Adventdalen and an increase in Barentsburg (Table 1). Interpolated data indicate an active layer thickness of ca. 463 cm at Hornsund. This is tentatively attributed to a combination of local meteorological conditions with higher air temperatures, ground water flow and the advection of heat to the thawing front. Analysis of extended data series will help to better understand the relation of active layer thickness and environmental variables in Svalbard.

3. Future permafrost challenges in Svalbard

3.1 Permafrost conditions in other geographic areas in Svalbard

Recent efforts by Norwegian permafrost researchers have centred on expanding the ground temperature monitoring network in Svalbard as part of the SIOS-InfraNor project[1]. In summer 2019, a 30 m deep borehole was drilled and instrumented at Verlegenhuken on the northernmost part of the island Spitsbergen at 80°N, next to the existing meteorological station. Measurements, recorded one day after drilling, indicated ground temperatures at 30 m depth were -4.3 °C. However, temperatures might be out of equilibrium due to the energy introduced during drilling. Future measurements, when collected during 2020, will be very interesting to study to provide the first data on the permafrost thermal regime in northern Svalbard.

1 https://sios-svalbard.org/InfraNor

The Russian team drilled and equipped two temperature monitoring boreholes (15 m each) in the top of two pingos in Grøndalen and has already fed data into GTN-P. Hopefully, it will also be possible to expand the permafrost observation network to cover the Pyramiden settlement located centrally in Svalbard, where no permafrost observations are yet collected, but where meteorological observations take place. It will hopefully be possible to establish permafrost observations in Pyramiden as a result of our international cooperation.

3.2 Permafrost conditions at greater depth in the ground

As part of the SIOS-InfraNor project, a drilling campaign was conducted during spring 2019 to extend existing boreholes in central Svalbard to 20 m depth. This will provide additional information on ground temperatures below the depth of annual temperature fluctuations, further increasing our ability to analyse the impacts of permafrost thermal conditions on environmental change. In addition, analysis of permafrost cores taken during this drilling campaign will improve our understanding of the physical properties of permafrost, necessary to make better predictions of future changes. These investigations will aid in answering questions regarding permafrost thermal conditions at depth and in portions of Svalbard not previously instrumented.

4. Connections and synergies

Permafrost is the foundation for the built environment and many landforming processes in Svalbard. Changes in permafrost conditions impact many other research areas including ecology, glaciology, hydrology, greenhouse gas cycling and nutrient transport. The effects of permafrost change are likely to spill-over and impact other realms. The contents are relevant for other research themes addressed in the current SESS report including understanding spatial variations in plant productivity, ecological and seismic monitoring, and glacier change. Future versions of SESS reporting may seek to better integrate permafrost related research outcomes with other aspects of the terrestrial cryosphere and environmental monitoring initiatives.

5. Recommendations for the future

- *Maintain existing monitoring networks and instrumentation*. Long-term, field-based monitoring of the permafrost essential climate variables (ECV) is essential to develop knowledge of the impacts of climate change on polar landscapes. The monitoring network operated between the international partners contributing to this SESS report will be critical in evaluating permafrost conditions in Svalbard into the future.
- *Expand the permafrost ECV monitoring network and making the data available online*. Currently, there are large areas with little or no permafrost observations in northern, southern, and eastern Svalbard. Recent (e.g. instrumenting the borehole at Verlegenhuken) and planned future permafrost observation efforts through SIOS will contribute to improving our knowledge about permafrost conditions in these relatively unknown areas. New boreholes using modern technology should be able to provide online access to the permafrost data both for improved process understanding, but also for use during potential landslides preparedness situations and educational and outreach purposes.
- *Assessing the response of permafrost landscapes to changes in climate by obtaining more knowledge about the ground ice content*. Only a few of the permafrost observation borehole in Svalbard have full scale cryostratigraphical information, with the key parameter the ground ice content being very important for understanding potential consequences at landform scale for warming permafrost and thicker active layers.
- *Investigate avenues to increase the time-scale of permafrost observations*. Efforts should be made to rehabilitate sites where permafrost conditions may have been monitored in the recent past – either as part of mining exploration or scientific research in Svalbard.
- *Continue to develop remote sensing tools for monitoring permafrost conditions and landscape response*. Site-specific monitoring information can be upscaled using remote sensing tools that SIOS also provides.
- *Improve interdisciplinary networking on permafrost related issues*. Increase the dialogue between the research scientists and practitioners on engineering and other key cryospheric issues related to permafrost. Additionally, very little is known about conditions at the base of permafrost (total thickness, permeability, and pressures) – increasing dialogue between other branches of geosciences may allow for new breakthroughs and understanding of the role of permafrost in trapping hydrates and greenhouse gases.

6. Data availability

The data included in this report have been made available through the Global Terrestrial Network for Permafrost (GTN-P) database.

Acknowledgements

We are grateful to SIOS for supporting the development of this report. Both the meteorological and permafrost data that this report is based upon have been funded by our national research councils and the participating institutions, which the authors are based in. Financial support at Hornsund was provided by the Polish National Science Centre through grant No. 2016/21/B/ST10/02509. This work was supported by the Research Council of Norway, project number 251658, Svalbard Integrated Arctic Earth Observing System - Knowledge Centre (SIOS-KC).

References

Boike J, Juszak I, Lange S et al. (2018) A 20-year record (1998–2017) of permafrost, active layer and meteorological conditions at a high Arctic permafrost research site (Bayelva, Spitsbergen). Earth System Science Data 10:355

Burn CR (1998) The active layer: two contrasting definitions. Permafrost Periglac Process 9: 411-416

Christiansen HH, Humlum O (2008) Interannual variations in active layer thickness in Svalbard. In: Proceedings Ninth International Conference on Permafrost, June, pp. 257-262

Christiansen HH, Etzelmüller B, Isaksen K et al. (2010) The thermal state of permafrost in the nordic area during the international polar year 2007–2009. Permafrost Periglac Process 21:156–181

Christiansen HH, Gilbert GL, Demidov N, Guglielmin M, Isaksen K, Osuch M, Boike J (2019) Permafrost thermal snapshot and active-layer thickness in Svalbard 2016-2017. In: Orr et al (eds): SESS report 2018, Svalbard Integrated Arctic Earth Observing System, Longyearbyen, pp. 26–47. https://sios-svalbard.org/SESS_Issue1

Demidov NE, Verkulich SR, Karaevskaya ES, Nikulina AL, Savatyugin LM (2016) First results of permafrost monitoring on the cryospheric site of Russian Scientific Center on Spitsbergen (RSCS). Problems of Arctic and Antarctic 110: 67-79

Gilbert GL, Instanes A, Sinitsyn A, Aalberg A (2019) Characterization of two sites for geotechnical testing in permafrost: Longyearbyen, Svalbard. AIMS Geoscience, In press.

Hanssen-Bauer I, Førland E, Hisdal H, Mayer S, Sandø A, Sorteberg A (2019) Climate in Svalbard 2100 – a knowledge base for climate adaptation. Norsk klimaservicesenter (NKSS)/Norwegian Centre for Climate Services (NCCS)

Isaksen K, Holmlund P, Sollid J, Harris C (2001) Three deep Alpine-permafrost boreholes in Svalbard and Scandinavia. Permafrost Periglac Process 12:13-25

Shiklomanov NI, Streletskiy DA, Nelson FE (2012) Northern hemisphere component of the global circumpolar active layer monitoring (CALM) program. In: Proc 10th Int Conf on Permafrost, 1:377-382

Spitsbergen Oceanic and Atmospheric interactions (SOA)

Manuel Bensi[1], Vedrana Kovačević[1], Leonardo Langone[2], Stefano Miserocchi[2], Maurizio Demarte[3], Roberta Ivaldi[3]

1 National Institute of Oceanography and Experimental Geophysics, Sgonico (Trieste), 34010, Italy
2 Institute of Polar Sciences, National Research Council of Italy, Via P. Gobetti 101, 40129 Bologna, Italy
3 Italian Navy Hydrographic Institute, Genova, 16126, Italy

Corresponding author: Manuel Bensi, mbensi@inogs.it, https://orcid.org/0000-0002-0548-7351

Keywords: Deep sea thermohaline variability, along slope currents, shelf-slope dynamics

1. Introduction

The Fram Strait is a crossroad of water masses that along its eastern part head towards the Arctic Ocean, and along its western edge, towards the Atlantic Ocean. This region is therefore strongly characterized by the interaction between waters of Atlantic and Arctic origins and by the local/remote atmospheric forcing and sea ice formation/melting, which contribute to driving the global thermohaline circulation (Skogseth et al. 2007; Nilsen et al. 2016; Onarheim and Årthun 2017; Polyakov et al. 2017; Bensi et al. 2019a). To understand the oceanic long-term

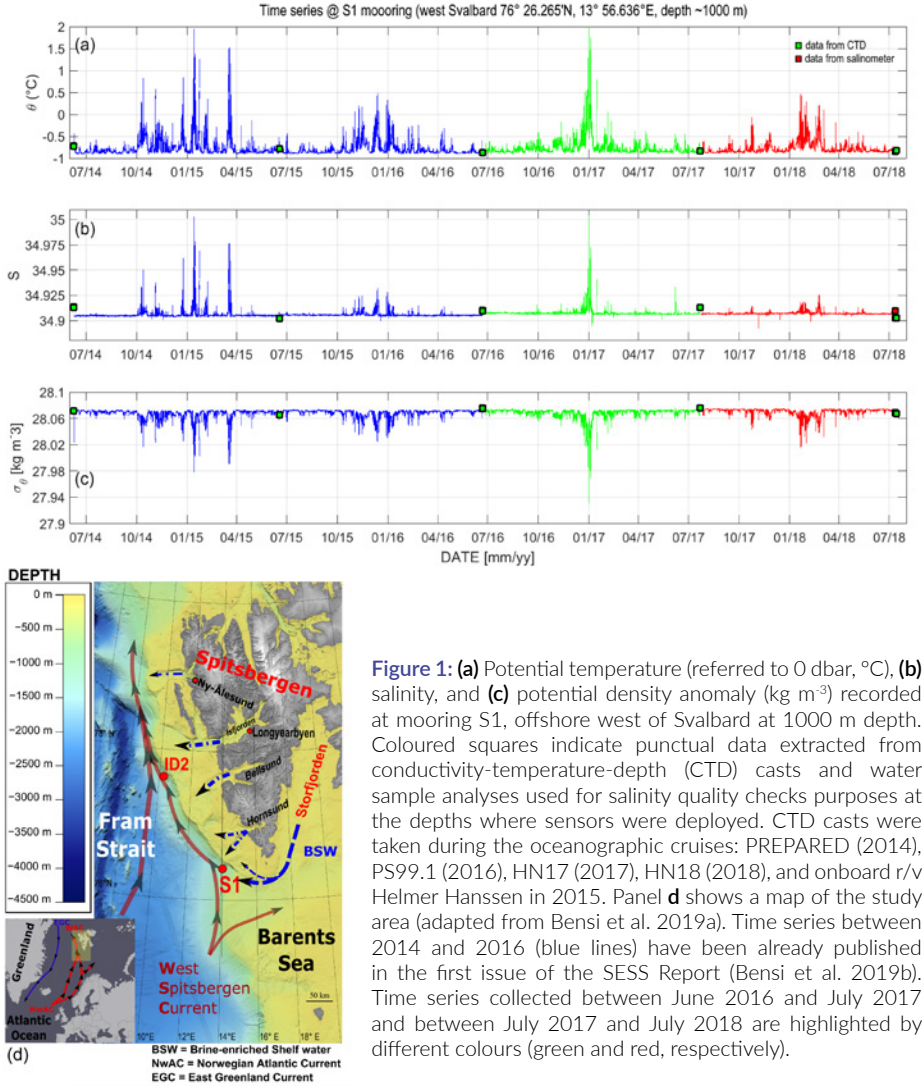

Figure 1: **(a)** Potential temperature (referred to 0 dbar, °C), **(b)** salinity, and **(c)** potential density anomaly (kg m^{-3}) recorded at mooring S1, offshore west of Svalbard at 1000 m depth. Coloured squares indicate punctual data extracted from conductivity-temperature-depth (CTD) casts and water sample analyses used for salinity quality checks purposes at the depths where sensors were deployed. CTD casts were taken during the oceanographic cruises: PREPARED (2014), PS99.1 (2016), HN17 (2017), HN18 (2018), and onboard r/v Helmer Hanssen in 2015. Panel **d** shows a map of the study area (adapted from Bensi et al. 2019a). Time series between 2014 and 2016 (blue lines) have been already published in the first issue of the SESS Report (Bensi et al. 2019b). Time series collected between June 2016 and July 2017 and between July 2017 and July 2018 are highlighted by different colours (green and red, respectively).

variability related both to natural and anthropogenic causes, especially in sensitive areas such as the Svalbard Archipelago, it is fundamental to collect long time series. At the same time, efficient monitoring and predicting of the world ocean must be a collaborative effort, useful to optimize and integrate ocean observing systems, sensors deployment and usage, and quality check of the data (Pearlman et al. 2019). Moreover, oceanographic data have to be analysed together with atmospheric ones, and with data collected on land, to provide a comprehensive view of the links between the different Earth's spheres. Here, we briefly present the updated time series collected by means of the deep-sea oceanographic mooring named S1, located south-west offshore Svalbard at ~1040 m depth (Lat. 76° 26.28'N Lon. 13° 56.91'E, Figure 1). Actually, the data series for temperature, salinity, dissolved oxygen, turbidity, and horizontal currents span over a time interval from June 2014 until July 2018. Data from June 2016 to July 2018 integrate those presented in the first issue of the SESS report released in January 2019 (Bensi et al. 2019b, data from 2014-2016). The comparison of oceanographic time series collected at S1 with atmospheric data (air temperature, wind speed and direction, heat fluxes at the air-ocean interface) provides information about the variability that characterizes the deep-sea layer along the West Svalbard continental margin (Bensi et al. 2019a). Atmospheric time series (air temperature, wind speed and direction, heat-fluxes at the air-ocean interface) are obtained from the ECMWF ERA-interim (European Centre for Medium-range Weather Forecasts) dataset.

2. The state of the oceanographic time series from mooring station S1 (76° N, 013° E)

Thermohaline data collected at S1, at depths between ~900 m and ~1000 m, reveal periodical peaks in temperature and salinity, which are translated into temporary reductions of the deep layer density, in particular between October and April. During 4 years of measurements, the most extreme episode was recorded between the end of 2016 and the beginning of 2017, when data showed that the potential temperature and salinity exceeded 2.5 °C and 35,

Table 1: Extreme values recorded at 1000m depth, at S1 mooring station, between October and April. Typical values of potential temperature, salinity, and potential density within the Norwegian Deep Sea Water at 1000 m depth in this region are -0.91 °C, 34.91, and 28.07 kg m^{-3}.

	Oct-Apr 2014-2015	Oct-Apr 2015-0216	Oct-Apr 2016-2017	Oct-Apr 2017-2018
Potential temperature (°C)	max 1.94	max 0.48	max 2.53	max 0.47
Salinity	max 35.00	max 34.97	max 35.00	max 34.92
Potential density anomaly (kg m^{-3})	min 27.978	min 28.02	min 27.93	min 28.01
Current magnitude (cm s^{-1})	max 60	max 35	max 85	max 49

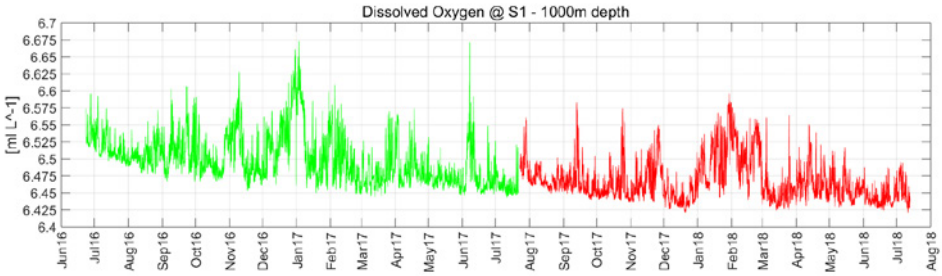

Figure 2: Dissolved oxygen (ml l^{-1}) recorded at S1. Data cover the period from June 2016 to July 2018. The optical sensor used was the Sea-Bird Electronics SBE 63, mounted on a SBE-37-ODO microcat. Time series collected between June 2016 and July 2017 and between July 2017 and July 2018 are highlighted by different colours (green and red, respectively).

respectively (Figure 1). Peak values of thermohaline properties and currents that occurred between 2014 and 2018 on the West Svalbard continental slope are reported in Table 1. Peaks in temperature and salinity were recorded in winters in which the maximum current speeds were also higher. The most extreme event, at the end of 2016 and the beginning of 2017, was indeed characterized by currents with magnitude up to 85 cm/s. The analysis of the direction revealed also an abrupt change from NW to SE, similarly to what was observed during other events within the period 2014-2016 (Bensi et al. 2019a). This change in flow direction followed a several-days period of enhanced temperature variations. From June 2016 onwards, dissolved oxygen concentrations were also recorded at S1. This parameter can provide information about the origin of the water that temporarily reaches a depth of 1000 m. In fact, higher values of dissolved oxygen are a signal that water intrusions belong to water masses that have been more or less recently in contact with the atmosphere. Apart from a slight negative trend that could be attributable to the instrumental drift of the sensor (Figure 2) we observed that peaks in temperature and salinity were accompanied, usually, by larger oxygen values. This fact suggests that water intrusions in the deep layer occupied by the Norwegian Deep Sea Water provide not only heat and salt, but also increased oxygenation. During the deployment phase between July 2017 and July 2018, 4 temperature sensors recorded data at different depths, spanning from 885 m to 1006 m (Figure 3). The time-depth diagram of temperature interpolated in the deep layer helps to better understand the origin and propagation of the warm water intrusions within this layer. We found that they occur about every 3-4 weeks. During the sub-period between January and March (Figure 3, lower panel), their occurrence increased, and the sensors recorded at least 5 episodes in which temperature peaks were close or above 1.5 °C. Individual episodes lasted about 10-24 hours, although sometimes they were included in longer events (lasting several days) that characterized a general increase in temperature in the deep layers. Temperature peaks usually were higher in the upper part of the bottom layer, and sometimes they did not reach the deepest sensors (see e.g. episodes in October 2017 and on 1-2 March 2018), proving that the warm water intrusions are connected with the water masses from the layer above.

2.1 Periodic oscillations and low-frequency variability

During the investigated time interval (2016-2018) the mooring station S1 was also equipped with a pressure sensor, positioned at ~ 40 m from the sea bed (at depth of ~ 1004 m), which showed large-amplitude periodic oscillations (Figure 4). Statistical and harmonic analysis techniques applied to the data provided information about the tidal signal. Moreover, de-tided bottom pressure time series are able to reveal oscillations of the water column

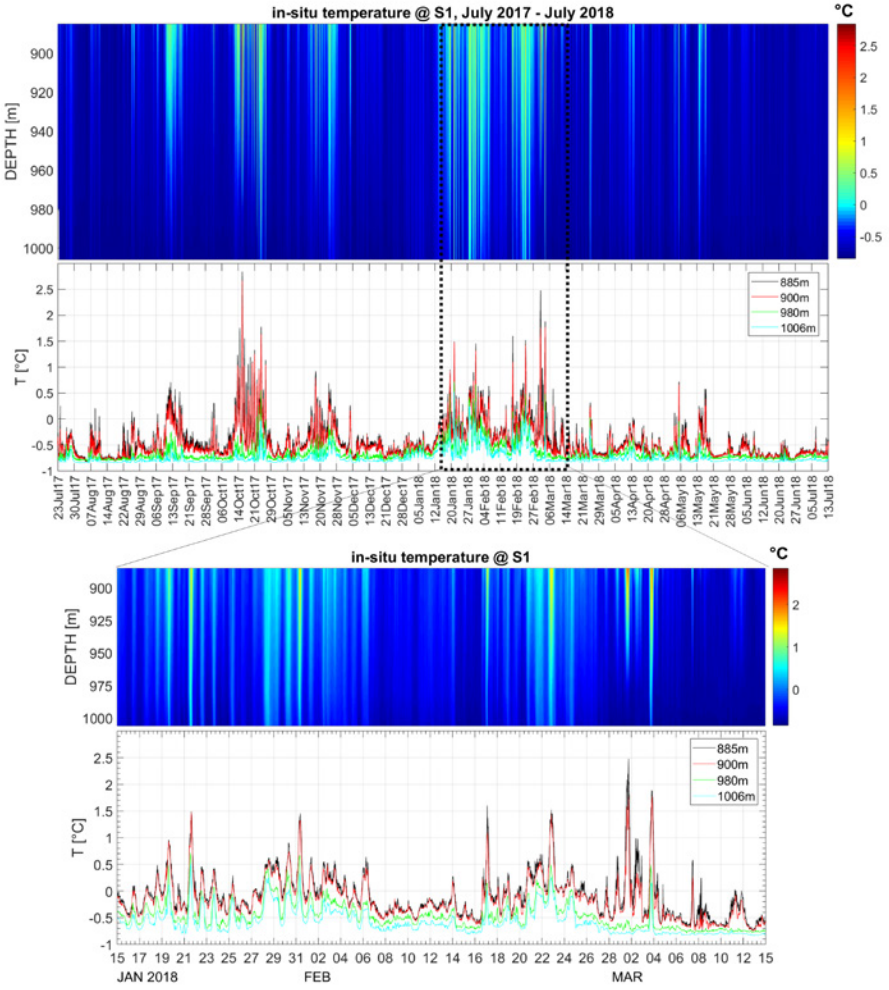

Figure 3: Time series of *in situ* temperature (°C) collected at different depths at S1 mooring station, between July 2017 and July 2018. The lower panel shows the same data with a zoom on the period 15 Jan - 15 Mar 2018.

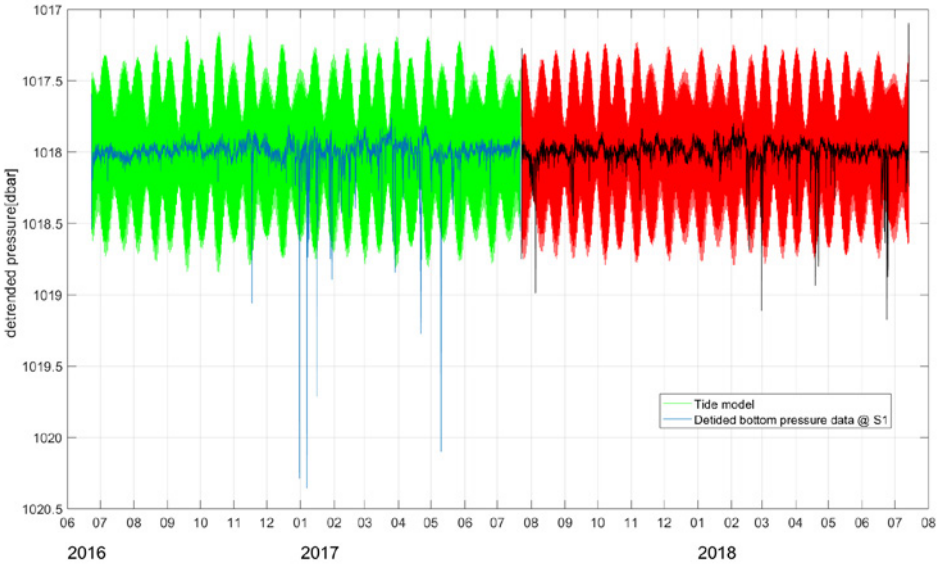

Figure 4: Tidal records (green and red refers to the two deployment phases) and residual bottom pressure time series (blue and black) obtained at S1 mooring station, offshore west of Svalbard at 1000 m depth between June 2016 and July 2017.

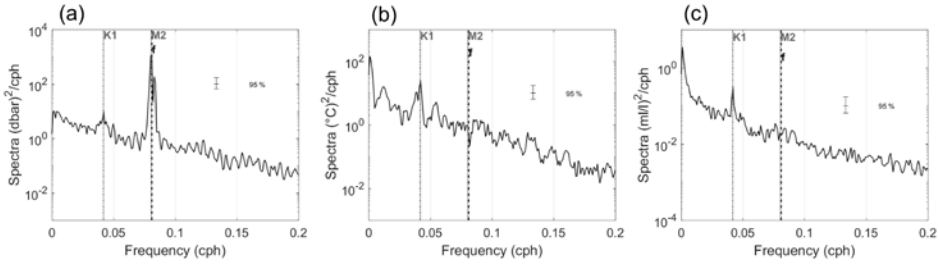

Figure 5: Spectral analysis of June 2016 - July 2017 hourly time series: raw pressure (a), potential temperature (b), dissolved oxygen concentration (c). Spectra of salinity and potential density anomaly are quite similar to those of the potential temperature, and therefore not shown. The spectra referred to the period 2017-2018 are alike. K1 (period 23.94 h) and M2 (12.42 h) are the most typical representatives of the diurnal and semidiurnal tidal constituents, respectively, while f is the inertial frequency at the latitude of S1 (period 12.34 h).

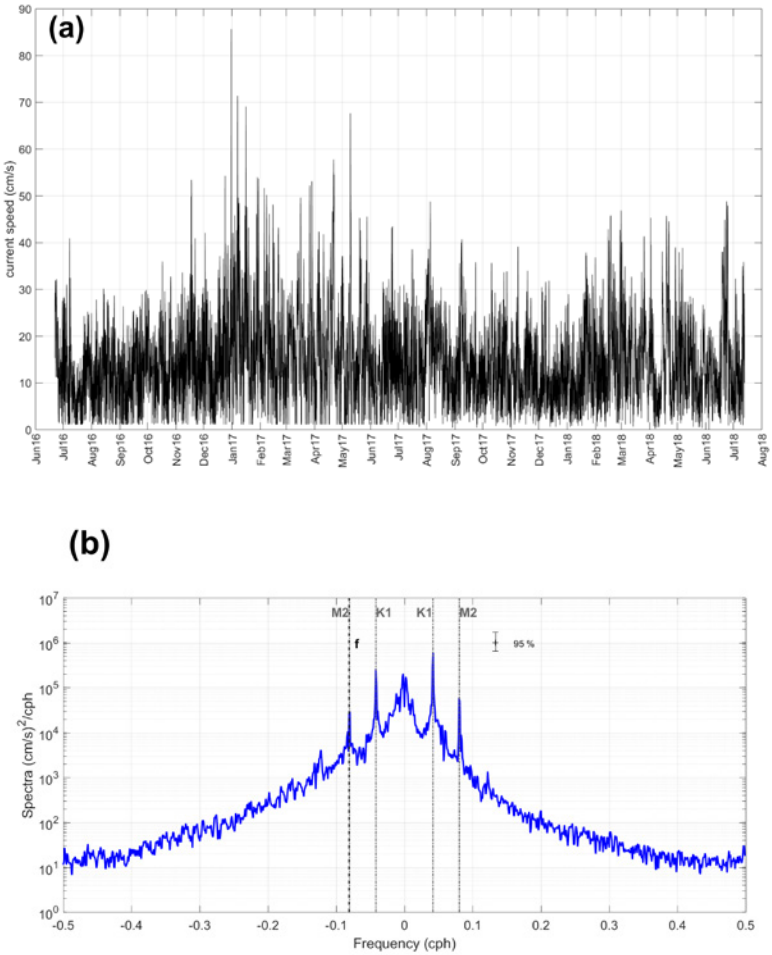

Figure 6: (a) Time series of the current speed (cm s^{-1}) at S1 (1000m depth) in the period June 2016 - July 2017**. (b)** The rotary spectrum of u (eastward) and v (northward) components of the same current time series (negative/positive frequencies refer to anticyclonic/cyclonic rotations). The power spectrum of the same dataset from July 2017 - July 2018 has very similar characteristics.

that are not related to the tides, and hence can be associated with other signals. The power spectrum analysis has been performed separately for each yearly deployment period due to the time gap between the mooring recovery and re-deployment. Both periods confirm that the large-amplitude diurnal and semidiurnal oscillations are due to the tidal movements of the sea level (corresponding to about 1 m amplitude). The variance due to these oscillations is far more important than any other periodic signals of the pressure and the semidiurnal is more energetic than the diurnal one (Figure 5a). The low-frequency part is emerging only in

the residual pressure values (tidal constituents filtered out). Oscillations of the thermohaline properties, as shown for the potential temperature (Figure 5b), and dissolved oxygen (Figure 5c) seem to be significantly energetic at the low-frequency spectrum end (i.e., at periods of about 3-4 days and about 40 days). Tidal peaks are also evident, but the diurnal one is more energetic than the semi-diurnal, contrary to that of the pressure. The significant oscillations of the turbidity at 1000 m depth are concerning the low-frequency band, and there are only some correspondences with the already evident tidal bands (not shown). Note also that turbidity during 2016-2017 refers to the 900 m depth (140 m above the sea bed). Its power spectrum (not shown) has no significant oscillations at that depth, except at the very low-frequency spectrum end. We believe that the different depth at which the turbidity sensor was placed during 2016-2017 (900 m) and 2017-2018 (1000 m) can explain the slightly higher energy both at the diurnal and long-period time scales found during the second year of measurements. This behaviour could be partially related to the fact that some periodic turbidity oscillations are mostly driven by a sediment resuspension from the sea bed, while the occasional significant turbidity increase, often unlinked with the thermohaline parameters, is related possibly to another kind of phenomena, e.g. the advection of the sediment-rich near-bottom flow from slope/shelf areas. The deep horizontal currents appeared also influenced by the diurnal and semidiurnal signals, as well as by the low-frequency fluctuations (with periods of about 3 weeks, Figure 6). The rotations in the positive sense (cyclonic) were slightly more energetic than in the negative (anti-cyclonic) sense and diurnal oscillations have more variance than the semidiurnal ones. The particularity of the semidiurnal band of the current flow is the overlapping of the semidiurnal tidal and inertial frequencies, the latter being present in marine currents, and absent in the sea-level (pressure). The only ECMWF atmospheric variables showing the diurnal, although rather weak, signal are air temperature at 2 m height and to a lesser extent, the mean sea level air pressure. Wind components are oscillating energetically only at long periods, from a week onward (not shown).

2.2 Concluding remarks

As observed during four years (2014-2018) of thermohaline and current recordings, the deep layer at the West Svalbard slope was perturbed several times with peculiar manifestations of thermohaline properties, currents, and turbidity, as noticed above and in Bensi et al. (2019a, b). Not all the phenomena occurred simultaneously, and often turbidity variations were decoupled from the thermohaline variability. As an example of such events we took those from the period December 2016 - January 2017, when the amplitudes of variability were particularly large concerning temperature and currents. An exceptional increase in temperature, changing its sign from negative to positive, was reflected in simultaneous salinity increase, and density decrease. Each of such events lasted about 10 days (one in the period December - January 2016-2017 and two in the period January -

February 2018). There was no concomitant significant increase of turbidity, which, instead, increased significantly during a similar event occurred at the beginning of March 2018 at the depth of about 1000 m. The current field appeared quite uniform during such events, and NW direction was almost unperturbed, except for the daily oscillations, manifesting as cycloidal motions. However, as these events ceased, and the temperature returned to the usual level (-0.9 °C), the current flow reversed for about several days (e.g. two weeks after the event recorded at the end of 2016), before resuming its prevalent NW direction.

Synergies with other SESS report chapters: in the SESS Report 2018 the SOA chapter (Bensi et al. 2019b) included considerations on the relation between atmospheric processes (wind data) and the dynamic response of the deep sea west of Svalbard. Here we foresee a potential for greater interaction among scientists working on different research topics to discuss important aspects such as: the carbonate system and the CO_2 uptake from the land and ocean (e.g. link with chapters in this report on "Atmospheric black Carbon at Svalbard" (Gilardoni et al. 2020) and "Mapping of plant productivity" (Karlsen et al. 2020), and the effects of melt water runoff from fjords on the offshore marine system (e.g. link with chapters on "The state of Svalbard glaciers" (Schuler et al. 2020) and "Atlantification of Svalbard fjords" (Cottier et al., 2019).

3. Unanswered questions

How do internal dynamics influence the mixing rate between upper and deep layers along the West Spitsbergen continental slope, contributing to the slow modification of the deep layer (> 800 m depth) in this Arctic region?

What is the long-term effect of these continuous intrusions of warmer and saltier water into the deep layers of the Fram Strait? Will they, in turn, have an effect on the progressive warming of the Arctic Ocean?

Can numerical models help resolve the processes observed experimentally in the deep sea west of Svalbard, and help predicting long-term changes possibly induced by them?

4. Recommendations for the future

The *integration of in situ data (fixed ocean and land stations, hydrographic cruises) with other data collection platforms, such as ARGO floats*[1] *and high-resolution satellite images would ensure a better interpretation of the oceanographic phenomena, especially the extreme ones*. In addition, the Synthetic-aperture radar (SAR) satellite images, which are not affected by the cloud cover, could be used for the analysis of wind, waves, and the sea ice cover variability.

Output from high-resolution numerical models could be used to better interpret the dynamic response of the deep ocean to changes in atmospheric pressure, and thus to study the generation and propagation of internal topographically trapped waves.

Set up access programmes to marine infrastructure open to third parties as well, with the aim of guaranteeing implementation and maintenance of the offshore observational sites, to achieve time series useful for climatic considerations. SIOS could extend the call for access to infrastructure including marine sites (within fjords and offshore), and providing the necessary logistic support to access such infrastructures. This would ensure greater visibility of the data, greater collaboration, and optimisation of the existing infrastructure. A specific example could be the possibility, through transnational access calls, to add biogeochemical sensors and/or more levels of turbidity sensors at mooring station S1. This approach would also ensure greater interaction between coastal (fjords) and offshore studies (e.g., concerning carbonate system, organic and inorganic outflow from fjords).

A programme of harmonisation of marine measurements around Svalbard would be desirable in the near future in order to ensure homogeneous data collection in different areas. *A medium-term objective could be to create a handbook of best practices applicable to the measurements carried out around the archipelago.*

1 http://www.argo.ucsd.edu

5. Data availability

Table 2 summarizes the datasets used and presented in this SESS report card.

Table 2: Dataset presented in the SESS report chapter SOA

Parameter (time series) [depth ~ 1000 m; *Latitude: 76° 26.28' N; Longitude: 013° 56.91' E*	Period covered	Data provider	Metadata/Data access
Temperature/Salinity	June 2014 - July 2018	OGS/ISP	NODC (OGS)/Seadatanet/ Data will be available through the SIOS data access point
Turbidity	June 2014 - July 2018	OGS/ISP	NODC (OGS)/Seadatanet/ Data will be available through the SIOS data access point
Dissolved Oxygen	June 2016 - July 2018	OGS/ISP	NODC (OGS)/Seadatanet/ Data will be available through the SIOS data access point
Horizontal currents (u, v)	June 2014 - July 2018	OGS/ISP	NODC (OGS)/Seadatanet/ Data will be available through the SIOS data access point

Acknowledgements

We thank the Captains and crew (scientific and technical) of the research vessel Alliance during High-North cruises (The 'High North' programme is managed by the Italian Navy Hydrographic Institute). We appreciate SIOS-KC staff for their continuous effort spent in promoting research and outreach activities in Svalbard. This work was supported by the Research Council of Norway, project number 251658, Svalbard Integrated Arctic Earth Observing System - Knowledge Centre (SIOS-KC).

References

Bensi M, Kovačević V, Langone L, et al. (2019a) Deep Flow Variability Offshore South-West Svalbard (Fram Strait). Water 11:683. https://doi.org/10.3390/w11040683

Bensi M, Kovačević V, Ursella L, Rebesco M, Langone L, Viola A, Mazzola M, Beszczyńska-Möller A, Goszczko I, Soltwedel T, Skogseth R, Nilsen F, Wåhlin A (2019b) Spitsbergen Oceanic and Atmospheric interactions -SOA. In: Orr et al. (eds): SESS report 2018, Svalbard Integrated Arctic Earth Observing System, Longyearbyen, pp. 130-146. https://sios-svalbard.org/SESS_Issue1

Cottier F, Skogseth R, David D, Berge J (2019) Temperature time-series in Svalbard fjords. A contribution from the "Integrated Marine Observatory Partnership". In: Orr et al. (eds): SESS report 2018, Svalbard Integrated Arctic Earth Observing System, Longyearbyen, pp. 108-118. https://sios-svalbard.org/SESS_Issue1

Gilardoni S, Lupi A, Mazzola M, Cappelletti DM, Moroni B, Ferrero L, Markuszewski P, Rozwadowska A, Krejci R, ZiegerP, Tunved P, Karlsson L, Vratolis S, Eleftheriadis K (2020) Atmospheric Black Carbon in Svalbard. In: Van den Heuvel et al. (eds): SESS report 2019, Svalbard Integrated Arctic Earth Observing System, Longyearbyen, 196 - 211 . https://sios-svalbard.org/SESS_Issue2

Karlsen SR, Stendari L, Nilsen L, Malnes E, Eklundh L, Julitta T, Burkhart A, Tømmervik H (2020) Sentinel based mapping of plant productivity in relation to snow duration and time of green-up. In: Van den Heuvel et al. (eds): SESS report 2019, Svalbard Integrated Arctic Earth Observing System, Longyearbyen, 42 - 57 . https://sios-svalbard.org/SESS_Issue2

Nilsen F, Skogseth R, Vaardal-Lunde J, Inall M (2016) A Simple Shelf Circulation Model: Intrusion of Atlantic Water on the West Spitsbergen Shelf. J Phys Oceanogr 46:1209–1230. https://doi.org/10.1175/JPO-D-15-0058.1

Onarheim IH, Årthun M (2017) Toward an ice-free Barents Sea. Geophys Res Lett 44:8387–8395. https://doi.org/10.1002/2017GL074304

Pearlman J, Bushnell M, Coppola L, et al. (2019) Evolving and Sustaining Ocean Best Practices and Standards for the Next Decade. Front Mar Sci 6. https://doi.org/10.3389/fmars.2019.00277

Polyakov IV, Pnyushkov AV, Alkire MB, et al. (2017) Greater role for Atlantic inflows on sea-ice loss in the Eurasian Basin of the Arctic Ocean. Science 356:285–291. https://doi.org/10.1126/science.aai8204

Schuler TV, Glazovsky A, Hagen JO, Hodson A, Jania J, Kääb A, Kohler J, Luks B, Malecki J, Moholdt G, Pohjola V, van Pelt W (2020), SvalGlac: New data, new techniques and new challenges for updating the state of Svalbard glaciers. In: Van den Heuvel et al. (eds): SESS report 2019, Svalbard Integrated Arctic Earth Observing System, Longyearbyen, 108 - 135 . https://sios-svalbard.org/SESS_Issue2

Skogseth R, Sandvik AD, Asplin L (2007) Wind and tidal forcing on the meso-scale circulation in Storfjorden, Svalbard. Cont Shelf Res 27:208–227. https://doi.org/10.1016/j.csr.2006.10.001

The Continuous Plankton Recorder Survey – Monitoring plankton in the Nordic Sea (CPR Survey)

Martin Edwards[1], Pierre Helaouet[1], Clare Ostle[1], David Johns[1], Marianne Wootton[1], Espen Strand[2] & Espen Bagoien[2]

1 Continuous Plankton Recorder Survey, Marine Biological Association, Plymouth, U.K.
2 Institute of Marine Research, P.O. Box 1870 Nordnes, N-5817 Bergen, Norway

Corresponding author: M. Edwards, maed@mba.ac.uk

Keywords: CPR Survey, Plankton, zooplankton, phytoplankton

1. Introduction

The marine ecosystems of the Arctic and its associated regional seas have been undergoing a rapid transformation over the last few decades which includes loss of sea ice cover and ocean warming. The Arctic sea regions in particular are experiencing the strongest warming on the planet (twice as fast as the planetary average) and the loss of sea ice in recent decades has been unprecedented (Smetacek and Nicol 2005). This persistent warming in the Arctic, caused predominantly by the ice-albedo feedback, has pushed the region into 'uncharted territory' (Caesar *et al.* 2018). Many regional seas that were once considered as being inhabited exclusively by Arctic flora and fauna have become more influenced by more southerly species as these species move northward as the Arctic warms (Polyakov *et al.* 2017). These changes are having huge consequences on the biodiversity and populations of plankton, fish, marine mammals and seabirds of these northern seas.

Plankton are highly sensitive to these rapid environmental changes and are excellent indicators of the state of the environment by acting as biological 'sentinels'. As plankton are at the base of the food-web, by monitoring changes in the plankton we can also understand changes to other animals and trophic levels such as fish and seabirds (Edwards *et al.* 2013). The Continuous Plankton Recorder (CPR) Survey has been operating in the North Sea and North Atlantic since 1931 and is one of the most geographically extensive and oldest continuous marine biological surveys in the world (Edwards *et al.* 2010). It has now been operating for over 10 years in Nordic waters beginning in November 2008. Within this region of the Nordic Seas, the CPR survey adds to and complements other monitoring methods by providing a broader spatial and temporal perspective. For example, most other surveys are coastal or are only sporadically sampled (e.g. once per year) through time. The CPR survey also adds value by providing multi-decadal data at the Atlantic basin scale that can help disentangle and interpret changes observed in the Nordic Seas and help predict changes over the next coming decades. For example, regions that currently support Arctic ecosystems will instead support sub-Arctic systems within the next 10 to 20 years (if not sooner). The biological signals of change we see further south in Atlantic sub-polar systems now can be used to detect the early warning signs of change in the Arctic.

The CPR survey has been operating on a monthly basis using ships of opportunity from northern Norway to Svalbard since 2008 (refer Edwards et al. 2019 for a detailed CPR methodology). Generally, the route operates every month from Tromso in northern Norway to Longyearbyen in Svalbard when conditions are favourable (Figure 1). Sometimes there can be reduced sampling during the winter period. The northern Norwegian routes were initially established due to the rapid changes to plankton and climate and the movement of plankton northwards observed over the last 50 years in the sub-polar Atlantic. These rapid changes in plankton were originally observed in the North East Atlantic, where the majority of CPR routes operate, with plankton northerly movement measured at a rapid ~ 23 km

per year in this region (Beaugrand et al.2009) . To continue these observations of rapid biological movement and biodiversity changes it was considered crucial to establish more northerly CPR routes covering the Nordic Seas to continue to document these changes as well as to monitor for possible trans-Arctic migrations.

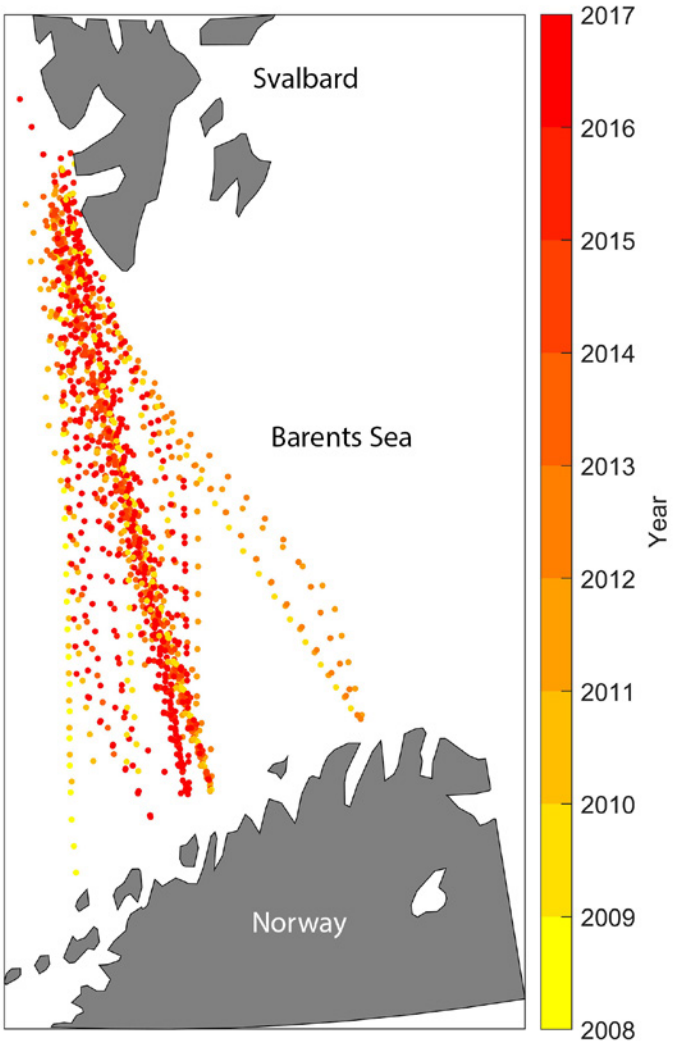

Figure 1: Distribution of CPR samples in the Barents Sea region between northern Norway and Svalbard.

2. The state of plankton

The Barents Sea ecosystem supports some of the world's largest stocks of commercially exploited fish species such as cod (*Gadus morhua*) and haddock (*Melanogrammus aeglefinus*) as well as being the home to some of the largest concentrations of seabirds in the world coupled with a diverse assemblage of marine mammals (Dalpadado et al. 2014). These rich ecosystems are sustained by very high biomasses of phytoplankton and zooplankton found in this region leading to these lucrative marine bio-resources and abundant higher trophic levels.

Generally, the plankton sampled in the Barents Sea consists of a cold-boreal/Arctic to an Atlantic assemblage with the occasional temperate species recorded particularly in the warmer waters of the North Atlantic current to the west and south of Svalbard (Aarflot *et al.* 2018) . Warmer Atlantic water is found to the south and west of Svalbard (known as the Norwegian Current), particularly near the coast of northern Norway, and can also be found to branch as far north as the western coast of Svalbard (as the West Spitsbergen Current). Colder and fresher Arctic waters can be found flowing southward to the east of Svalbard and along the southern coast of Svalbard as far west as Bear Island (approximately halfway between Spitsbergen and Norway's North Cape) (Loeng et al. 1997). As the Barents Sea sits at the doorstep to the Arctic Ocean a number of boreal-Arctic species are also found such as diatom *Ephemera planamembranacea*, the dinoflagellate *Ceratium arcticum* and the copepod *Calanus hyperboreus* (data based on the CPR time-series for this region).

The most commonly recorded phytoplankton in this region are the diatom groups *Chaetoceros* spp., *Thalassiosira* spp., *Rhizosolenia* spp. and *Pseudo-nitzschia* spp which dominate the spring bloom biomass. The dinoflagellate genus *Ceratium* is also very common particularly during the more stratified summer months. Coccolithophore blooms are also a common phenomenon in this region. Calanoid copepods typically dominate the zooplankton assemblage, particularly the boreal species *Calanus finmarchicus*. Euphausiids and hyperiids also contribute to high zooplankton biomasses. Collectively the copepod species *C. finmarchicus* and *C. glacialis* and the krill (*Thysanoessa inermis and T. raschii*) are considered the primary herbivores of this region and as such are the key food sources for higher trophic level predators in the Barents Sea ecosystem (Dalpadado *et al.* 2014).

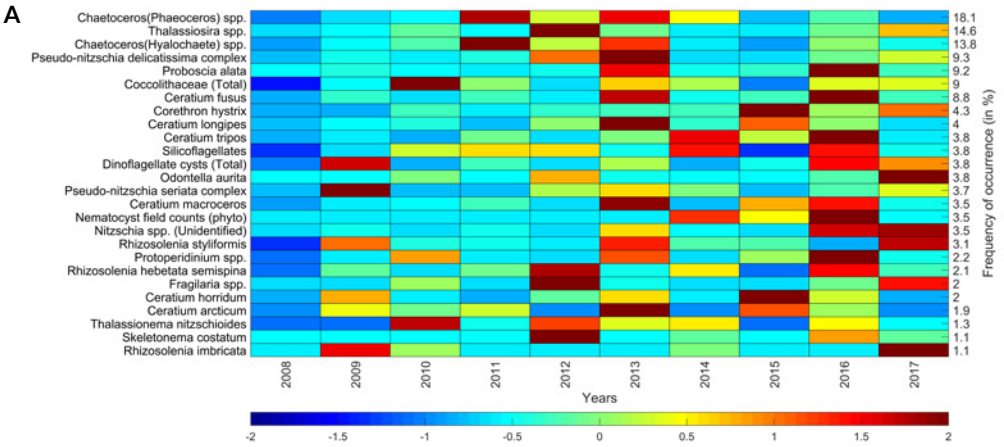
A
Chaetoceros(Phaeoceros) spp. 18.1
Thalassiosira spp. 14.6
Chaetoceros(Hyalochaete) spp. 13.8
Pseudo-nitzschia delicatissima complex 9.3
Proboscia alata 9.2
Coccolithaceae (Total) 9
Ceratium fusus 8.8
Corethron hystrix 4.3
Ceratium longipes 4
Ceratium tripos 3.8
Silicoflagellates 3.8
Dinoflagellate cysts (Total) 3.8
Odontella aurita 3.8
Pseudo-nitzschia seriata complex 3.7
Ceratium macroceros 3.5
Nematocyst field counts (phyto) 3.5
Nitzschia spp. (Unidentified) 3.5
Rhizosolenia styliformis 3.1
Protoperidinium spp. 2.2
Rhizosolenia hebetata semispina 2.1
Fragilaria spp. 2
Ceratium horridum 2
Ceratium arcticum 1.9
Thalassionema nitzschioides 1.3
Skeletonema costatum 1.1
Rhizosolenia imbricata 1.1
Frequency of occurrence (in %)
2008 2009 2010 2011 2012 2013 2014 2015 2016 2017
Years
-2 -1.5 -1 -0.5 0 0.5 1 1.5 2

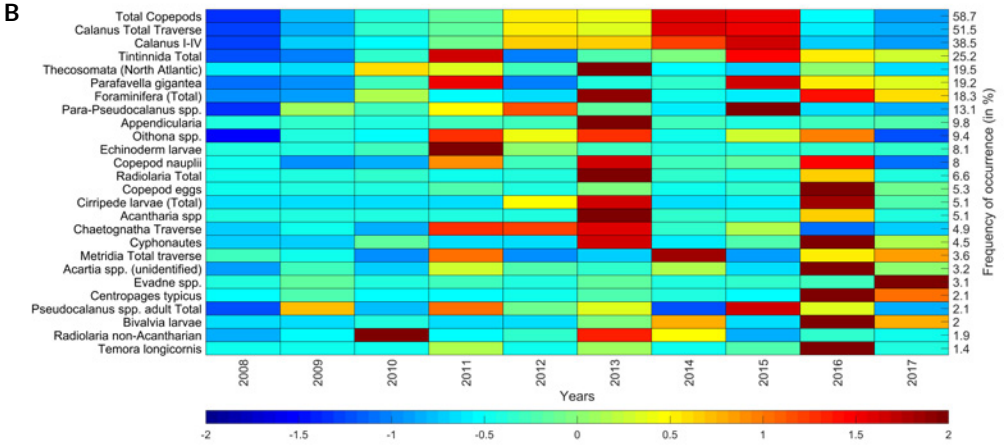
B
Total Copepods 58.7
Calanus Total Traverse 51.5
Calanus I-IV 38.5
Tintinnida Total 25.2
Thecosomata (North Atlantic) 19.5
Parafavella gigantea 19.2
Foraminifera (Total) 18.3
Para-Pseudocalanus spp. 13.1
Appendicularia 9.8
Oithona spp. 9.4
Echinoderm larvae 8.1
Copepod nauplii 8
Radiolaria Total 6.6
Copepod eggs 5.3
Cirripede larvae (Total) 5.1
Acantharia spp 5.1
Chaetognatha Traverse 4.9
Cyphonautes 4.5
Metridia Total traverse 3.6
Acartia spp. (unidentified) 3.2
Evadne spp. 3.1
Centropages typicus 2.1
Pseudocalanus spp. adult Total 2.1
Bivalvia larvae 2
Radiolaria non-Acantharian 1.9
Temora longicornis 1.4
Frequency of occurrence (in %)
2008 2009 2010 2011 2012 2013 2014 2015 2016 2017
Years
-2 -1.5 -1 -0.5 0 0.5 1 1.5 2

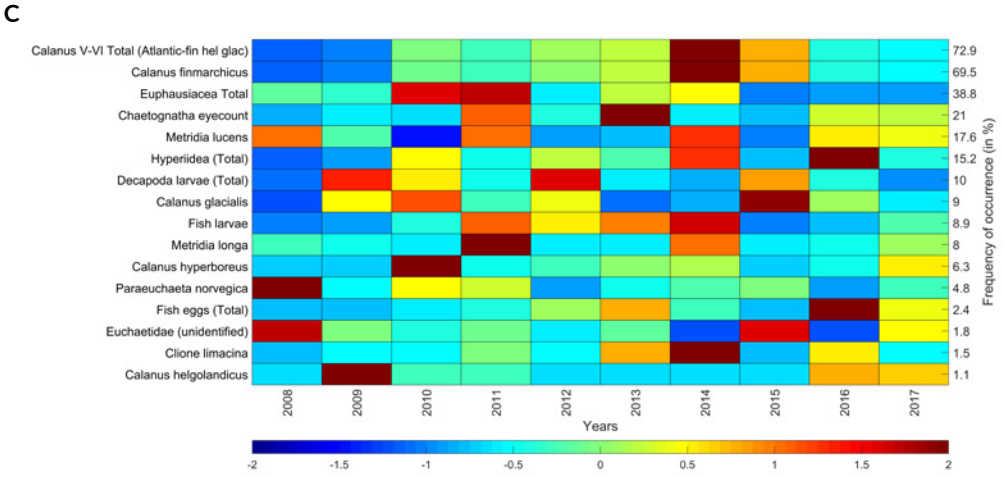
C
Calanus V-VI Total (Atlantic-fin hel glac) 72.9
Calanus finmarchicus 69.5
Euphausiacea Total 38.8
Chaetognatha eyecount 21
Metridia lucens 17.6
Hyperiidea (Total) 15.2
Decapoda larvae (Total) 10
Calanus glacialis 9
Fish larvae 8.9
Metridia longa 8
Calanus hyperboreus 6.3
Paraeuchaeta norvegica 4.8
Fish eggs (Total) 2.4
Euchaetidae (unidentified) 1.8
Clione limacina 1.5
Calanus helgolandicus 1.1
Frequency of occurrence (in %)
2008 2009 2010 2011 2012 2013 2014 2015 2016 2017
Years
-2 -1.5 -1 -0.5 0 0.5 1 1.5 2

Figure 2: The average annual abundance of the most common plankton taxa recorded since 2008, (A) phytoplankton; (B) small zooplankton (C) large zooplankton. Standardised abundance, 0=mean. Aggregated data for the whole Svalbard transect.

Annual trends (2008-2017) in the CPR data for the most common phytoplankton and zooplankton species are shown in Figure 2. Figure 2 also show the most dominant phytoplankton and zooplankton recorded in this region ordered by the percent frequency of occurrence on CPR samples. In 2017 a total of 87 zooplankton and 38 phytoplankton taxonomic entities were routinely recorded for this region on CPR samples representing a fairly diverse plankton community considering the high latitude of these observations. Of particular note for 2017 was the large numbers of *C. hyperboreus* (highest since 2010) and low numbers of *C. finmarchicus* recorded as well as a high number of fish larvae sampled in April. The abundance of the marine cladoceran *Evadne* spp was well above its long-term mean. In the phytoplankton very large blooms of *Pseudo-nitzschia delicatissima* were recorded in July 2017 and the abundances of *Odentella aurita* and *Rhizosolenia imbricata* were well above the long-term mean.

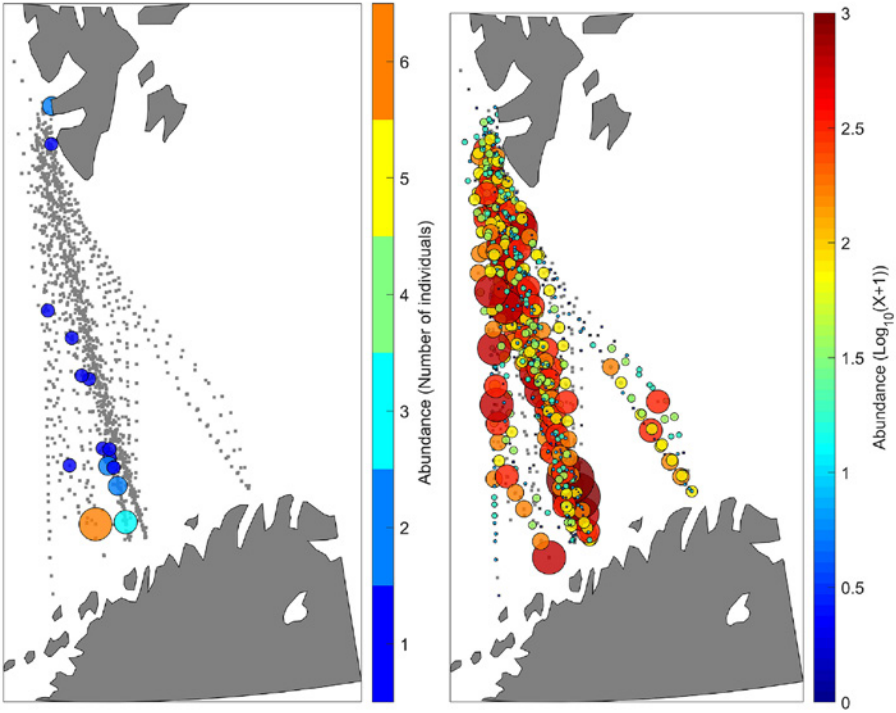

Figure 3: The spatial distribution and abundance of the calanoid species *Calanus helgolandicus (left)* and *Calanus finmarchicus (right)*. Colours represent abundances per sample.

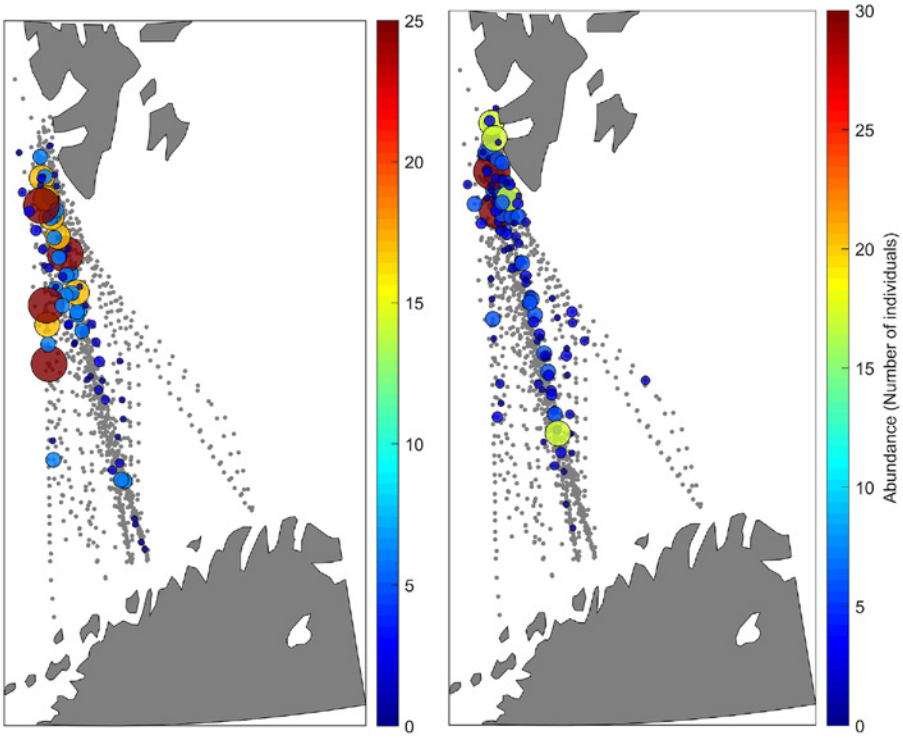

Figure 4: The spatial distribution and abundance of the calanoid species *Calanus hyberboreus (left)* and *Calanus glacialis (right)*. Colours represent abundances per sample.

The spatial distribution of the most common zooplankton *C. finmarchicus* and its relatives are show in Figure 3 and 4. We have focused on *C. finmarchicus* and its congeneric relatives *C. helgolandicus*, *C. glacialis* and *C. hyperboreus* as they are the numerically dominant zooplankton found in this region and they also occupy distinctive thermal preferendums and niches. As such, these species can act as useful indicators and 'sentinel' species to environmental changes and in particular highlight the consequences of climate warming in this region. Thermal niches mentioned in the text have been calculated from gridded CPR North Atlantic data. By far the most numerically dominant species *C. finmarchicus* shows the most cosmopolitan thermal envelope for this region ranging between 0-11°C with an optimum of around 5-6 °C. The more southerly distributed and warmer-water species *C. helgolandicus* has a thermal preferendum ranging between 9-18 °C with a thermal optimum of 11 °C. To put the two species into context from the Svalbard region into the wider North Atlantic region we have shown the biogeographical distributions of the two species for the whole North East Atlantic and Norwegian Sea (Figure 5). In the North Sea *C. finmarchicus* is at its southern edge and *C. helgolandicus* is close to its optimum (Helaouët, Beaugrand and

Edwards, 2013). For the more cold water species *C. glacialis* the thermal range was between 0-7 °C with a thermal optimum of ~4 °C. The larger and lipid rich species *C. hyperboreus* shows a strong affinity towards more polar waters with a thermal range between 0-7 °C and a thermal optimum of between 0-2 °C in these waters.

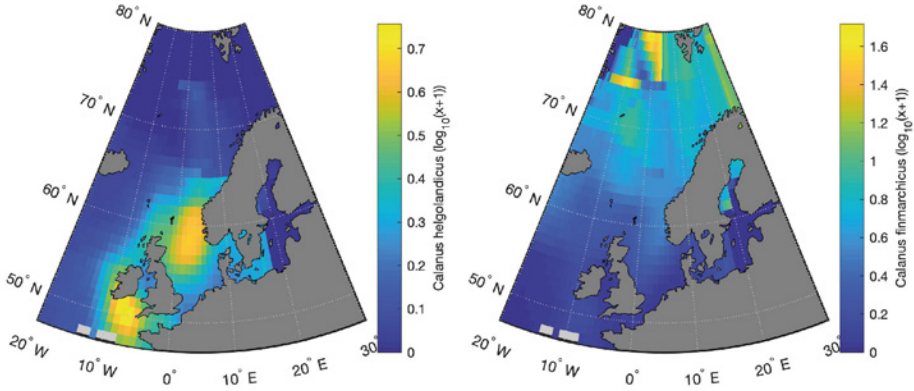

Figure 5: The mean spatial abundance of *C. helgolandicus* and *C. finmarchicus* in the North East Atlantic and Nordic Seas. Data based on CPR sampling and interpolated using objective mapping procedures.

C. finmarchicus is most abundant off the northern coast of Norway with the more colder distributed species *C. glacialis* and *C. hyperboreus* found most abundant off the south-west coast of Svalbard and Storfjord Channel following the penetration of the colder Arctic Current from the east. Interestingly the warm-temperate species *C. helgolandicus* is also recorded on this route with highest abundances recorded off northern Norway. Rather surprisingly, the species has also been recorded off the west coast of Svalbard itself, presumably being carried northward there by the warmer West Spitsbergen Current. The northernmost record of this southerly distributed species *C. helgolandicus* (from CPR records) is currently 77.902 °N recorded off the west coast of Svalbard. There is increasing evidence that temperate species are becoming more commonly recorded in the Barents Sea over the last few years. This is in line with the observed and rapid increase in temperatures recorded in the Barents Sea over the last decade (Lind et al. 2018). Seasonally the *C. finmarchicus* season extends from March to October, whereas the warmer-water species *C. helgolandicus* is generally only present in the autumn months in this region. The seasonal presence in the surface waters of *C. hyperboreus* is generally restricted to the late spring/early summer in this region.

2.1 Trans-Arctic invasive species

Apart from shifting species boundaries (e.g. *Calanus helgolandicus*) that are moving progressively poleward and, in some cases, expanding, the rapid climate change observed the Arctic may have even larger consequences for the establishment of invasive species and the biodiversity of these northern seas (Reid et al. 2007). The thickness and areal coverage of summer ice in the Arctic have been melting at an increasingly rapid rate since records began (Lind et al. 2018). In the spring following the unusually large ice free period in 1998 large numbers of a Pacific diatom *Neodenticula seminae* were found in samples taken by the CPR survey in the Labrador Sea in the North Atlantic. *N. seminae* is an abundant member of the phytoplankton in the subpolar North Pacific and has a well-defined palaeo history based on deep sea cores.

According to the palaeo evidence and modern surface sampling in the North Atlantic since 1948 this was the first record of this species in the North Atlantic for at least 800,000 years. The reappearance of *N. seminae* in the North Atlantic, and its subsequent spread southwards and eastwards to other areas in the North Atlantic, after such a long gap, could be an indicator of the scale and speed of changes that are taking place in the Arctic and North Atlantic oceans as a consequence of climate warming (Reid *et al.* 2007).

The species has been recently found in the Barents Sea north of Iceland and west of Svalbard and also on the ST route in the spring of 2016 at 77.387 N and 13.557 E which is currently its most easterly record. Independent of the CPR survey, the presence of *N. seminae* has recently been recorded from sediment samples along the west Spitsbergen slope (Miettinen, Koç and Husum, 2013). It is possible we could witness more trans-Arctic exchanges in the near future if the ongoing warming trend and reduction of sea ice continues in the Arctic.

The diatom species may itself could be the first evidence of a trans-Arctic migration in modern times and be a harbinger of a potential inundation of new organisms into the North Atlantic. The future consequences of such a change to the biodiversity, productivity and health of Arctic systems caused by these trans-Arctic migrations as well as the encroachment and establishment of more southerly distributed species are at present unknown but are being closely monitored by the CPR survey. Figure 6 shows the distribution of *N. seminae* in the Northern Hemisphere from CPR records in the North Pacific and records from the North Atlantic from 1998 and also the first record from the Svalbard region.

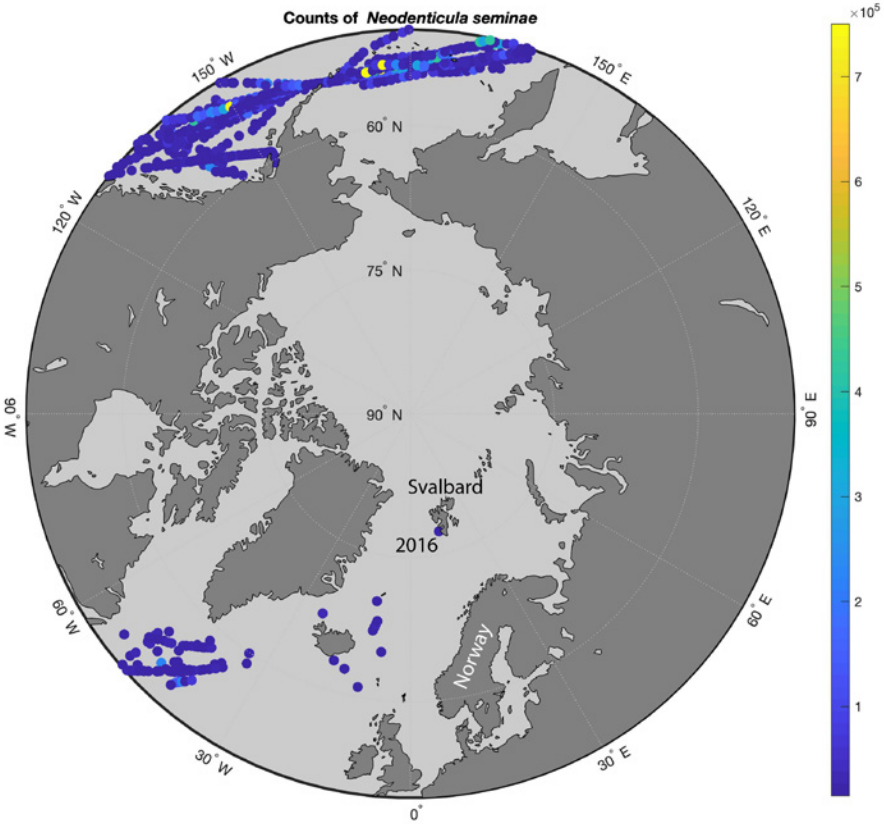

Figure 6. The distribution of the Pacific diatom species *N. seminae* in the Northern Hemisphere from CPR records in the North Pacific and records from the North Atlantic from 1998. The species was recorded off Svalbard in 2016, its most easterly observation in the North Atlantic.

3. Unanswered questions

Many unanswered questions concern the impact of climate change on plankton including the potential acidification of the marine environment and the consequences of these changes to higher trophic levels. Some key emerging issues are listed below.

- Establishing mechanistic links between climate warming, plankton and fisheries (and other higher trophic levels such as seabirds) to form a predictive capacity.
- Identifying species and habitats particularly vulnerable or resilient to climate change impacts and separating the impacts of climate from other anthropogenic pressures such as nutrients/overfishing.
- Understanding the risks to species and habitats and the potential opportunities for new species colonisations as well as potential new pathogens and Harmful Algal Bloom species.
- Understanding the risks caused by warming temperatures and acidification on native marine organisms.
- Understanding the rate of genetic adaptation to climate change impacts.

4. Recommendations for the future

It is envisioned that in the near future the CPR survey will form part of a more integrated observation system within this region and enhance its monitoring with an additional suite of biogeochemical and molecular sensors. It will also endeavour to explore where possible synergies between other oceanographic monitoring and the biological monitoring conducted by the CPR survey. For example, the CPR survey works closely with Norwegian scientists to coordinate its sampling on board of this ship of opportunity and shares data with the Norwegian ferrybox system to obtain further and complimentary information such as pCO_2. Although this region has limited commercial shipping activities, if the CPR monitoring was to be expanded in this region, additional CPR routes could be towed using other ships of opportunity in this region such as tourist vessels.

5. Data availability

All data are freely available on request by contacting the Continuous Plankton Recorder Survey at the Marine Biological Association (MBA), United Kingdom. Data requests (Dan Lear: dble@mba.ac.uk).

Dataset	Parameters	Period	Location or area	Dataset landing page	Comment
CPR Survey: Svalbard plankton data	>100 plankton taxa	Monthly data since 2008-11-01	CPR tow route from Tromso in northern Norway to Longyearbyen in Svalbard	http://doi.dassh.ac.uk/data/1629	Data requests (Dan Lear: dble@mba.ac.uk).

Acknowledgements

This work was supported by the Research Council of Norway, project number 251658, Svalbard Integrated Arctic Earth Observing System - Knowledge Centre (SIOS-KC). The Svalbard CPR route is funded by the Institute of Marine Research (Norway).

References

Aarflot, J. M. et al. (2018) Contribution of Calanus species to the mesozooplankton biomass in the Barents Sea. ICES Journal of Marine Science 75(7):2342–2354. https://doi.org/10.1093/icesjms/fsx221

Beaugrand G, Luczak C and Edwards M (2009) Rapid biogeographical plankton shifts in the North Atlantic Ocean. Global Change Biology, 15(7):1790–1803. https://doi.org/10.1111/j.1365-2486.2009.01848.x

Caesar L et al. (2018) Observed fingerprint of a weakening Atlantic Ocean overturning circulation. Nature, 556(7700):191–196. https://doi.org/10.1038/s41586-018-0006-5

Dalpadado P et al. (2014) Productivity in the Barents Sea - Response to recent climate variability PLoS ONE 9(5). https://doi.org/10.1371/journal.pone.0095273

Edwards M et al. (2010) Multi-decadal oceanic ecological datasets and their application in marine policy and management, Trends in ecology & evolution, 25(10):602–10. https://doi.org/10.1016/j.tree.2010.07.007

Edwards M. et al. (2013) Marine ecosystem response to the Atlantic Multidecadal Oscillation. PloS one 8(2):e57212. https://doi.org/10.1371/journal.pone.0057212

Edwards M, Helaouet P, Ostle C, Wootton M, Strand E, Bagoien E (2019) The Continuous Plankton Recorder Survey - Monitoring plankton in the Nordic Sea. In: Orr et al (eds): SESS report 2018, Svalbard Integrated Arctic Earth Observing System, Longyearbyen, pp. 120 - 129. https://sios-svalbard.org/SESS_Issue1

Helaouët P, Beaugrand G and Edwards M (2013) Understanding long-term changes in species abundance using a niche-based approach. PLoS ONE, 8(11). https://doi.org/10.1371/journal.pone.0079186

Lind S, Ingvaldsen RB and Furevik T (2018) Sea linked to declining sea-ice import, Nature Climate Change 8(634). https://doi.org/10.1038/s41558-018-0205-y

Loeng H, Ozhigin V and Ådlandsvik B (1997) Water fluxes through the Barents Sea. ICES Journal of Marine Science 54(3):310–317. https://doi.org/10.1006/jmsc.1996.0165

Miettinen A, Koç N and Husum K (2013) Appearance of the Pacific diatom Neodenticula seminae in the northern Nordic Seas - An indication of changes in Arctic sea ice and ocean circulation. Marine Micropaleontology99:2–7. https://doi.org/10.1016/j.marmicro.2012.06.002

Polyakov IV et al. (2017) Greater role for Atlantic inflows on sea-ice loss in the Eurasian Basin of the Arctic Ocean. Science 356(6335):285–291. https://doi.org/10.1126/science.aai8204

Reid PC et al. (2007) A biological consequence of reducing Arctic ice cover: arrival of the Pacific diatom Neodenticula seminae in the North Atlantic for the first time in 800 000 years. Global Change Biology 13(9):1910–1921. https://doi.org/10.1111/j.1365-2486.2007.01413.x

Smetacek V and Nicol S.(2005) Polar ocean ecosystems in a changing world. Nature 437(7057):362–368. https://doi.org/10.1038/nature04161

Grand Challenge Initiative – Cusp: observational network for solar wind-driven dynamics of the top atmosphere (GCI-Cusp)

Jøran Moen[1,2], Andres Spicher[1], Toru Takahashi[1,3], Douglas E. Rowland[4], Craig Kletzing[5], James LaBelle[6], Miguel Larsen[7], Mark Conde[8], Yoshifumi Saito[9], Kolbjørn Blix[10]

1 University of Oslo, Oslo, Norway
2 University Centre in Svalbard, Longyearbyen, Norway
3 National Institute of Polar Research, Tokyo, Japan
4 NASA Goddard Space Space Flight Center, Greenbelt, Maryland, USA
5 University of Iowa, Iowa, USA
6 Dartmouth College, Hanover, New Hampshire, USA
7 Clemson University, South Carolina, USA
8 University of Alaska, Fairbanks, USA
9 JAXA Institute of Space and Aeronautical Science, Kanagawa, Japan
10 Andøya Space Center, Andenes, Norway

Corresponding author: Jøran Moen, jmoen@fys.uio.no
ORCID number 0000-0002-8176-0954

Keywords: GCI-Cusp, polar ionosphere, aurora, reconnection, atmospheric heating, outgassing

1. Introduction

The magnetic cusp is a unique place in near Earth space, where energy from the solar wind transfers down into Earth's atmosphere and visualizes as *Daytime Auroras*. The *Grand Challenge Initiative – Cusp* is a gigantic rocket project that umbrellas nine sounding rocket missions, with in total twelve sounding rockets (Moen et al. 2018). In winter 2018/19 three missions (5 rockets) were successfully completed with acquisition of high-quality data while they traversed daytime cusp auroras over Svalbard. This report card is devoted to give an overview over which physical parameters are measured and some of the open science questions that these data are suitable to study.

Open access data in a standardized format are a prerequisite in order to enable efficient collaboration between many international teams of researchers, and also to inspire new research teams to take advantage of the heavy investments in experimental work. Due to complexities associated with rocket experiments, including spin modulations, wake effects etc., the data need to be skilfully prepared and calibrated, and adequate documentation has to follow in order to enable other than the rocket experiment team to make use of the data. The main purpose of this report card is to outline the ongoing development of a *multi-instrument cusp observing system* for efficiently exchange and reuse of data provided by the *GCI-Cusp* project. All *GCI-Cusp* partners are recommended to share equally their data in a combined database accessible through the SIOS Data Management System (SDMS)[1].

2. The state of the GCI-Cusp Earth observing system

The global picture of the Sun-Earth coupling is routinely monitored by the Super Dual Auroral Radar Network (SuperDARN) of radars, ground magnetometers, and numerous satellite missions. For detailed process studies, however, Svalbard is a unique observing platform to investigate multi-scale plasma processes. This is carried out on campaign basis by combined efforts in operating optical instruments and radars during sounding rocket campaigns. One aim of the *GCI-Cusp* project is to create an observing system for multi-scale process studies of the Sun-Earth coupling in the auroral *cusp*. Svalbard is the only place in the world where we can combine optics, radar and in-situ to study the *cusp*.

National Aeronautics and Space Administration (NASA), Japan Aerospace Agency (JAXA), SIOS, and the University of Oslo (UiO) signed a joint venture agreement in Tokyo 6 April, 2017 stating that all partners will share equally the combined database produced by *GCI-Cusp*[2].

1 https://sios-svalbard.org/metadata_search
2 https://sios-svalbard.org/News_20170406

The VISIONS-2 rockets, Visualizing Ion Outflow via Neutral Atom Sensing-2, were launched into a region of strong auroral and electrodynamic forcing, and observed its main target – atmospheric escape in the form of ion outflow. As shown in Figure 1 Left panel, the trajectories of the two rockets were almost coplanar, with one rocket (35.039 – pink trajectory) launched to 800 km apogee and the other (35.040-black) to 600 km apogee two minutes later. The resulting configuration has proven very valuable in studying the mechanisms that drive the ion outflow. In particular, studies of the variations in the plasma wave environment at the two different altitudes in conjunction with the ion measurements have been very illuminating. All the instruments functioned, and the data analysis is ongoing. Another rich dataset is the limb-imaging "Rocket-borne Auroral Imager" (RAI) dataset, which is providing altitude profiles of auroral and airglow emission at 630.0, 557.7, 864.4, and 391.4 nm, and is showing potential signatures of high altitude N2+ upwelling. The energetic neutral atom imaging analysis is in the early stages, but the instruments functioned well and returned data throughout the flight.

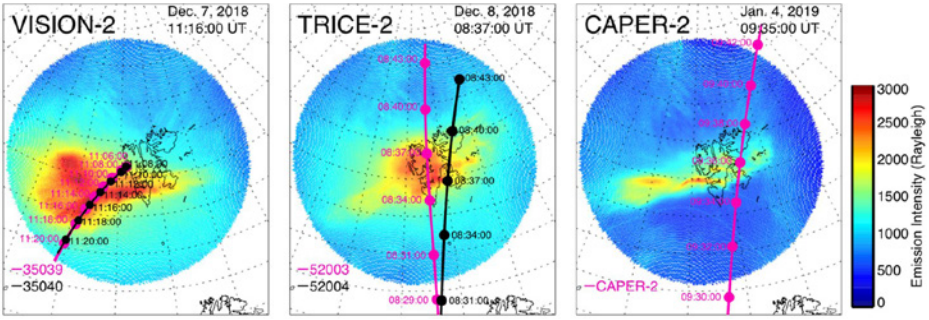

Figure 1: The all-sky image of the auroral 630.0 nm oxygen line has been projected onto a geographic map assuming 250 km as the peak altitude of the aurora emission. The emission intensity is colour coded with Rayleigh bar on the right. The rocket trajectories are overlaid. Left panel: VISIONS-2, two rockets launched from Svalrak, Ny-Ålesund Dec 7, 2018, the first at 11:06 UT and the other two minutes later at 11:08 UT. The auroral image was taken at 11:16 UT. Middle panel: TRICE-2, two rockets launched simultaneously from Andøya Space Center, December 8, 2018. The auroral omages was taken at 08:37 UT. Right panel: CAPER-2, one single rocket launched from Andøya Space Center on January 4, 2019. The all-sky image was taken ab 08:35 when the rocket entered the cusp aurora.

The TRICE-2 rockets, Twin Rockets to Investigate Cusp Electrodynamics, were launched from Andøya Space Center over Svalbard on December 8, 2018. The mission consisted of two, well-instrumented sounding rockets, launched two minutes apart through the auroral cusp. The high-flier (payload 52.003) reached an apogee of 1040 km and the low-flier (52.004) reached the top height of 755 km altitude. The TRICE-2 strategy was to fly two sounding rockets along same magnetic coordinates. However, as illustrated in Figure 1 middle panel, the low-flyer trajectory (black) diverted slightly to the east of the high-flier (pink). Nevertheless, the TRICE-2 mission was very successful in high resolution observation

of ion steps caused by variability in the solar wind plasma injections; i.e. contain signatures of magnetic reconnection in the cusp as well as other cusp electrodynamics. Combined with ground radar and optical data, the TRICE-2 data provide a unique opportunity to have a great potential to study spatial and temporal variability in the energy transfer from the solar wind to the top atmospheres which is the mission main objective.

CAPER-2, Cusp Alfvén and Plasma Electrodynamics Rocket, was launched from Andøya Space Center on January 4, 2019 and reached an apogee of 774 km over Svalbard. As illustrated in the Figure 1 right panel, the traversing of the cusp was starting around apogee. CAPER-2 was dedicated to explore the physical nature of Magnetosphere-Ionosphere (MI) coupling in terms of waves and acceleration processes. There are least two separate electron acceleration processes of broad significance to space plasma physics: acceleration in electrostatic electric fields and in time-varying electromagnetic fields associated with Alfvén waves. In addition, a host of microscopic wave modes play a role in redistributing energy from the resulting electron beams to the thermal plasma, including most ubiquitously Langmuir waves. CAPER-2 observed strong Langmuir waves for the first half of the cusp traversal. CAPER-2 observed several intense wave signatures comprising continuous strong Langmuir waves for the first half of the cusp traversal. CAPER-2 also observed whistler mode waves in front of and within the cusp, suggesting a method of remotely detecting the cusp using VLF waves. The CAPER-2 observations are thus well suited to make significant advances in our understanding of wave-wave and wave-particle interactions the polar cusp.

Sounding rocket data are notoriously difficult to access and, as their existence is often unknown by other researchers, and their use is frequently confined to the rocket teams. We aim to make a step forward by making data from the GCI cusp openly accessible and in a standardized format. This is a prerequisite to enhance usability, transparency and reproducibility, allowing to facilitate international collaboration, and to inspire new research teams to take advantage of the heavy investments in experimental work. This also complies with the new requirement for several scientific journals to make the data and related products available in a repository practicing the FAIR principles[3], i.e. making data findable, accessible, interoperable and reusable (Wilkinson et al. 2016). This has the aim to "accelerate scientific discovery and enhance the integrity, transparency, and reproducibility of this data"[4].

In order to achieve this, data from the VISIONS-2 sounding rocket are used as a pioneering example, with the ambition to inspire other sounding rocket PIs in the future. The plan is to archive Visions-2 data on the Space Physics Data Facility (SPDF)[5] and on NIRD[6] , and make

3 https://publications.agu.org/author-resource-center/text-requirements/ (11.10.2019)
4 https://copdess.org/enabling-fair-data-project/ (11 October2019)
5 https://spdf.gsfc.nasa.gov/
6 https://archive.norstore.no/

it findable through SIOS[7] using NetCDF format, following examples of the latest NASA missions GOLD and ICON[8] The metadata are designed to account for preferences of SPDF and SIOS to follow the International Solar Terrestrial Programme (ISTP) Guidelines[9] and Attribute Convention for Data Discovery (ACDD).

Due to the complexities of spacecraft experiments, including spin modulations, charging or wake effects etc. (Mozer 2016; Paulsson et al. 2018), the data need to be skilfully prepared for it to be useful for scientific purposes. Documents describing the instruments and the calibration methods will be provided and each instrument team on VISIONS-2 and ICI-5 will follow the level definitions mentioned below, loosely inspired (and simplified) by the Magnetospheric Multiscale Mission (MMS) data level description (Baker et al. 2016) and adapted to satisfy attributes from the ISTP guidelines. The levels are labelled by "Hn", standing for "High Resolution data" with "n" taking values between 0 and 3:

- Raw: Raw telemetry data received on the ground and raw data that have been reconstructed, but unprocessed (remove artefacts, combine frames etc.)
- H0 (Level 0): Uncalibrated raw data at full resolution, i.e. quantity versus time.
- H1 (level 1): Calibrated (SI units) data.
- H2 (level 2): Processed calibrated units.
- H3 (level 3): Higher-order products.

Furthermore, refinements and updated versions of the data may be generated in the future when new calibrations are available. Those will be annotated by different versions V01, V02, V03, etc. Release notes describing changes in the new versions will also be provided from the source webpages.

3. Unanswered questions

Further three rocket missions are scheduled in November/December 2019, the Cusp Heating Investigation (CHI), the Cusp-RegionEXperiment (C-REX-2) and the SIOS Investigation of Cusp Irregularities (ICI-5). CHI will measure the flow of plasmas and neutral gasses in the cusp, testing current model of how they interact with one another and become heated and accelerated in the process. C-REX-2 measures wind and ion velocity at around 400 km in altitude on the cusp to trace causes of increased densities there. The mission differentiates between possible causes such as changes in wind, temperature or ion velocity. C-REX will be launched at Andøya, North-Norway over Svalbard, and CHI will be launched from

7 https://sios-svalbard.org/metadata_search

8 e.g. https://spdf.gsfc.nasa.gov/pub/data/gold/documentation/GOLD%20Public%20Science%20Data%20Products%20Guide%20-%20Rev%203.0.pdf

9 https://spdf.gsfc.nasa.gov/sp_use_of_cdf.html

Ny-Ålesund, Svalbard. The aim is a simultaneous launch and the two rockets will provide complementary data sets. ICI-5 was launched in the morning of 26 November 2019. Following the launch, it was quickly reported that the science team picked a prime science event. All payload events were reported as nominal and a solid track was provided by both the Norwegian and NASA ground assets. After data review, it was apparent that a roll rate anomaly was experienced, precluding the instruments from functioning as intended, i.e. no scientific data. The ICI-5 objective was to discover the drivers of plasma turbulence in the cusp auroral region, and specifically determine the size of turbulent eddy structures, and to explore why cusp aurora disturbs radio signals. Efforts will be made to redo the experiment.

Table 1 lists the physical parameters for each *GCI-Cusp mission*. Table 2 lists the science objectives for each *GCI-Cusp* mission. Rocket science is highly competitive, and the research questions selected for each mission are indeed questions of fundamental importance in space science and of relevance to Earth space climate and Earth system models.

The science objective for each mission is indeed very specific. However, data from each mission have the potential for a wide range of research questions in Earth system science and planetary science; i.e. the data have great potential for re-use in general research topics of fundamental relevance in space plasma physics (Table 3).

The topside neutral ionosphere is indeed affected by the solar wind coupling towards the Earth ionosphere and thermosphere system. Weather systems include the atmosphere up to 150 km, however it is uncertain how much the solar wind coupling to the polar atmosphere may affect weather and regional climate prediction models. Energetic particle precipitation modifies atmospheric chemistry in the mesosphere-stratosphere which in turn modifies the vertical energy transport that indeed is relevant for climate models (Semeniuk 2011).

We are now mobilizing for the *Grand Challenge Initiative - Mesosphere and Lower Thermosphere* (*GCI-M/LT*). In the stratosphere and mesosphere, between 10-90 km altitude, the residual meridional circulation is driven by dissipating gravity waves. Gravity wave forcing is included in global circulation models (GCM) merely as a factor, but is not properly modeled. This indeed introduces uncertainties in climate scenario predictions (Shepherd 2014). The GCI-M/LT project will investigate sub-grids scale processes in the mesosphere-lower thermosphere in order to develop more realistic models for global circulation. The need for in-situ small-scale 3D measurements of waves, structures and turbulence in the altitude range 40-120 km by a structured program of sounding rockets was emphasized in the SIOS Infrastructure Optimization Report (Ellis-Evans and Holmén 2013). This will be essential in order to make progress in understanding the vertical transport of energy and mass flow dynamics, including the role of meteor components (Ellis-Evans and Holmén 2013).

Table 1: The physical parameters measured/to be measured by each rocket mission are marked by crosses. E (Electric field), B (Magnetic field), Ne (electron density), HF/ELF/VLF (High Frequency/ Extreme Low Frequency/Very Low Frequency), e-flux (electron fluxes), i-flux (ion fluxes), Vi (ion velocity), Vn (Neutral wind), Te (electron temperature), N (neutral density), velocity of H+, He+, O+, Phase space of H+, He+, O+, core ground experiments ASC (All-Sky Camera), EISCAT Svalbard Radar to measure Ne,Vi, Te, Ti and Cutlass High Frequency Radar to measure Vi flow field and plasma irregularities.

Mission/ Parameter	TRICE-2	VISIONS-2	CAPER-2	AZURE	ICI-5	C-REX 2	CHI	SS-520-3
E	x	x	x		N/A			x
B	x	x	x		N/A			x
Ne	x	x	x		N/A			x
HF/ELF/VLF	x	x	x					
e-flux	x	x	x		N/A			x
i-flux	x	x						
Vi				x		x	x	
Vn				x		x	x	
Te		x						x
N								x
velocity H+, He+, O+								x
Phase space H+, He+, O+								x
narrowband auroral / airglow imaging		x						
Key Ground Support for the completed missions								
ASC	x	x	x	-	x	-	-	-
EISCAT	x	x	x	-	x	-	-	-
Cutlass HF	x	x	x	-	N/A	-	-	-

Table 2: Specific science objectives of each mission.

Mission name	Specific mission objectives	#rocket	Launch Site	Launch date	Lead
TRICE-2	Magnetopause reconnection -steady or pulsed	2	ASC	8DEC2018	US
VISIONS-2	Energization of O+- Ion upflow/outflow	2	Svalrak	7DEC2018	US
CAPER-2	Alfvén wave acceleration of auroral particles	1	ASC	4JAN2019	US
G-Chaser	Student rocket Technology testing	1	ASC	13JAN2019	US
AZURE	Auroral effects on the atmosphere/energy gain or loss	2	ASC	6APR2019	US
SIOS ICI-5	Plasma instabilities processes/turbulence in the cusp ionosphere	1	Svalrak	DEC2019	NO
C-REX 2	Neutral & plasma winds to study enhanced density at 400 km	1	ASC	DEC2019	US
CHI	Auroral forcing of cusp upwelling effects	1	Svalrak	DEC2019	US
SS-520-3	Energization of O+- Ion upflow	1	Svalrak	TBD	JP

Table 3: The GCI-Cusp missions have the potential to address fundamental questions in space physics.

Fundamental Questions	TRICE-2	VISIONS-2	CAPER-2	AZURE	ICI-5	C-REX 2	CHI	SS-520-3
Magnetic reconnection	x	x	x		x	x	x	x
Particle acceleration	x	x	x				x	x
Atmospheric heating		x		x	x	x		x
Plasma instabilities	x	x	x	x			x	x
Plasma Turbulence	x	x	x		x			x

4. Recommendations for the future

The greatest success with the *GCI-Cusp* collaboration so far, is that we so far have been successful with the launches, and that we are developing a *multi-scale Cusp atmosphere observing system*. We adapt to the SIOS data management system and the Space Physics Data Facility (SPDF) for storing and making data openly accessible and reusable for new research projects developed, within and outside the *GCI-Cusp* consortium, and hence to maximize the return of the investments made by each participation, and puts the Svalbard oriented research into a global context. We also hope that in the near and distant future, other rocket experiments will follow the footsteps of the GCI-Cusp with VISIONS-2, and make their data standardized in a similar way.

The GCI-Cusp programme has already resulted into its successor initiative. That is a new international effort to create the *Grand Challenge Initiative Mesosphere/Lower Thermosphere (GCI-M/LT)* that was initiated at the CEDAR 2018 workshop in Santa Fe. If SIOS decides to participate in *GCI-M/LT*, it will be an excellent opportunity to close further knowledge gaps defined by SIOS. As reported in the SIOS Infrastructure Optimisation Report (Ellis-Evans and Holmén 2013), there is an observational gap in the altitude range 40-80 km, that only can be filled by rockets. Taken together, GCI-Cusp and *GCI-M/LT* will be an important contribution to optimize an ESS monitoring program for vertical coupling of atmospheric layers.

Recommended future investments:

i) New SIOS infrastructure investment plans should consider a high-resolution time and space 4D all-sky imaging system to enhance the features of the cusp-observational network, i.e. 3 identical imagers placed at 3 different sites. Key parameters derived from routine ground optical and radar instruments should be given status as SIOS core data.

ii) SIOS should make a strategic effort to also become a central partner in the GCI-M/LT rocket initiative, by prioritizing to investment into the planned SIOS ICI-6 sounding rocket.

5. Data availability

The objective is to have the first release of VISIONS-2 data before 31 December 2019. This will include data from the VISIONS-2 experiments listed in Table 4 .

Table 4: List of the instruments on-board both VISIONS-2 payloads (35.039 and 35.040) with the data levels (see section 2) expected at the time of data release. The abbreviations stand for Fields and Thermal Plasma (FTP) instrument, Cubesat Electric Field Instrument (CEFI), multi-needle Langmuir probe system (mNLP), the Energetic Electron Analyzer/Energetic Ion Analyzer (EEA/EIA), Acute precipitating electron spectrometer (APES), MIniaturized Low-energy Energetic Neutral Atom imager (MILENA), Rocket-borne Auroral Imager (RAI), and miniaturized plasma imagers (MPI). This list may be subject to minor changes. The name of the instruments PIs and data repositories are also included.

Mission/ Parameter (instrument)	VISIONS-2 35.040	VISIONS-2 35.039	Provider, access
Magnetic field (FTP/CEFI)	H2	H2	Pfaff/Rowland/spdf
DC electric field (FTP)	H2		Pfaff/Rowland/spdf
VLF (FTP/CEFI)	H2	H2	Pfaff/Rowland/spdf
HF (FTP)	H2		Pfaff/Rowland/spdf
Langmuir probe (FTP/CEFI)	H1	H1	Pfaff/Rowland/spdf
Electron temperature (FTP/CEFI)	H2	H2	Pfaff/Rowland/spdf
Electron density (mNLP)		H1	Moen/NIRD
Electron particle data (EEA)	H2		Clemmons/Rowland/spdf
Electron particle data (APES)	H0		Michell/Rowland/spdf
Electron particle data (MILENA)	H0	H0	Collier/Rowland/spdf
Ion particle data (EIA)	H2		Clemmons/spdf
In-situ auroral imager (RAI)		H0	Hecht/spdf
Ion Velocity (MPI)		H2	Burchill/spdf
Trajectory, attitude, mechanical	H1	H1	Rowland/spdf
All-Sky Imager	H2	H2	Moen/NIRD

Acknowledgements

The Norwegian contribution to the Grand Challenge Initiative - Cusp program is funded by grants from the Research Council of Norway and the Norwegian Space Agency. This work was supported by the Research Council of Norway, project number 251658, Svalbard Integrated Arctic Earth Observing System - Knowledge Centre (SIOS-KC), and project number 275653, 4DSpace investigation of plasma turbulence in the cusp ionosphere. Thanks to the SIOS-KC staff for their assistance to develop the GCI-Cusp initiative.

References

Baker DN, Riesberg L, Pankratz CK, Panneton RS, Giles BL, Wilder FD, Ergun RE (2016) Magnetospheric Multiscale Instrument Suite Operations and Data System. Space Sci Rev, 199: 545. https://doi.org/10.1007/s11214-014-0128-5

Ellis-Evans C, Holmén K (2013) SIOS Infrastructure Optimisation Report. SIOS-PP Work Package 3, Deliverable 3.4. https://sios-svalbard.org/sites/sios.metsis.met.no/files/common/D3.4_SIOSInfrastructureOptimisationreport.pdf

Moen J, Spicher A, Rowland DE, Kletzing C, LaBelle J (2019) Grand Challenge Initiative – Cusp: Rockets to explore solar wind-driven dynamics of the top side polar atmosphere. In: Orr et al. (eds): SESS report 2018, Svalbard Integrated Arctic Earth Observing System, Longyearbyen, pp. 184-204. https://sios-svalbard.org/SESS_Issue1

Mozer FS (2016) DC and low-frequency double probe electric field measurements in space. J. Geophys. Res. Space Physics, 121:10,942– 10,953. https://doi.org/10.1002/2016JA022952

Paulsson JJP, Spicher A, Clausen LBN, Moen JI, Miloch WJ (2018) Wake potential and wake effects on the ionospheric plasma density measurements with sounding rockets. Journal of Geophysical Research: Space Physics, 123: 9711– 9725. https://doi.org/10.1029/2017JA025004

Semeniuk K, Fomichev VI, McConnell JC, Fu C, Melo SML, Usoskin IG (2011) Middle atmosphere response to the solar cycle in irradiance and ionizing particle precipitation. Atmos. Chem. Phys., 11: 5045–5077. https://doi.org/10.5194/acp-11-5045-2011

Shepherd TG (2014) Atmospheric circulation as a source of uncertainty in climate change projections, Nature Geoscience, 7:703-708.https://doi.org/10.1038/ngeo2253

Wilkinson MD, et al. (2016), The FAIR Guiding Principles for scientific data management and stewardship, Scientific Data, 3: 160018. https://doi.org/10.1038/sdata.2016.18

Frequently Asked Questions

Sentinel satellite-based mapping of plant productivity in relation to snow duration and time of green-up (GROWTH)

Why is measuring annual plant production important?

Plants provide food for wildlife, and plant production plays a key role in the global carbon budget, nutrient cycling, surface energy budget and large-scale climate.

How can plant production be measured over large areas?

Time-series of satellite data provide copious amounts of information and cover vast areas, even in the most inaccessible regions. Information on plant production can be extracted from satellite data. However, to interpret those remote-sensing signals correctly, we must calibrate them against data from field measurements and near-ground sensors.

Climate-Ecological Observatory for Arctic Tundra (COAT)

What is the High Arctic tundra?

The High Arctic tundra is the most northerly community of plants and animals. They inhabit a very dry and cold climate with short cool summers and long cold winters when the ground is covered with snow. Permafrost (ground that remains frozen for two or more years) is a characteristic of the High Arctic tundra, which is mostly treeless and covered with low-lying vegetation. The ecosystems of the High Arctic tundra contain a diverse range of plants and animals, many of which are found there and nowhere else.

What is the Climate-ecological Observatory for Arctic Tundra?

The Climate-Ecological Observatory for Arctic Tundra (COAT) is a response to the urgent international calls for establishment of scientifically robust observation systems that will enable long-term, real-time detection, documentation, understanding and predictions of climate impacts on arctic tundra ecosystems. The activities in Svalbard are an integral part of COAT.

Are there geese in Svalbard in the winter?

There are three species of goose in Svalbard, pink-footed goose, barnacle goose and light-bellied brent goose. All three species breed in Svalbard, but spend the winter further south in different areas in Europe. For example, most of the pink-footed goose population in Svalbard migrates along the Norwegian coast, and winters in Denmark, the Netherlands and Belgium. They return to Svalbard in May and start nesting in June as soon as the snow melts.

How big is the Arctic fox?

The Arctic fox is a small top predator in the Svalbard tundra ecosystem. It is about the size of a house cat, with a body mass between 2.5 and 5 kg. However, it is an efficient predator and scavenger; its diet includes eggs, chicks and even adults of geese, ptarmigans and seabirds. It can also traverse great distances. One female was recorded moving 3 500 km across sea ice from Svalbard to Canada in March 2018!

Is a milder climate bad for herbivores on the Svalbard tundra?

A milder climate influences the herbivore species in the Svalbard tundra both negatively and positively. It increases the frequency and extent of ground ice during the winter as precipitation that previously fell as snow falls as rain and forms a thick ice cover over the ground. This can lead to increased starvation and death for the entire overwintering community of birds and mammals. A milder climate also advances spring and extends the summer grazing season. This can be positive because breeding grounds for migratory geese are accessible earlier and herbivore forage for non-migrating species will be available longer into autumn.

Environmental Monitoring in the Kapp Linné-Grønfjorden Region (KLEO)

Why did you develop an “environmental observatory” in the Kapp Linné–Grønfjorden region?

The area is strongly influenced by the high arctic maritime setting of the west coast of Spitsbergen, in contrast to the region around Longyearbyen which is distinctly more continental. Warmer and wetter conditions in Svalbard have been attributed to increasing Atlantification of the Barents Sea and the west coast of Spitsbergen is especially impacted by the changes in ocean currents.

Why study lakes and lake sediments?

Lakes are commonly viewed as sentinels of climate and environmental change, since they respond to changes in physical, biological, chemical and climatological processes in the watershed – and this information is recorded in the sediments deposited on the lake floor. Linnévatnet is one of the largest lakes in Svalbard and its sediment record provides a detailed history of glacier meltwater changes through time. Long-term "Paleo" records that extend back centuries and millennia provide a baseline, a context against which we can compare current status and future changes.

How are Svalbard's lakes changing in response to global change?

Ice cover on Linnévatnet has been forming later over the past five years than it did a decade ago. The timing of ice melt in the spring has not changed significantly. Water temperatures are higher in the summer. Future work will examine how the organisms living in the lake respond to these changes.

How often does your weather station in Linnédalen record measurements?

The weather station in Linnédalen is programmed to record measurements every 30 minutes. Unfortunately, the weather station is old and unreliable and there are data gaps when it has stopped working.

Will glaciers in Svalbard disappear due to global warming?

Yes, some of them. Linnébreen has become so small that it is behaving more like a static ice field than as a glacier which moves under its own weight. But it will take at least several decades before the ice of Linnébreen melts away completely. Large glaciers in Svalbard are getting smaller but will likely not disappear.

New data, new techniques and new challenges for updating the state of Svalbard glaciers (SvalGlac)

Do all glaciers on Svalbard melt/shrink?

All glaciers in Svalbard experience melting during the summer period. This does not automatically mean that they are losing mass, which is the quantity we are most interested in. Glaciologists study the balance between processes of mass gain and mass loss: the "mass balance". A mass change manifests itself first as a change in the glacier's thickness. Over time its length and area will adjust. The total mass of ice on Svalbard is decreasing. We have good knowledge of the total mass budget, even though each individual glacier is not monitored.

What will happen to the glaciers in the future?

Given continued warming, the glaciers will continue losing mass. However, we lack the quantitative studies required to quantify the expected changes through 2100.

How much ice is there in Svalbard? How many glaciers? And how many of them are monitored?

Svalbard has about 2200 individual glaciers (larger than 1 km^2), covering a total area of about 34000 km^2 (about 60% of the total land area of the archipelago). About 10 glaciers are monitored with glaciological mass balance studies. Together they cover a total of ~1650 km^2, corresponding to about 5% of Svalbard's glacier area. However, several other methods allow us to survey glacier changes over large areas (for example satellite remote sensing, modelling).

What are the differences between calving glaciers and land-terminating glaciers?

Glaciers that end in the sea lose mass by calving and submarine melting (melting of ice in contact with warmer ocean water) in addition to meltwater runoff, which is the main mechanism for land-terminating glaciers.

What are glacier surges?

A glacier surge is a switch from a slow- to a fast-flowing mode. Typically the glacier will accelerate from a few metres per year to as much as several metres per day. Some glaciers surge periodically. Surges are often accompanied by an advance of the glacier front; they from last several months up to years, and typically lead to thickening in the lower part of the glacier, and thinning in the upper part. The time between surges – the "quiescent phase" when the glacier "recharges" – characterized by thickening in the upper parts and thinning in lower parts. This phase can last several decades to centuries.

Seismological monitoring of Svalbard's cryosphere: current status and knowledge gaps (CRYOSEIS)

What is cryoseismology?

Cryoseismology is the study of ground shaking (seismic waves) generated in the cryosphere – the frozen part of our planet. These vibrations are caused by processes such as the movement of glaciers, iceberg break-up events (calving), and flowing meltwater. Cryoseismology also includes continuously measuring changes in ice and frozen ground (permafrost) using ambient seismic vibrations (noise).

How can cryoseismology be used to monitor climate change?

Climate change affects processes at glaciers such as calving, and causes changes in the permanently frozen ground (permafrost) in polar regions. Cryoseismology allows us to use seismic waves to measure these changes with high temporal resolution (days or even seconds) or over longer periods (up to decades) by going back to data gathered since the installation of the recording station.

How can cryoseismology contribute to glaciology?

Cryoseismology can help us estimate the mass of ice that glaciers lose due to calving and observe and better understand glacial processes like crevassing or meltwater discharge. For example, strong calving in Svalbard can be registered as much as 100 km away, and seismological records are fully independent of visibility, which guarantees calving observations despite polar night or bad weather. The high temporal resolution (sampling on the sub-second scale) may provide much more detailed information about the calving process than for example satellite images (weekly images during summer). A seismic station can even be used to monitor different glaciers in parallel.

What is an icequake?

Analogous to earthquakes, icequakes result from sudden movements or cracks opening in the ice or at the base of the glacier. Since the underlying physics is similar, icequakes can be often analysed using the same methods as applied for earthquake research.

Multidisciplinary research on biogenically driven new particle formation in Svalbard (SVALBAEROSOL)

What are aerosols?

Aerosols are tiny particles suspended in the air. Primary aerosols are already in particle form when they enter the atmosphere. Secondary aerosols form from vapour molecules suspended in the air. In secondary aerosol formation, volatile gases (both anthropogenic and biogenic emissions) are oxidised in the atmosphere and transformed to condensable vapours, including sulphuric acid, methane sulphonic acid, iodic acid and a variety of highly oxidised organic compounds.

Why are secondary aerosols relevant in the Arctic?

Clouds do not form without seed particles – so-called cloud condensation nuclei (CCN) – on which water vapour can condense. Arctic CCN consist largely of secondary aerosol particles. Therefore, secondary aerosol has a great impact on cloudiness, precipitation, cloud radiative properties and climate in the Arctic.

How does warming affect clouds and climate?

Warming leads to sea ice decline and promotes plant growth on land. Enhanced phytoplankton productivity owing to reduced sea ice coverage, and warming-induced increases in terrestrial vegetation both probably enhance emission of several key gases to the atmosphere. This will likely be reflected in higher concentrations of aerosol and cloud condensation nuclei (CCN) which, in turn, influence cloud properties and climate. Clouds can both cool and warm the regional climate. Whether sea ice decline exerts negative or positive feedback on temperature has not yet been properly established.

How do the suggestions given in this report help to mitigate climate warming and Arctic change?

Here, we propose an upgrade to SIOS that would enable scientists to resolve and to monitor mechanisms of secondary aerosol formation. All this information would be fed to the CERN-CLOUD experiment, where processes can be experimentally simulated and parameterised. These parameterisations and correct description of secondary aerosol formation can be deployed in large-scale models, including global climate models, that help mankind to understand and mitigate the ongoing global change.

Atmospheric black carbon in Svalbard (ABC Svalbard)

What is Black Carbon (BC)?

Black carbon, often abbreviated BC, is a component of the small particles that make up atmospheric aerosols – particles in the air. BC is emitted during combustion, including fuel combustion for residential heating, transportation, energy production, as well as during wildfires. BC observed in the Arctic can be emitted by local sources, but can also be transported from long distances to Arctic areas.

Why is atmospheric black carbon important?

BC is an atmospheric pollutant, as it can be harmful for human health, but it is also a short-lived climate forcer. This means that it can contribute to altering the climate, but its life-time in the atmosphere (a few days) is shorter than that of greenhouse gases, like CO_2 (5 to 200 years). Together with the reduction of greenhouse gases, reduction of short-lived climate forcers is necessary if we are to keep global warming below the limit of 2°C.

What is the effect of black carbon on the Arctic climate?

BC contributes to Arctic warming through different mechanisms. Black carbon in the Arctic region can absorb incoming solar radiation during spring and summer; it darkens snow and ice promoting their melting, and modifies the way clouds interact with radiation. In addition, BC outside the Arctic can still have an effect of the Arctic climate, by changing the transport of energy from lower latitudes to the polar regions.

Why are atmospheric black carbon measurements important in the Arctic?

BC measurements in the Arctic are crucial to improving the ability of climate models to replicate the present warming and to predict the future climate change. In addition, ongoing

warming will increase human activities in the Arctic, including shipping and oil extraction, both of which generate BC. At the same time international efforts are being made to reduce BC emissions in the Arctic areas, as well as at lower latitudes. BC measurements are essential to monitor the impacts of changing human activities and policy actions on the Arctic atmosphere.

Probing the vertical structure of the lower atmosphere over Svalbard (ProVeSAS)

How many radiosonde balloons are launched every day?

Worldwide, weather balloons are released simultaneously at least once a day every day of the year from almost 900 locations, including many in the Arctic!

How can the measurements done in Ny-Ålesund be made representative on a broader scale?

There are two main strategies for this: (1) Better cooperation with modellers. We will need a Large Eddy Simulation model for Kongsfjorden to interpret the various measurements; (2) Closer links to the satellite community. Data from the cloud radar and Raman LIDAR equipment in Ny-Ålesund are directly comparable to data from the upcoming EarthCare mission planned by the European and Japanese space agencies. UAV (drone) flights could be performed below the track of the satellite and connect properties measured locally in Kongsfjorden to the undisturbed conditions over the Arctic Ocean.

Which factors determine the maximum altitude a tethered balloon can reach?

The two main factors are (1) the weight of the payload, which increases due to the increased weight of the tether line as the tethered balloon ascends; and (2) the wind conditions. Often, especially in the Ny-Ålesund area, strong wind jets at low altitude may hamper the vertical motion of the balloon.

Which is your strategy for aerosol research?

The retrieval of aerosol properties from LIDAR requires the solution of an inverse equation that depends on a scattering theory. For this reason, LIDAR data must be calibrated regularly against measurements done on site at altitude (e.g. by balloon or drone). The aim is to obtain reliable height-resolved LIDAR data on aerosol type and concentration that can be directly compared to chemistry and transport models.

Would you like to be part of the SESS report?

SIOS frequently publishes calls for contributions to the SESS report. Visit our web portal and follow us on twitter/facebook to stay updated.

www.sios-svalbard.org
twitter.com/sios_kc
facebook.com/SIOSKnowledgeCentre

You can find this and previous SESS reports on our webpage:
https://sios-svalbard.org/SESSreport

Visit the SIOS data access point to find metadata and datasets described in this report: https://sios-svalbard.org/metadata_search

SIOS
SVALBARD INTEGRATED ARCTIC EARTH OBSERVING SYSTEM

ISSN 2535-809X (printed)
ISSN 2535-6321 (pdf)
ISBN 978-82-691528-7-6 (printed, stapled)
ISBN 978-82-691528-6-9 (pdf)